**Luz K. Polo Osorio**

**Versão corregida**

# Physiological responses, bioactivity and differential analysis of protein abundance of the brown seaweed *Sargassum* (Phaeophyceae, Fucales) submitted to UV radiation

# Respostas fisiológicas, bioatividade e análises diferencial da abundância de proteínas da alga parda *Sargassum* (Phaeophyceae, Fucales) submetida a radiação UV

**São Paulo**

**2019**

**Luz K. Polo Osorio**

# Physiological responses, bioactivity and differential analysis of protein abundance of the brown seaweed *Sargassum* (Phaeophyceae, Fucales) submitted to UV radiation

# Respostas fisiológicas, bioatividade e análises diferencial da abundância de proteínas da alga parda *Sargassum* (Phaeophyceae, Fucales) submetida a radiação UV

Thesis presented to the Institute of Biosciences of the University of São Paulo, to obtain a PhD Degree in Biological Sciences, in the area of Botany.

Advisor: Profa. Dra. Fungyi Chow

**São Paulo**

**2019**

Ficha catalográfica elaborada pelo Serviço de Biblioteca do Instituto de Biociências da USP,
com os dados fornecidos pelo autor no formulário:
http://www.ib.usp.br/biblioteca/ficha-catalografica/ficha.php

Polo Osorio, Luz Karime
Respostas fisiológicas, bioatividade e análises diferencial da abundância de proteínas da alga parda Sargassum (Phaeophyceae, Fucales) submetida a radiação UV / Luz Karime Polo Osorio; orientadora Fungyi Chow. -- São Paulo, 2019.

245 f.

Tese (Doutorado) - Instituto de Biociências da Universidade de São Paulo, Departamento de Botânica.

1. Abiotic stress. 2. Algae. 3. Phenolic compounds. 4. Photoprotection. 5. Proteomics. I. Chow, Fungyi , orient. II. Título.

Bibliotecária responsável pela estrutura da catalogação da publicação:
Elisabete da Cruz Neves - CRB - 8/6228

**Prof(a). Dr(a).**
Ana Beatriz Furlanetto Pacheco

**Prof(a). Dr(a).**
Maria Teresa Menezes Széchy

**Prof(a). Dr(a).**
Estela Maria Plastino

**Prof(a). Dr(a).**
Fungyi Chow
Orientadora

*A mi amado y sabio padre*

## ACKNOWLEDGMENTS

To Coordenação de Aperfeiçoamento de Pessoal de Nível Superior (CAPES) for the PhD fellowship during 2015-2016.

To Fundação de Amparo à Pesquisa do Estado de São Paulo (FAPESP) for the PhD fellowship (Proc. No. 2016/03095-0) and the research internships abroad (BEPE Proc. No. 2018/17758-7) for the execution of this research; and to BIOTA/FAPESP for the research grant (Proc. No. 2013/50731-1).

To my dear supervisor Fungyi Chow for the sharing knowledge, patient and dedication through my academic process. Gracias profe profe.

To Professors Valéria Cassano and Mariana Oliveira for the contribution in my qualification exam, and the help in the taxonomy area.

To the technicians William Oliveira, Rosário Petti, André Nakasato from the Laboratory of Marine Algae "Édison José de Paula" (LAM), for all the help during experiments and laboratory analysis.

To Professor Eny Floh from the Laboratory of Cellular Biology of Plants (BIOCEL) for availability of the equipment during the proteomic stage and Dr. Andre Luis Wendt dos Santos for being my tutor along this complex area; thanks for the time and patience. To the technicians Amanda Macedo e Silvia Blanco for all the help during the time spent at BIOCEL.

To Professor Marilene Demasi from the Laboratory of Biochemistry and Biophysics (Butantan Institute) for the availability of the equipment for gel electrophoresis and to the technician Adrian Hand for the help during my stay in this laboratory.

To Professor Antonio Carlos Teixera from the Center for Chemical System Engineering - Department of Chemical Engineering, for the spectroradiometer loan.

To Caro (sonrri sonrri) for all the timeshare and for make our home a special place.

To all the colleagues from the LAM, specially Alexandre Souza and Talissa Harb for the help, discussions and laughter. Thank you for making this process more enjoyable; and to my dear Vanessa Victoria-Urrea. Thanks for the support and for bringing a little home!

To my dear Professor Félix López Figueroa from the research group Photobiology and Biotechnology of Aquatic Organisms (FYBOA) in the Department of Ecology and Geology at University of Málaga-Spain. Thank you for receiving me and giving me the opportunity and experience to work with you. To Professor Nathalie Korbee for the discussions and help in High Performance Liquid Chromatography (HPLC) analysis. To Julia who helped me 100% during my internship abroad. To Francisca De La Coba Luque for all the help in gas chromatography (GC) analysis.

To Jota. Thanks for being by my side and supporting me all the time.

To my family, mom, dad, brother. Thanks a lot for all the unconditional support and words of encouragement in difficult times.

## GENERAL ABSTRACT

The incidence of light in terms of quality and quantity into the aquatic ecosystem is an important factor determining the distribution and abundance of macroalgae. Ultraviolet radiation which is one of the most debated factors that can affect these responses can cause significant cellular damage through photooxidation and oxidative stress, resulting in several vital metabolic changes such as DNA replication, transcription and translation, growth rate and development, photosynthesis and respiration, and promotion of apoptosis. Based on the aforementioned information, the present study aimed to contribute to the knowledge of the effect of UV radiation on macroalgae by using *Sargassum* spp. as biological model by integrating diverse physiological, cellular defenses, biological activities, and proteomic approaches for understanding the impact and sensitivity of this stressor under laboratory conditions. The different responses of the seaweed were evaluated under PAR, PAR+UVA and PAR+UVB treatments. Physiological parameters showed little variation between the treatments suggesting that moderate UV radiation doses could regulate resistance responses through the activation of antioxidant defense system by production of UV-absorbing compounds with photoprotective function, such as phlorotannins, flavonoids, and carotenoids that could provide adaptive advantages for organisms exposed to UV radiation. Moreover, extracts from the treated algal material presented high antiviral potential, which may be related to the presence of phenolic compounds and sulfated polysaccharides in the tested extracts. Then, the species can be considered as a potential biotechnology source of natural bioactive compounds. In relation to the proteomic profile of *S. filipendula*, were identified 40 proteins differentially abundant with respect to the UV treatments, which were mainly related to photosynthesis (32%), energy metabolism (12%), carbohydrate metabolism (7%), ROS scavenging defense and stress related metabolism (7%). Proteomic results showed target proteins that could improve the ability of the species to adapt to UV exposure, contribuiting significantly in our understanding of the molecular mechanisms underlying stress tolerance. Additionally, composition and abundance of fatty acids, chlorophylls, and carotenoids of *S. vulgare* after exposure to different light qualities: SOX (low pressure sodium lamps as control), SOX+Blue, SOX+Green, SOX+Red, and SOX+UV, showed that SOX supplemented with UV radiation provoked the decrease of certain carotenoids. On the other hand, the content of certain fatty acids under these SOX treatments showed slighty variation under the different light qualities, presenting a high percentage of PUFAs; however, there is need to perform future researches that allow the establishment of light condition for the stimulation of these compounds from *S. vulgare*.

## RESUMO GERAL

A incidência de luz em termos de qualidade e quantidade no ecossistema aquático é um fator importante que determina a distribuição e a abundância de macroalgas. A radiação ultravioleta é um fator que pode afetar essas respostas, causando danos celulares significativos por fotooxidação e estresse oxidativo, resultando em alterações metabólicas vitais. Com base nestas informações, o presente estudo teve como objetivo contribuir para o conhecimento do efeito da radiação UV em macroalgas, usando *Sargassum* spp. como modelo biológico, integrando abordagens de defesas fisiológicas, celulares, atividades biológicas e proteômica para entender o impacto desse estressor em condições de laboratório. Diferentes respostas das algas foram avaliadas nos tratamentos PAR, PAR+UVA e PAR+UVB. Os parâmetros fisiológicos mostraram pouca variação entre os tratamentos, sugerindo que doses moderadas de radiação UV poderiam regular as respostas de resistência mediante a ativação do sistema de defesa antioxidante, produzindo compostos que absorvem radiação UV com função fotoprotetora, como florotaninos, flavonoides e carotenoides, que poderiam fornecer vantagens adaptativas para os organismos expostos à radiação UV. Além disso, extratos obtidos do material em tratamento apresentaram altos potenciais antivirais, o que pode estar relacionado à presença de substâncias fenólicas e polissacarídeos sulfatados nos extratos testados. Em relação ao perfil proteômico de *S. filipendula*, identificamos 40 proteínas diferencialmente abundantes em relação aos tratamentos, relacionadas principalmente com fotossíntese (32%), metabolismo energético (12%), metabolismo de carboidratos (7%); defesa de sequestro de ROS e relacionados a estresse (7%). Os resultados mostraram proteínas alvo que poderiam melhorar a capacidade das algas em se adaptar à exposição à radiação UV. Além disso, a composição e abundância de ácidos graxos, clorofilas e carotenoides de *S. vulgare* após exposição a diferentes qualidades de luz: SOX (lâmpadas de sódio de baixa pressão como controle), SOX+Azul, SOX+Verde, SOX+Verde, SOX+Vermelho e SOX+UV, mostraram que a luz SOX suplementado com radiação UV reduziu certos carotenoides. Por outro lado, o conteúdo de certos ácidos graxos sob esses tratamentos SOX mostrou uma leve variação, apresentando uma alta porcentagem de PUFAs; entretanto, é necessário realizar pesquisas futuras que permitam o estabelecimento de condições de luz para a estimulação desses compostos em *S. vulgare*

## LIST OF ABBREVIATION

A: Absorbance

ABTS: 2,2'-azino-bis (3-ethylbenzothiazoline-6-sulphonic acid)

AIDS: Acquired immune deficiency syndrome

AOX: Antioxidant

BCM: Bromochloromethane

BSA: Bovine serum albumin

CAT: Catalase

CDOM: Coloured dissolved organic matter

CFCs: Chlorofluorocarbons

$CH_4$: Methane

$CO_2$: Carbon dioxide

CPDs: Cyclobutane pyrimidine dimers

CTC: Carbon tetrachloride

DOC: Dissolved organic carbon

DPPH: 2,2-diphenyl-1-picrylhydrazyl

DW: Dry weight

EC50: Half maximal effective concentration

F-gases: Fluorinated gases

FRAP: Ferric reducing antioxidant power

FW: Fresh weight

GAE: Gallic acid equivalent

GHGs: Greenhouse gases

GPx: Glutathione peroxidases

GR: Growth rate

GSH: Glutathione

HAT: Hydrogen atom transfer

HBFCs: Hydrobromofluorocarbons

HCFCs: Hydrochlorofluorocarbons

HFCs: Hydrofluorocarbons

HIV: Human immunodeficiency virus

HRP: Horse radish peroxidase

IC50: Half maximal inhibitory concentration

IN: Integrase

ITS-2: Internal transcribed spacer

MB: Methyl bromide

$N_2O$: Nitrous oxide

$O_3$: Ozone

OAPCI: Overall antioxidant potency composite index

ODS: Ozone depleting substances

PAR: Photosynthetically active radiation

PFCs: Perfluorocarbons

POS: Preparation for oxidative stress

ROS/RNS: Reactive oxygen species/reactive nitrogen species

RT: Reverse transcriptase

RT-HIV: Reverse Transcriptase enzyme for human immunodeficiency virus

RubisCO: Ribulose-1,5-bisphosphate carboxylase/oxygenase

$SF_6$: Sulphur hexafluoride

SET: Single electron transfer

SOD: Superoxide dismutase

SPs: Sulfated polysaccharides

TCA: Trichloroacetic acid

TPC: Total phenolic compounds

UNEP: United Nations Environment Program

UV: Ultraviolet

## LIST OF FIGURES

## LIST OF TABLES

## CONTENTS

# General introduction

## 1. ULTRAVIOLET RADIATION (UV) AND OZONE ($O_3$)

Solar radiation is essential to life on Earth, but its UV component may also damage both living organisms and non-living matter. UV radiation is a band of the electromagnetic spectrum, which is subdivided into three specific spectral regions: (a) UVA radiation (400-315 nm) that passes through the atmosphere with little attenuation by the $O_3$ layer, being the largest component of ground-level solar UV radiation; (b) UVB radiation (315-280 nm), absorbed efficiently but not completely by $O_3$; and (c) UVC radiation (280-100 nm), which is potentially the most harmful UV radiation, but absorbed completely by $O_3$ and does not reach the surface of the Earth (Madronich et al. 1998) (Fig. 1).

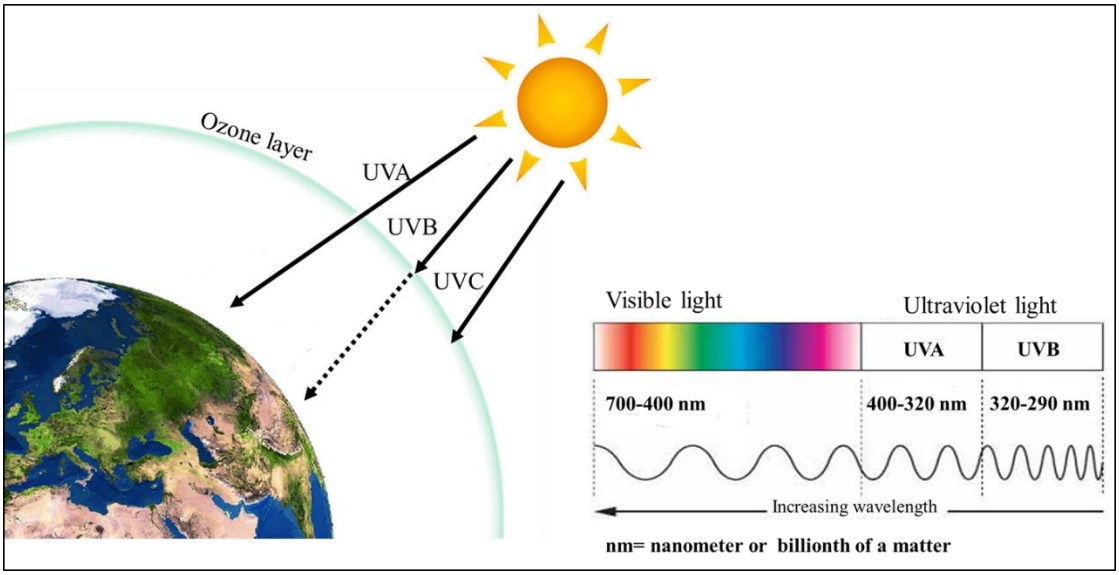


**Figure 1.** Schematic representation of incidence of UV radiation on Earth's surface and gradual spread until pass through the ozone layer. Visible (700-400 nm) and UV (400-200 nm) spectra.

Ozone makes up the atmosphere in minimal quantities (a molecule of $O_3$ to 2.5 million molecules present in the atmosphere), concentrating mainly on the stratosphere, 15 to 25 km above the Earth's surface. This region is known as ozonosphere, being responsible for the absorption of part of the incident solar UV radiation. Ozone is constantly formed in the stratosphere and corresponds to the chemical bonding of a molecular oxygen with an

atomic oxygen, the latter coming from the photodissociation of $O_2$ by a photon of UV radiation with wavelengths less than 242 nm (Okuno et al. 1996)

Eventhough natural phenomena are responsible of causing temporary $O_3$ loss; depletion has been linked to various anthropogenic factors. Human-made chlorofluorocarbons (CFCs) were consider the principal compounds to cause this depletion since they tend to react with the $O_3$ molecules, decomposing it, resulting in a diminution that cause an increase in UV radiation that reach the Earth's surface. These compounds are stable and have atmospheric long life enough to be carried by the wind into the stratosphere. When these $O_3$-depleting substances (ODS) are broken into the atmosphere, they release chlorine or bromine, which attack $O_3$. Each chlorine or bromine atom reacts with $O_3$ repeatedly combining with it and breaking down about 100,000 $O_3$ molecules during its stratospheric life (EPA 2010) (Fig. 2).

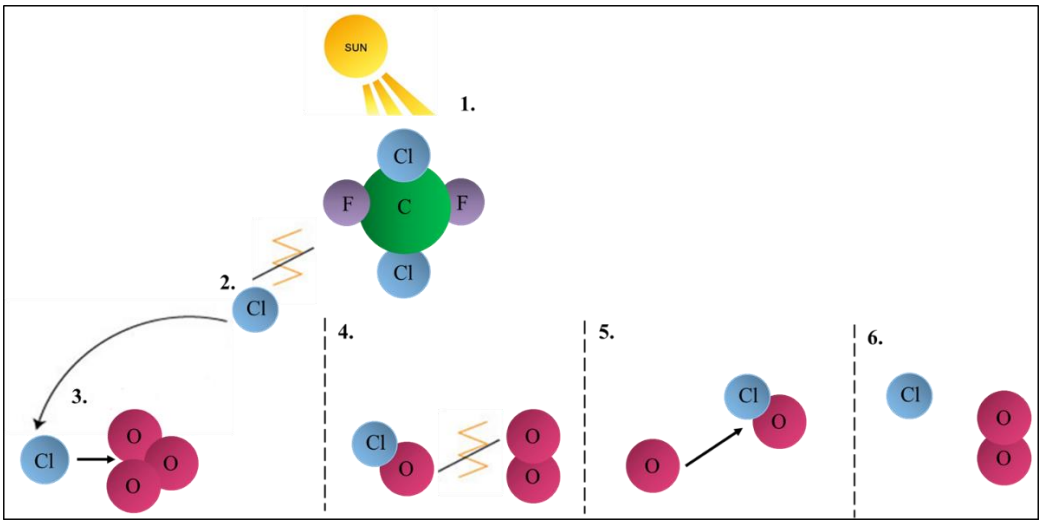


**Figure 2.** Ozone depletion process. 1) UV radiation heats a chlorofluorocarbon (CFC) molecule; 2) Chlorine atom (Cl) breaks away; 3) Chlorine atom hits $O_3$ molecule; 4) Chlorine atom takes one oxygen atom to create monoxide, leaving one molecule of oxygen; 5) Oxygen atom heats chlorine monoxide molecule; 6) Two oxygen atoms form an oxygen molecule; chlorine atom is free and repeats the $O_3$ depletion process. Based on Sivasakthivel and Kumar (2011).

However, CFCs and other compounds as halons, carbon tetrachloride (CTC), 1,1,1-trichloroethane (TCA), hydrochlorofluorocarbons (HCFCs), hydrobromofluorocarbons (HBFCs), bromochloromethane (BCM), and methyl bromide (MB), are now referred as controlled substances due to the success of the Montreal Protocol and subsequent

amendments (Europea Enviromet Agency 2018). Other ODS including nitrous oxide ($N_2O$), methane ($CH_4$), and carbon dioxide ($CO_2$) receive less attention in part because their effects over short time periods (*e.g.* decades) are relatively small, but have gained focus in relation to the long-term recovery of the $O_3$ layer (Portmann et al. 2012).

However, the introduction of other gases has led to new indirect problems. As substitutes for ODS, fluorinated gases (F-gases) have been introduced in sectors such as refrigeration and air conditioning applications. These gases include hydrofluorocarbons (HFCs), perfluorocarbons (PFCs), and sulphur hexafluoride ($SF_6$), and do not deplete the $O_3$ layer, but they are greenhouse gases, contributing to climate change. Additionally, F-gases often have a far larger impact on the climate than 'traditional' greenhouse gases such as carbon dioxide ($CO_2$), since some of them have a greenhouse effect up to 23,000 times more powerful than the same amount of $CO_2$ (European Environment Agency 2018).

Although $O_3$ depletion in low and medium latitudes practically does not occur, there is naturally more solar radiation available at the surface close to the Equator, where the solar angle is most directly overhead. Ozone also is naturally thinner in the tropics compared to the mid- and high-latitudes, so there is less $O_3$ to absorb the UV radiation as it passes through the atmosphere in tropical and subtropical regions (Correa 2015).

Since the creation of the Montreal Protocol, ODS like CFCs, methyl bromide, carbon tetrachloride, among others, have been controlled. Conversely, climate-related changes in the incidence of UV radiation at Earth's surface may result from variations in cloud, snow, ice cover, land-use, and atmospheric and oceanic circulation, varying depending on the region (Williamson et al. 2014). In addition, strong interactions exist between stratospheric $O_3$ depletion and climate-induced changes that are caused by an increase of greenhouse gases (GHGs), alterations that likely decrease total stratospheric $O_3$ in the tropics and increase total $O_3$ at mid and high latitudes (Bais et al. 2015). Also circulation patterns, such as the North Atlantic Oscillation that account for a high proportion of the variability in the total $O_3$ column, are predicted to alter by the accumulation of GHGs, bringing with it changes in UVB radiation levels at Earth's surface (Ossó et al. 2011). Moreover, fluctuation in the stratospheric $O_3$ due to global warming may occur by the increase of atmospheric water content and its rate of transport through the cold tropopause (the troposphere–stratosphere boundary). Water vapor is involved in $O_3$ destruction by accelerating the gas-phase hydrogen oxides (HOx) catalytic cycle and by increasing the surface area of stratospheric aerosol particles on which $O_3$-depleting halogen molecules

can be activated (Anderson et al. 2012). Therefore, global warming clearly may have significant impacts on the future of stratospheric $O_3$ depletion, independently of the concentration of ODS in the atmosphere (Williamson et al. 2014).

## 2. EFFECTS OF SOLAR UV RADIATION ON AQUATIC ECOSYSTEMS

More than 60% of the biomass produced on the planet comes from aquatic ecosystems, making them a key component of the Earth's biosphere with an incorporation of atmospheric carbon dioxide very similar to the amount from the terrestrial ecosystems (Zepp et al. 2011). Additionally, aquatic ecosystems are a major source for human food supply and drinking water, and are economically important for pharmaceutical and chemical industries (Häder et al. 2007).

Abiotic environmental factors such as solar UV radiation strongly affect organisms living in aquatic ecosystems, a situation that has been widely discussed as part of global climate change scenarios (Hoepffner 2008). Nowadays, it is known that climate change has important effects on the underwater UV radiation, including changes in UV transparency and depth mixing of the surface waters. These shifts in UV exposure have important implications for processes such as UV inactivation of water-borne human pathogens to carbon cycling (Häder et al. 2011).

UV radiation levels in which aquatic organisms are exposed depend on different drivers such as the solar irradiance reaching the Earth's surface, incidence of wavelength, type and concentration of atmospheric gases (*i.e.* mainly $O_3$), altitude and particulate, and dissolved material in the water column (Blumthaler and Webb 2003). In the case of open ocean waters, transparency is higher than coastal areas and shallow continental shelf waters, since runoff of silt and dissolved organic carbon (DOC) from shores do not reach in a significant way these kind of waters. Thus, the optical properties of open oceans are largely determined by plankton occurrence and their degradation products, with zooplankton being an additional source of DOC (Piazena et al. 2002; Kramer and Herndl 2004). One of the major factors controlling the optical characteristic of freshwater and coastal habitats is the coloured dissolved organic matter (CDOM), which helps reducing UV exposure of organisms in the water (Fig. 3).

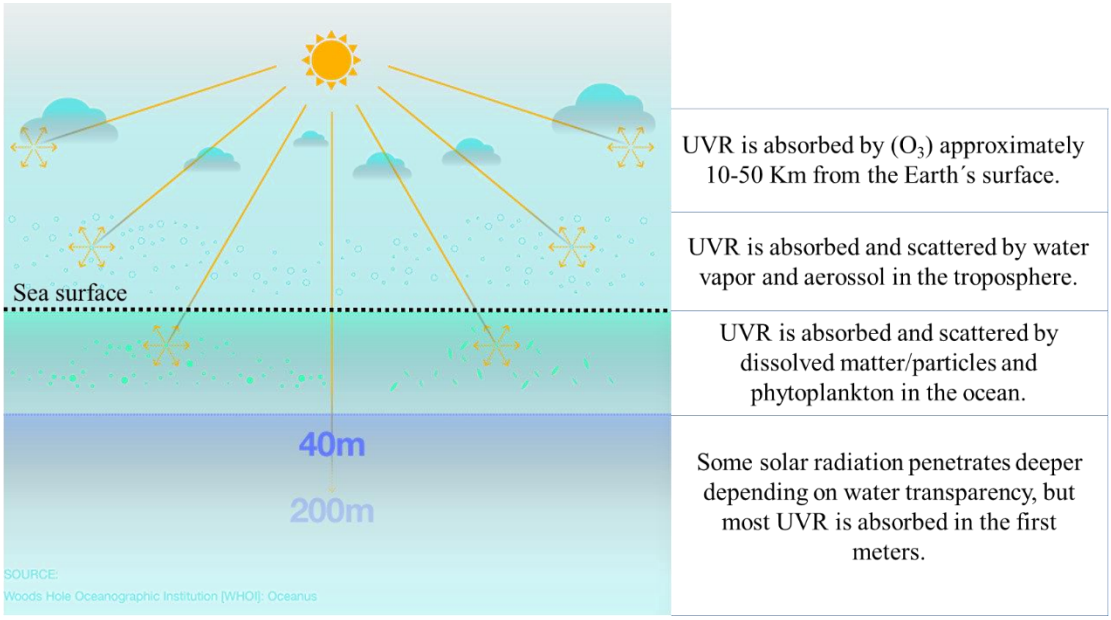


**Figure 3.** Interaction between UV radiation (UVR) from the incidence on the Earth's surface and the ocean (Source: Woods Hole Oceanographic Institution, WHOI).

Generation of CDOM is done by microbial degradation of organic material from macroalgae and plankton as well as land plants (Hudson et al. 2007; Thomas et al. 2009). Thus, its quality and quantity vary seasonally due to variations in these aquatic processes and rainfall events (Hayakawa and Sugiyama 2008). Hyper-oligotrophic water systems are characterized by its high transparency due the extremely low CDOM concentrations, and in some cases diffuse attenuation coefficients indicate that 1% of incident surface UV radiation (at 325 nm) can reaches as deep as 84 m (Raimbault et al. 2007).

When UV radiation levels increase, the ecosystem becomes susceptible to negative alterations that may reduce the photosynthetic uptake of atmospheric carbon dioxide, also affecting species diversity, ecosystem stability, trophic interactions, and global biogeochemical cycles (Häder et al. 2011). Solar UV radiation causes photodegradation of CDOM, which increases its transmission in the water column, potentially enhancing deleterious effects on aquatic organisms (Zhang et al. 2009). Biological and physiological performance processes as growth, photosynthesis, and reproduction can lead to mortality of individuals (Lao and Glazer 1996). Highly energetic photons of the UV radiation has indirect consequences as they can be absorbed by nucleic acids, lipids, amino acids, chlorophylls, and carotenoids (Diffey 1991), causing substantial cellular damage through photooxidation and oxidative stress in several organisms. Changes in these cell

components would result in many vital metabolic alterations such as replication, transcription, and translation.

## 3. THE GENUS *Sargassum*

Within the macroalgae, *Sargassum* is one of the most worldwide distributed genera (Phillips, 1995; Guiry and Guiry, 2014), and is of great importance as a component of the marine flora in tropical and subtropical regions of both hemispheres (Paula 1988). It is one of the most representative genera among the 41 genera of the Order Fucales (Phaeophyceae, Ochrophyta), with an estimated of 358 species, currently flagged as taxonomically accepted, showing the following synopsis (AlgaeBase 2019).

**Kingdom** Chromista

**Phylum** Ochrophyta

**Class** Phaeophyceae

**Order** Fucales

**Family** Sargassaceae

**Genus** *Sargassum*

*Sargassum* is mainly formed by a holdfast, which is disciform and constituted by filaments that are compactly superimposed and interlaced. Thallus with main axes from whose apex arise numerous, long, primary lateral branches that support lateral laminar structures and resemble the leaves of the angiosperms, called phylloids. A representative specimen of *Sargassum filipendula* C. Agardh is shown in Figure 4. From the axil of the phylloids, floating vesicles (air bladders or aerocysts) or receptacles are differentiated. The receptacles consist of a system of branched cylindrical branches containing the reproduction elements situated in conceptacles. Other structures of great importance in the genus are the cryptostomes that are cavities immersed in the phylloids with a communication pore to the external environment (Paula 1988). The thallus could be monoecious or dioecious with unisexual and bisexual receptacles, with scattered conceptacles that could be unisexual or bisexual (AlgaeBase 2019).


**Figure 4.** General habit of a specimen of *Sargassum filipendula* collected in Cigarras Beach, São Sebastião, São Paulo. Photo: Fungyi Chow.

Species of the genus have dominance in the coverage of coastal consolidate substrate areas, both in tropical and subtropical regions, often forming the so-called *Sargassum* beds (Széchy et al. 2001). Studies in the Brazilian coast underline *Sargassum* species as the most abundant in the lower intertidal and upper sublittoral zones of the coastal ecosystems (Paula and Eston 1987; de Eston and Bussab 1990; Széchy and Paula 2000; Ghilardi 2007). The genus stands out for its sensitivity to variations in salinity, temperature, and different pollutants (Paula and Eston 1987; Gorostiaga and Díez 1996; Amado Filho et al. 1999). In addition, the position they occupy on the coast, implies that they are subjected to higher levels of UV radiation with possible consequences on its general biological performance, which may cause shifts within the whole ecosystem due to the role as structural habitat as ecosystem engineering and as an energy source (Häder et al. 2007).

It is important to emphasize that these algae play an important ecological role as shelter, protective, and food resource for several marine species (Széchy et al. 2001), and are considered hosts since its occurrence provides microhabitats for several other algae and marine fauna (hydrozoans, amphipods, copepods, among others). Another aspect of

great relevance referred to chemical ecology is the profile of secondary metabolites produced as defense mechanism that contribute with reducing algal palatability from herbivores and providing protection to other palatable species; thus, the ecological alteration of *Sargassum* from its natural environment may lead to the local extinction of these species (Pereira 2002).

The economic potential of the genus is due to its use as source of alginate, a phycocolloid found in the cell wall of many brown algae. This phycocolloid presents a wide commercial application, being used in food, textile, and pharmaceutical industries (Lee and Mooney 2012). Close to 50% of the produced alginate is destined to the textile industry, serving as an emulsifying agent for inks employed as fabric dye. In the food industry, a diversity of products uses this phycocolloid to increase the commercial value (Széchy and Paula 2000), and species like *S. myriocystum* Grunow, *S. plagiophyllum* C. Agardh, and *S. ilicifolium* (Turner) C. Agardh, are highly suitable for industrial exploitation in India, as a source of alginates and other secondary metabolites (Ganapathi et al. 2013). In addition, *S. fusiforme* (Harvey) Setchell, which is an edible seaweed, presents a great economic importance in countries like China, Korea and Japan, due to its widely use as food source, having a high nutritional value rich in minerals, vitamins, and non-caloric dietary fibers (Arasaki and Arasaki 1981).

*Sargassum* species such as *S. thunbergii* (Mertens ex Roth) Kuntze, *S. siliquosum* J. Agardh, *S. paniculatum* J. Agardh and other unidentified species have been tested experimentally as food supplement in domestic animal feeds (Ang Junior 1985; Trono and Lluisma 1990; Thomas and Subbaramaiah 1991; Széchy and Paula 2000), as well as food additive to fish diet in coastal regions (Ohno et al. 1990) and goat herd (Marín et al. 2009). In addition, it is possible to highlight the use of species like *S. wightii* Greville ex J. Agardh in the production of fertilizers (Williams and Feagin 2010; Thambiraj et al. 2012; Ganapathi et al. 2013).

On the other hand, a large number of studies report that species of this genus including *S. fulvellum* (Turner) C. Agardh, *S. hemiphyllum* (Turner) C. Agardh, *S. thunbergii*, *S. siliquastrum* (Mertens ex Turner) C. Agardh, *S. micracanthum* (Kützing) Endlicher, *S. macrocarpum* C. Agardh, *S. oligocystum* Montagne, *S. fusiforme*, *S. pallidum* (Turner) C. Agardh, *S. swartzii* C. Agardh, *S. polycystum* C. Agardh, and *S. ilicifolium* (Turner) C. Agardh have bioactive compounds such as sulfated polysaccharides, plastoquinones, phlorotannins, fucoidan, sargaquinoic acid, sargachromenol (nerve growth factor),

steroids, terpenoids, and flavonoids (Iwashima et al. 2005; Zhu et al. 2006). These compounds present significant therapeutic prospection (Yende et al. 2014) with hepatoprotective properties (Wong et al. 2000), dietary antioxidants (Kim et al. 2007; Zubia et al. 2007; Hwang et al. 2010), antitumoral potential (Taskin et al. 2010; Zandi et al. 2010; Manojkumar 2013), antiviral action (Iwashima et al. 2005; Sinha et al. 2010), neuroprotective activity (Tsang and Kamei 2004; Ina et al. 2007), and immunomodulatory agents (Chandraraj et al. 2010).

Nowadays is recognized the importance of UV radiation effects on aquatic ecosystem being an important factor in determining community structure in aquatic systems. However, ecosystem response to climate variability involves both synergistic and antagonistic influences with respect to UV radiation-related effects on these ecosystems, which significantly complicates the comprehension and prediction of its consequences at the ecosystem level. Then, under the perspectives of ecological importance, economical exploitation, and prospecting potential, laboratorial researches involving species of *Sargassum* are of great relevance since they give insights of how ecosystems could respond to the changes in atmospheric or aquatic conditions that alter the UV radiation-depending processes.

## 4. JUSTIFICATION

Since the publication of the United Nations Environment Program (UNEP) in 1998, studies with UV radiation have been rapidly expanding and many of them have shown the inverse relationship between the amount of $O_3$ and the incidence of UV radiation on the surface of the Earth.

Nowadays, there are evidences that the main cause of $O_3$ depletion is the anthropogenic pollution of the atmosphere due to rapid industrialization in recent decades, leading to the increase of polluting gases and volatile organic compounds that are responsible for the destruction of the $O_3$ layer, which acts as a natural UV filter in the stratosphere (McKenzie et al. 2003). These abrupt changes in the levels of UV radiation incidence can compromise the survival of marine organisms, as they experience substantially higher levels of UV radiation in the environment where they occur, especially benthic algae, which are attached to the substrate and often exposed to the atmosphere during the tidal fluctuation. Thus, its effects on these organisms has become an important issue to be investigated, as its long-term consequences on the balance of ecosystems are still uncertain.

Laboratory studies of physiological and metabolic UV radiation-triggered responses from an integrated perspective, including physiological performance, antioxidant defenses, cellular and DNA damage, and proteomic profile are important assessments for better understanding the potential biological implications of the increasing environmental UV radiation on *Sargassum* spp. sensitivity, a valuable species as community structuring in tropical and subtropical marine habitats. Furthermore, the high sensitivity of *Sargassum* to changes of abiotic factors can be an important feature that allows its use for environmental monitoring, which could subsidize decision-making of monitoring and mitigation programs. On the other hand, studies on antioxidant potential as well as bioactivity of *Sargassum* will be useful initial profiles to design further possibilities for prospecting the species.

Additionally, proteomic studies have become a helpful complementary tool to understand how organisms changes the protein regulation under abiotic and biotic stresses. In Brazil, this kind of research is unique and innovative for macroalgae, and only few studies have been performed in Brazil for microalgae. Thus, the initial proteomic studies addressed in this research could provide a useful platform for future researches on biochemical and molecular regulations associated with abiotic stressor in brown macroalgae and other aquatic biological models.

Therefore, this study intends to contribute to the knowledge of the effect of UV radiation on macroalgae by using the brown seaweed *Sargassum* spp. as biological model, an ecological important species with biotechnological potential, and by integrating diverse physiological, cellular defenses, biological activities and proteomic approaches for understanding the impact and sensitivity of this stressor under laboratory conditions.

## 5. GENERAL OBJECTIVES

- Extend the existing knowledge of the effect of UV radiation on macroalgae and provide support for a better understanding of the impact and sensitivity of the stressor in laboratory conditions by using *Sargassum* spp. as biological model.
- Verify the existence of variation in *Sargassum* spp. responses under UV radiation exposure by integrating physiological, cellular defenses, biological activities and proteomic approaches.

- Establish and provide a working platform for proteome studies in marine macroalgae that may be useful in approaches of biochemical and molecular regulation associated with stress conditions.

# General material and methods

## 1. COLLECTION SITE AND ALGAL MATERIAL

Specimens of *Sargassum* spp. were collected at Cigarras Beach (24°43'55.74"S and 45°23'54.48"W), São Sebastião District (Fig. M1 A-B), during the summer season (February-March 2016), a local having a great abundance of *Sargassum* beds. São Sebastião is located on the North coast of the São Paulo State, Brazil (Fig. 5), in the region of Atlantic Forest with 72.24% of its area covered by natural vegetation. It has around 100 km of coastline and 34 beaches. The municipality has a rugged development, with a very narrow and steep coastline, characterized by bays and coves. It has a territorial strip limited on one side by the foothills of the Atlantic mountain chain Serra do Mar and on the other by the Atlantic Ocean (Gouveia 2012). A tropical humid climate prevails without a dry season. The average temperature of the hottest month is between 24 and 25 °C, with the hottest trimester corresponding to the months of January to March, which also are the ones with highest precipitation (Gouveia 2012). The coldest trimester corresponds to the period from June to August.

For this study, two collections were carried out and all collected material was used to evaluate different aspects of *Sargassum* after UV exposure. Material from the first collection (February 2016) was used to perform the experiments of Chapter I (growth rate, total soluble proteins, and photosynthetic pigments) and Chapter II (DNA damage, antioxidant activity, the bioactive potential. In the second collection (October 2016), the obtained material was used for performing the experiments of Chapter III (differential abundance of proteins. Description of Material and Method of Chapter IV will be in the respective chapter as it correspond to a specific study during the research internships abroad.

The algae were collected from the lower intertidal zone of the rocky shore (Fig. 5) and wet transported in net bags into cooler boxes to the Laboratory of Marine Algae "Édison José de Paula" (LAM) of the Institute of Biosciences at the University of São Paulo, localized at approximately 5 h distance. In the laboratory, algae with similar morphology were selected, cleaned of macroepiphytes and washed with abundant filtered seawater. Portions of five individuals (phylloids) from each collection were silica gel-dried for further taxonomic-molecular analysis and the remained fixed in formaldehyde 4% (v/v, diluted in seawater) for taxonomic identification by morphological characters and

subsequent herborization process. The remaining clean collected biomass was used for UV experiments.

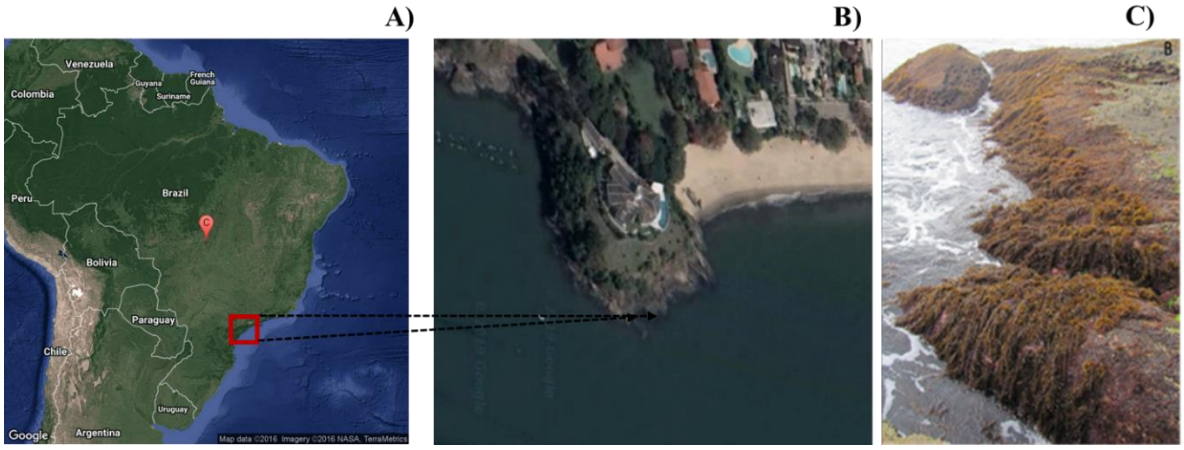


**Figure 5.** A) Brazil's map with the localization of São Sebastião, in the North coast of São Paulo State; B) Cigarras Beach (24°76'1"S and 45°41'7"W) and the localization of the right rocky shore coast which correspond to the collection site; C) Distribution of *Sargassum* bed along the lower intertidal and upper infralittoral zones of the littoral.

## 2. TAXONOMIC AND MOLECULAR IDENTIFICATION

### 2.1. Taxonomic identification

The taxonomic identification by morphological characters was carried out using the work by Paula (1988), Camacho et al. (2015), and Algaebase (http://www.algaebase.org/). The morphological characteristics considered for identifying purposes from the collected specimens are summarized in Table S1 (supplement material), including shape, size, and characteristics of the holdfast, main axis, branches, phylloids, cryptostomata, vesicles, and receptacles. To analyze the shape and size of the cryptostomata, specimens were observed under a stereomicroscope. Morphological measurements included length and width of phylloids and receptacles performed under a stereomicroscope. Additionally, results from the morphological features of the samples were discussed with the expert taxonomists Dra. Maria Tereza Széchy, Dra. Valéria Cassano, and Dra. Mariana Cabral de Oliveira. The herborized material was deposited in the SPF Herbarium of the University of São Paulo (voucher SPF 58087 for collection 1; and SPF 58086 for collection 2).

## 2.2 Molecular identification

The identification of the species by morphological characters was validated by molecular biology techniques, using DNA barcode markers. For DNA extraction, approximately 20 mg dry weight (DW) of silica gel-dried material (five different individuals) were grinded in liquid nitrogen until a fine powder was obtained and DNA extraction was done using the NucleoSpin Plant II kit (Macherey-Nagel, Düren, Germany), following the manufacturer's instructions. The total DNA extracted was analyzed in 0.7% agarose gel electrophoresis and then submitted to a polymerase chain reaction (PCR) using primers to amplify the rDNA second internal transcribed spacer (ITS-2), a nuclear marker. The reaction profile included: a) an initial 1 min long step of denaturation at 94 °C, b) 40 cycles of denaturation at 94 °C for 40 s, c) primer annealing at 55 °C for 30 s, d) extension at 72 °C for 45 s, and e) a final extension step at 72 °C for 7 min. Primers used were following (Yoshida et al. 2000):

**SARG-ITS2F (5'-CGATGAAGAACGCAGCGAAATGCGAT-3'**

**SARG-ITS2R (5'-TCCTCCGCTTAGTATATGCTTAA-3')**

The PCR product was analyzed by 0.7% agarose gel electrophoresis, with a 1 Kb DNA Ladder marker (Invitrogen, USA) to verify the success of the reaction and the sizes of the amplified fragments. PCR products were purified using the GTX™ PCR DNA and Gel Band Purification kit (GE Healthcare, Buckinghamshire, UK), according the manufacturer's instructions.

The purified amplified DNA was quantified in NanoDrop 2000-Spectrophotometer (Thermo Scientific, USA) for subsequent sequencing reaction by using the BigDye Terminator Cycle Sequencing Ready Reaction kit (Applied Biosystems, USA).

After the sequencing, forward and reverse sequences were obtained and manually aligned using the BioEdit 7.0.4.1 software and the divergent nucleotides occurring at the same position were verified with the electropherograms of the sequences. Each sequence obtained from each sample was compared to the sequences available from GenBank (http://www.ncbi.nlm.nih.gov), using the BLASTn software (Altschul et al. 1990). The DNA barcode consensus sequences of all samples were aligned in a matrix in the MEGA 7 software (Tamura et al. 2011) and, finally, a maximal neighbor-join (NJ) tree with 2000 replicates of Bootstrap was done for the marker, in the same program.

Results obtained for the morphological and molecular identification are presents in Supplement 1. After evaluating the results, combining morphological and molecular data set, the identity of *Sargassum* was concluded as *S. filipendula*.

## 3. LABORATORY CONDITIONS AND EXPERIMENTAL SETUP

Cleaned apical portions of *S. filipendula* (± 8 cm) were acclimated for one week under laboratory conditions, in a ratio of 3 g of alga per 1 L of culture medium, consisting in sterilized seawater 32 psu enriched with von Stosch solution diluted at 50% (Ursi and Plastino (2001), based on Edwards (1970)), photosynthetically active radiation (PAR) of 60 ± 5 μmol photons.$m^{-2}$.$s^{-1}$, 25 ± 1 °C, photoperiod of 14 h and intermittent aeration every 30 min.

Seawater used in the culture was collected in front of the Center of Marine Biology of University of São Paulo (CEBIMar/USP) with an average salinity of 32 psu. Sterilization was done by double filtration (5 μm and 1 μm) in a pressure filter (Cuno-AP230) and further radiation with UVC ionizing radiation (UVC lamp, QUIMIS Q884-21 - 3.8 L/min system).

The irradiance was provided by fluorescent lamps (Philips, daylight model, 5200K/40 W), measured with a quanta meter Li-Cor Biosciences Model Li-250A, connected to the US-SQS/LS/N model sensor SQSA0235 (Heinz Walz GbmH, 91090, Effeltrich, Germany). Aeration was provided in alternating periods of 30 min (on/off) by IBRAM CR03 radial compressor, oil free, initially bubbled into a vial containing distilled water that serves as a filter and humidifier.

After the acclimation period, the material was exposed for 10 days to three different radiation treatments: a) PAR (control treatment), b) PAR+UVB, and c) PAR+UVA under the same laboratory culture conditions described above. UVB (312 nm; 1.5 W.$m^{-2}$) and UVA (365 nm; 7 W.$m^{-2}$) radiations were provided by Philips lamps models TL 20W/12 and Actinic BL TL-K 40 W/10-R, respectively.

The PAR irradiance intensity measurements were obtained as in the acclimation condition. The UV radiation intensity was obtained in W.$m^{-2}$ with a MACAM Ultraviolet Radiometer (Scotland), connected to the UVB or UVA specific sensors. The measurements of total radiation spectrum emitted by radiation sources (PAR and UV)

were obtained using the SphereOptics SMS-500 (Spectral Measurements System) spectroradiometer and summarized in Figure 6.

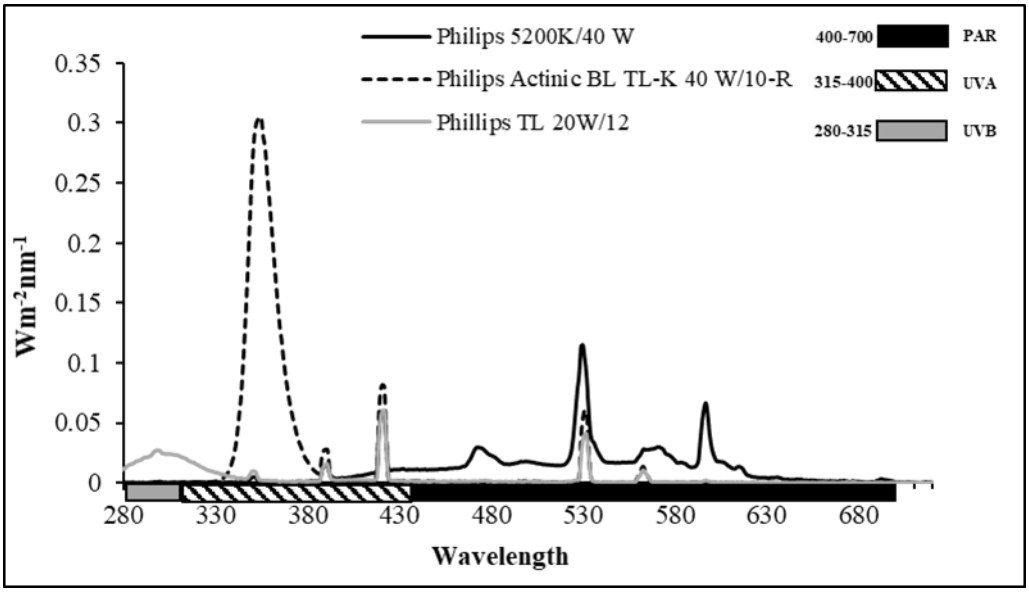


**Figure 6.** Total radiation spectrum emitted by radiation sources: PAR (400-700 nm), UVA (315-400 nm), and UVB (280-315 nm).

The UVA and UVB intensities were chosen after performing a bibliographic review on studies that evaluated the effect of UV radiation on different brown macroalgal species (Table 1). The used intensities are considered as moderate so the evaluation here performed will allowed to give insights on the behavior of different parameters of *S. filipendula* without provoke chronic damage. Table 2 shows the conversion factor for radiation according to McCree (1981).

Total doses of UVB and UVA were 162 $kJ.m^{-2}$ and 756 $kJ.m^{-2}$, respectively. These doses were calculating by using the following formula:

$$UV\ dose\ (kJ.m^{-2}) = UV\ intensity\ (W.m^{-2}) \times Exposure\ time\ (h)$$

The experiments were performed under 3 h exposure to UV radiation per day. During the exposure to UV radiation, aeration was increased in all treatments to encourage greater movement of the algal fragments in order to promote a homogenize exposure for all branches (Polo et al. 2014a, b) For the experiments whose duration was 10 day, culture medium was added at the seventh day of exposure to avoid nutrient limitation.

**Table 1.** Summary of intensities of laboratory UVA and UVB doses ($W.m^{-2}$) used in different studies with brown macroalgal species. This bibliographic review served as parameter for further choice of experimental intensities of this study, considering a moderate level intensity.

| Species | UVA ($W.m^{-2}$) | UVB ($W.m^{-2}$) | Reference |
|---|---|---|---|
| *Laminaria digitata; Laminaria hyperborea; Laminaria saccharina* | 11-15 | 0.8-1.4 | (Dring 1986) |
| *L. saccharina; Fucus distichus; Palmaria palmata* | 9 | 0.06 | (Dieter et al. 1997) |
| *Alaria esculenta; L. saccharina; Saccorhiza dermatodea* | 7 | 0.7 | (Bischof et al. 1998) |
| *L. saccharina; L. digitata; A. esculenta; Chordaria flagelliformis* | 8 | 0.851 | (Wiencke et al. 2000) |
| *Fucus serratus* | 17 | 0.8 | (Altamirano et al. 2003) |
| *F. serratus; Fucus spiralis* | 8 | 1.2 | (Schoenwaelder 2003) |
| *Myriogloia chilensis; Desmarestia ligulata; Colpomenia sinuosa; Scytosiphon lomentaria* | 8.6 | 2.4 | Huovinen et al. (2007) |
| *Lessonia nigrescens* | 8.75 | 2.35 | Gomez et al. (2007) |
| *L. nigrescens; Lessonia trabeculata* | 0.38-3.18 | 0.86-6.88 | Tala et al. (2007) |
| *S. dermatodea* | 5.63-7.03 | 0.47--0.58 | (Roleda et al. 2006a) |
| *L. nigrescens* | 2.4 | 8.8 | Gomez and Huovinen (2010) |
| *Macrocystis pyrifera* | 46.9- 47- 67.1 | 1.3- 1.4- 1.9 | (Rothäusler et al. 2011)) |
| *Saccharina latissima* | 4.3 | 0.4 | (Holzinger et al. 2011) |
| *L. nigrescens; Durvillaea antarctica* | 11.1 | 1.9 | (Cruces et al. 2013) |
| *argassum hystrix* | 14.3 | 1.6 | (Harnita et al. 2013) |
| *Sargassum cymosum* | 0.7 | 0.35 | (Polo et al. 2014a, b) |

**Table 2** Conversion factor for radiation (McCree 1981).

| Irradiance | | |
|---|---|---|
| **From** | **To** | **Conversion** |
| µmol photons.$m^{-2}.s^{-1}$ | Watts/$m^2$ | ÷ 4.6 |
| Watts/$m^2$ | µmol photons.$m^{-2}.s^{-1}$ | x 4.6 |

After the UV exposure treatment, the respective evaluation was performed and samples were collected for further analysis. Growth rate, content of pigments, and total soluble proteins were measure before starting the experiment (initial time, T0) and along

10 days of experiment on days 4, 7, and 10 (T4, T7, and T10, respectively), using five independent repeats for each treatment and time. Samples for analyzing antioxidant activity, bioactive potential, and DNA damage were collected at time 0 and time 10, using five independent repeats for each treatment and time. Finally, analysis of differential protein abundance were performed after 24 h and 4 days of experiment using three independent repeats for each treatment.

Collection site, algal material, laboratory conditions, and experimental setup of the current research were the same for chapters I, II, and III. Thus, descriptions about these topics are not addressed in the specific chapter. Specific Material and Methods, as the methodological procedures, are addressed in each chapter. Additionally, chapter IV is composed by results obtained from the internship abroad research BEPE and details about collection site, algal material, laboratory conditions, and experimental setup are addressed in the respective chapter.

A summary of the experimental setup performed at LAM for chapters I, II, and III is shown in Figure 7.

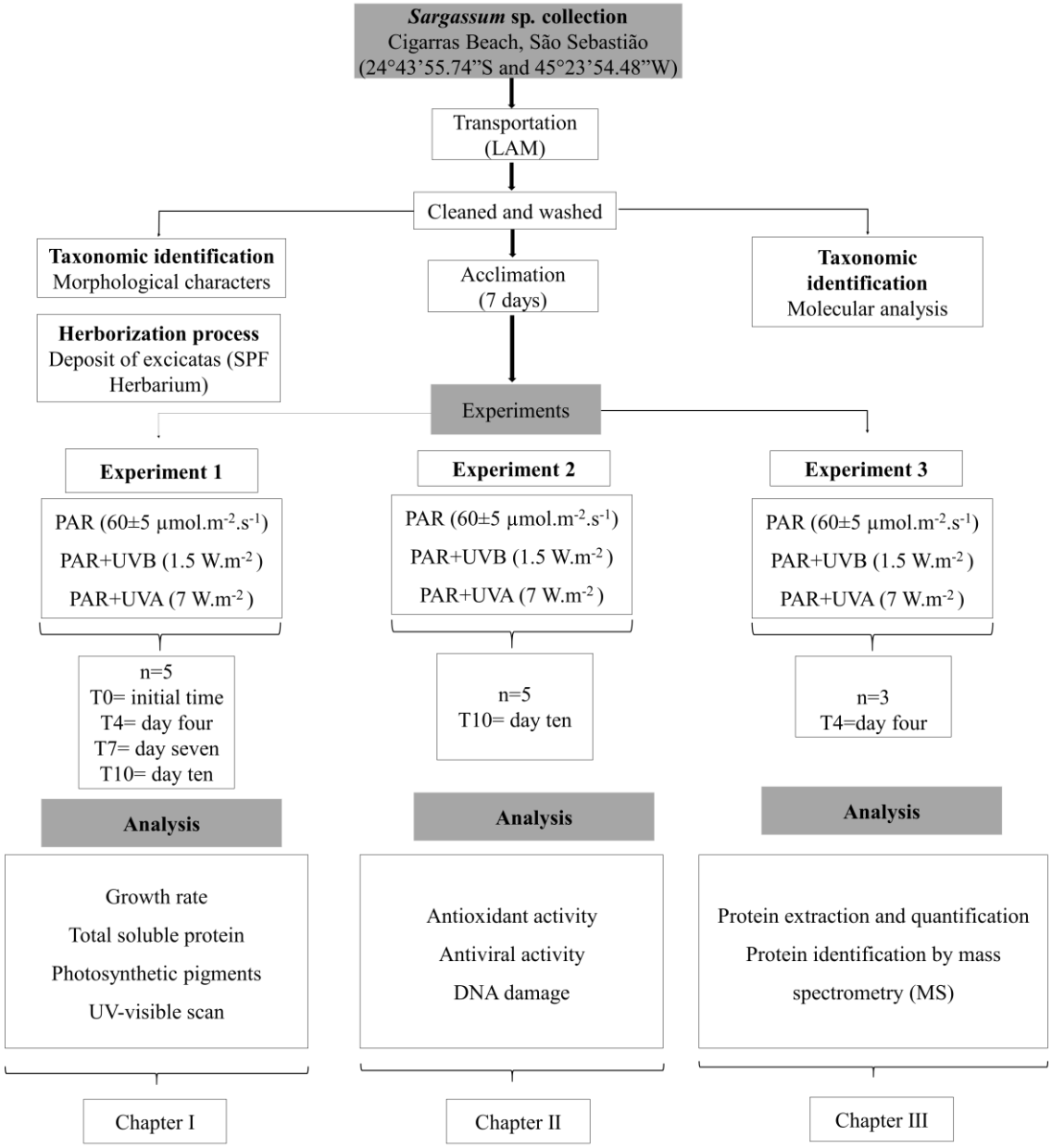


**Figure 7**. General scheme of the experimental design to evaluate the effect of UV radiation on the brown alga *Sargassum filipendula*.

# Chapter I

## Growth, pigments and proteins

## Chapter I

Assessment on physiological performance and sensibility of *Sargassum filipendula* (Fucales, Ochrophyta) induced by moderate UV radiation exposure in laboratory.


## ABSTRACT

The effect of UV radiation is a major factor affecting distribution and physiology of photosynthetic organisms on aquatic ecosystem. Studies with macroalgae indicate diverse biological disturbances in response to UV radiation, including growth rate alterations, photoinhibition of photosynthesis, pigment degradation, protein, and DNA damages, among others. In the present work, sensibility of the brown macroalga *Sargassum filipendula* to UV radiation was studied by analyzing its physiological performance when exposed to three different radiation treatments: PAR (control), PAR+UVB, and PAR+UVA during ten experimental days at moderate doses of UV and 3 h per day. Changes in the physiological parameters growth rate, total soluble proteins, photosynthetic pigments, and the UV-vis absorbing compounds were analyzed after T0, T4, T7, and T10 (days) of UV exposition. Physiological parameters showed little variation between the treatments and over time, suggesting that moderate UV radiation doses as the used in this study could regulate resistance responses to reestablish the cellular homeostasis condition through the activation of antioxidant defense system, as overproduction of phenolic compounds, since phenolic release was verified in the treatments. The responses registered in *S. filipendula* would be related to acclimation mechanisms against acute UV radiation stress, triggering resistance responses to avoid serious damage to the metabolic machinery, activating control systems to maintain the hormesis, and the homeostasis of the deleterious actions of reactive species, similar to the phenomenon coined as preparation for oxidative stress (POS). Finally, the UV-visible absorption spectra showed absorption bands that evidence the presence of mainly UV-absorbing compounds with photoprotective function, such as phlorotannins, flavonoids, and carotenoids that could provide adaptive advantages for organisms exposed to UV radiation.

## INTRODUCTION

Solar radiation is the most important prerequisite for life on Earth, since it provides light, heat, and energy demanded for photosynthesis processes. This radiation mainly consists of UV radiation, visible light (photosynthetically active radiation, PAR), and infrared radiation (IR) (Diffey 2002). The UV radiation corresponds to a small part of the electromagnetic spectrum and is divided into three spectral regions: 1) UVA (400–315 nm) being the closest radiation to the visible spectrum, and it is not absorbed by ozone ($O_3$) layer; 2) UVB (315-280 nm) which is not completely absorbed by $O_3$ and is harmful to living organisms; and 3) UVC (280-100 nm) which is extremely harmful, but is completely absorbed by $O_3$ (Madronich et al. 1998).

Since the reports of man-made changes in the stratospheric $O_3$ layer, the effect of UV radiation on the aquatic ecosystem has become a relevant subject. Interactions between global climate change, $O_3$, and UV radiation are bringing important consequences for UV exposure in that ecosystem (Bais et al. 2015). Although, the attenuation of UV radiation that penetrates to the water column varies according to the location (*e.g.*, oceanic versus coastal environments), latitude, and concentrations of particulate and dissolved matters (Villafañe et al. 2003). UV radiation has been considered as one of the main factors affecting the distribution of photosynthetic organisms in aquatic ecosystem, having diverse biological effects and most of them with unfavorable consequences (Björn 2007).

Macroalgae are major biomass producers on rocky shores and continental shelf, which provide microhabitats for many larval stages of fishes, crustaceans, epibionts and epiphytes, and other marine organisms (Lippert et al. 2001). Due to tidal exposure, intertidal macroalgae are constantly imposed to fluctuating environmental stresses such as high temperature, desiccation, and elevated radiation levels (PAR and UV radiation) (Sampath-Wiley et al. 2008) that could easily lead to the formation and accumulation of free radicals and reactive species, triggering oxidative stress. Photobiological studies in macroalgae indicate diverse physiological disturbances in response to UV radiation, including alterations on growth and development (Altamirano et al. 2003; Gao and Xu 2008; Schmidt et al. 2010c; Navarro et al. 2016), pigment degradation (Heo and Jeon 2009), dynamic or chronic photoinhibition of photosynthesis (Gómez and Figueroa 1998; Lopez et al. 1998; Figueroa and Vinegla 2001; Sampath-Wiley et al. 2008; Barufi et al. 2011; Ayres-Ostrock and Plastino 2014; Figueroa et al. 2014), protein and DNA damage (Buma et al. 2001; Kumar et al. 2004), decrease in lipid/fatty acid contents

(Khotimchenko and Yakovleva 2005; Liang et al. 2006), inhibition of enzyme activity (Lee and Shiu 2009), alterations in polyamines content (Polo et al. 2014a), and modifications in cellular organization and ultrastructure (Poppe et al. 2003; Holzinger and Lütz 2006; Schmidt et al. 2009, 2010a, 2010b, 2012, 2015; Polo et al. 2014b; Álvarez-Gómez et al. 2017; Ouriques et al. 2017). However, UV radiation at low levels have been reported positive influence on some metabolic processes (Table 3).

**Table 3**. Main effects caused by UV radiation on algae (modified from Pessoa (2012)).

| UV radiation (nm) | Negative effects | Positive effects |
|---|---|---|
| UVA (315-400) | Indirect damage to DNA | Stimulation of photosynthesis and growth at low levels |
| UVB (280-315) | Direct damage to DNA<br>Oxidative stress<br>Reduction of growth rate and photosynthetic pigments<br>Apoptosis promotion<br>Mutation | Induction of photorepair signaling process at low-moderate level |
| UVC (200-280) | Degradation of photosynthetic apparatus<br>High oxidative stress<br>Programed cell death | Unknown |

As a photoprotective mechanism against UV radiation , especially UVB, macroalgae can increase the production of UV-absorbing compounds, such as mycosporine-like amino acids, phenolic compounds, and carotenoids, which play protective roles by mitigating the damages caused for the increase of reactive species (Ruhland et al. 2007); therefore, giving advantages that enables macroalgae to survive in the presence of UV radiation.

The genus *Sargassum* C. Agardh has dominance in the coverage of coastal consolidate substrate areas, both in tropical and subtropical regions, often forming the so-called *Sargassum* beds. It plays an important ecological role as shelter, protection, and food resource for several marine species (Széchy et al. 2001) and is considered hosts since its occurrence provides microhabitats for several other algae and marine fauna. The genus stands out for its sensitivity to variations in salinity, temperature, and different pollutants (Paula and Eston 1987; Gorostiaga and Díez 1996; Amado Filho et al. 1999), an

interesting feature requisite of bioindicator species. In addition, the position that *Sargassum* occupy on the littoral zone, between the lower intertidal to infralittoral, implies that they are subjected to higher levels of UV radiation with possible consequences on its general performance, which may cause shifts within the whole ecosystem due to its role as community engineers providing habitat and energy source (Häder et al. 2007).

Given the many changes that UV radiation may have on seaweeds, it is important to study the sensitivity and tolerance of these organisms for understanding the possible biological consequences under an extremely dynamic environment and predicted global climate changes scenarios. Therefore, the aim of this study was to evaluate the biological effect of moderate dose of UV radiation (UVA and UVB) on the physiological performance and sensibility of the brown macroalga *Sargassum filipendula* C. Agardh by analyzing growth rate, photosynthetic pigments (Chl *a*, Chl *c*, and carotenoids), total soluble proteins, and UV-absorbing compounds, under laboratorial conditions.

## MATERIAL AND METHODS

**Collection of algal material and experimental setup**. Specimens of *S. filipendula* were collected at Cigarras Beach (24°43'55.74"S and 45°23'54.48"W), localized in São Sebastião, north coast of São Paulo State, Brazil, during the summer season (February-March 2016). Cleaned apical portions (± 8 cm length) were acclimated for one week under laboratory conditions (details addressed in General material and methods, section 1). After the acclimation period, the material was exposed for 3 h to different radiation treatments: a) PAR (control treatment), b) PAR+UVB (UVB 312 nm; 1.5 $W.m^{-2}$; 16.2 $kJ.m^{-2}$ /day), and c) PAR+UVA (UVA 365 nm; 7 $W.m^{-2}$; 75.6 $kJ.m^{-2}$ /day). Radiations were provided by Philips lamps models TL 20W/12 for UVB and Actinic BL TL-K 40 W/10-R for UVA (details addressed in General material and methods, section 3).

Growth rate, total soluble proteins, photosynthetic pigments, and UV-visible absorbing compounds were evaluated before start the experiment (T0) and after 4, 7, and 10 days (T4, T7 and T10, respectively).

**Growth rate.** Growth rate (GR) was evaluated through measurements of fresh biomass weight over the experimental period, following the formula from Penniman et al. (1986) as following:

$$GR\ [\%.day^{-1}] = [(Wf / Wi)^{1/t} - 1] \times 100$$

where Wi = initial wet mass, Wf = final wet mass, and t = time in days.

**Total soluble proteins, photosynthetic pigments, and UV-visible absorbing spectrum.** The extraction of soluble proteins and photosynthetic pigments was carried out from frozen fresh samples of approximately 70 mg of fresh weight (FW) at T0, T4, T7, and T10. Material was ground in liquid nitrogen until a fine powder was obtained, and extracted in 1 mL of cold sodium phosphate buffer 0.05 mM (pH 5.5), protecting the extract from photo- and thermooxidation, and then centrifuged for 15 min at 4 °C and 12,000 rpm. The obtained supernatant was called buffered extract.

From an aliquot of the buffered extract, the total soluble protein content was analyzed according to the Bradford's spectrophotometric method (Bradford 1976), using the Bio-Rad solution for the protein assay (Bio-Rad, USA), and the absorbance at 595 nm was recorded in a UV-visible 96-wells microplate spectrophotometer. Bovine serum albumin (BSA) was used for the standard curve with concentrations ranging from 2 to 16 $\mu g.mL^{-1}$ ($y = 0.0434x + 0.049$; $R^2 = 0.97$).

From the pelleted material obtained after the extraction of soluble proteins, photosynthetic pigments were analyzed by resuspending the pellet in 1.5 mL of methanol, extracted for 3 h at 4 °C, protecting the extract from photo- and thermooxidation. Subsequently, centrifugation was carried out for 15 min at 12,000 rpm and 4 °C. The obtained supernatant was called methanolic extract. Chlorophylls *a* (Chl *a*) and *c* (Chl *c*) contents were measured from aliquots of 380 µL, read in a UV-visible 96-wells microplate spectrophotometer and then calculated using the absorbance coefficients (Eλ) from Ritchie (2008) for methanol, where $E\lambda_{632} = 16.4351$ and $E\lambda_{665} = 3.2416$ for Chl *a*; and $E\lambda_{632} = 34.2247$ and $E\lambda_{665} = 1.5492$ for Chl *c*; following the formulas:

$$Chl\ a\ (\mu g.g^{-1}) = 16.4351\ A_{665} - 3.2416\ A_{632}$$

$$Chl\ c\ (\mu g.g^{-1}) = 34.2247\ A_{632} - 1.5492\ A_{665}$$

where A = absorbance at the respective wavelength.

From the same methanolic extract (380 µL), the absorbance at 470 nm was used for calculating the total carotenoid concentration using the model proposed by Hartmut and Lichtenthaler (1987), in which absorbance coefficients for Chl *a* ($E\lambda = 1.63$) and Chl *c* ($E\lambda = 119.5$) were based on Lichtenthaler and Buschmann (2001) and Jeffrey (1963), respectively, following the formula modified by Urrea-Victoria and Chow (pers. comm.):

$$Carotenoids\ (\mu g.g^{-1}) = (1000 \times A_{470} - 1.63 \times Chl\ a - 119.5 \times Chl\ c) / 221$$

where A = absorbance at the respective wavelength.

**UV-visible absorption spectra of buffer and methanolic extracts.** From aliquots of 300 µL of the buffered and methanolic extracts UV-absorbing and visible-absorbing compounds were assessed by determining the absorption spectra in a UV-visible microplate spectrophotometer by reading the absorbance in the range of 200 to 750 nm. From the UV- and visible-absorbing spectra of the both extracts, maximal absorption bands were identified and analyzed by calculating the area under the curve (AUC) based on the Riemann sum. Data were standardized by the sample biomass in grams (absorbance/biomass).

**Seawater UV-visible absorption spectrum**. The absorption spectrum (200-750 nm) of the seawater, in which samples were cultivated during the experiment, was also registered by using a 300 µL aliquot of seawater and read it in a UV-visible microplate spectrophotometer. Maximal absorption bands were identified and analyzed by calculating the area under the curve (AUC) of each band based on the Riemann sum.

**Data analysis.** Statistical analysis of data set was performed with the software STATISTICA (version 10.0). Five replicates were used for all studied parameters. Data were checked in their normality (Kolmogorov-Smirnov test) and homoscedasticity (Bartlet's test) and then submitted to one-way, multi-way or repeated measures analysis of variance (ANOVA), followed by the Newman-Keuls *post-hoc* test to verify the significance of the differences ($p < 0.05$).

## RESULTS

**Growth rate.** After 10 days of experiment with different radiation treatments (PAR, PAR+UVA, and PAR+UVB), growth rate of *S. filipendula* analyzed by radiation and time (two-way evaluation) did not show differences within the treatments over time (Fig. 8). Despite these results, it was possible to denote higher growth rate values for PAR treatment over time followed by PAR+UVA and then by PAR+UVB (Fig. 8). Nevertheless, an increase on the growth rate was observed in samples treated with PAR+UVA at the ten day (T10), being closer to the value presented in PAR at the same time. At T10, *S. filipendula* exposed to UVB treatment showed the most negative growth

rate (-1.53 %.day$^{-1}$) when compare to PAR and PAR+UVA (0.68 %.day$^{-1}$ and 0.25 %.day$^{-1}$, respectively) (Fig. 8).

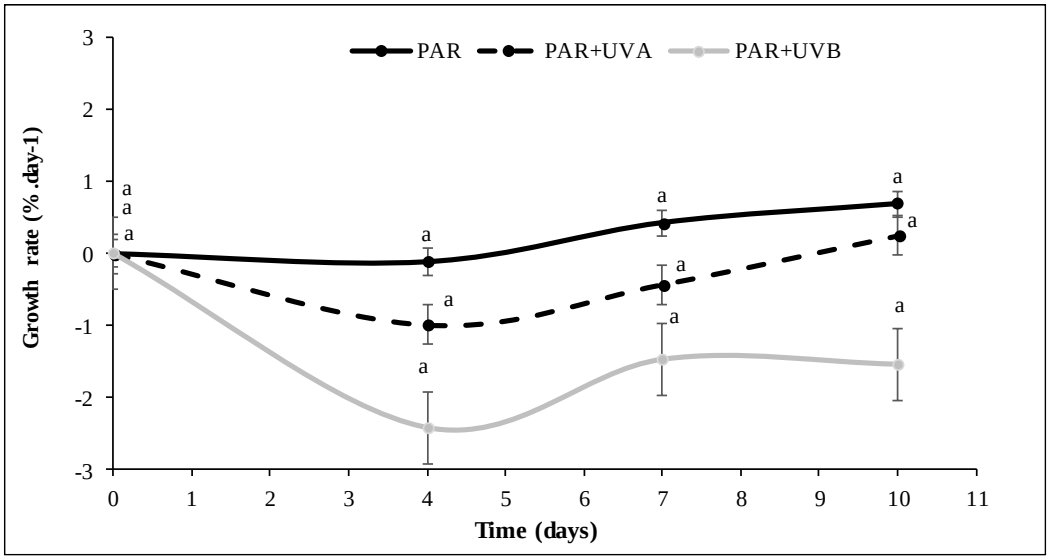


**Figure 8**. Growth rate of *Sargassum filipendula* along 10 days of exposure to PAR, PAR+UVA, and PAR+UVB radiation treatments ($n$ = 5; mean ± SD). Letters indicate differences according to repeated measures ANOVA.

**Proteins and photosynthetic pigments.** The Figure 9A shows the content of total soluble proteins of *S. filipendula* over 10 days of exposure to PAR, PAR+UVA, and PAR+UVB radiations. In general, with few exceptions, no differences were observed within the days for each radiation treatment, within the radiation for the same time and between the interaction time x radiation. PAR treatment at T10 showed a remarkable increase of proteins when comparing over time at the same treatment and between the other radiation treatments. Differences were also observed at T7 in PAR+UVA and T10 in PAR+UVB when comparing to PAR. It was not possible to notice a clear response pattern.

The content of photosynthetic pigments (chlorophylls *a* and *b* and carotenoids) in *S. filipendula* showed little variation when compared over time and after treated with UV (Fig. 9B-D). No differences were observed in the concentration of chlorophyll *a* (Fig. 9B) when comparing within times and UV treatments, except for PAR+UVB at T10 (606.46 ± 2.88 µg.g$^{-1}$), in which a significant reduction was evidenced in relation to the other radiation treatments at the same time (846.90 ± 3.82 µg.g$^{-1}$ for PAR and 833.46 ± 2.88

µg.g$^{-1}$ for PAR+UVA). The content of chlorophyll *c* did not presented a clear response trend (Fig. 9C); nevertheless, it varied significantly over time and among the treatments, showing a reduction at T4 in PAR+UVA and at T10 in PAR+UVB when comparing to the other times and between treatments. Finally, carotenoid concentrations showed no differences over time and between the treatments (Fig. 9D). The samples of PAR at T4 were lost then the mean ± SD does not appear in the figure.

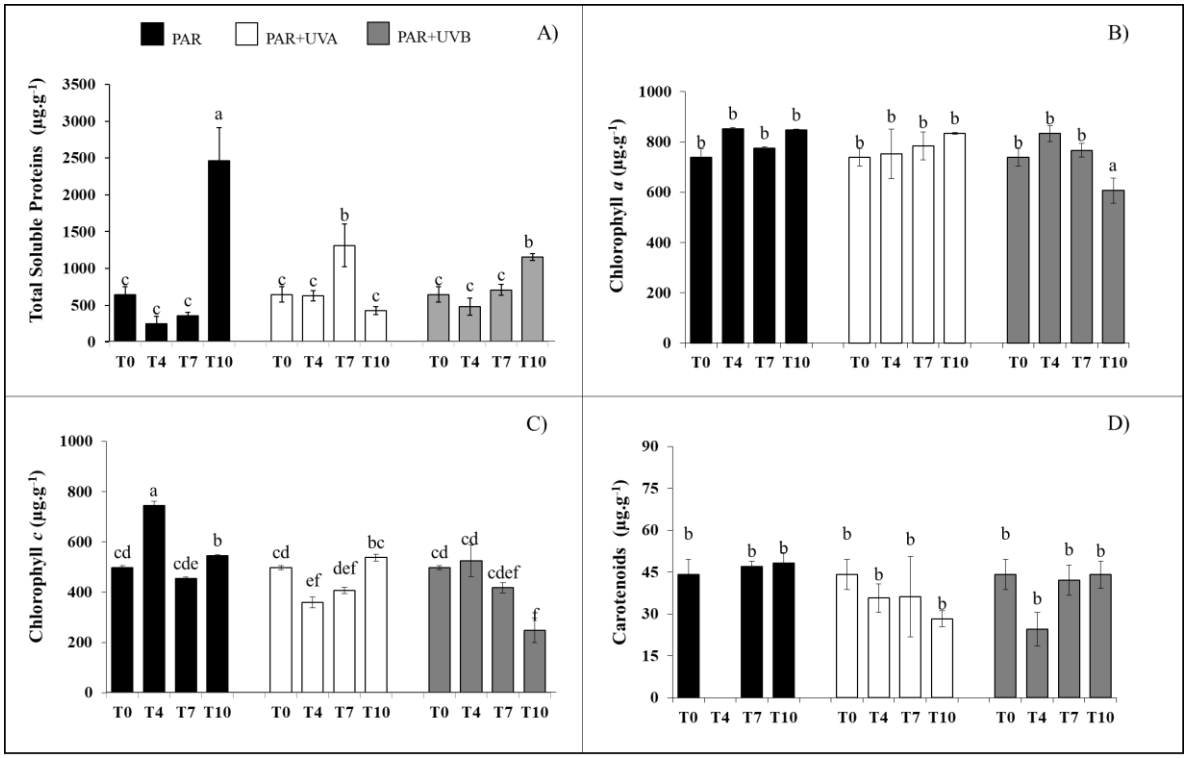


**Figure 9**. A) Total soluble proteins; (B) Chlorophyll *a*; (C) Chlorophyll *c*; and (D) Carotenoids of *Sargassum filipendula* along 10 days of exposure to PAR, PAR+UVA, and PAR+UVB radiation treatments ($n$ = 5; mean ± SD). T0 represents samples before start the experiment and T4, T7, and T10 correspond to the respective exposition time. Letters indicate differences according to bifactorial ANOVA and Newman-Keuls *post-hoc* test ($p < 0.05$).

**UV-visible absorption spectra of buffer and methanolic extracts and seawater.** Considering independently the buffer and methanolic extracts and the seawater samples, a similar pattern of the spectrum profile was observed for all treatments and over time (T4, T,7, and T10), then, only one spectrum (T4) for each one is presented. The absorption spectra of buffer and methanolic extracts and seawater are shown in the Figures 10A, 11A and 12A, respectively. Additionally, the area under the curve (AUC) for the maximal

absorption bands for buffer and methanolic extracts and seawater are represented in Figures 10B-D, 11B-D and 12B-D for T4, T7, and T10.

The Figure 10A presents the general UV absorption spectrum for buffer extract. Since no maximal absorption bands were observed in the visible region for this extract, the spectrum between 400 nm and 750 nm is not shown. Maximal absorption bands were identified between 220-240 nm and 260-280 nm for T4 (Fig. 10B), T7 (Fig. 10C), and T10 (Fig. 10D). For the times T4 (Fig. 10B) and T7 (Fig. 10C) similar trends were observed, with differences for both wavelength ranges (220-240 nm and 260-280 nm) and higher AUC for UV radiation treatments than PAR treatment. For T10, the amplitude of variances between PAR and UV radiation treatments was higher for 260-280 nm (Fig. 10D).

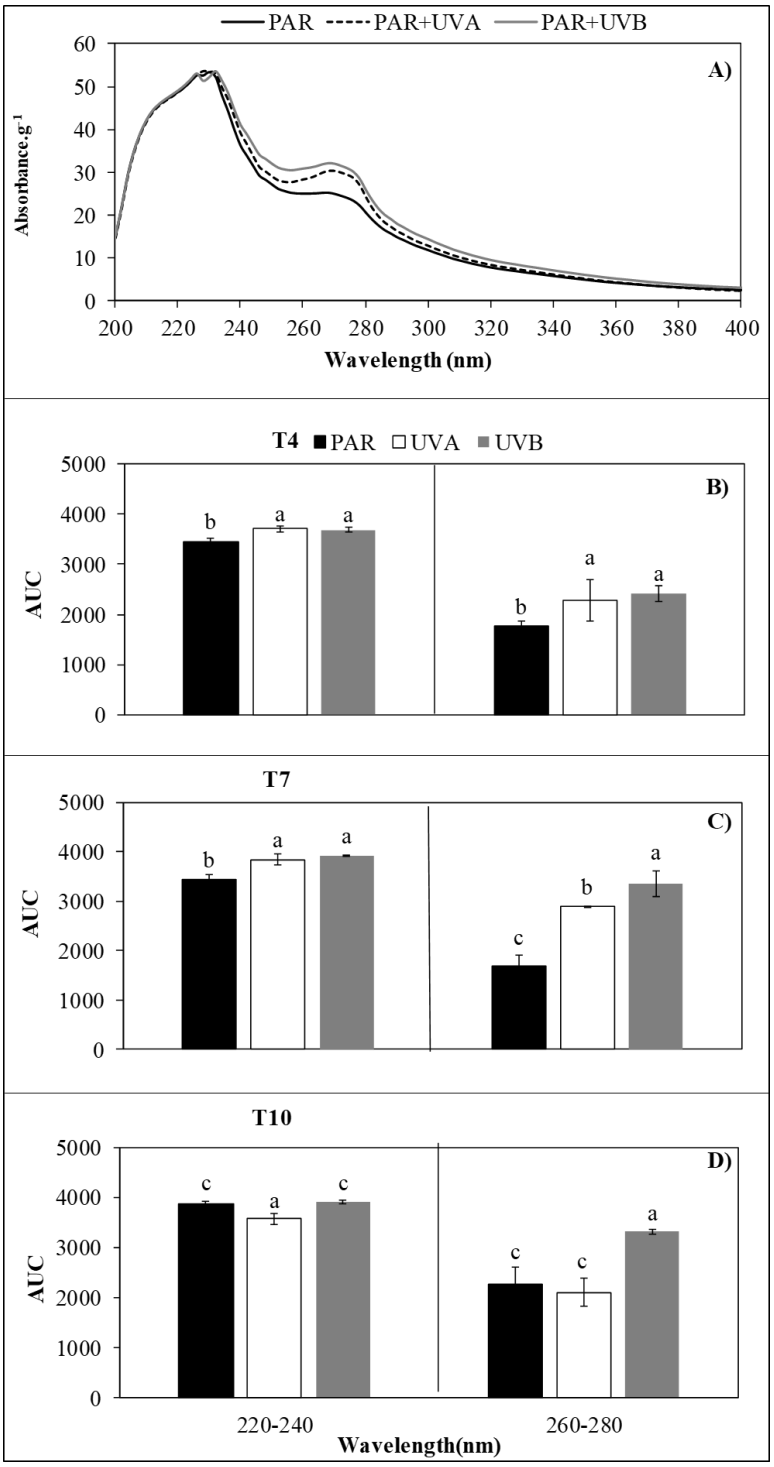


**Figure 10.** Absorption spectrum of buffer extract and area under the curve (AUC) of maximal absorption bands at 220-240 nm and 260-280 nm. (A) General UV spectrum at T4; (B) (C), and (D) represent the AUC ($n$ = 5; mean ± SD) at T4, T7 and T10 of radiation exposure, respectively, at two specific absorption bands: 220-240 nm and 260-280 nm. Letters indicate differences according to unifactorial ANOVA and Newman-Keuls *post-hoc* test ($p < 0.05$). The analysis were performed for each absorption band separately.

For the absorption spectrum of methanolic extract we identified five maximum bands in the UV-visible spectrum: 208-218 nm, 260-276 nm, and 328-350 nm for the UV spectrum, and 430-450 nm and 600-670 nm for the visible spectrum (Fig. 11). Major visible-absorption compounds than UV-absorption compounds were registered (Fig. 11A). For T4 (Fig. 11B), T7 (Fig. 11C), and T10 (Fig. 11D) similar lower AUC values at UV maximum bands of 260-276 nm, 328-350 nm, and 430-450 nm than visible maximum bands of 430-450 nm and 600-670 nm were observed. When compare the treatments over time, higher absorbance values were registered in PAR exposure at both UV and visible regions for T10 (Fig. 11D).

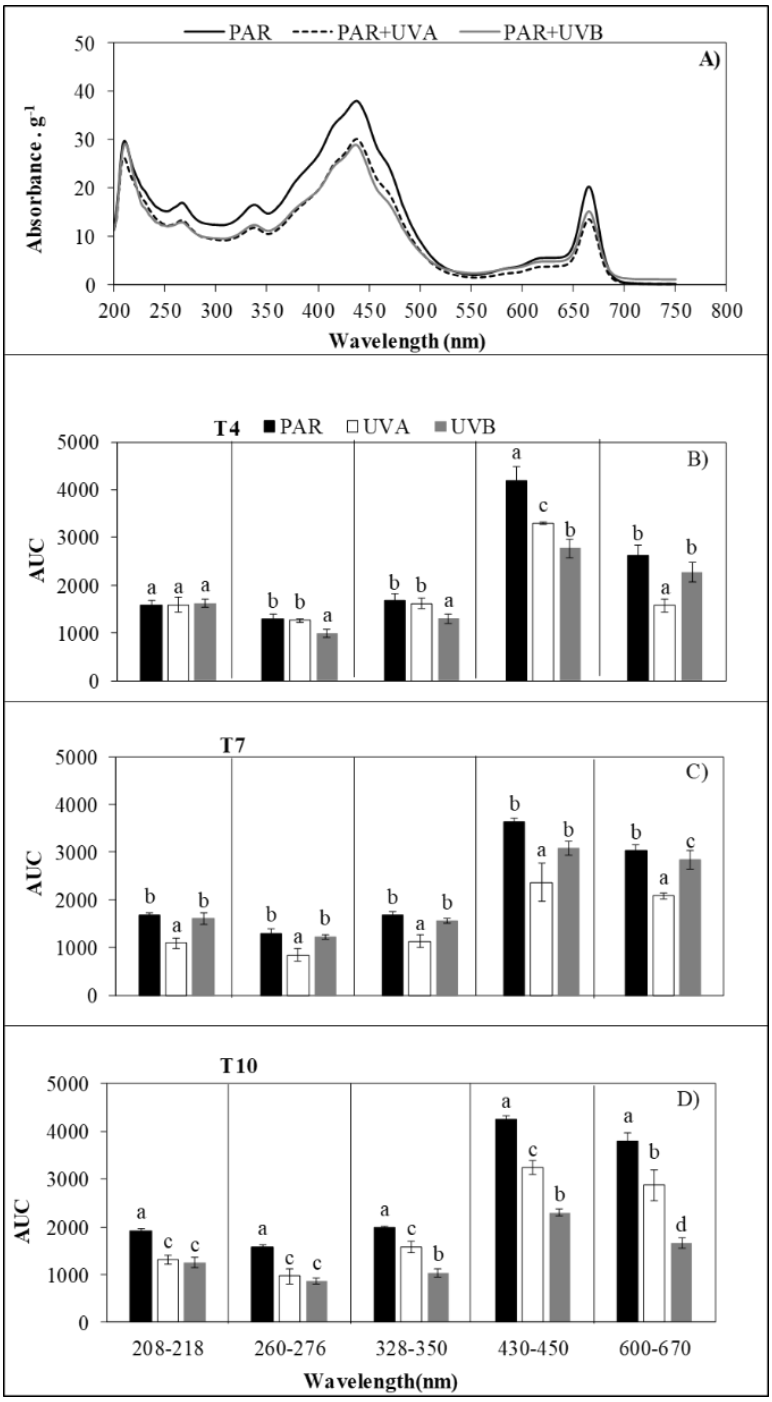


**Figure 11.** Absorption spectrum of methanolic extract and area under the curve (AUC) of maximal UV-visible absorption bands. (A) General UV spectrum at T4; (B) (C), and (D) represent the AUC ($n$ = 5; mean ± SD) at T4, T7, and T10 of radiation exposure, respectively, at three specific UV-absorption bands: 208-218 nm, 260-276 nm, and 328-350 nm, and two specific visible-absorption bands: 430-450 nm and 600-670 nm. Letters indicate differences according to unifactorial ANOVA and Newman-Keuls *post-hoc* test ($p < 0.05$). The analysis were performed for each absorption band separately.

The seawater samples in which the algae were cultivated during the experiment show maximal absorption bands in the UV region, specifically in the range of 208-218 nm (Fig.

12A), and no absorption was observed at visible wavelengths. No differences for AUC among the treatments were observed at T4 (Fig. 12B), whereas at T7 and T10 major AUC levels were observed for PAR+UVB > PAR+UVA > PAR (Fig. 12C-D, respectively); additionally, the magnitude of UV-absorbing compounds was major at T10. This last result agrees with the yellowish color of the seawater after 10 days of UV radiation exposure that presented more brownish coloration over experimental time for PAR+UVB treatment (Fig. 13).

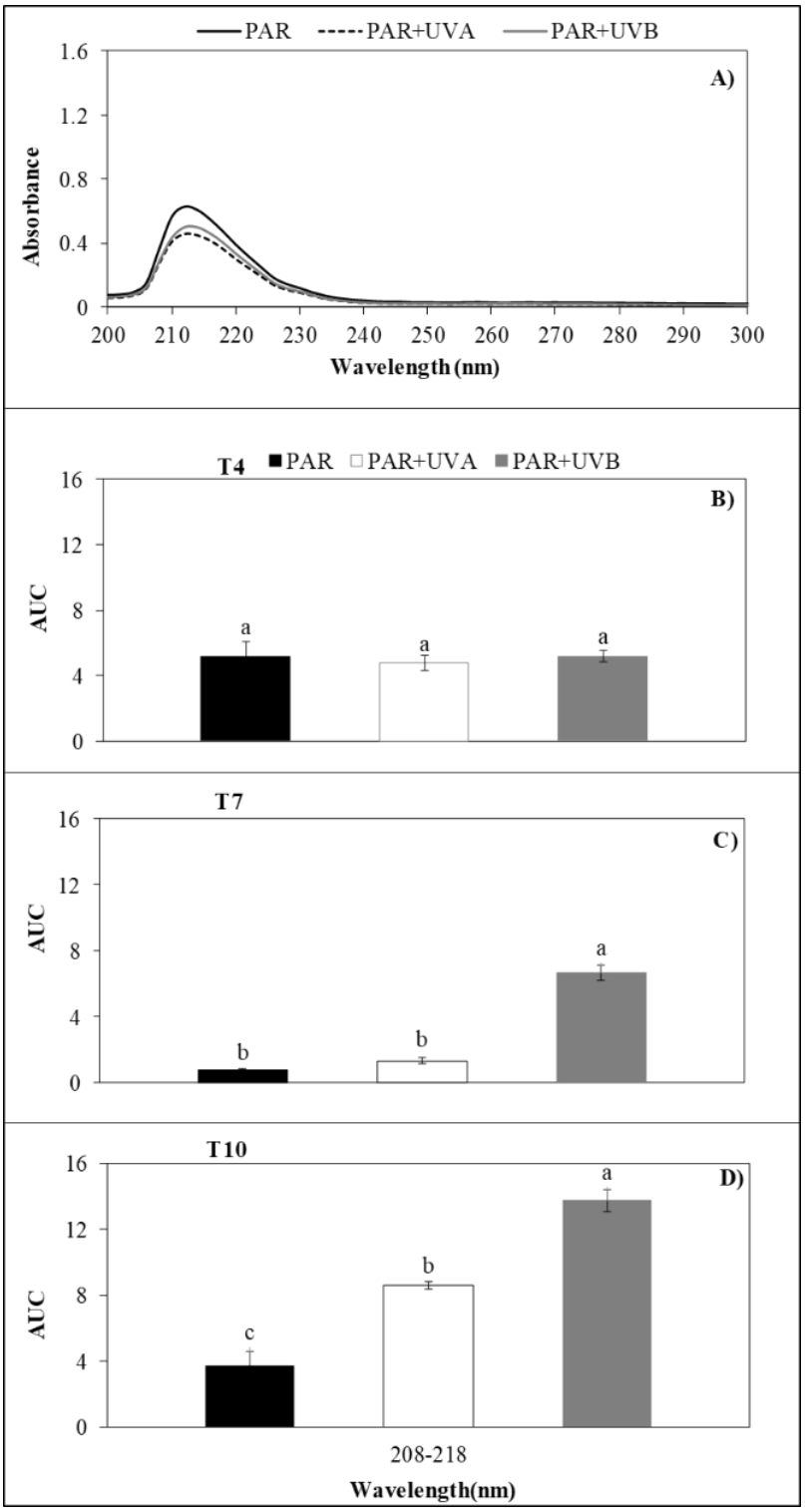


**Figure 12.** Absorption spectrum of seawater and area under the curve (AUC) of maximal UV-visible absorption bands. (A) General UV spectrum at T4; (B) (C), and (D) represent the AUC ($n$ = 5; mean ± SD) at T4, T7, and T10 of radiation exposure, respectively, at the 208-218 nm. Letters indicate differences according to unifactorial ANOVA and Newman-Keuls *post-hoc* test ($p < 0.05$).


**Figure 13.** Appearance of seawater in which *Sargassum filipendula* was cultivated, after 10 days of experimentation at three different radiation treatments.

## DISCUSSION

Ultraviolet radiation can lead to manifold effects on biological systems, resulting in anatomical, physiological, biochemical, and molecular alterations. Therefore, elevated doses of UV radiation trigger acclimation mechanisms in exposed benthic macroalgae, enabling them to tolerate the stressful condition and generating, in turn, a series of responses to maintain control over biological homeostasis (Vinegla and Figueroa 2009). Furthermore, UV-induced oxidative stress seems to elicit diverse and complex defense mechanism as a response to avoid cellular damage and assure the hormesis.

The present study shows that growth rate of *S. filipendula* did not present differences when treated with the specified doses of PAR+UVA and PAR+UVB along 10 days of experiment. Usually, UVA radiation causes indirect DNA damage through the formation of chemical intermediates, such as oxygen and hydroxyl radicals that interact with DNA to form cross-links and breaks in the DNA-protein chain (Dahms et al. 2011). However, moderate doses of UVA such as the one used for this experiment (75.6 $kJ.m^{-2}$ per day) have shown to stimulate photosynthesis and macroalgal growth as reported by Döhler et al. (1995) and Xu and Gao (2010). Additionally, as stated by Xu and Gao (2010), UVA radiation can activate photoprotective mechanisms to counteract the negative effect of UVB radiation, resulting in a decreasing impact of UV radiation on growth rates.

In a previous study, using *Sargassum cymosum* C. Agardh as a biological model to evaluate the combined effects of UV radiation and salinity, Polo et al. (2014b) found that UVA and UVB together in minor doses as the ones used herein (7.56 $kJ.m^{-2}$ and 3.78 $kJ.m^{-2}$ per day, respectively) stimulated the growth rate, leading to an increase in the

amount of mitochondria, which could support the metabolic energy demand required for this process. Indeed, studies with different algal species at minor doses of UV radiation show that UV level modulate diverse physiological responses besides growth, through up- or downregulation, such as induction of chlorophyll *a*, phenolic compounds, and antioxidant activity (Polo et al. 2014b), alteration in putrescine/spermidine ratio (Polo et al. 2014a), variation of photosynthetic performance and accessory pigments (Polo et al. 2014b; Simioni et al. 2014; Schmidt et al. 2015), carbon and nitrogen contents (Polo et al. 2014b), and ultrastructural organization (Bouzon et al. 2012; Pereira et al. 2018).

At elevated doses of UV radiation (98 $kJ.m^{-2}$ and 27 $kJ.m^{-2}$ per day for UVA and UVB, respectively), negative effects on algal growth and development are usually related to the damage caused to photosynthetic machinery, photosynthetic pigments, antioxidant enzymes, and lipid peroxidation (Xu and Gao 2010). Makarov (1999) reported a decrease in growth rate of the brown algae *Laminaria saccharina* (Linnaeus) J.V. Lamouroux, *Alaria esculenta* (Linnaeus) Greville, *Saccorhiza dermatodea* (Bachelot de la Pylaie) J. Agardh, *Fucus distichus* Linnaeus, *F. serratus* Linnaeus, and *F. vesiculosus* Linnaeus when exposed to UVB radiation. Likewise, Michler et al. (2002) reported a pronounced thallus necrosis and loss of parts of the thalli in the arctic *L. solidungula* J. Agardh after one week of daily exposure (18 h) to UV radiation, process that ultimately led to weight loss. However, it must be taken into account that the former study was carried out in field, with higher doses of UV radiation (324 $k.Jm^{-2}$ and 12.96 $kJ.m^{-2}$ per day for UVA and UVB, respectively) and longer exposition time than the experimented with *S. filipendula* in this study (75.6 $kJ.m^{-2}$ and 16.2 $kJ.m^{-2}$ for UVA and UVB per day, respectively). Tissue deformation observed as partial necrosis of the apical segments has also been reported for red macroalgae such as *Gracilaria domingensis* (Kützing) Sonder ex Dickie (Schmidt et al. 2010a), *Kappaphycus alvarezii* (Doty) Doty ex P.C. Silva (Schmidt et al. 2010b), and *Gelidium floridanum* W.R. Taylor (Schmidt et al. 2012a) after UV radiation exposure. For the present study, thallus necrosis was not observed. However, it could be expected that long-term and higher dose exposures to UV radiation may result in tissue deformation and serious damage in *S. filipendula*, and long-term growth measurements and observations on morphological integrity of the algal tissue may represent a more holistic indication of the negative impact of this stress factor (Roleda et al. 2004a).

Protein contents of *S. filipendula* showed increase in certain radiation treatments, indicating the possibility of stimulate their accumulation. At control radiation (PAR

treatment), increase of protein level at T10 could represent a response to the nutrient reload by the addition of von Stosch enrichment solution to the culture medium after seven days of cultivation. However, that response is unclear. Proteins are known to be strong absorbers of UVB radiation (Karentz 1994) and an increased protein degradation followed by resynthesis in order to replace UVB sensitive proteins could thus be expected during UVB exposure (Cullen and Neale 1994). Repair-mechanisms for UVB harm induce damage of membranes and electron transport components, which demand increasing enzymatic activity with higher nitrogen requirements. For example, photosynthetically relevant proteins like ribulose-1,5-biphosphate carboxylase/oxygenase (RubisCO) or D1 protein show an increased turnover under UV exposure, leading to a decrease in photosynthetic activity (Aro et al. 1993; Bornman and Teramura 1993; Strid et al. 1994). Moreover, it has been shown that UVB can directly affect the nitrogen uptake system in phytoplankton and leads to decreased uptake rates of ammonium and nitrate (Behrenfeld et al. 1995; Dohler 1997).

Changes in carbon, nitrogen, and protein contents and carbohydrate storage have frequently been used as indicators of physiological state of seaweeds health (Gagné et al. 1982). The variation of the chemical composition probably is related to carbon-nutrient balance (Lerdau and Coley 2002), in which the seaweeds allocate differentially C:N sources depending of the metabolic demands (Rosenberg and Ramus 1982; Polo et al. 2014b). The influence of nitrogen, as like proteins, amino acids, and other N-components on macroalgal metabolism is important since it is an essential element for the maintenance of several metabolic routes. In addition, algae are more sensitive to environmental variations when their intracellular nitrogen reserves are exhausted. As reported by some authors, an increase in nitrogen availability, such as nitrate and ammonium, will result in higher growth rates in various algae (Chow and Oliveira 2008). In addition, (Bischof et al. 2000b) suggest a possible mechanistic linkage between susceptibility to UV radiation and N metabolism since the limitation of this element could inhibit D1 protein turnover and the synthesis of RubisCO in the brown macroalga *A. esculenta*. Other aspect that could be affected as result of the interaction between UV radiation and nitrogen limitation is nutrient uptake and assimilation as reported for *F. vesiculosus*, in which this factor reduces ammonium uptake (Döhler et al. 1995). Furthermore, (Davison et al. 2007) reported that nitrogen could reduce the negative effects of UV radiation by either

increasing protection against UV radiation damage or enhancing the ability to repair damage in *L. saccharina*.

Photosynthetic pigments showed little variation along UV exposure within and between treatments. Some authors reported that UVB radiation is responsible for the loss of photosynthetic pigments (Bischof et al. 2000a; Holzinger and Lütz 2006b) and can also reduce the expression of genes involved in photosynthesis (Holzinger and Lütz 2006b). When analyzing the visible spectrum from methanolic extract, maximal absorption bands where registered in region between 430-450 nm and 600-670 nm, indicating the presence of chlorophyll *a* (Chl *a*, with maximal absorption bands at 432, 617, and 666 nm). However, no differences were observed for *S. filipendula*. Chlorophyll *a* is the main pigment constituent of the reaction center, in which the D1 protein is closely associated with the occurrence of the electron transport chain of the photosystems. Moreover, the alteration of the size of harvesting antenna complex and the carotenoid antioxidant composition indicate that photosynthesis is a dynamic process that attempts to safeguard the integrity of the reaction center and Chl *a*. Therefore, specifically Chl *a* must be tolerant to different stressing impact, and as demonstrated in our study this stability is also observed at moderate UV exposure, being able to acclimate to variations in light intensity and spectral quality (Senger and Bauer 1987; Falkowski and LaRoche 1990).

Additionally, accessory pigments such as chlorophyll *c* (Chl *c*, with maximal absorption bands at 445, 584, and 633) and carotenoids were also observed. These pigments serve as an antenna to increase the energy absorption capacity to be directed to the reaction center. However, under stress conditions, the accessory pigments may be degraded in order to reduce the excess energy being directed to the reaction center and thus not overburden the Chl *a* and hence prevent oxidation. These facts could explain the reduction of Chl *c* here observed. Similar results were observed by Polo et al. (2014b), in which Chl *c* was diminished, thus preventing oxidative damage of the photosynthetic apparatus under exposure to UV radiation.

On the other hand, carotenoids have a recognized antioxidant activity, in which an increase will act as antioxidant mechanism for protecting the photosynthetic apparatus against oxidative stress. For the present study, content of total carotenoids did not presented significant variations. According to Teramura (1983), carotenoids are generally less affected than chlorophylls in cropland plants exposed to UVB radiation. Additionally, accumulation of carotenoids specifically in response to UV radiation in both

phytoplankton (Goes et al. 1994) and macroalgae (Polo et al. 2014b) suggests that this condition could induced antioxidant defenses triggering by this pigments. Within these pigments, the fucoxanthin (maximal absorption bands at 428, 448, and 468 nm), one of the most abundant carotenoids in brown algae has attracted considerable interest due to biological properties, such as antioxidant, anti-inflammatory, anticancer, anti-obese, antidiabetic, antiangiogenic, and antimalarial activities (D'Orazio et al. 2012). The fact that the protection mechanism by pigment degradation and/or increase of carotenoids apparently was not very evident for *S. filipendula* under UV radiation effect, could indicate the participation of other mechanisms in response to UV radiation. As has been registered for other macroalgae, the establishment of physical barriers like the increase of cell wall polysaccharide layer can shield the photosynthetic apparatus against damaging radiation or the induction and synthesis of UV-absorbing compounds, such as phenolic compounds, which are additional mechanisms that might be involved in UV radiation acclimation of radiation protecting processes (Schoenwaelder 2002a).

For a large group of organisms, it has been reported a biological phenomenon referred as preparation for oxidative stress (POS) (Hermes-Lima and Storey 1998), in which an antioxidant upregulation linked exclusively in response to low oxygen stress is established. Different laboratory studies have shown increases in activity of the enzymes catalase (CAT), superoxide dismutases (SOD), and glutathione peroxidases (GPx) and in the levels of reduced glutathione (GSH) under hypoxia conditions (Moreira et al. 2017). Although POS has not been reported for other conditions different from low oxygen, changes in enzymatic and non-enzymatic antioxidant systems have been widely reported for another stress conditions than hypoxia; thus, we suggest the expansion of this term for other situations, in which there is activation of the antioxidant systems as occur in response to other types of stressors such as UV radiation.

Macroalgae produce a large diversity of UV-absorbing compounds that are known to protect against UV radiation stress (Korbee et al. 2005; Abdala-Diaz et al. 2006). The measurement of UV-visible absorption spectrum is an easy and valuable tool for comparing the presence and biosynthesis of UV-absorbing compounds and elucidating hypothetic chemical classes with photoprotective function. For *S. filipendula*, maximal absorption bands in the UV region were widely observed, suggesting the presence of secondary metabolites such as phenolic compounds, which are largely distributed among

brown algae acting as defense mechanism (Li et al. 2011) and potent antioxidant (Al-Azzawie and Alhamdani 2006).

From the maximal UV absorption bands identified in *S. filipendula* some compounds can be suggested like tannins with λmax near 278 nm, phlorotannins with λmax close to 220-240 nm and 260-280 nm, flavone/flavonols with λmax about 210 nm, 240/260 nm, and 370 nm (like apigenins), and phenolic acids with λmax by 220 nm and 320 nm. Polyphenols are the most prominent phenolic compounds in brown seaweeds, particularly phlorotannins, which are exclusively of this taxon. They are found free or forming complexes with different components of the cell walls (Wang et al. 2012), such as polysaccharides, and are essential to the physiological integrity of alga with important roles involved in chemical defenses and protection against oxidative damage in response to changes in nutrient availability and UV radiation (Li et al. 2017).

In addition, the λmax at 210 nm was previously reported by (Salgado et al. 2007) in *Padina gymnospora* (Kützing) Sonder, and attributes this absorption band to a linkage between phenolic compounds and alginates. Other studies in which this linkage has been observed (Schoenwaelder 2002a; Berglin et al. 2004; Salgado et al. 2005), reveals that this coupling preserves the UV absorption capability of phenolic compounds along time. Moreover, there is an extensive literature reporting their properties especially for their capacity to act as antioxidant, with positive effects on human and animal health improving the current interest for disease therapy and chemoprevention (Panche et al. 2016).

Phlorotannins such as fucophloroethol, phloroethol, eckol, and dieckol have been identified in several species of brown algae, including species of the genus *Sargassum* (Li et al. 2011). No identification of these compounds was performed in our study; nevertheless, our results suggest the presence of phlorotannins since they have maximal absorption bands within the ranges here observed. Additionally, Polo et al. (2014b) by analyzing the ultrastructure of *S. cymosum* reported the degradation and high migration of phlorotannins contained in physoids through the cell wall as a response caused by UV radiation. This phenomena leads to the liberation of phenolic compounds into the surrounding medium creating an UV-absorbing microenvironment (UV-refuge) (Roleda et al. 2010a); an acclimation strategy against UV radiation that has also been reported for the present study, in which the appearance of the seawater that *S. filipendula* was cultivated during radiation exposure presented a yellowish color as an indicator of this exudation, with more intensity in PAR+UVB treatment.

Our results for *S. filipendula* show the capacity of the species to synthesize and accumulate UV- and visible-absorbing compounds, probably phlorotannins and carotenoids, respectively, that could provide adaptive advantages for organisms exposed to different ambient stressors such as UV radiation, since brown algae could be more sensitive to UV exposure. This feature is of great importance for macroalgae inhabiting the coasts of Brazil due to high radiation levels to which are subjected, especially during low tides and summer season. In addition, the proper isolation, identification, and comprehension of the biosynthesis action of these compounds will undoubtedly be of great benefit for the development of functional bioproducts with potential application in medical, pharmaceutical, alimentary, and agricultural fields.

The present work is a base research that contributes to the knowledge of sensibility and tolerance of *S. filipendula* to UV radiation, a valuable species as community structuring in tropical and subtropical marine habitats that is widely distributed in the Brazilian coast in the lower intertidal zone. The integrative data on physiological performance here presented give insights of the biological implications for the species due to this stressor factor. Additionally, possible prediction of environmental consequences such as decrease in primary production due to the possible inhibition of photosynthesis at population level can be appreciated, affecting growth rate and reproduction, having as consequence the devastation of the trophic base for associated species that could lead to the elimination of the ecological niche diversity in this ecosystem. Then, the sensitivity of *S. filipendula* to changes of abiotic factors can be an important feature that allows its use for environmental monitoring which could subsidize decision-making of monitoring and mitigation programs

# Chapter II

## DNA damage and bioactivity

## Chapter II

Variation of antioxidant capacity and antiviral activity of the brown seaweed *Sargassum filipendula* (Fucales, Ochrophyta) under laboratorial UV radiation treatments


### ABSTRACT

Ecophysiological responses as well as the potential use of macroalgae are closely influenced by environmental conditions such as UV radiation among others abiotic factors. Thus, the production of UV-absorbing compounds is a well-known strategy for protecting organisms against UV radiation stress due to the ability of absorb and dissipate short wavelengths. Besides the natural photoprotective sunscreen features of UV-absorbing compounds, there are strong evidences on its potential as antioxidant, anti-inflammatory, antibacterial, antifungal, antimalarial, antiproliferative, immunomodulatory, and anticancer agents. In this sense, we aim to investigate the potential cell damage and its relationship with antioxidant activity and bioactive property of the brown macroalga *Sargassum filipendula* under the effect of radiation treatments: PAR (control), PAR+UVA, and PAR+UVB after 10 days of exposure. Cell damage was assessed as DNA impairment by the quantification of cyclobutane pyrimidine dimers (CPDs). For antioxidant evaluation, five different antioxidant assays including ABTS, DPPH, Folin-Ciocalteu, FRAP, and chelating activity were performed using methanolic crude extracts at different concentrations. Antiviral activity was assessed by the ability of the sample to inhibit the enzyme HIV-1 reverse transcriptase (HIV-1 RT) using different concentration of methanolic and aqueous extrats. PAR+UVB treatment affected negatively the DNA integrity, which increasing CDP-DNA complexes were registered. Higher antioxidant activity was observed under PAR treatment than UVA and UVB radiation treatments. Inhibition of HIV-1 RT showed percentages between 25% to 90% for methanolic extracts, while aqueous extracts presented inhibition near to 100% for all treatments and tested concentrations. Results showed that UV-absorbing compounds present in *S. filipendula* provide adaptive advantages against UV radiation exposure. Additionally, the species can be considered as a potential biotechnology source of natural bioactive compounds, and proper isolation of these compounds or obtaining extract rich in bioactive compounds will undoubtedly be of great benefit for the development of functional bioproducts.

## INTRODUCTION

Marine organisms like seaweeds are constantly exposed to combined stressors such as high irradiance and UV radiation. Changes in irradiance and light quality can either promote or inhibit many of their biological processes if radiation becomes excessive, or if short wavelength radiations with high energy content such as UVB radiation are absorbed by biomolecules (Vass et al. 1997). As a consequence, important components in macroalgae metabolism are particularly affected such as proteins (destruction of C-C bonds, or the tertiary protein structure due to S-S bond cleavage), lipids (peroxidation at C=C bonds), and nucleic acids (especially cyclobutyl pyrimidine dimers and pyrimidine (6-4) pyrimidone photoproducts). It has been reported for these organisms that conformation changes in the reaction center protein (D1) of photosystem II and the $CO_2$ fixing enzyme in the Calvin cycle (ribulose-1,5-bisphosphate carboxylase/oxygenase, RubisCO) lead to several negative effects as the inhibition of photosynthesis and subsequent decrease in productivity (Bischof et al. 2007).

Two major classes of mutagenic DNA lesions induced by UV radiation are cyclobutyl pyrimidine dimers (CPDs) and 6–4 photoproducts (6–4PPs, which are pyrimidine adducts) (Fig. 14). The CPDs and 6–4PPs make up around 75 and 25%, respectively, of the UV-induced DNA damage products and both classes of lesions distort the DNA helix (Britt and May 2003), causing inhibition in DNA replication and transcription, with consequent disruption on cell metabolism and division (Buma et al. 2000) that could directly inhibit growth and survival. To counteract the lethal effects of DNA lesions, efficient DNA repair mechanisms have been developed by the organisms, in which specialized repair proteins continuously scan the genome for the presence of DNA lesions. When a mismatched base, an apurinic or apyrimidinic sites, is found by a lesion recognition protein, it triggers an efficient DNA repair that restores the genetic information. Within the DNA repair mechanism, photoreactivation is an important defense against UVB radiation-induced DNA damage in land plants (Quaite et al. 1994). This system consist on a single enzyme called photolyase, which specifically binds to CPDs (CPD photolyase) or 6–4PPs (6–4 photolyase) and reverses the damage using the energy of light through removing DNA lesions caused by UVR (Essen and Klar 2006). More complex repair pathways such as excision repair (BER–Base Excision Repair and NER–Nucleotide Excision Repair), which do not directly reverse DNA damage but

replace the damaged DNA with new, undamaged nucleotides appear to have a complementary role (Quaite et al. 1994).

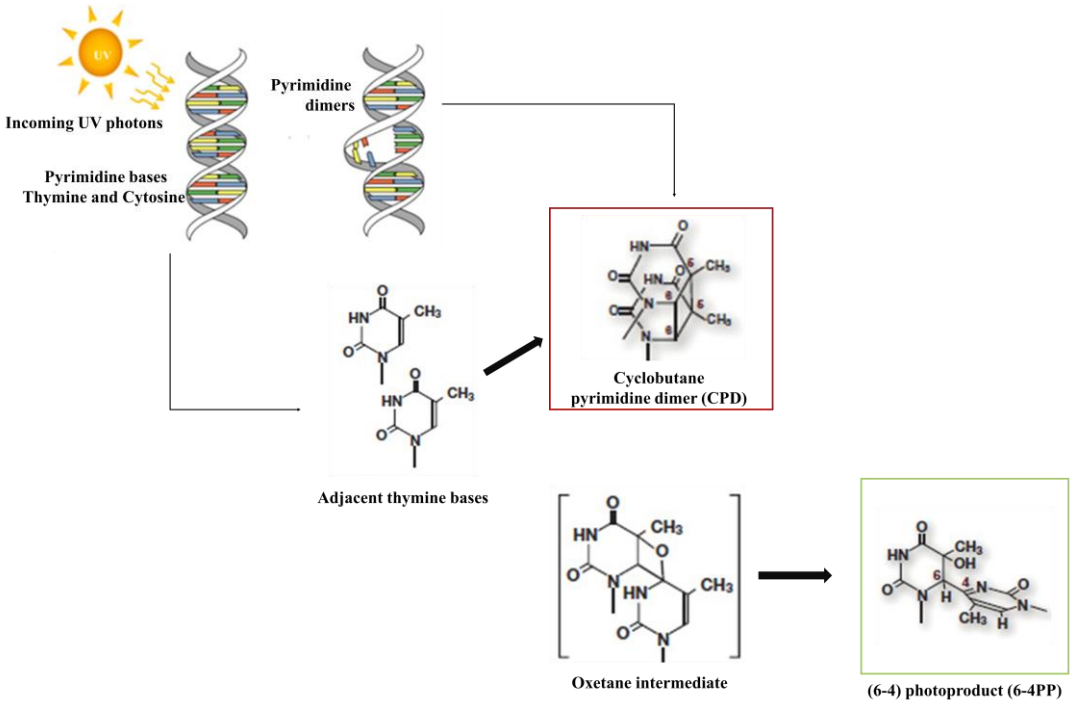


**Figure 14.** Production process of thymine dimer lesion in DNA. Incoming UV photons induce the bind together of two consecutive nitrogenous bases on one DNA strand, destroying the normal base-pairing double-strand structure in that area. Then, pyrimidine dimers (CPDs) and 6–4 photoproducts (6–4PPs) are formed.

DNA damage by the accumulation of CPDs has been reported for all seaweed groups (Van de Poll et al. 2001; Bischof 2002; Roleda et al. 2004b, 2007a). For brown seaweeds, significant CPDs accumulation in *L. saccharina* was observed after 15 days of exposure to UV radiation. However, repair process was observed, resting only 10% of the initial CPDs concentration, suggesting the presence of photolyase activity (Van de Poll et al. 2002). DNA damage and repair processes have also been reported in gametes on the brown alga *Ascoseira mirabilis* Skottsberg exposed to UV radiation. The authors found CPDs formation in propagules after 1 h of exposure, which increased after 8 h of exposure. Effective DNA repair in *A. mirabilis* was register after two days post-cultivation in low visible light intensity (Roleda et al. 2007b). Likewise, induction and accumulation of CPDs in zoospores of *Laminaria digitata* (Hudson) J.V. Lamouroux increased with increasing UVB dose, and repair of the damaged DNA was registered after two days of recovery in low visible light (Roleda et al. 2010a).

Additionally to the photorepair system for damaged DNA and proteins in the photosynthetic apparatus caused by UV radiation, macroalgae have developed other efficient protective mechanisms against excessive solar radiation. It has been observed the presence of antioxidant substances in algal cells (*e.g.* vitamins, pigments, mycosporine-like amino acids, and polyphenols) that act as defense systems and photoprotective molecules against UV radiation and other environmental stressors (Gates 2014).

Physiological changes in algae in response to alteration of environmental light, temperature, and nutritional conditions directly influence their chemical composition. Under non-stressing metabolic condition, algae produce homeostatic amounts of reactive species (free radical and non-radical species) as byproducts of the electron transport system in chloroplasts and mitochondria and other biological reactions. Free radicals are formed when molecules contain one or more unpaired electrons (Fig. 16), thus giving reactivity to the molecules; the non-radical forms are produced when two free radicals share their unpaired electrons.

Environmental drivers such as high sunlight or elevated exposure to UV radiation can increase the overproduction of reactive species and subsequently cause oxidative stress. The altered state in which reactive oxygen species and reactive nitrogen species (ROS/RNS) overwhelm antioxidative defenses of the organism, that lead to oxidative modification of biological macromolecules (lipids, proteins, DNA, among others), causes cell/tissue injuries and accelerates cellular death (Trevisan et al. 2001). To counteract the oxidant effects (adverse modifications to lipids, proteins, and DNA) and restore the redox balance, cells can activate or silence genes encoding defensive enzymes, transcription factors, and structural proteins (Dalton et al. 1999). Thus, efficient antioxidant mechanisms are essential to withstand photooxidation (Okamoto et al. 2001).

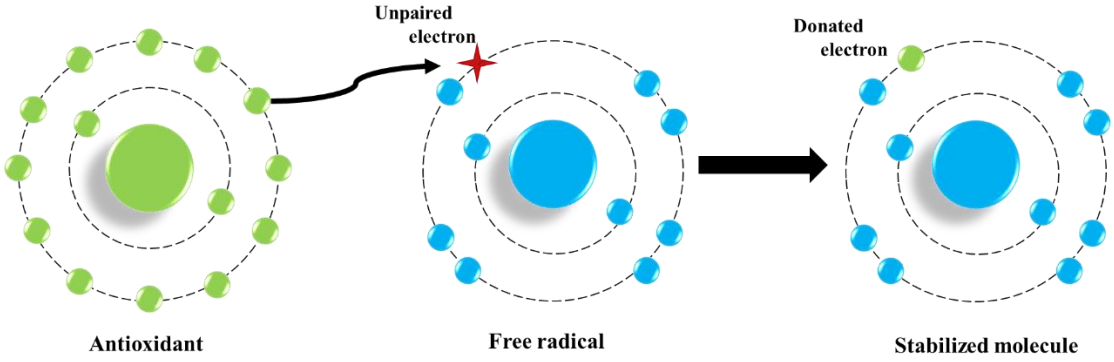


**Figure 15**. Stabilization of a free radical molecule by antioxidant electron donation.

In the case of brown seaweeds, it is known that they are rich in natural antioxidants as phenolic compounds like phlorotannins, carotenoids mainly fucoxanthin, and isoprenoids. Among antioxidants, phenolic compounds, which are characterized by the presence of large multiple phenol units and widely produced among brown algae, are secondary metabolites that act as oxidative defense mechanism in this group (Li et al. 2011). The interaction of phenolic compounds binding to sulfated polysaccharides, another secondary metabolite with biological activity, has been also investigated due to the linkage into the cell wall as an integrated mechanism of environmental defense. In the study of Salgado et al. (2007) was investigated the interactions between phenolic compounds, alginates, and UV absorption capacity in *P. gymnospora*, and a strong relationship between both phenolic compounds and alginates was observed, wherein such interaction would preserve the absorption capacity of UV radiation by phenolic compounds over time.

Other investigations on algal polyphenol concentrations have shown variations according to season, habitat, and local environmental factors such as salinity, UV radiation, sunlight, and nutrient availability (Svensson et al. 2007; Jormalainen and Honkanen 2008). In addition, their distribution may vary into the cells with differential life stages and functions, as well as within and among the species. In general, phenolic compounds clearly tend to be more abundant in young, actively growing, and highly productive portions. Species with apical growth trend to have the highest concentrations of this compound in the apical portions when compare to their branches (Hay and Fenical 1988). On the other hand, those with intercalary like-meristematic growth have the highest concentration in this region, as species of the genus *Laminaria* and *Ascophyllum*

*nodosum* (Linnaeus) Le Jolis, *Sargassum muticum* (Yendo) Fensholt, and *Cystoseira tamariscifolia* (Stackhouse) Papenfuss (Connan et al. 2006a; Abdala-Diaz et al. 2014).

Phenolic compounds have been recognized as having antioxidant properties. Antioxidant substances are probably the most relevant bioactive compounds found in algae (Munir et al. 2013) and have attracted great interest because their mechanisms of action go far beyond the modulation of oxidative stress. Evidences strongly demonstrate the contribution of these compounds to the prevention of cardiovascular diseases and neurodegenerative diseases (Urquiaga and Leighton 2003; Oueslati et al. 2012) with potential as anti-aging, anti-inflammatory, antibacterial, antifungal, cytotoxic, antimalarial, antiproliferative, and anticancer (Fujimura et al. 2000; Cornish and Garbary 2010; Thomas and Kim 2011). A recent research performed with *Sargassum linifolium* C. Agardh reported a significantly pronounced antioxidant activity, suggesting that the species could offer new potential sources of bioactive (Ismail 2017). Likewise, Chakraborty et al. (2017) suggested that seaweeds belonging to *Anthophycus longifolius* (Turner) Kützing, *S. plagiophyllum*, and *S. myriocystum* be utilized as a source of naturally occurring antioxidant substances, after evaluating the role of phenolic compounds responsible for antioxidant activities within these species. Additionally to the scavenging activity, polysaccharides from *Sargassum* have demonstrated significant anticancer activity, making it useful for therapeutic studies to treat cancer cell lines (Chitra et al. 2018).

Among these groups of substances, phenolic compounds have demonstrated superior *in vitro* activity than the other antioxidants like pigments (β-carotene, lutein, fucoxanthin, phycoerythrin), polysaccharides (fucoidans, sulfate galactans), and mycosporine-like amino acids (Munir et al. 2013). Other studies have provided evidences that phenolic compounds as phlorotannins from marine brown algae have a key role as bioactive ingredients and play a vital role in algae itself as well as human health and nutrition. A study performed with Japanese Laminariaceae, reported that phlorotannins present in this group might be useful as a novel functional foodstuff or supplement with anti-inflammatory activity (Shibata et al. 2008). Reviews by Jung et al. (2010), Li et al. (2011), and Thomas and Kim (2011) reported that the brown algae *Ecklonia cava* Kjellman, *Ecklonia stolonifera* Okamura, *Ecklonia kurome* Okamura, *Eisenia bicyclis* (Kjellman) Setchell, *Ishige okamurae* Yendo, *S. thunbergii*, *Hizikia fusiformis* (Harvey) Okamura, *Undaria pinnatifida* (Harvey) Suringar, and *L. japonica* Areschoug present anticancer,

bactericidal, and anti-allergic biological activities, as well as potential application in the treatment for Alzheimer's disease and other health-related activities associated with its phlorotannins content.

Moreover, besides the bioactivities mentioned above, a variety of bioactive compounds from brown seaweeds have demonstrated antiviral properties and tested against the Human Immunodeficiency Virus (HIV). HIV belongs to a class of viruses called retroviruses and a subgroup of retroviruses known as lentiviruses (Chiu et al. 1985). Isolates from this virus are grouped in two types: HIV-type 1 (HIV-1) and HIV-type 2 (HIV-2) and the former is the main agent of Acquired Immune Deficiency Syndrome (AIDS), which by 2017 has affected 36.9 million of people around the world (Joint United Nations Programme on HIV/AIDS (UNAIDS) 2018) (Fig. 17).

A)

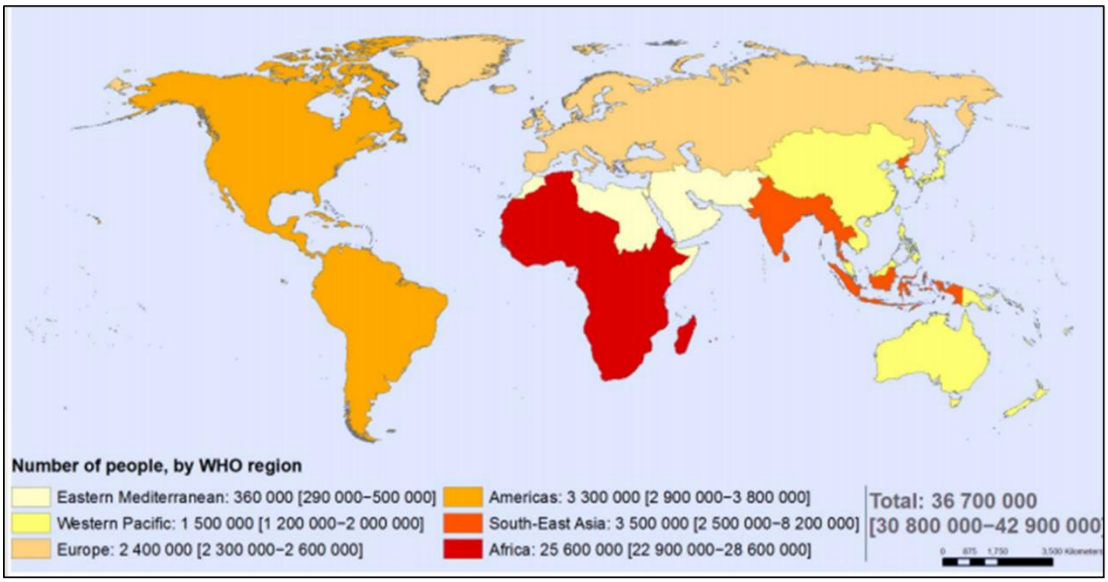


B)

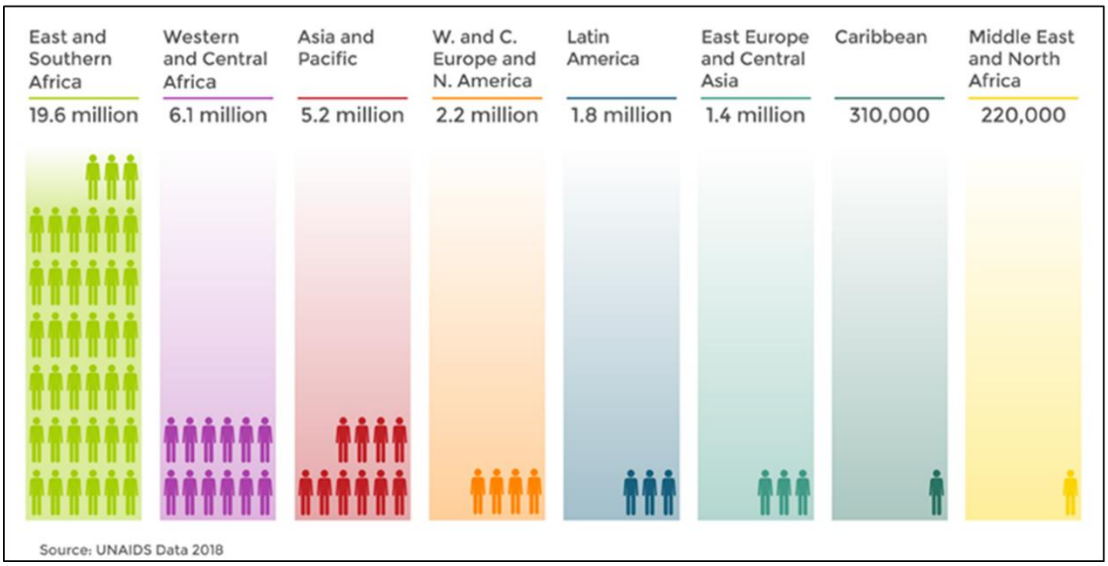


**Figure 16.** Worldwide statistics review of A) Prevalence of HIV among adults aged from 15 to 49 around the world (Source: World Health Organization (WHO), 2018); B) Number of people living with HIV per region (Source: Global information and education on HIV and AIDS, 2017).

Important viral enzymes are encoded by the *pol* gene of HIV-1 (Fig. 18): HIV-1 reverse transcriptase (RT) which converts the viral RNA into DNA before its integration into human cell's genes (Smith and Daniel 2006); and HIV-1 integrase (IN) that incorporates the double-stranded DNA product resulting from the reverse transcription of viral RNA into a host genome. Finally, when viral DNA is integrated into the host cell

DNA, the cell will go on to make viral proteins to initiate the replication process (Smith and Daniel 2006). These enzymes are considered an appropriate target for antiretroviral agents as they play key roles in the virus replication cycle.

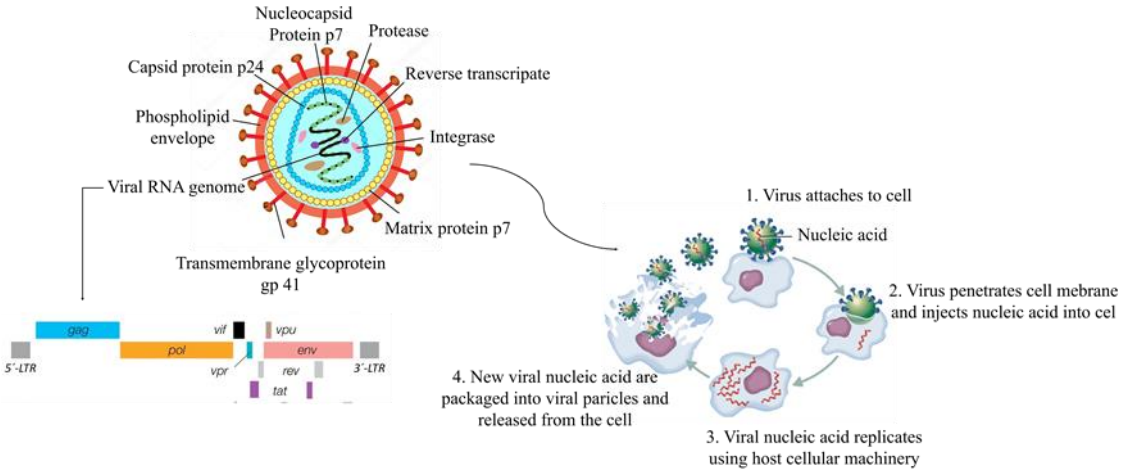


**Figure 17.** General organization of the HIV virus showing the viral genome composed by three genes: *gag*, *pol* and *env*; and the replication cycle into the host. Modified from source: (http://autocww.colorado.edu).

Despite the significant advances in rational drug design against the HIV-1, issues like drug resistance, side effects, and the need for long-term antiviral treatment urge the development of new anti-HIV agents, targets, and therapies (Worm et al. 2010). In this regard, marine resources can be an invaluable basis for the discovery of new bioactive compounds for the treatment of diseases like AIDS, since many of these have been reported to exhibit significant anti-HIV activity and are able to inhibit almost every stage of the viral life cycle (Jiang et al. 2010).

These compounds, which have been successfully extracted from macroalgae, includes phlorotannins, lectins, steroids, sulfoglycolipids, and polysaccharides, and within this group, natural and synthetic sulfated polysaccharides have been the focus of most of the researches. In the particular case of antiviral activity, inhibition of HIV-1 RT by sulfated polysaccharides from brown seaweeds has shown to be efficient in disrupting the viral peptide attachments which are supposed to be highly preserved in the drug-resistance mutation process (Karadeniz et al. 2015). Among sulfated polysaccharides, fucans from species like *Dictyota mertensii* (C. Martius) Kützing, *Lobophora variegata* (J.V. Lamouroux) Womersley ex E.C. Oliveira, *Spatoglossum schroederi* (C. Agardh) Kützing,

and *F. vesiculosus* have shown to inhibit successfully HIV RT activity up to 99% (Queiroz et al. 2008).

As state before, marine algae are exposed to a combination of stressors such as UV radiation and other environmental conditions, easily leading to the formation and accumulation of free radicals and reactive species, triggering oxidative stress. However, it has been observed the presence of antioxidant substances in algal cells that act as a defense system and photoprotective molecules against different environmental stressor. Additionally, these compounds can play a key role as bioactive ingredients and a vital role in human health. Therefore, the present chapter has as aim to investigate the potential cell damage and its relationship with antioxidant activity and bioactive properties of *Sargassum filipendula* under the effect of radiation treatments: PAR (control), PAR+UVA, and PAR+UVB after 10 days of exposure by measuring the possible damage to DNA together with the antioxidant and antiviral activities.

## MATERIAL AND METHODS

**Collection site and algal material.** Specimens of *S. filipendula* were collected at Cigarras Beach (24°43'55.74"S and 45°23'54.48"W), localized in São Sebastião, North coast of São Paulo State, Brazil, during the summer season (February-March 2016). Cleaned apical portions (± 8 cm) were acclimated for one week under laboratory conditions (details are addressed in General material and methods, section 1).

**Laboratory conditions and experimental setup.** After the acclimation period, the material was exposed for 3 h to different radiation treatments: a) PAR (control treatment), b) PAR+UVB, and c) PAR+UVA. UVB (312 nm; 1.5 $W.m^{-2}$; 16.2 $kJ.m^{-2}$ /day) and UVA (365 nm; 7 $W.m^{-2}$; 75.6 $kJ.m^{-2}$ /day) radiations were provided by Philips lamps models TL 20W/12 and Actinic BL TL-K 40 W/10-R, respectively (details are addressed in General material and methods, section 3).

In this chapter, we analysed the effect of UV radiation on *S. filipendula* after 10 days of exposure by evaluating the DNA damage, antioxidant potential, and antiviral activity. In the case of antioxidant activity, evaluation was performed using methanolic extracts, while antiviral activity was assessed using both methanolic and aqueous extracts.

**Oxidative DNA damage evaluation.** The potential DNA damage caused by UV radiation was evaluated by the OxiSelect™ UV-Induced DNA Damage ELISA kit (CPD Quantitation; Cell Biolabs Inc, USA), according to the manufacturer's specifications. Cyclobutane pyrimidine dimers (CPDs) are a type of DNA damage caused specifically by the absorption of UV radiation that results in a transition of C (cytosine) to T (thymine) and CC to TT, which are the most frequent mutations of gene *p53* in both human and mouse skin cancers. After UV exposure, cells activate *p53* genes and stall the cell cycle for repair. If the damage is too severe, the cell will trigger apoptosis to get rid of DNA damaged, potentially mutant cells.

Algal samples of 20 mg fresh weigh (FW) exposed to different radiation treatments during 10 days were grounded in liquid nitrogen until a fine powder was obtained. DNA extraction was done using the NucleoSpin Plant II kit (Macherey-Nagel, Düren, Germany), following the manufacturer's instructions. The DNA samples (2 μg/mL) were first heat denatured before adsorbed onto a 96-well DNA high-binding microplate. The CPDs present in the sample or standard were probed with an anti-CPD antibody, followed by an HRP (Horse Radish Peroxidase) conjugated secondary antibody. Absorbance of the samples and controls were read at 450 nm using a UV-visible microplate spectrophotometer (Epoch Biotek, USA). The CPDs content in the samples was determined by comparing with a standard curve prepared from predetermined CPD-DNA standards and expressed as CPD-DNA ng.

**Antioxidant potential.** Crude methanolic extracts of *S. filipendula* were tested for their antioxidant potential after exposure to PAR and UV radiations after 10 days of exposure. Samples of 200 mg FW were grounded in liquid nitrogen, suspended in 1 mL of methanol and extracted for 3 h at room temperature, protected from light and temperature to avoid photo- and thermoxidation. The samples were centrifuged at 14.000 rpm for 15 min at room temperature and the supernatant was recovered for further antioxidant assays.

In general, the analytical tests for the determination of the antioxidant potential are based on two mechanisms of reaction: 1) Hydrogen Atom Transfer (HAT) mechanism that evaluate the ability of antioxidants to donate hydrogen atoms to block the action of peroxyl radicals (ROO•) and 2) Single Electron Transfer (SET) mechanism that detect the ability of the sample to reduce the oxidant by electron reduction, which does not need to be strictly a free radical, unlike the HAT mechanism assays (Castelo-Branco and Torres

2011). In addition, each antioxidant assay has a particular chemical principle and affinity with the components of the extract. Thus, the evaluation of the antioxidant potential using several assays allows more complete antioxidative responses of the studied species (Matanjun et al. 2008). Thus, antioxidant activity was evaluated using five different assays: a) ABTS (2,2'-azino-bis(3-ethylbenzothiazoline-6-sulphonic acid) free radical scavenging activity; b) DPPH (2,2-diphenyl-1-picrylhydrazyl) free radical scavenging activity; c) Ferric Reducing Antioxidant Power (FRAP); d) Folin-Ciocalteu reducing capacity; and e) ferrous ion-chelating ability.

Each antioxidant potential assay was analyzed in six concentrations of the algal methanolic extract (2, 4, 6, 8, 10 and 12 $mg.mL^{-1}$). All the assays were protected from photooxidation. Respective blanks at different crude algal extract concentrations were prepared as sample blank for discount from the assay absorbance.

Commercial gallic acid and Trolox (Sigma-Aldrich, Brazil) were used as standard references for antioxidant activity evaluation. Samples were analyzed in a UV-visible 96-well microplate spectrophotometer (Epoch Biotek, USA) by reading the absorbance in the specific wavelength of each assay. Final volume of the each reaction assay was 300 µL.

Results were expressed as:

**1.** percentage of antioxidant activity for ABTS, DPPH, and ferrous ion-chelating using the formula:

$$\%AOA = [(A_c - A_s)/A_c] \times 100$$

where: $A_C$ = absorbance of the negative control, and $A_S$ = absorbance of the sample.

The percentages of activity for FRAP and Folin-Ciocalteu assays were calculated by considering as 100% of activity the algal extract concentration at 10 $mg.mL^{-1}$ and 12 $mg.mL^{-1}$, respectively, and at T10 of the PAR treatment, as the antioxidant activity varies depending on the extract concentrations and the maximal antioxidant potential.

Additionally, the respective concentration in gallic acid equivalent (µg $GAE.mL^{-1}$) was calculated for each percentage, using the curves obtained with the standards.

**2.** milligrams of standard equivalent per gram of algal FW ($mg.g^{-1}$ FW), using the curves obtained with the standards;

3. half-maximal effective concentration (EC50), which is the concentration of the sample to reach 50% of antioxidant activity, using dose-response curves with the software GraphPad Prism v. 6.0 and hyperbolic dose-response adjustment model. Lower values of EC50 represent extracts with better antioxidant potential.

***ABTS free radical scavenging activity.*** The antioxidant assay by ABTS free radical capture was performed according to Torres et al. (2017) and (Santos et al. 2019b), modified from Rufino et al. (2007) and Yang et al. (2011). This assay gives a general screening of the antioxidant potential, since is based on the SET and HAT mechanisms, and consists on the reduction of the ABTS radical (ABTS•) by antioxidants, producing a decrease in absorbance at 734 nm, generated by electrochemical or enzymatic reactions. This methodology is applicable to both lipophilic and hydrophilic antioxidants.

The reaction assay was prepared by mixing 280 μL of ABTS• solution to 20 μL of algal extract, after the incubation for 20 min at room temperature and light-protected the absorbance was read at 734 nm. Gallic acid curve was performed with concentrations in a range of 0 to 1.5 $\mu g.mL^{-1}$ (equivalent to 0 to 0.45 μg) and Trolox curve with concentrations in a range of 0 to 10 $\mu g.mL^{-1}$ (0 to 3 μg) (Table 5).

***DPPH free radical scavenging activity.*** The antioxidant assay by DPPH free radical scavenging activity was determined according to (Pires et al. 2017a) and (Santos et al. 2019b), modified from Brand-Williams et al. (1995) and Rufino et al. (2007a). This method comprises the reduction of the DPPH radical by antioxidants, producing a decrease in absorbance at 515 nm. It is based primarily on the SET mechanism and, marginally, on the HAT mechanism. In the assay, an oxi-reduction reaction occurs when antioxidants react with this stable free radical. DPPH, which presents a violet coloration, is reduced (the unpaired electron of N pairs with the electron yielded by the radical H of an oxidant), making the reaction yellowish and occurring the formation of DPPH-H.

The reaction mixture was prepared with 280 μL of DPPH• solution and 20 μL of algal extract, after the incubation for 30 min at room temperature and light-protected the absorbance was read at 517 nm. Gallic acid curve was performed with concentrations in a range of 0 to 3 $\mu g.mL^{-1}$ (equivalent to 0 to 0.9 μg) and Trolox curve with concentrations in a range of 0 to 10 $\mu g.mL^{-1}$ (equivalent to 0 to 3 μg) (Table 5).

***Ferric Reducing Antioxidant Power (FRAP).*** The antioxidant activity through the FRAP assay was evaluated following the method described in Urrea-victoria et al. (2016)

and Santos et al. (2019), modified from Rufino et al. (2006). This method comprises the SET mechanism and determines the iron reduction in biological fluids and aqueous solutions of pure compounds. At low pH, when ferric tripyridyl hydrazine complex ($Fe^3$ + TPTZ; 2,4,6-Tris(2-pyridyl)-*s*-triazine) is reduced to ferric ion ($Fe^{3+}$), an blue color is produced with a maximum absorption at 595 nm. The reaction is non-specific and any reaction with low reducing power, under the established reaction conditions, will form the ferrous ion ($Fe^{2+}$) from the ferric ion ($Fe^{3+}$). The change in absorbance is directly related to the total reducing power of the electron-donating antioxidants present in the reaction mixture Tandon et al. (2012).

For reaction mixture, the FRAP solution (265 µL) was mixed with 20 µL of algal extract and 15 µL of ultrapure water, incubated for 30 min at 37°C and light-protected, and then the absorbance was read at 595 nm. Gallic acid curve was performed with concentrations in a range of 0 to 4.5 $\mu g.mL^{-1}$ (equivalent to 0 to 1.35 µg) and Trolox curve with concentrations in a range of 0 to 10 $\mu g.mL^{-1}$ (equivalent to 0 to 3 µg) (Table 5).

***Folin-Ciocalteu reducing capacity.*** This procedure was modified by Pires et al. (2017b) and Santos et al. (2019) from Singleton and Rossi (1965) and Waterman and Mole (1994). This method was initially proposed for the analysis of proteins taking advantage of the reagent's activity toward protein tyrosine residue (containing a phenol group) (Folin and Ciocalteu 1927). This method is often used for measuring total phenolic content in a sample and is based on the reducing property of phenolic compounds, which reacts with the Folin-Ciocalteu reagent (a mixture of the heteropoly acids phosphomolybdic acid and phosphotungstic acid) under alkaline conditions reached with the addition of sodium carbonate ($Na_2CO_3$). This leads to the dissociation of a phenolic proton and formation of phenolate anion. The anion is more prone to donating electrons and is able to reduce the reactant, which means that it has a higher reducing capacity, thus forming a blue molybdenum complex (Huang et al. 2005). It should be mentioned that the Folin-Ciocalteu reagent is non-specific for phenolic compounds as it can be reduced by many non-phenolic compounds like vitamin C, Cu(I), nitrogen-containing compounds, reducing sugars, and some inorganic ions (Ikawa et al. 2003).

The reaction mixture was prepared by mixing 200 µL of ultrapure water, 20 µL of algal extract, 20 µL of Folin-Ciocalteu reagent 2 N and 60 µL of $Na_2CO_3$ at 10 $mg.mL^{-1}$, incubated for 30 min at room temperature and light-protected, and then the absorbance was read at 760 nm. Gallic acid curve was performed with concentrations in a range of 0

to 10 μg.mL$^{-1}$ (equivalent to 0 to 3 μg) and Trolox curve with concentrations in a range of 0 to 100 μg.mL$^{-1}$ (equivalent 0 to 30 μg) (Table 5).

***Ferrous ion-chelating ability.*** The antioxidant activity through the ferrous ion-chelating ability was evaluated according to Harb et al. (2016) and Santos et al. (2019) modified from Min et al. (2011). This method also follows the SET mechanism, is based on the ferrozine method from Carter (1971) and determines the ability of the extracts in chelating ferrous ion ($Fe^{2+}$). The ferrozine in the presence of this ion forms a pink complex whose absorbance is determined at 562 nm. When there are chelating agents, less $Fe^{2+}$ ions are available for complex formation with ferrozine, causing a decrease in absorbance at 562 nm.

The reaction mixture was prepared with 250 μL of ammonium acetate solution 10%, 15 μL of ammonium sulfate solution (2 mM), and 20 μL of algal extract, then incubated for 5 min at room temperature and light-protected. After incubation, 15 μL of the ferrozine solution (6.1 mM) was added, incubated for additional 10 min with shaking at 100 rpm and the absorbance was read at 562 nm. Gallic acid curve was performed with concentrations in a range of 0 to 15 μg.mL$^{-1}$ (equivalent to 0 to 4.5 μg) (Table 4).

***Overall Antioxidant Potency Composite Index (OAPCI).*** This index was calculated based on Seerem et al. (2008) by using the obtained values of antioxidant assays for the EC50. An overall antioxidant potency composite index was determined by assigning all assays an equal weight, fixing an index value of 1 to the lowest value of EC50 for each assay, and then calculating an index score for all other samples within the test as follows:

*Antioxidant index score = (sample score/best score)*

The OAPCI was calculated for each assay considering all treatments and for each type of radiation treatment considering an estimation for all assays. For the chelating assay, the index was not calculated, since samples did not reach 50% of the antioxidant activity and then EC50 was not calculated.

**Table 4.** Summary of linear function (y = ax + b) and regression coefficient ($R^2$) for gallic acid and Trolox standards (expressed in µg.mL$^{-1}$ of standard) for each antioxidant assay and the respective conversion factor (CF) in relation to gallic acid.

| Assay | Gallic acid | Trolox |
|---|---|---|
| ABTS | y = -0.3447x + 0.7516<br>R² = 0.9901 | y = -0.0619x + 0.8064<br>R² = 0.9685<br>CF = 5.56 |
| DPPH | y = -0.1912x + 0.7572<br>R² = 0.98 | y = -0.0554x + 0.8135<br>R² = 0.9793<br>CF = 3.45 |
| Folin-Ciocalteu | y = 0.0698x - 0.0033<br>R² = 0.9986 | y = 0.0113x - 0.0024<br>R² = 0.9851<br>CF = 6.17 |
| FRAP | y = 0.4603x + 0.0987<br>R² = 0.994 | y = 0.1198x + 0.1024<br>R² = 0.9948<br>CF = 3.86 |
| Ferrous ion-chelating | y = -0.0591x + 1.6528<br>R² = 0.9747 | --- |

**Antiviral activity.** Antiviral activity of *S. filipendula* under UV radiation treatments during 10 days was assessed by the ability to inhibit the activity of the enzyme HIV-1 reverse transcriptase (HIV-1 RT) using the colorimetric kit for RT assay (Roche, Germany) and based on Woradulayapinij et al. (2005). Two kinds of algal extracts were tested:

a) Methanolic extract: samples of 200 mg FW were grounded in liquid nitrogen, suspended in 1.2 mL of methanol and extracted for 3 h at room temperature. The samples were centrifuged at 8.000 rpm for 5 min at room temperature and the supernatant was recovered into a new microtube. This procedure was repeated two more times and the final methanolic extract was concentrated at 40 °C and then stored at room temperature for further analysis.

b) Aqueous extract: the precipitated material obtained after methanolic extraction was back extracted with 2.4 mL of ultrapure water for 3 h at 80 °C and the supernatant was recovered into a new microtube. This procedure was repeated two more times and the final aqueous extract was concentrated by freeze-dried during three days and stored at room temperature until the analysis.

To choose the algal concentrations for the assay, a preliminary test was conducted with samples exposed to UV radiation (PAR, PAR+UVA, and PAR+UVB) during 10

days. Samples were diluted in DMSO 10% and both methanolic and aqueous extracts were tested for antiviral activity in a concentration of 200 μg.mL$^{-1}$.

Based on the data obtained from the preliminary assay, the following concentrations were tested for the inhibition of the enzyme HIV-1 RT: 200, 400, 600, and 800 μg.mL$^{-1}$ for methanolic extract and 50, 100, 150, and 200 μg.mL$^{-1}$ for aqueous extract, diluting the extracts in DMSO 10% to reach the desire concentrations. A solution of the Foscarnet (sodium phosphonoformate tribasic hexahydrate), which is a commercial antiviral medication and classified as a pyrophosphate analog DNA polymerase inhibitor, was diluted in DMSO 10% at a concentration of 3 μg.mL$^{-1}$ and used as positive control.

The reaction mixture was obtained by adding 20 μL of samples or standards, 19 μL of lysis buffer, 20 μL oligo $(dT)_{15}$+ polyA, and 1 μL of the HIV-1 RT enzyme, in a 200 μL microtube. DMSO 10% without the addition of the enzyme was used as blank and DMSO 10% with the addition of the enzyme as negative control. After incubation for 1 h at 37 °C, the solution was transferred to the reaction modules provided by the kit and remained for a another 1 h at 37 °C. After this incubation period, the modules were washed with wash buffer. The mix prepared with buffer and antibody (200 μL) was added to the wells and incubated for a 1 h at 37 °C. After incubation, the modules were washed with wash buffer and added 200 μL of ABTS solution. Absorbance at 405 and 490 nm was read with UV-visible microplate spectrophotometer (Epoch Biotek, USA). Inhibition of RT was calculated using the following formula:

$$\%\ RT\ inhibiton = \frac{(\mathrm{Abs405\ NC} - \mathrm{Abs490NC}) - (\mathrm{Abs405\ S} - \mathrm{Abs490\ S})}{(\mathrm{Abs405\ NC} - \mathrm{Abs490\ NC})}\ x\ 100$$

where: Abs405 NC: absorbance of negative control at 405 nm; Abs409 NC: absorbance of negative control at 409 nm; Abs405 S: absorbance of sample at 405 nm; Abs409 S: absorbance of sample at 405 nm.

Additionally, effective concentration of the sample to inhibit 50% of viral activity (IC50) was calculated using dose-response curves with the software GraphPad Prism v. 6.0 and hyperbolic dose-response adjustment model. Lower values of IC50 represent extracts with better antiviral potential.

**RESULTS**

**Oxidative DNA damage evaluation**. The oxidative DNA damage was assessed by the quantification of cyclobutane pyrimidine dimers (CPDs). Figure 19 presents the CPD-DNA levels (ng) of *S. filipendula* after 10 days of exposure to PAR, PAR+UVA, and PAR+UVB radiations. No changes were observed when comparing PAR and PAR+UVA treatments, presenting CPDs values of 0.034 ± 0.01 ng and 0.088 ± 0.03 ng, respectively. Nevertheless, samples treated with PAR+UVB presented differences with a notable increase in the CDP-DNA content (2.11 ± 0.82 ng).

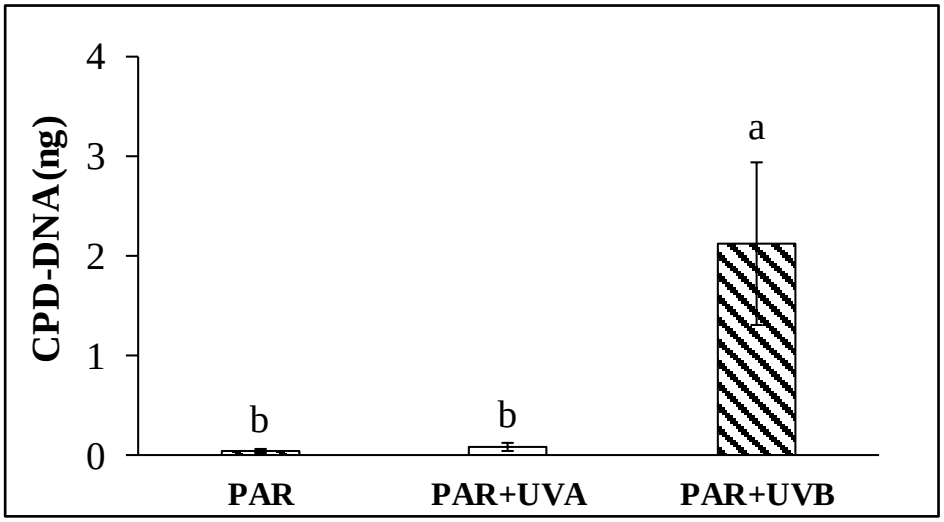


**Figure 18.** CPD-DNA levels of *Sargassum filipendula* after 10 days of exposure to PAR, PAR+UVA, and PAR+UVB radiation treatments ($n$ = 5; mean ± SD). Letters indicate differences according to one-way ANOVA and Newman-Keuls *post-hoc* test ($p < 0.05$).

**Antioxidant potential.** Antioxidant activities from *S. filipendula* extracts at different concentrations using diverse antioxidant assays (except for ferrous ion-chelating ability) are presented in Figure 20, as percentage of antioxidant activity (principal Y axis) and concentration of gallic acid equivalent (µg GAE.mL$^{-1}$). For each radiation treatment, the linear function (y = $a$x +$b$; being $a$ = angular coefficient and $b$ = intercept) and the regression coefficient ($R^2$) were calculated. Dose-dependency was observed for all antioxidant assays, where the lowest concentrations and highest concentrations of crude extract presented the lowest and the highest percentages of antioxidant activity. EC50 was calculated for all assays, except for ferrous ion-chelating ability, since for this assay the antioxidant activity reached values up to 30%. For the other assays, PAR showed the lowest EC50 values, representing major efficiency of antioxidant potential, followed by

PAR+UVA and PAR+UVB (PAR < PAR+UVA < PAR+UVB) (Table 5). Result specifications will be presented below in the respective item for each antioxidant assay.

***ABTS free radical scavenging activity.*** Antioxidant potential by ABTS method showed as percentages of antioxidant activity was close to 100% for all treatments at the major extract concentration tested (12 mg.mL$^{-1}$ of algal extract) (Fig. 20A). Differences among the concentrations of crude extract were observed when considering independently each radiation treatment, being 2 mg.mL$^{-1}$ and 12 mg.mL$^{-1}$ the concentrations with the lowest (~40%; ~0.80 µg GAE.mL$^{-1}$) and highest (~100%; 2.20 µg GAE.mL$^{-1}$) values of ABTS radical scavenging activity, respectively, for all treatments. Changes in antioxidant potential were observed when analyzed between radiation treatments and over the same concentration of crude extracts. At algal concentration of 6 mg.mL$^{-1}$, antioxidant activity for PAR+UVA (~48%) and PAR+UVB (~53%) were lower when comparing against PAR (~64%); a similar trend was observed at algal concentration of 10 mg.mL$^{-1}$, which PAR, PAR+UVA, and PAR+UVB presented ~80%, 64%, and 65% of activity, respectively (Fig. 20A). As angular coefficient represents the level of slope between the variables and dose-dependence relationship, the magnitude of angular coefficient were PAR > PAR+UVB > PAR+UVA (10.201, 9.936, and 10.327, respectively; Fig. 20A).

When analyzed EC50 data for ABTS assay (Table 5), the most efficient treatment was PAR (3.00 ± 0.14 mg.mL$^{-1}$) followed by PAR+UVA (3.60 ± 0.15 mg.mL$^{-1}$) and PAR+UVB (4.15 ± 0.18 mg.mL$^{-1}$).

***DPPH free radical scavenging activity.*** Antioxidant potential by DPPH method is shown in Figure 20B, which differences were observed when comparing within each radiation treatment. Values between 30% and 97% were observed for PAR treatment, which correspond to the algal concentrations of 2 mg.mL$^{-1}$ and 12 mg.mL$^{-1}$, respectively (Fig. 20B). These values represent ~1.00 µg GAE.mL$^{-1}$ and ~4.00 µg GAE mL$^{-1}$, respectively. Differences were also observed when compared radiation treatments at the same crude extract concentration, with a significant reduction in antioxidant activity for PAR+UVA and PAR+UVB in most algal concentrations in relation to the PAR control. Samples treated with PAR+UVB radiation presented the lowest activity potential, registering percentages between 16% and 76%. Lower angular coefficient ($\alpha$) from the linear equation ($y = ax + b$), indicates minor slope between the proportionality of

antioxidant activity and algal crude extract concentration, being this values as PAR > PAR+UVB > PAR+UVA (13.321, 12.226, and 9.681, respectively; Fig. 20B). Samples treated with PAR+UVB radiation showed higher values of EC50 (6.66 ± 0.32 $mg.mL^{-1}$) when compared with PAR (3.80 ± 0.08 $mg.mL^{-1}$) and PAR+UVA (4.45 ± 0.11 $mg.mL^{-1}$) (Table 5).

***Folin-Ciocalteu reducing capacity.*** Antioxidant potential by Folin-Ciocalteu method showed antioxidant activity with values up to 100% for PAR treatment at concentration of 12 $mg.mL^{-1}$ of algal extract (Fig. 20C). Differences between algal extract concentrations were observed when compared individual radiation treatment, with significant increase in antioxidant activity while enhance the concentration of the extract. Differences were observed between the same concentration of crude extracts and the radiation treatments, with the lowest activity for PAR+UVA and PAR+UVB (78% and 67%, respectively, at the highest algal concentration) when compared to the PAR control (Fig. 20C). As angular coefficient represents the level of slope between the variables and dose-dependence relationship, the magnitude of angular coefficient were PAR > PAR+UVA > PAR+UVB (15.251, 11.218, and 9.290, respectively; Fig. 20C). EC50 data for Folin-Ciocalteu assay (Table 5) indicate that extracts exposed to UV radiation treatments showed lower effective phenolic concentration (PAR+UVA = 7.30 ± 0.14 $mg.mL^{-1}$ and PAR+UVB = 9.08 ± 0.25 $mg.mL^{-1}$) than PAR treatment (5.35 ± 0.09 $mg.mL^{-1}$). Additionally, the total phenolic compounds in *S. filipendula* under PAR treatment was calculated with respect to gallic acid equivalent (GAE) and algal extract concentration and compared with literature for *Sargassum* species (Table 6). Since the present study performed the analysis by using extracts from fresh biomass and most of the works use dry extracts, we transformed our data to mg $GAE.g^{-1}$ of dry algal extracts. This transformation was based in the extract yield of *Sargassum* species, which corresponds to 12% ( (Khaled et al. 2012; Pires 2016 pers. comm). For *S. filipendula*, the phenolic concentration was 10 ± 0.11 mg $GAE.g^{-1}$, 8.16 ± 0.10 mg $GAE.g^{-1}$, and 7.16 ± 0.11 mg $GAE.g^{-1}$ for PAR, PAR+UVA, and PAR+UVB, respectively; similar to other species of *Sargassum* (Table 6).

***Ferric Reducing Antioxidant Power (FRAP).*** Antioxidant potential by FRAP method showed antioxidant activity with values near to 100% for PAR and PAR+UVA treatments at the algal concentration of 12 $mg.mL^{-1}$ (Fig. 20D). Dose-dependence was observed between 2 $mg.mL^{-1}$ to 12 $mg.mL^{-1}$ of algal crude extract, equivalent to ~1.00

µg GAE.mL$^{-1}$ and ~2.50 µg GAE.mL$^{-1}$. When compared among the radiations at the same concentration of crude extract, PAR+UVB treatment was significantly lower (~64% antioxidant activity) in relation to PAR and PAR+UVA (~100% antioxidant activity). Lower angular coefficient was reached by PAR+UVB treatment (10.682; Fig. 20D), followed by PAR (12.826) > PAR+UVA (13.599). EC50 values also presented differences (Table 6), showing a better antioxidant efficiency at PAR control samples (2.85 ± 0.12 mg.mL$^{-1}$), followed by PAR+UVA (3.41 ± 0.26 mg.mL$^{-1}$) and finally by PAR+UVB (5.70 ± 0.07 mg.mL$^{-1}$) (Table 5).

***Ferrous ion-chelating ability.*** Antioxidant potential by the metal chelating method achieved values up to 30% for all the tested samples and due to the low antioxidant activity data are not shown. No differences were observed between or within concentrations of extracts and radiation treatments. Since the percentage of antioxidant activity did not reach 50% of antioxidant activity by this assay, EC50 values were not calculated.

***Overall Antioxidant Potency Composite Index (OAPCI).*** As a complementary data, OAPCI was calculated for each antioxidant assay and radiation treatment (Table 7). The OAPCI values were calculated based on the EC50, in which the lowest EC50 value per antioxidant assay represents the index 1 (or 100%), therefore, a lower index means higher potency for the assay. The lowest index per assay was registered for PAR treatment (index 1), followed by PAR+UVA (1.19), and PAR+UVB (1.50). In relation to the assays, ABTS scavenging assay was the most sensitive antioxidant method (Index for assay = 1.05), followed by DPPH (1.25), FRAP (1.30) and finally Folin-Ciocalteu (1.33).

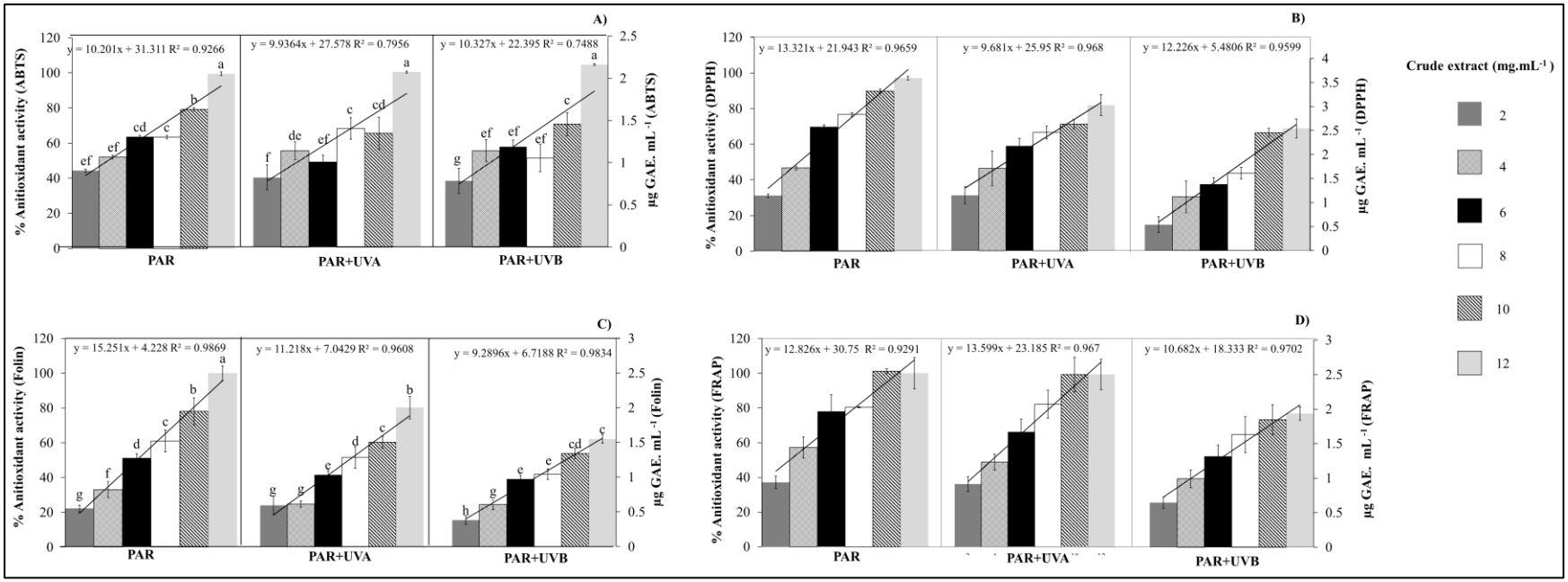


**Figure 19**. Antioxidant activity expressed as percentage and concentration of gallic acid equivalent (reference standard; µg GAE.mL$^{-1}$) of methanolic extracts of *Sargassum filipendula* after 10 days of exposure to different laboratory radiation treatments ($n$ = 5; mean ± SD), assayed at six different concentrations of algal crude extracts (2, 4, 6, 8, 10, and 12 mg.mL$^{-1}$). (A) ABTS free radical scavenging activity; (B) DPPH free radical scavenging activity; (C) Total phenolic compounds; (D) Ferric Reducing Antioxidant Power (FRAP). Letters indicate differences according to bifactorial ANOVA and Newman-Keuls *post-hoc* test ($p < 0.05$). Each assay and radiation treatment includes the linear function ($y = ax + b$) and coefficient of regression ($R^2$).

**Table 5.** Values of EC50 (half maximal effective concentration; $mg.mL^{-1}$) of the methanolic extracts obtained from *Sargassum filipendula* after 10 days of exposure to different laboratory radiation treatments ($n = 3$; mean ± SD). Regard that lower values of EC50 represent extracts with better antioxidant potential. Letters indicate differences according to unifactorial ANOVA, for each assay separately, and Newman-Keuls *post-hoc* test ($p < 0.05$).

| | **EC50 ($mg.mL^{-1}$)** | | |
|---|---|---|---|
| | **PAR** | **PAR+UVA** | **PAR+UVB** |
| **ABTS** | 3.00 ± 0.14 ***c*** | 3.60 ± 0.15 ***b*** | 4.15 ± 0.18 ***a*** |
| **DPPH** | 3.80 ± 0.08 ***c*** | 4.45 ± 0.11 ***b*** | 6.66 ± 0.32 ***a*** |
| **Folin** | 5.35 ± 0.09 ***c*** | 7.30 ± 0.14 ***b*** | 9.08 ± 0.25 ***a*** |
| **Frap** | 2.85 ± 0.12 ***c*** | 3.41 ± 0.26 ***b*** | 5.70 ± 0.07 ***a*** |
| **Chelating** | * | * | * |

* Since the percentage of antioxidant did not reach 50%, EC50 values could not be calculated.

**Table 6**. Total phenolic content by the Folin-Ciocalteu method of *Sargassum filipendula* after exposure to UV radiation and a summary obtained from other authors for *Sargassum* species. Data are expressed as gallic acid equivalent and mass of dry algal extract (mg GAE.$g^{-1}$).

| Species | Extraction information | Total phenolic compounds (mg GAE.$g^{-1}$) | Site | Reference |
|---|---|---|---|---|
| ***S. filipendula* PAR** | Methanol | 10.00 ± 0.11 | Brazil | Present study |
| ***S. filipendula* PAR+UVA** | Methanol | 8.16 ± 0.10 | Brazil | Present study |
| ***S. filipendula* PAR+UVB** | Methanol | 7.16 ± 0.09 | Brazil | Present study |
| ***S. furcatum*** | Dichloromethane/methanol 9 days extraction | 17.00 ± 3.00 | Brazil | (Vasconcelos et al. 2018) |
| ***S. linearifolium*** | Ethanol 70% - Ultrasonic bath 3 times | 47.06 ± 0.65 | Australia | (Dang et al. 2018 |
| ***S. vestitum*** | Ethanol 70%- Ultrasonic bath 3 times | 141.91 ± 3.95 | Australia | (Dang et al. 2018) |
| ***Sargassum* sp.** | | 0.084 ± 0.050 | Indonesia | (Sinjal et al. 2018) |
| ***S. plagiophyllum*** | | 7.48 ± 0.02 | India | (Chakraborty et al. 2017) |
| ***S. myriocystum*** | | 8.71 ± 0.17 | India | (Chakraborty et al. 2017) |
| ***S. linifolium*** | | 10.35 ± 0.92 | Egypt | (Ismail 2017)) |
| ***S. nipponium*** | Methanol 70% | 17.59 ± 0.30 | Korea | (Lee and Kim 2015) |
| ***S. muticum*** | Methanol 70% | 37.98 ± 0.53 | Korea | (Lee and Kim 2015) |
| ***S. fulvellum*** | Methanol 70% | 27.33 ± 0.57 | Korea | (Lee and Kim 2015) |
| ***S. thunbergii*** | Methanol 70% | 19.51 ± 0.42 | Korea | (Lee and Kim 2015) |
| ***S. micracanthum*** | Methanol 70% | 31.29 ± 1.83 | Korea | (Lee and Kim 2015) |
| ***S. tenerrimum*** | | 2.13 ± 0.19 | Iran | (Movahedinia and Heydari 2014) |
| ***S. polycystum*** | Methanol - 3 days | 45.00 ± 3.00 | India | (Matanjun et al. 2008) |
| ***S. siliquastrum*** | Ethanol 24 h extraction - 3 times | 127.37 | Korea | (Cho et al. 2007) |

**Table 7.** Overall antioxidant potency composite index based on EC50 values of *Sargassum filipendula* after exposure to UV radiation. The index was calculated for each antioxidant assay and then used for calculate the Index for assay and the Index for radiation as the mean of columns (Index for assay) or lines (Index for radiation).

| Overall Antioxidant Potency Composite Index | | | | | |
|---|---|---|---|---|---|
| **Radiation treatment** | **ABTS** | **DPPH** | **Folin** | **FRAP** | **Index for radiation** |
| **PAR** | 1.00 | 1.00 | 1.00 | 1.00 | 1.00 |
| **PAR+UVA** | 1.11 | 1.19 | 1.32 | 1.13 | 1.19 |
| **PAR+UVB** | 1.04 | 1.56 | 1.66 | 1.76 | 1.50 |
| **Index for assay** | 1.05 | 1.25 | 1.33 | 1.30 | |

### *Inhibition of HIV-1 reverse transcriptase*

After 10 days of experiment with three different radiation treatments (PAR, PAR+UVA, and PAR+UVB), *S. filipendula* showed inhibitory effects against HIV-1 RT by using different concentrations of methanolic (Fig. 21A) and aqueous extracts (Fig. 7B). The methanolic extracts showed differences between concentrations of algal crude extracts when analyzed each radiation treatment independently (Fig. 21A), presenting a dose-dependency response. For PAR, inhibition values between 45% and 90% were registered; nevertheless, UV radiation treatments did not stimulate the antiviral activity compared to PAR treatment, which decreased values were observed with percentages between 23% and 86% for PAR+UVB, and were lower for PAR+UVA with inhibition between 25% and 65% (Fig. 21A).

Differences were also observed for IC50 of the methanolic extracts, remembering that a low value of IC50 means better inhibitory efficiency. In this case, extracts from PAR samples were more efficient than extracts treated with UV radiation, presenting an IC50 of 264.77 ± 15.07 $\mu g.mL^{-1}$. Within UV extracts, PAR+UVB had better efficiency than PAR+UVA, showing values of 417.40 ± 6.50 $\mu g.mL^{-1}$ and 589.70 ± 56.14 $\mu g.mL^{-1}$, respectively (PAR+UVA > PAR+UVB > PAR). Although the treatments with UV radiation did not stimulate the antiviral activity when comparing to PAR, samples reached values up to 60% for PAR+UVA and 80% for PAR + UVB.

For aqueous extracts (Fig. 21B), the antiviral activity achieved values close to 100% for all the tested samples and in general no differences were observed among concentrations of

algal extracts (50, 100, 150, 200, and 300 µg.mL$^{-1}$) and radiation treatments; therefore, IC50 was not calculated (Fig. 21B).

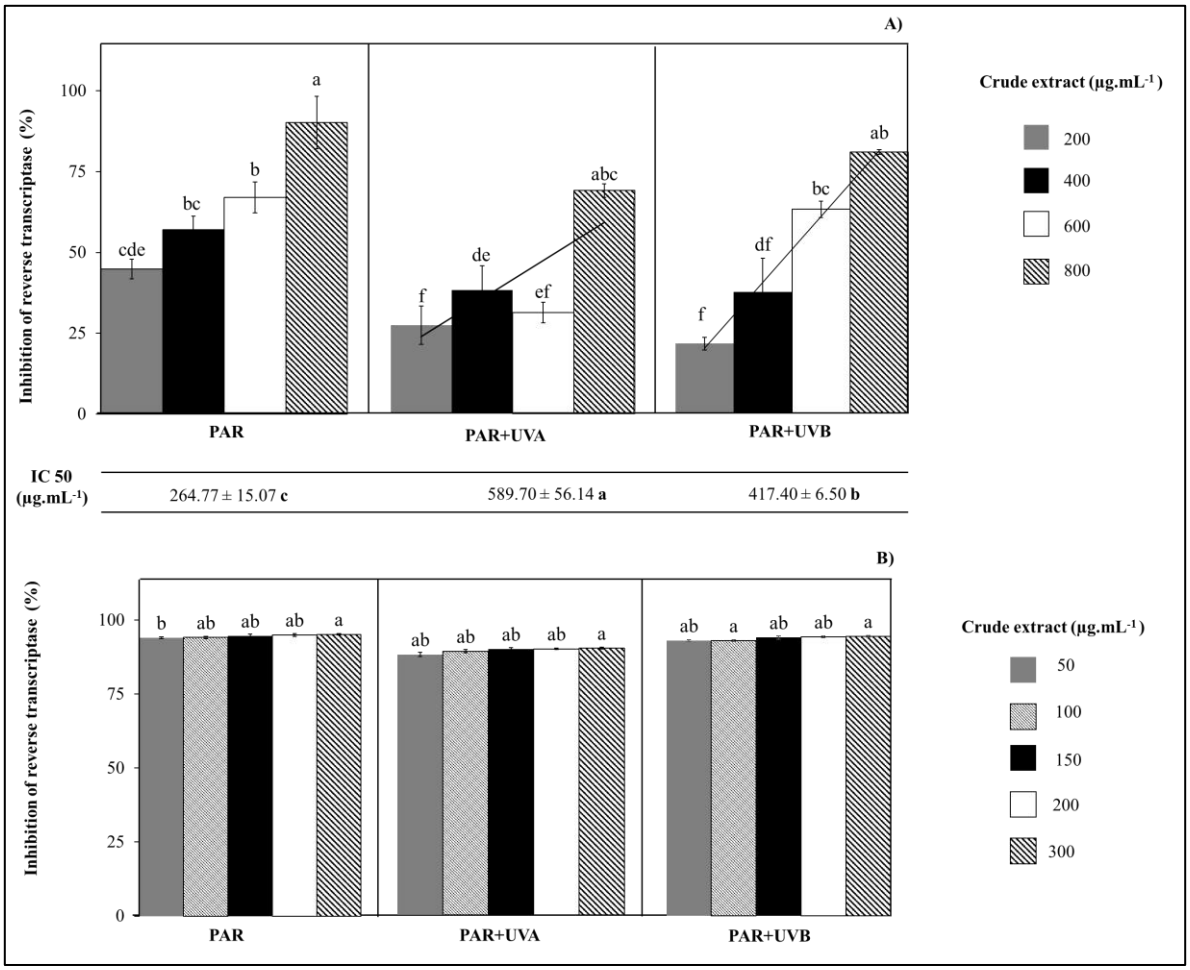


**Figure 20.** Antiviral activity tested as inhibition of HIV-1 RT of *Sargassum filipendula* after 10 days of exposure to different laboratory radiation treatments ($n$ = 3; mean ± SD;). A) Methanolic extracts assayed at four concentrations (200, 400, 600, and 800 µg.mL$^{-1}$); B) Aqueous extracts assayed at five concentrations (50, 100, 150, 200, and 300 µg.mL$^{-1}$). Regard that lower values of IC50 represent extracts with better antioxidant potential. Letters indicate differences according to bifactorial ANOVA and Newman-Keuls *post-hoc* test ($p$ < 0.05). IC50 (µg.mL$^{-1}$) was only calculated for methanolic extracts.

## DISCUSSION

*Sargassum* species are vertically distributed between the lower intertidal ribbon until depths of the infralittoral and constitute an important ecosystem engineering for a diverse marine flora and fauna. As many species of *Sargassum* inhabit the tide interphase, they are

commonly exposed to fluctuating adverse air-water stressors. UV radiation is expected to increase with the human population growth and development and global climate changes. Particularly, because of the highly deleterious effect of UV radiation, it is relevant to understand the biological mechanisms underlying acclimation, sensitivity, tolerance, and repair.

Cyclobutane pyrimidine dimers (CPDs) formation is a DNA mutagenic lesion typically reported after UV radiation exposure for several brown seaweed, responsible for the inhibition in replication of DNA and transcription, and consequent disruption of cell metabolism and division, affecting growth and survival. For the present study, after 10 days of experiment, the moderate UVB radiation dose used here increased at 35-times the CPDs level in *S. filipendula* in relation to PAR and PAR+UVA treatments. The same trend of CPDs spread have been reported for early stages (gametes and zoospores) of the brown seaweeds *L. saccharina*, *L. digitata*, *L. hyperborean* (Gunnerus) Foslie, and *A. mirabilis* (van de Poll et al. 2002; Roleda et al. 2005, 2007b, 2010b), in which the susceptibility to UV exposure is greater compared to adult stages. For *L. saccharina* the authors observed CPDs accumulation after 15 days of exposure to UV radiation and repair process was identified as only 10% of the UV-induced CPDs remained (van de Poll et al. 2002), suggesting then the presence of photolyase activity. Mechanisms of DNA repair, as the enzyme photolyase, are essential dynamic tools for life maintenance and evolution, where specialized repair proteins trigger efficient DNA repair processes, which restore the genetic information, reverse the damage by using the energy of light, and remove the DNA lesions caused by UV radiation (Essen and Klar 2006). Our results did not evaluate a recovery period without the incidence of UV radiation; however, since *S. filipendula* was exposed to a moderate UV dose, we can expect a gradual recovery of the species by lesion recognition proteins.

Excess of UV radiation has been reported to increase the production of reactive species via photosensitizing chromophores in cells, such as tryptophan, nicotinamide adenine dinucleotides, riboflavins, and porphyrins, causing oxidative stress (Wondrak et al. 2006). Moreover, complexes I and II of the respiratory chain favor the generation of mitochondrial reactive oxygen species (ROS) under exposure to this factor (Turrens and Boveris 1980; Turrens 1997), and ROS formed at the NADH dehydrogenase site of complex I are released

into the mitochondrial matrix (Chen et al. 2003). Thereby eliciting oxidative damage to the mitochondrial enzymes, including the complexes of the respiratory chain, enzymes of the Kreb's cycle, and several other sensitive proteins, as well as mtDNA (Bandy and Davison 1990; Zhang et al. 1990; Hausladen and Fridovich 1996). Then, as a photoprotective mechanism to prevent and ameliorate oxidative damage caused by UV radiation, macroalgae improve the production of UV-absorbing compounds, serving as sunscreen (Ruhland et al. 2007). In the case of brown seaweeds, phenolic compounds act as a photoprotection mechanism by the absorption of incident photons (Abdala-Diaz et al. 2006). Therefore, the capability of synthesizing these compounds provides macroalgae the advantage of enhancing tolerance, which enables them to maintain all metabolic processes and to survive in the presence of UV radiation that can induce the activation of antioxidant cell defenses.

High antioxidant activity, close to 100%, was registered at concentrations of crude extracts of *S. filipendula* at 10 and 12 $mg.mL^{-1}$, results that are in agreement with diverse literature data, in which brown seaweed species tend to have high antioxidant potential (Lim et al. 2002; Demirel et al. 2009; Zubia et al. 2009; Budhiyanti et al. 2012). Tropical macroalgae, such as *Sargassum* spp., are expected to develop a very effective antioxidant defense system due to the strong UV radiation in the tropical environment (Zubia et al. 2007) and their partial exposure to air stress during tide fluctuation. Additionally, several studies have shown that many seaweed increase their antioxidant activity in response to this stress condition (Figueroa and Vinegla 2001; Roleda et al. 2006b; de la Coba et al. 2008; Schmidt et al. 2012a; Aigner et al. 2013).

The values of EC50 for *S. filipendula* showed a better index at PAR treatment for all antioxidant assays, evidencing the active action of antioxidant system in the species at non-stressing conditions. However, when *S. filipendula* was submitted to UV radiation, EC50 were higher for the samples exposed to this stress. As a defense strategy, it has been reported for brown seaweeds, the exudation of phenolic compound into the surrounding medium to create an UV-absorbing microenvironment (Roleda et al. 2010a); fact that was observed for the present study (see details in Chapter I). When analyzing UV-visible absorbing spectra of seawater after UV exposure in *S. filipendula*, it was possible to observe maximal absorption bands in the UV region (208-218 nm) suggesting the presence of these compounds, as was reported (Salgado et al. 2005, 2007) the similar wavelength absorption for complex of

phenolic compound and sulfated polysaccharides. The wavelength bands identified for *S. filipendula* presented higher values in PAR+UVA and PAR+UVB treatments, corresponding to an increase of 100% and 200%, respectively in relation to PAR (Chapter I). Then, the general low antioxidant activity after UV radiation exposure, which is attributed to phenolic compounds, could be explained by the significant extrusion into the seawater, thereby reducing the content inside the cells. Moreover, yellowish brown color in the water of these treatments, is another indicator of phenolic compounds into the medium and had been also described for other brown algae (Roleda et al. 2010b; Polo et al. 2014a).

By comparing data from total phenolic compounds (mg GAE.$g^{-1}$) within several *Sargassum* species, our results showed similar content in relation to other species as *S. furcatum* Kutzing (Vasconcelos et al. 2018), *S. plagiophyllum* (Chakraborty et al. 2017), and *S. linifolium* (Ismail 2017), which presented values of 17.00 ± 3.00 mg GAE.$g^{-1}$, 7.48 ± 0.02 mg GAE.$g^{-1}$, and 10.35 ± 0.92 mg GAE.$g^{-1}$, respectively. Other species as *S. linearifolium* (Turner) C. Agardh (Dang et al. 2018), *S. muticum* (Lee and Kim 2015), and *S. siliquastrum* reported higher phenolic contents than *S. filipendula*, 47.06 ± 0.65 mg GAE.$g^{-1}$, 37.98 ± 0.53 mg GAE.$g^{-1}$, and 127.37 mg GAE.$g^{-1}$, respectively. These findings indicate that phenolic content can vary depending on the species and several biotic factors (reproductive stages, age, herbivory) and abiotic factors (sun exposure, depth, salinity) modulating the accumulation of phlorotannins (Connan et al. 2006b).

Even with this reduction of antioxidant activity caused by UV radiation, samples of *S. filipendula* reached more than 50% of activity at the higher algal extract concentration for all assays, and showed to be more effective than other species of *Sargassum*. For example, in the study of Rastian et al. (2016), algal extract concentration nearly of 100 mg.$mL^{-1}$ of ethanolic extract (from dry samples) in *S. boveanum* J. Agardh resulted in 90% of antioxidant potential by the DPPH assay, while in our study we registered at 2.4 mg.$mL^{-1}$ of methanolic extract of *S filipendula* ~97%, 82%, and 76% for PAR, PAR+UVA, and PAR+UVB, respectively, for the same DPPH assay; and similar results were found for the other tested assays.

It has been reported that the interaction between antioxidant and DPPH could be dependent on the structural conformation of antioxidant (Sánchez-Moreno 2002); feature that

may give the assay the ability to differentiate phenolic compounds among several compounds usually present in natural system capable of exhibit antioxidant activity. Then, from our results we can infer that the obtained methanolic extracts from *S. filipendula* have antioxidant composition, which may act as free-radical inhibitors. Besides the presence of phenolic compounds with antioxidant action, other compounds such as sargaquinoic acid, sargachromenol, and fucosterol, capable of deactivating DPPH and $ABTS^{+}$ radicals, have been also reported within the genus (Wang et al. 2009).

When compare the EC50 values obtained by DPPH and ABTS assays (methods based on radical scavenging activity), differences were observed between other *Sargassum* species. Here, we reporting EC50 values of ~0.68 $mg.mL^{-1}$, ~0.8 $mg.mL^{-1}$, and ~1.0 $mg.mL^{-1}$ for PAR, PAR+UVA, and PAR+UVB, respectively, different than Vinayak et al. (2011), where EC50 from methanolic extracts was 2.87 $mg.mL^{-1}$. Higher EC50 was also reported by Zubia et al. (2007) when analyzed ethanolic extracts from *S. ramifolium* Kuetzing and *S. pteropleuron* Grunow, being 6.64 $mg.mL^{-1}$ and 7.14 $mg.mL^{-1}$, respectively. These findings demonstrate that even at UV radiation treatments, *S. filipendula* extracts kept an efficient antioxidant characteristic. Additionally, DPPH and $ABTS^{+}$ activities might be explained because the presence of compounds with multiple -OH groups and/or center of unsaturation, which enabled them to donate a proton to free radical by hydrogen atom transfer (HAT) to deactivate the free radicals, as reported by Maneesh et al. (2017) when analyzed antioxidant activity in methanolic/ethyl acetate extracts with in *S. wightii*.

Potential $Fe^{2+}$ ion chelating ability has been reported for brown seaweeds and attributed to phenolic compounds, such as phlorotannins (Karawita et al. 2005). Despite low activity reported by *S. filipendula* in all treatments when testing the ferrous ion-chelating ability; FRAP method at a concentration of 12 $mg.mL^{-1}$ showed antioxidant values ~100% for PAR and PAR+UVA, and ~80% for PAR+UVB. This chelating ability is probably related to the vicinity of phenolic moieties, which bond with $Fe^{2+}$, diminishing the redox potential and balance out the oxidized type of $Fe^{2+}$ (Maneesh et al. 2017).

When analyzed together all assays for testing the antioxidant activity of extracts from *S. filipendula*, it was possible to observe that ABTS and DPPH methods based on radical scavenging activity presented the lowest OAPCI, followed by ferric reducing power, and

finally Folin index reported the highest value. As stated before, index calculations were based on EC50 values, then lower values means higher sensitive to the assay. Differences could be related with the pH condition sample (neutral for the present study), since ABTS and DPPH index showed higher sensitivity at neutral pH, in relation to the assays with acidic (FRAP) or alkaline (Folin-Ciocalteu) reaction pHs (Apak et al. 2016).

For the present study, five different antioxidant methods were tested, however, several assays have been developed due to the complexity and diversity of research topics, and none has gained universal acceptance. Thus, a major challenge in this kind of investigations is to know which method is best suited for a particular future application, knowing that antioxidants may exert their effect through various mechanisms such as scavenging radicals, sequestering transition metal ions, decomposing hydrogen peroxide or hydroperoxides, quenching active prooxidants, and repairing biological damage (Niki and Noguchi 2000).

Another standpoint highlighted in relation to the effect of UV radiation is the activation or suppression of secondary metabolites with different biological activity, such as antiviral activity. Therefore, in the present study, the inhibition of the HIV-1 RT by methanolic and aqueous extracts from *S. filipendula* were studied under UV treatments. Methanolic extracts of *S. filipendula* at concentrations of 200 to 800 $\mu g.mL^{-1}$ showed values of RT inhibition ranging from 25% to 90%, close that found by Ahn et al. (2002) for some species of *Sargassum*, reached an inhibition of HIV-1 RT above 50% at concentration of 200 $\mu g.mL^{-1}$. These results are similar to our findings when we compare samples from the control (PAR), in which the percentage of inhibition achieved similar values in the same algal extract concentration. Nevertheless, samples treated with UV radiation only achieved inhibition values higher than 50% when using concentrations of methanolic extract between 600 and 800 $\mu g.mL^{-1}$. Currently, there is no evidence that confirm affection of the antiviral activity of seaweed by UV radiation. However, the low inhibition observed in *S. filipendula* after exposure to UV could be related with the exudation and migration of phenolic compounds to the seawater, more specifically phlorotannins, through the cell wall in response to the stimuli caused by this type of radiation (Polo et al. 2014), which means that there is a reduction of these compounds inside the algae, as was stated for the antioxidant activity.

Despite the percentage of inhibition reached by methanolic extracts of samples exposed to UV radiation, we can suggested that phenolic compounds could be responsible for this activity, since it has been reported that phlorotannins can inhibit the polymerase and ribonuclease activities of HIV-1 RT (Ahn et al. 2004, 2008). Some researchers have been focused on the isolation of these compounds from brown algae in order study the potential to inhibit of HIV-1 RT. Ahn et al. (2004) isolated two phlorotannins from *E. cava*: 8,8'-bieckol and 8,4'''-dieckol which are dimers of eckol. Both compounds presented inhibition against HIV-1 RT with IC50 values of 0.0005 $\mu g.mL^{-1}$ and 0.0053 $\mu g.mL^{-1}$, respectively. Since the 8,8'-bieckol showed a higher activity, it has been suggested that it might be employed as a drug candidate for the development of new generation therapeutic agents against HIV. Another phlorotannin isolated from the same species is 6,6'-bieckol, which has presented inhibition of HIV-1 RT with a IC50 value of 0.00107 $\mu g.mL^{-1}$ and reduction of cytopathic effects; thus, having potential as a safe therapeutic agent (Artan et al. 2008).

The diphlorethohydroxycarmalol is another phlorotannin that has been assayed for inhibitory activity against HIV-1 RT, presenting a IC50 value of 0.0091 $\mu g.mL^{-1}$ (Ahn et al. 2006). This compound has also been isolated from the brown algae *I. okamurae.* In relation to these studies, *S. filipendula* presented IC50 values of 238.97, 644.01 and 372.94 $\mu g.mL^{-1}$ for PAR, PAR+UVA, and PAR+UVB, respectively. However, we must take into account that inhibition of HIV-1 RT here tested, was made from methanolic crude extracts, without any fractioning, pre-extraction or purification processes that could cleanse or concentrate the most active metabolites, and even though it was possible to reached up 90% of inhibition.

For aqueous extracts of *S. filipendula*, HIV-1 RT inhibition reached almost 100% for all samples at all tested extract concentrations that could be attributed to sulfated polysaccharides, compounds containing ester sulfate groups in their sugar residues, and are rich constituents of seaweed's cell wall that represents more than 50% of the dry weight (Wang et al. 2012). Several authors have reported that antiviral activity of macroalgae aqueous extracts is associated to the presence of these compounds (Kremb et al. 2014; Thuy et al. 2015; Zaid et al. 2017). Sulfated polysaccharides can act as virus adsorption blockers in the host cell (De Clercq 2000) and as competitive inhibitors, preventing the connection

between the reverse transcriptase enzyme and the reverse transcription initiator (Viennois et al. 2013).

Additionally, sulfated polysaccharides have attracted the attention due to the many beneficial biological activities such as anticoagulant (Mao et al. 2009), anticancer (Synytsya et al. 2010; Zandi et al. 2010), anti-inflammatory (Na et al. 2010), and antiviral (Schaeffer and Krylov 2000). Moreover, isolated sulfated polysaccharides from some species of *Sargassum* like *S. patens* C. Agardh (Zhu et al. 2004), *S. tenerrimum* J. Agardh (Sinha et al. 2010), and *S. trichophyllum* (Kützing) Kuntze (Lee et al. 2011) have been tested for antiviral activity, showing promising results against retroviruses. Thus, they are a very important resource for the development of novel drugs.

Summarizing, our results suggest that *S. filipendula* develop an effective antioxidant defense system against UV radiation, which may be consider an adaptation to high solar radiation. The presence of phenolic compounds within the extracts and the seawater, in which they were cultivated, are important characteristic responsible for the evolutionary success of the group (Abdala-Diaz et al. 2006), playing a vital role in scavenging free radicals and assure the protection of the species from photoxidation. Moreover, our research shows, that even without stimulation of the antiviral activity by UV radiation, the species presented efficient inhibition against HIV-1 reverse transcriptase when using methanolic and aqueous extracts at different concentrations., reinforcing the elevate bioactivity of *S. filipendula* composition. Thus, we can suggest that the species could be a potential rich source of a natural antiviral and further isolation of compounds will help us to understand the mechanisms behind the antiviral activity observed herein. In addition, this kind of studies are valuable since they bring an initial screening of potential compounds suitable for development of nutraceutical, cosmeceutical, and pharmaceutical products.

# Chapter III

## Proteomics

## Chapter III

Assessment of quantitative proteomic profile of the brown seaweed *Sargassum filipendula*: UV-mediated responses


### ABSTRACT

Increasing exposure to UV radiation is a factor that can have a negative impact on the health of aquatic organisms as seaweeds, which are of particular significance within the coastal ecosystems. Then, changes in the metabolic control mechanisms hidden behind this physiological trait still need to be further investigated; however, information on the physiological and molecular regulation in algae associated with rising exposure to UV radiation is still scarce. Therefore, our objective was to evaluate the proteome changes of the sub-tropical seaweed *Sargassum filipendula* exposed to PAR (control), PAR+UVA, and PAR+UVB treatments by the analysis of differential abundance of proteins based on the shotgun proteomic approach. In order to obtain the highest yield of protein extraction, three extraction methods were tested: TCA-acetone, phenol, and phenol/protease inhibitor cocktail extractions. Phenol/protease inhibitor cocktail extraction method yielded 2-times more protein amount than phenol method, showing to be the most efficient procedure. Differential abundance of proteins were assessed by two-dimensional electrophoresis (2-DE) analysis and shotgun mass spectrometry analysis; nevertheless, 2-DE analysis provided very limited information and restrictions on its feasibility, then label-free shotgun proteomic analysis allowed a more comprehensive and mid-scale proteomic analysis. The obtained peptide data from *S. filipendula* under the UV radiation treatments were blasted against Sargassum-, Fucales-, and Ectocarpus-Uniprot databases, and larger matches were gained with Ectocarpus-Uniprot database. From the data against Ectocarpus-Uniprot database, 767 proteins were identified, in which 40 of these proteins were differentially abundant within treatments. The 40 proteins were classified according to its metabolism function and were mainly related with photosynthesis (32%), energy (12%), carbohydrate (7%), ROS scavenging defense and stress (7%). Additionally, 17% corresponds to other metabolisms, and 24% of uncharacterized peptides. Our results have giving so far insights into UV stress responses in *S. filipendula* from a proteomic view, which suggests that this stressor may have a severe effect on proteins by the inhibition of its functions. Additionally, this analysis could

provide target proteins that could improve the ability of *S. filipendula* to adapt to UV exposure. Therefore, proteome studies may lead to identify the proteins involved in stress responses and contribute significantly in our understanding of the molecular mechanisms underlying stress tolerance.

## INTRODUCTION

Discover the function of genes whose expression responds to the stress caused by the effects of UV radiation is essential for understanding the molecular bases that determine the main characteristics of the dynamic responses of stress-responsive genes (de Nadal et al. 2011). However, it is important to correlate and confirm the information through systematic integrated data sets on transcription studies of messenger RNA (transcriptomic) with those that address the protein translation (proteomic). Several studies have shown that changes in transcripts do not correspond effectively to changes in protein synthesis, and only direct measurements of the proteins can reveal the correct functional changes (Ghazalpou et al. 2011).

Proteomic is the large-scale study of the total protein content of an organism or part of them, including their structure and physiological role or function that helps in the protein identification and their understanding of metabolic functioning and regulatory alterations during different stages of the life cycle or under stress conditions. One of the main challenges in proteomic studies is the analysis of differential abundance of proteins under different conditions as stages of life cycle or abiotic stress and, more precisely, the identification of proteins whose encoding genes that exhibit profile differences in composition and abundance.

Proteins are the direct effectors of all forms of live responses to stress, not only including enzymes that mediate changes in metabolic levels, but also serving as components of replication, transcription, and translation machineries (Xu et al. 2013). Therefore, proteome studies may lead to identify proteins involved in stress responses and contribute significantly in our understanding of the molecular mechanisms underlying stress tolerance.

With the development and enhancement of protein separation and identification techniques, comparative proteomic in land plants has evolved into a powerful tool for the identification of proteins previously unrecognized in response to an abiotic stress (*i.e.* heavy metal, UV radiation, light, temperature, nutrient availability) (Kosová et al. 2011). Although, there are few studies with marine algae, these technical tool advances have made possible to increase more pioneering researches with macroalgae. In general, the extraction of proteins in any macroalga is difficult due to the presence of large percentage of water into the cells

(*ca.* 80%), which yield low amount of total proteins. Additionally, many species such as brown algae present secondary metabolites, mainly polysaccharides and polyphenols that contaminate the sample and cause proteins to precipitate or degradation or generate artifact results, especially in approaches that include two-dimensional electrophoresis gels (2-DE) (Yotsukura et al. 2010). Therefore, the extraction procedure is a key point for proteomic approaches, in which the achievement of high protein yields with better purity and integrity are desirable.

Studies with brown macroalgae describe extraction methods to find the best protocol, and protein identification by 2-DE gels from *Scytosiphon gracilis* Kogame, *Ectocarpus siliculosus* (Dillwyn) Lyngb (Contreras et al. 2008), *Saccharina japonica* (Areschoug) C.E. Lane, C. Mayes, Druehl & G.W. Saunders (Kim et al. 2011), and *E. kurome* (Yotsukura et al. 2010). These works include Tris buffer (lysis buffer), trichloroacetic acid (TCA)/acetone precipitation, urea, and phenol extraction methods. Studies with *S. gracilis* comparing the extraction methods showed that no protein spots were yielded in the 2-DE gel with urea; however, phenol extraction gave the best results and 30 polypeptides appeared neatly identifiable over a pale background resulting from a low level of contaminants. In *E. siliculosus*, protein extraction was adequate with all methods and also approximately 30 polypeptides appear clearly resolved. The differences of efficiency in the extraction methods for both species could be related with the structure of the thallus with higher contents of polysaccharides and polyphenols in *S. gracilis*, which interfere with protein fractionation (Contreras et al. 2008). The results of the protein identification showed peptides involved in several primary metabolic pathways like carbon fixation, protein synthesis, and oxidative phosphorylation; and others related to stress responses, such as glutathione-*S*-transferase and peroxiredoxins, and heat-shock proteins (protein folding). Independent of the species, all the results from the studies mentioned above showed that the phenol extraction method is the one that presents the greater efficiency for the extraction of proteins in macroalgae.

Other proteomic studies include the identification of proteins involved in tolerance or stress defenses after exposure to abiotic factors such as high temperature and heavy metals such as copper (Cu) and cadmium (Cd). Proteome analysis in those studies identified new proteins that may reveal the relationship of other metabolic pathways involved in stress

tolerance. In *E. cava*, protein profile was markedly affected when the cultivation temperature was increased leading to a rise in the amounts of photosynthesis-related proteins, which catalyzes the elimination of active oxygen species (Yotsukura et al. 2012). In *E. siliculosus*, lethal Cu concentrations induced the expression of proteins that underlie the crucial importance of certain metabolic pathways during the response to Cu stress, and accumulation of proteins involved in pathways related to energy production such as the pentose phosphate pathway were identify. By employing a proteomic strategy, Zhang et al. (2015) and Zou et al. (2015) investigated patterns of differentially enriched proteins in *Sargassum fusiforme* when exposed to different concentration of Cd and Cu. Results shown that the global proteome profiling led to the identification of several pathways that are activated in response to both metals and distinct patterns of protein regulation were observed under these conditions. In the case of Cd exposure, a down-regulation of primary carbon metabolism was observed; nevertheless, the high abundance of proteins associated with mRNA translation and protein folding indicates that *S. fusiforme* attempts to correct the errors in gene information processing to maintain cell survival. Exposure to Cu lead to an induction to proteins related to carbohydrate metabolism, protein destination, RNA degradation, and signaling regulation; moreover, novel target proteins involved to other metabolic pathways in Cu tolerance, such as riboflavin metabolism, were identified.

The cited researches, and almost all studies with algal proteomic approaches, have employed the proteomic analysis by the implementation of two dimensional electrophoresis (2-DE) in polyacrylamide gel. In this technic, proteins are separated by two properties in two dimensions on 2-DE gels. In the first dimension, proteins are resolved according to their isoelectric points (pIs), and in the second dimension, proteins are separated according to their molecular weight (O'Farrell 1975). However, as a disadvantage this approach could underestimate the data provided leading to a loss of valuable information. One of the major issues within 2-DE analysis, is the fact that spots on a given gel often contain more than one protein, making quantification ambiguous since it is not immediately apparent which protein in the spot has changed. Additionally, any 2-DE gel approach is subject to the restrictions imposed by the gel method, as limited dynamic range, difficulty handling hydrophobic proteins, and difficulty detecting proteins with extreme molecular weights and pI values. Furthermore, reproducibility of gels, increased bench time, complexity of sample

preparation, requirement for higher sample concentration, and high cost of the reagents are other concern issues (Zhu et al. 2010).

Due to the limitations that arise from 2-DE, the development of non-gel-based, "shotgun" proteomic techniques together label-free quantification (LFQ) method, provides powerful tools for studying large-scale protein expression and characterization in complex biological systems. LFQ determines the relative amount of proteins in two or more biological samples, but unlike other quantitative methods, is does not use a stable isotope that chemically binds and labels the protein. In this approach, each sample is separately prepared, then subjected to individual Liquid Chromatography coupled with tandem Mass Spectrometry (LC-MS/MS) or two-dimensional Liquid Chromatography (LC/LC). Protein quantification is generally based on the measurements of ion intensity changes such as peptide peak areas or peak heights in chromatography, and the spectral counting of identified proteins after MS/MS analysis. The spectral count-based label-free method allows both relative and absolute quantification of protein abundance. Additionally, these approaches have provided rigorous, powerful tools for analyzing protein changes in large-scale proteomic studies (Monteoliva and Albar 2004; Zhu et al. 2010).

Despite the advantages of shotgun proteomic techniques, there are not available researches that include this approach in brown seaweeds, and all studies are with microalgae; even more, the number of proteomic studies based on 2-DE gels, which evaluates stress responses in macroalgae, are scarce. Therefore, more studies are needed to expand our understanding of protein metabolic regulation under abiotic stress as UV radiation exposure and the mechanisms that underlie physiological acclimation and adaptation to this factor, especially with a more extensive and comprehensive mid- and large-scale analysis. Additionally, within the brown seaweeds, *Sargassum* species are valuable ecosystemic organisms as community structuring in tropical and subtropical marine habitats (Széchy et al. 2006) and include potentially prospecting species due the high content of bioactive compounds (Iwashima et al. 2005; Hwang et al. 2010; Sinha et al. 2010; Yende et al. 2014), thereafter, constitute a biological model extremely relevant for future outlines of ecophysiological studies and technological applications. Thereat, proteomic studies could contribute to a better understanding of its biology, as well as of responses to stress conditions

and global climate changes, besides providing subsidies for decision-making of monitoring and mitigation programs. In this context, the aim of the chapter was to identify the major revealed proteins and evaluate the differential proteome profile of the sub-tropical seaweed *Sargassum filipendula* under PAR, PAR+UVA, and PAR+UVB treatments.

## MATERIAL AND METHODS

**Collection site and algal material.** Specimens of *S. filipendula* were collected at Cigarras Beach (24°43'55.74"S and 45°23'54.48"W), localized in São Sebastião, North coast of São Paulo State, Brazil, during the spring season (October 2016). Cleaned apical portions (± 8 cm) were acclimated for one week under laboratory conditions (details are addressed in General material and methods, section 1).

**Laboratory conditions and experimental setup.** After the acclimation period, the material was exposed for 3 h to different radiation treatments: a) PAR (control treatment), b) PAR+UVB, and c) PAR+UVA. UVB (312 nm; 1.5 $W.m^{-2}$; 16.2 $kJ.m^{-2}$ /day) and UVA (365 nm; 7 $W.m^{-2}$; 75.6 $kJ.m^{-2}$ /day) radiations were provided by Philips lamps models TL 20W/12 and Actinic BL TL-K 40 W/10-R, respectively (details are addressed in General material and methods, section 3). Samples were collected after four days (T4) exposed to UV radiation from three independent replicates for each treatment.

**Proteomic analysis.** Proteomic analysis was performed in collaboration with Dr. Eny I.S. Floh and Dr. Andre Luis Wendt dos Santos from the Laboratory of Cellular Biology of Plants (BIOCEL) of the Institute of Biosciences at University of São Paulo. Initially, the proteomic profile of *S. filipendula* was analyzed using a 2-DE gels approach. This method enables separation of complex proteins mixtures in respect to their pI (isoelectric point), molecular weight, solubility, and relative abundance. Moreover, 2-DE provides information on protein changes in their quantitative and qualitative levels, isoforms, and posttranslational modifications (Rabilloud and Lelong 2011). However, due to several difficulties in this process such as degradation of the proteins in the gels, it was not feasible to compare differential protein abundance between the control and samples treated with UV radiation, as was initially proposed, then the few advances with 2-DE gels are presented. Consequently, we decided to analyze the protein identification by mass spectrophotometry with direct

injection of the protein solution to the equipment (shotgun analysis). Shotgun proteomic refers to a use of bottom-up proteomic techniques to study the whole proteins in a complex mixture, allowing a mid- and large-scale approaches. It utilizes the High Performance Liquid Chromatography (HPLC) in combination with Mass Spectrometry (MS) technologies. The most distinctive feature of shotgun proteomics is that it enables identification and comparative quantification of a wide range of proteins at the same time with minimal protein separation needed. Protein mixtures are first digested by protease, and the resulting peptides separated in HPLC, followed by tandem MS/MS analysis to identify the sequence of each peptide. The identified peptide sequences are compared with available databases, in searching for the corresponding protein identity (Zhang et al. 2013).

**Protein extraction.** Protein extraction is a crucial step for a successful proteomic analysis. In order to determine the best protocol for protein extraction, a bibliographical review was carried out on the methods used for brown algae, allowing the selection of possible procedures and know difficulties for further analysis. Based on the review, TCA-acetone and phenol extraction methods were tested with *Sargassum* spp. collected in Cibratel II Beach, localized in Ubatuba, South coast of São Paulo State, Brazil, during the spring season (November 2015), wet transported in net bags into cooler boxes to the laboratory where were cleaned of macroepiphytes and washed with abundant filtered seawater and kept in -80°C until analysis. For TCA-acetone method one sample was tested, while for phenol method two samples were used, one without proteinase inhibitor cocktail and one with it. After extraction with the three methodologies, proteins were quantified with the 2-D-Quant kit (GE Healthcare Life Sciences, USA), and details of the quantification process is described hereafter in the item *Protein quantification.*

***Extraction with TCA (trichloroacetic acid)-acetone.*** TCA-acetone precipitation method is commonly used to remove interfering compounds such as phenolic compounds, pigments, lipids, nucleic acids, among others. This procedure has shown that TCA precipitation efficiently inhibits protease activity in plant tissues (Wu and Wang 1984).

Approximately 10 g of fresh frozen sample were ground into a fine powder using the equipment TissueLysser II (Quiagen, Germany), suspended in 30 mL of extraction buffer containing TCA 10% and acetone and extracted by shaking for 1 h at 4 °C. The homogenate

was centrifuge at 6.500 rpm and 4 °C for 10 min to pelleted the proteins. Pellet was resuspended in isoelectric focusing buffer (9 M urea; 4% CHAPS; 20 mM DTT; 1.2% Pharmalytes pH 4 to 7 non-linear; and 10%PMSF added freshly) by shaking for 1 h at room temperature. Finally, the homogenate was centrifuged for 15 min at 13.500 rpm.

***Phenol extraction.*** Protein extraction using the phenol method allows efficient protein recovery and removes non-protein components as polysaccharides, lipids, and phenolic compounds, contaminants also found in brown algae. This procedure has a high clean-up capacity, also acting as a dissociating agent to decrease molecular interaction between proteins and other materials (Carpentier et al. 2005). Proteins were extracted following the phenol extraction method reported for brown algae and according to (Zou et al. 2015).

Two samples of approximately 10 g of fresh frozen biomass (Fig. 21A) were ground into a fine powder using the TissueLysser II (Fig. 21B-C) and suspended in 30 mL of extraction buffer (0.9 M sucrose; 0.1 M Tris–HCl; 0.01 M EDTA; 0.1 M KCl) (Fig. 21D). Just before the extraction, 2% β-mercaptoethanol and 1 mM phenylmethylsulfonyl fluoride (PMSF) were added. The biological material was extracted by shaking for 1 h at 4 °C and then mixed with an equal volume of saturated phenol (pH 8.0) and incubated on a shaker for 10 min at room temperature. The homogenate was centrifuge at 6.500 rpm and 4 °C for 10 min. Phenolic phase, which was on top of the homogenate (Fig. 21E), was carefully recovered to avoid contact with the interphase homogenate, poured into a new microtube and back-extracted with 30 mL of extraction buffer (Fig. 21F). Samples were shaken for 3 min, vortexed and centrifuged at 6.500 rpm and 4 °C for 10 min. The final collection of phenolic phase was mixed with five volumes of precipitation buffer (0.1 M ammonium acetate in cold methanol). Samples were incubated overnight at −20 °C. Proteins were pelleted by centrifugation at 6.500 rpm and 4 °C for 10 min and the pellet was washed three times with cooled precipitation solution and finally with cooled acetone. The pellets were air-dried and recovered by shaking for 1 h at room temperature with freshly isoelectric focusing buffer. One sample was recovered with buffer containing 9 M urea, 2 M thiourea, 4% CHAPS, 20 mM DTT, 1.2% Pharmalytes pH 4 to 7 non-linear, and 10% PMSF; and the other sample was recovered with the same previous buffer plus a Protease Inhibitor Cocktail (Sigma-

Aldrich, USA) for avoiding protein degradation. Finally, the homogenates were centrifuged for 15 min at 13.500 rpm and room temperature.

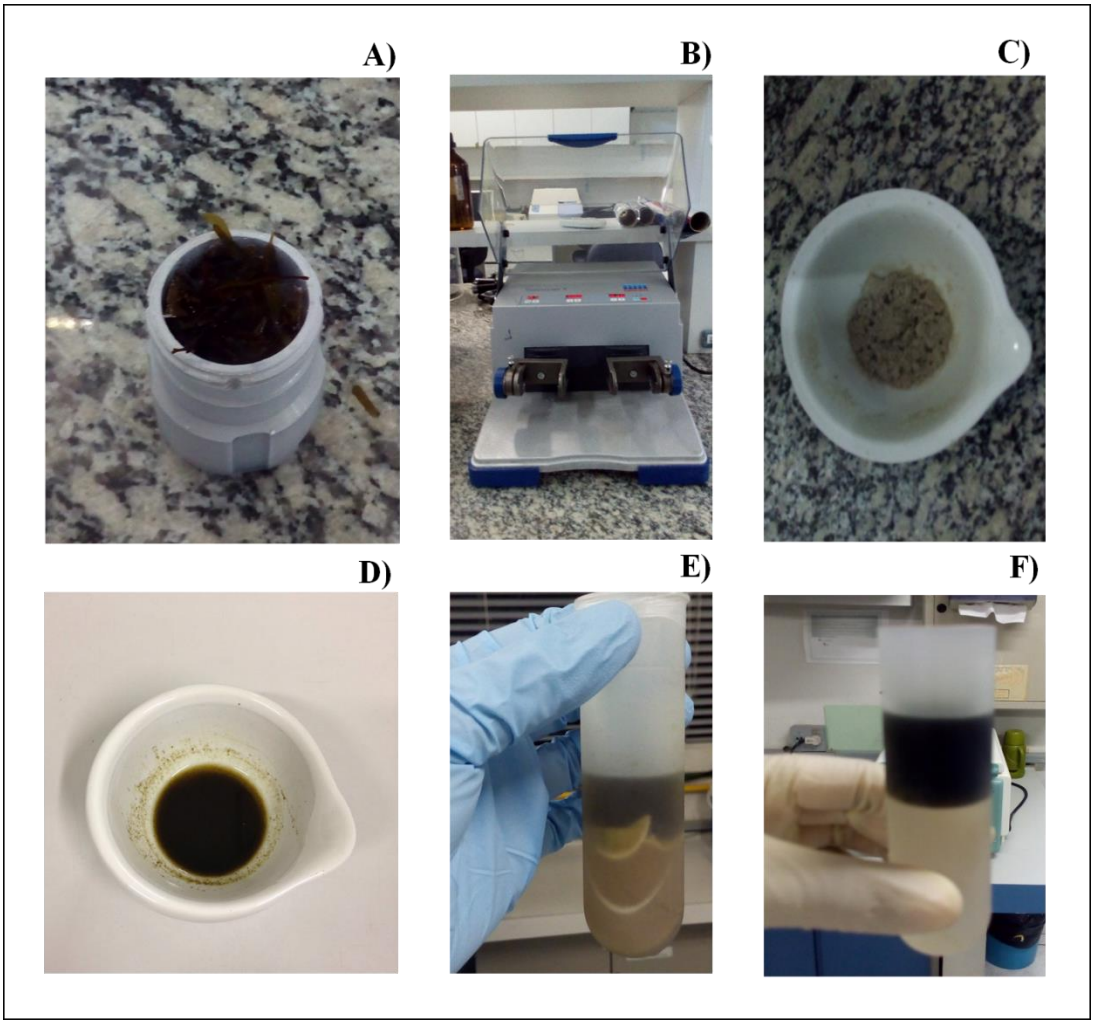


**Figure 21.** Methodological steps for protein extraction of *Sargassum filipendula*. A) Frozen sample in liquid nitrogen; B) Equipment for sample maceration, TissueLysser II; C) Sample ground into a fine powder; D) Sample resuspended in extraction buffer; E) Separation of phenol phase; F) Upper phase containing proteins.

***Protein quantification.*** Supernatants of extracted proteins were quantified with the 2-D-Quant kit (GE Healthcare Life Sciences, USA) according to manufacturer's specifications. This assay is based on the specific binding of copper ions to protein. Precipitated proteins were resuspended in a copper-containing solution and unbound copper is measured with a colorimetric agent (working color reagent). The assay had a linear response to protein in the range of 0–33 $\mu g.mL^{-1}$ and used BSA (bovine serum albumin) as standard. Absorbance's of each sample and standard were read at 480 nm using UV-visible microplate

spectrophotometer (Epoch Biotek, USA). Finally, a standard curve was generated by plotting the absorbance of the standard against the quantity of protein to determine the protein concentration of the samples.

After quantification process, we verified that the phenol method with the addition of the protease inhibitor cocktail was the best method for protein extraction (see Results item), then it was employed for the samples exposed to UV radiation for proteomic analysis.

***Two-dimensional electrophoresis (2-DE) analysis.*** Two-dimensional electrophoresis of the protein extracts was performed using a GE Healthcare 2-DE system (GE Healthcare, Waukesha, WI, USA) according to the manufacturer's instructions. Protein solution was resupended in 400 µL of isoelectric focusing buffer, added a small amount of bromophenol blue and centrifuged at 13.500 rpm for 5 min to pellet any indissoluble matter. Approximately 340 µL of the protein solution was loaded by rehydration into Immobiline Dry Strips 18 cm/ pH 4–7 non-linear (GE Healthcare, Waukesha, WI, USA). The strips were then transferred to an IPGphor II unit (GE Healthcare, Waukesha, WI, USA) and the separation was performed with the following parameters: 500V for 1 h, 1000V for 1 h, 8000V for 3 h, 8000V for 2 h and 30 min, and 1000V for 3 h. After isoelectric focusing, the strips are incubated with 10 mL of equilibration buffer I (6 M urea, 75 mM Tris–HCl, 2% SDS, 29.3% glycerol v/v, and 1% DTT) for 15 min followed with 10 mL of equilibration buffer (6 M urea, 75 mM Tris–HCl, 2% SDS, 29.3% glycerol v/v, and 2.5% 2-iodoacetamide) for 15 min.

The second dimension separation of proteins was performed on SDS-PAGE gel (12.5% polyacrylamide) using the Ettan Dalt Six apparatus (GE Healthcare, USA). The electrophoresis was carried out at 25 °C at 17.5 w/gel for 4 h and 30 min until the bromophenol blue dye front arrived at the bottom of the gels. Next, gels were fixed in a fixing solution containing 40% ethanol (v/v) and 10% glacial acetic acid (v/v) for 30 min under shaking, followed by two washing steps in ultrapure water for 10 min. Gels were incubated overnight in a dye work solution containing 80% Coomassie Blue (v/v) and 20% methanol (v/v) and washed in ultrapure water to remove unbound stain.

***Shotgun label-free quantitative proteomic analysis.*** Protein samples ($n$ = 3) obtained by the phenol extraction plus proteinase inhibitor cocktail were send to the Center of Facilities to Support Research (CEFAP) at the University of São Paulo for LC-MS/MS analysis.

Peptide samples were resuspended in 0.1% formic acid (FA) and analyzed using an LTQ-Orbitrap Velos ETD (Thermo, USA) coupled with Easy nanoLC II (Thermo, USA). The peptides were loaded onto a C18RP column (75 μm id × 10 cm, 3.5 μm particle size, 100 Å pore size; New Objective, Ringoes, NJ, USA) and separated on a 115 min gradient. The LTQ-Orbitrap Velos was operated in positive ion mode with data-dependent acquisition. The full scan was obtained in the Orbitrap with an automatic gain control (AGC) target value of 10e6 ions and a maximum fill time of 500 ms. Each precursor ion scan was acquired at a resolution of 60,000 FWHM in the 400–1500 m/z mass range. Peptide ions were fragmented by CID MS/MS using a normalized collision energy of 35. The 20 most abundant peptide were selected for MS/MS and dynamically excluded for a duration of 30s. The instrumental conditions were checked using 50 fmol of a tryptic digest of bovine serum albumin (BSA) as standard. The sample carryover was completely removed between run. The quantitation analyses was performed using MaxQuant (v 1.6.1.0) and Perseus (v 1.6.1.1) software's. Identity of the protein dataset was directly searched against three databases (http://www.ebi.uniprot.org) on April 2018 to obtain the corresponding blast information from the same genus Sargassum_Uniprot, same order Fucales_Uniprot, and a biological brown alga model Ectocarpus_UniProt that have its genome sequenced. A complementary search was made using Thermo Proteome Discoverer 1.4.0.288 software for list the identified proteins.

***Protein classification.*** The identified proteins were directly searched by using the accession numbers against the UniProt database (http://www.ebi.uniprot.org). Based on the obtained information, proteins were categorized according to its molecular weight and functional classification. Additionally, total identified proteins from the three Uniprot databases were registered, as well as the amount of differentially abundant proteins against the Ectocarpus_UniProt database, since this database lead the highest number of protein identity.

***Data analysis.*** Statistical analysis of data set was performed only for proteomic profile with proteins differentially abundant against the Ectocarpus_Uniprot data base with the software Perseus (v 1.6.1.1) by using three replicates for each UV radiation treatment. For find the differences in the radiation treatments, Student *t* tests ($p < 0.05$) based on the protein

abundance were performed by comparing between PAR and PAR+UVA (Group I); PAR and PAR+UVB (Group II); and PAR+UVA and PAR+UVB (Group III). Additionally, a multiple comparison for evaluating the integration of the composition and abundance of differentially abundant proteins in each sample, a bi-dimensional hierarchical clusterization of relativized data by the adjustment of standard deviation, followed by Euclidean distance and Paired group analyses combined with the Pearson correlation index was performed. The cluster results were associated to a heatmap graphic.

## RESULTS

**Protein extraction.** To analyze proteomic profile of *S. filipendula*, efficiency of protein extraction was tested by TCA-acetone, phenol, and phenol/protease inhibitor cocktail methods ($n$ = 1). Quantification results showed a protein concentration of 430 µg.mL$^{-1}$, 1300 µg.mL$^{-1}$, and 4000 µg.mL$^{-1}$ when extracted with TCA-acetone, phenol, and phenol with protease inhibitor cocktail (Fig. 22), respectively, thus demonstrating the effectiveness of this last extraction for the species. Consequently, the phenol/protease inhibitor cocktail extraction method was used for processing the experimental samples.

The obtained protein concentration of *S. filipendula* after exposure to UV radiation treatments for four days ($n$ = 3) was 3755 ± 485 µg.mL$^{-1}$ at PAR control treatment, 3353 ± 415 µg.mL$^{-1}$ at PAR+UVA treatment, and 3510 ± 388 µg.mL$^{-1}$ at PAR+UVB treatment.

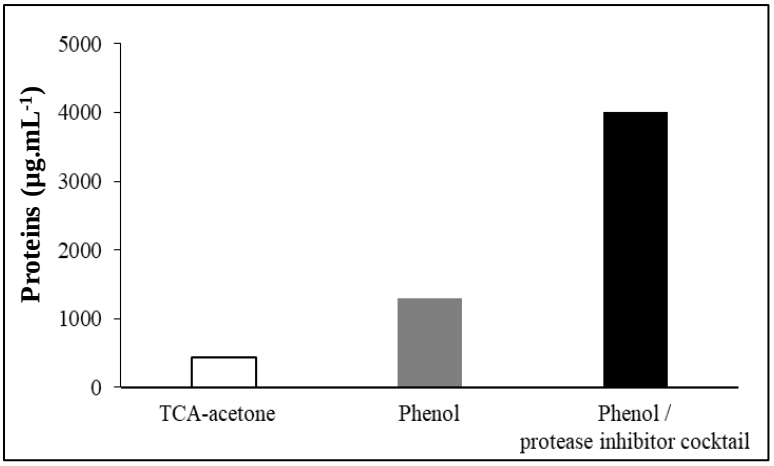


**Figure 22.** Protein yield (n = 1) of *Sargassum* spp. collected in Cibratel II Beach and used for testing protein extraction method by using TCA-acetone, phenol, and phenol containing protease inhibitor cocktail extractions.

**Two-dimensional electrophoresis analysis.** Figure 3 shows the 2-DE gels obtained from three extraction methods. When comparing between the methods, low content of proteins (spots) where visualized for the TCA-acetone (Fig. 23A). The both extraction by phenol method, without protease inhibitor cocktail (Fig. 23B) and with the addition of a protease inhibitor cocktail (Fig. 23C) presented higher content of spots when compared to TCA-acetone method, however, the addition of a protease inhibitor, resulted in higher quality gel with a clear resolution of the spots.

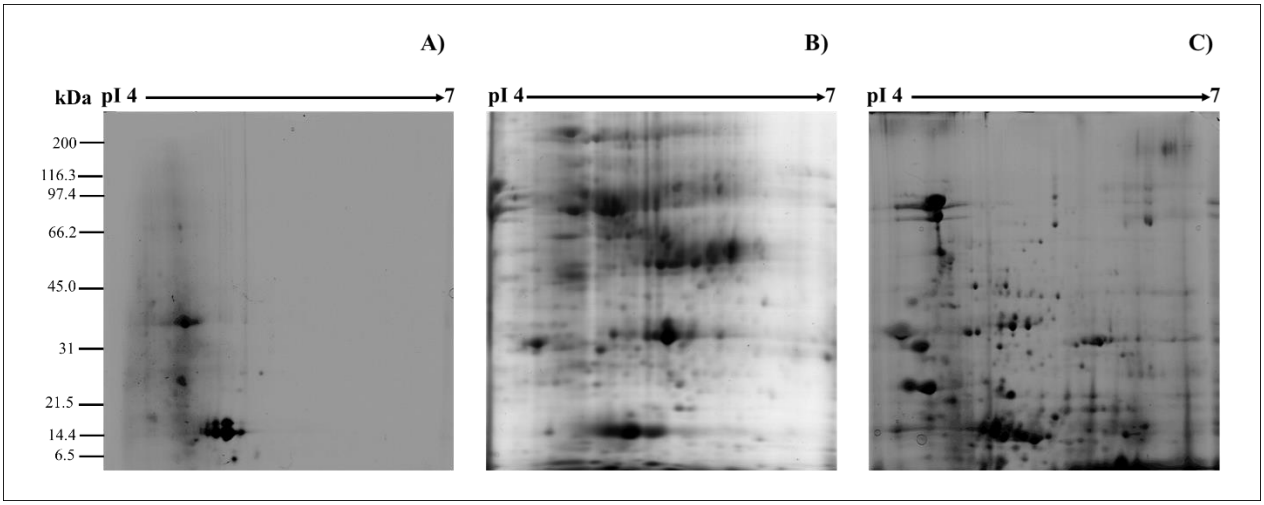


**Figure 23.** Two-dimensional electrophoresis gels of proteins extracted from *Sargassum* spp. by using different extraction methods. A) TCA-acetone method; B) phenol method); and C) phenol method containing protease inhibitor cocktail extractions. pI = isoelectric point.

***Shotgun label-free quantitative proteomic analysis.*** Results from proteomic analysis by shotgun LC-MS/MS were searched against three databases (http://www.ebi.uniprot.org) to obtain the proteins corresponding to blast information. The database from Sargassum_Uniprot contains 2500 proteins and, from this list, 45 are categorized as uncharacterized proteins until the date, corresponding to 2%. When searching our proteins from *S. filipendula* under UV radiation exposure against this set, 188 had a match and only one was uncharacterized (Fig. 4). In the case of database from Fucales_Uniprot it contains 3816 proteins and, from this total, 67 (1.8%) are still to be characterized. In the same way, our proteins from *S. filipendula* under UV radiation exposure were searched against this data set, and it was able to have a match with 248 proteins with only one uncharacterized protein (Fig. 24).

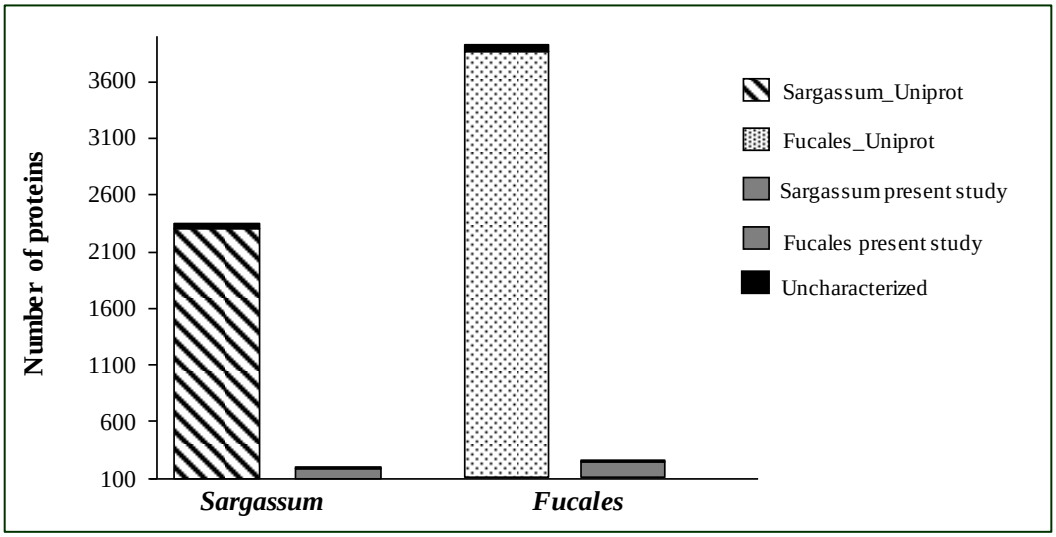


**Figure 24.** Total number of proteins from Sargassum_Uniprot and Fucales_Uniprot databases with the respective uncharacterized proteins, and the number of proteins from our study with *Sargassum filipendula* matched with the respective Uniprot database (Sargassum_Uniprot or Fucales_Uniprot) and the amount of uncharacterized proteins.

Finally, the last database used corresponds to Ectocarpus_Uniprot. This base was chosen since the species *Ectocarpus siliculosus* is one the few brown seaweeds with the complete genome sequenced, enabling a greater correspondence in protein identity. This database contains a list with 17169 proteins, nevertheless, a great number of proteins (10625, *ca.* 62%) are not yet characterized. When comparing against this set, 767 proteins from *S. filipendula*

under UV radiation exposure found a match and 254 from this identification were in the category of uncharacterized (*ca.* 32%; Fig. 25). Consequently, since the number of matched proteins for *S. filipendula* was higher with Ectocarpus_Uniprot, compared to the Sargassum_Uniprot and Fucales_Uniprot databases, results here obtained were selected to perform a deeper analysis of the proteomic profile of *S. filipendula* under the UV radiation treatments.

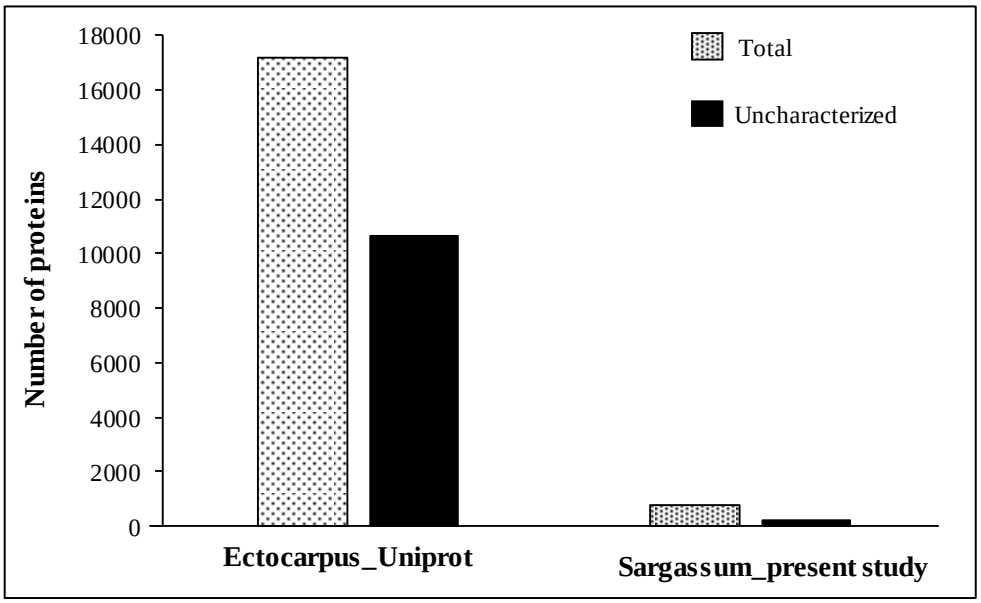


**Figure 25.** Total number of proteins from Ectocarpus_Uniprot database and the respective uncharacterized proteins, and the number of proteins from our study with *Sargassum filipendula* matched with this database and the amount of uncharacterized proteins.

The list of 767 proteins matched for *S. filipendula* with the information obtained from the Ectocarpus_Uniprot database was classified according to its molecular weight (low and high). Proteins with a molecular weight up to 50 kDa are considered as low molecular weight proteins (LMWP), and above this value corresponds to high molecular weight proteins (HMWP). From this classification, 529 were considered as LMWP and 258 as HMWP (Fig. 26). When comparing the significant abundance of proteins of *S. filipendula* between radiation treatments, it mean differences within PAR versus PAR+UVA (Group I), PAR versus PAR+UVB (Group II) and PAR+UVA versus PAR+UVB (Group III), 40 of them

were different in their abundance, then 29 proteins correspond to LMWP and 11 to HMWP (Fig. 26).

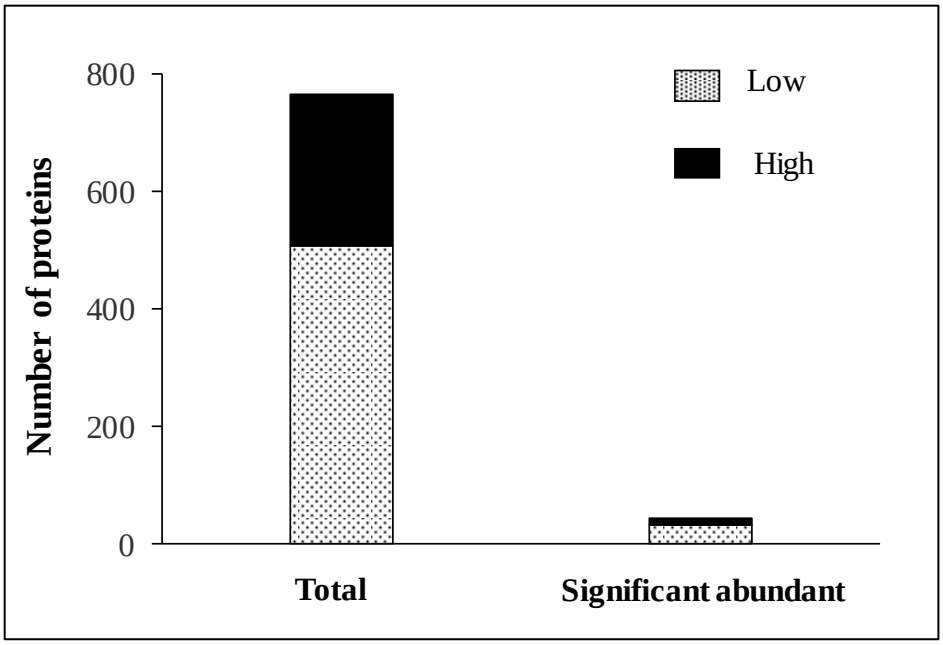


**Figure 26.** Classification of proteins of *Sargassum filipendula* matched with Ectocarpus_uniprot database (767 proteins) according to its molecular weight and the classification of proteins with differences in their abundances after UV radiation exposure (40 proteins). Low ≥50 kDa; High <50 kDa.

In the same way, the matched 767 proteins from *S. filipendula* were classified according to their metabolism or function by using the information content on the UniProt database (http://www.ebi.uniprot.org). From this list, the identities of all matched proteins are shown in Table Supplement 2 and the main identified metabolism were energy (9.3%), carbohydrate (5.4%), photosynthesis (5.2%), translation (3.4%), ROS scavenging, defense, and stress related (3.1%). Proteins with less representation were classified as *other functions* (16%) and a high number of proteins were categorized as uncharacterized (33%) (Table Supplement 2). Proteins that were different in relation to the abundance (40 proteins) were classified in 11 different metabolic pathways (Fig. 27), most of them belonging to photosynthesis (32%), energy (12%), carbohydrate (7%), and ROS scavenging defense (7%) metabolisms. Additionally, 17% correspond to other metabolisms, and uncharacterized proteins represents 24% of the total matched proteins.

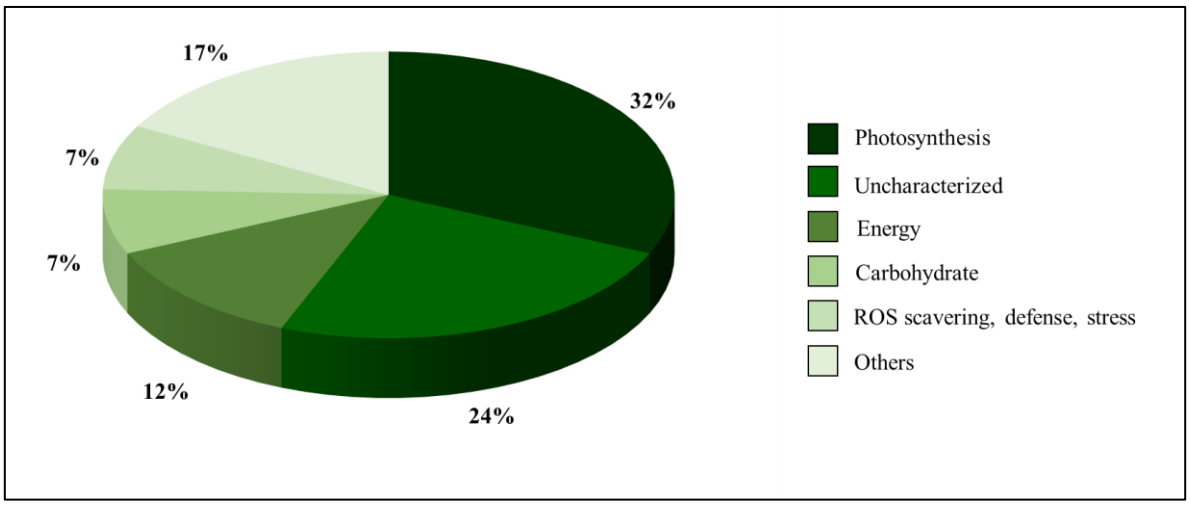


**Figure 27**. Metabolic classification of differential abundant proteins identified in *Sargassum filipendula* after exposure to UV radiation treatments (40 proteins) against the Ectocarpus_Uniprot database match.

The Student *t* test comparing Group I, Group II, and Group III showed 2, 20 and 21 proteins with significant changes in their abundance, respectively (Fig. 28), with some proteins being present in more than one group. The comparison within the Group I showed that one protein had a higher abundance at PAR+UVA treatment regard to the PAR treatment, while the other presented the opposite result. The Group II showed a lower abundance for 10 proteins at PAR+UVB treatment, in relation to PAR. Finally, the Group III presented 16 proteins at PAR+UVB treatment with higher abundance regarding to PAR+UVA treatment.

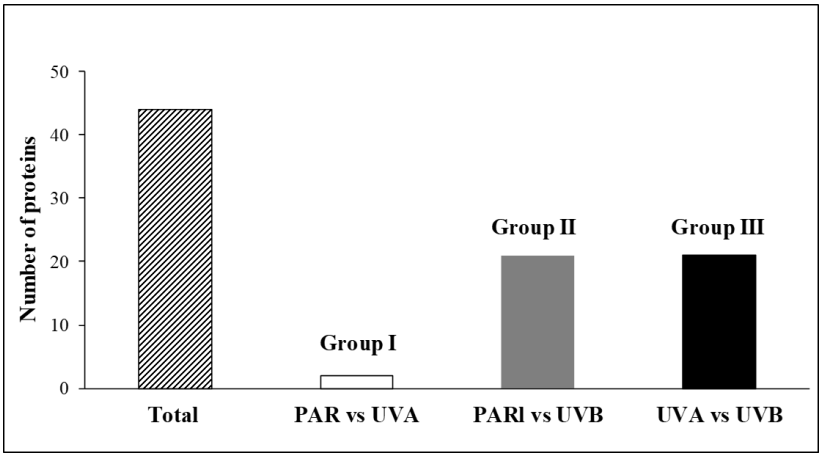


**Figure 28**. Total number of proteins identified in *Sargassum filipendula* with difference in their abundance and the respective protein number with different abundance for PAR versus PAR+UVA (Group I), PAR versus PAR+UVB (Group II), and PAR+UVA versus PAR+UVB (Group III) treatments.

The biplot cluster analysis (Euclidean distance) associated to a heatmap graph (Fig. 29) formed two associations in relation to treatments: PAR+UVA and PAR+UVB, which were more closely correlated (Pearson's correlation of 0.70), and a second low correlation between PAR and PAR+UVA/PAR+UVB (Pearson's correlation of 0.45). Additionally, considering the clusterization between the protein abundance, it was observed five associated groups with a significance of 60% of distance, which correlate the protein abundance (minimum, mean or maximal value) regarding to the mean abundance value for each protein. A first group (Group I) was formed by proteins related to transport and catabolism metabolisms, such as leucyl aminopeptidase, which presented the lowest abundance in PAR+UVA treatment. Similar trend was observed for superoxide dismutase from the same group, a protein associated to oxidative stress defense, with maximum abundance in PAR treatment and minimum at PAR+UVA treatment. A second group (Group II) includes 18 proteins, and all of them have a higher abundance in PAR+UVB treatment and is subdivided into two subgroups. The first subgroup includes two uncharacterized proteins, and seven associated to photosynthesis, carbohydrate, and energy metabolisms. The second subgroup includes four uncharacterized proteins and also presented proteins involve in amino acid pathway biosynthesis (enzymes) as alanine transaminase, carbohydrate metabolism as aldehyde dehydrogenase, and the others related to microtubule functions as tubulin beta chain and flagellar associated protein, and ROS scavenger metabolism as glutamate synthase. Besides from proteins related to carbohydrate, energy, and photosynthesis functions, Group III presented the importin subunit alpha which is related to membrane transport and the glutamine synthase related to nitrogen metabolism. Group IV presents proteins as peroxidase, similar to argenine/serine-rich splicing factor 7, and dihydrolipoamide acetyltransferase, which are related to stress, genetic information processing, and energy, respectively. The other proteins from this group are related to photosynthesis metabolism (photosystem II oxygen evolution complex protein PsbP, thylakoid lumen 15.0 kDa protein, cytochrome c-550, hydroxymethylbilane synthase putative chloroplast, and light harvesting complex protein), with major abundance at PAR and PAR+UVA treatments, and minimal abundance at PAR+UVB. Finally, ribulose-phosphate 3-epimerase involved in carbohydrate metabolism, two cytochrome proteins related to photosynthesis functions, and the ATP synthase O subunit involved in the energy metabolism formed the last association, Group V,

with major abundance at PAR and minimal abundance at PAR+UVA and PAR+UVB treatments.

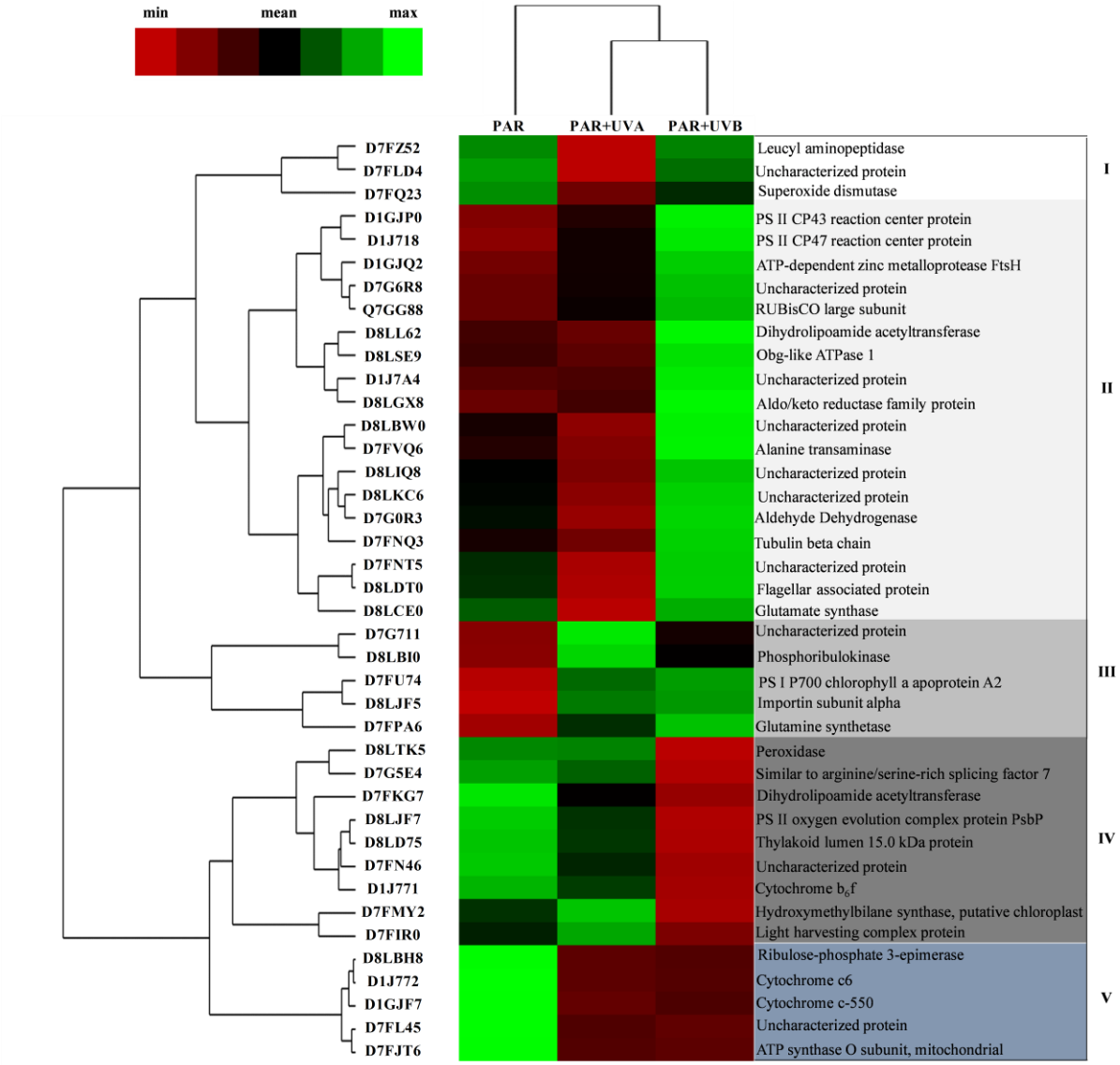


**Figure 29.** Biplot cluster analysis (Euclidean distance) of proteins differentially abundant of *Sargassum filipendula* after four days of exposure to UV radiation treatments, associated with a heatmap graph based on the mean value of abundance for each protein ($n$ = 3). Dataset represent the ID code identity and protein name. The scale represents minimum ± mean value ± maximum.

## DISCUSSION

Proteomic studies in algal research have been performed in both micro and macroalgae, however, applications are still quite limited, and this could be due the difficulty in the extraction of proteins, especially from brown seaweeds. Brown algae are characterized by elevate concentrations of phenolic compounds and polysaccharides, which make difficult to extract any type of metabolite, can contaminate samples, and degrade the metabolite of interest. On the other hand, cell disruption causes enzymes, such as proteases, to become free and active for the degradation of the target component, in this case the proteins. In addition to the difficulty of establishing a suitable protein extraction that yields high contents, the cellular disruption to facilitate the contact with the extraction solution is also important. Thus, it has been pointed out that there are certain key aspects for this type of researches as cellular disruption, efficient extraction with high yield and preservation of protein integrity (Contreras et al. 2008; Ritter et al. 2010).

One of the most versatile and widely applied method for protein extraction is homogenizing the biological material of interest in aqueous solution, followed by precipitation of proteins with TCA or acetone. Nevertheless, these methods for brown seaweeds tend to be inefficient since these algae have high levels of non-protein interfering compounds, as phenolic compounds, viscous polysaccharides (alginic acid or fucoidan), salts, and pigments (Contreras et al. 2008). Then, it is necessary to improve extraction methods that are capable to eliminate such contaminants that allow high quality proteins. In this context, methods based on phenol extraction have demonstrated to be successfully for protein extraction in these organisms, since compounds that may interfere in the protein quality are mostly remove (Contreras et al. 2008; Nagai et al. 2008; Ritter et al. 2010; Zou et al. 2015). These findings are in accordance with our results, where protein extraction of *S. filipendula* had a better effectiveness using phenol as extraction agent when compare to TCA-acetone method. Moreover, the stability of protein against protease activity is an essential issue for obtaining high protein quantity and quality, and then the phenol method was optimized by the addition of a protease inhibitor cocktail, which permit a higher quantity of proteins for *S. filipendula*, approximately 2-times more protein concentration with phenol/protease inhibitor cocktail than the usual phenol extraction method. Therefore, our

results provide an innovative method for protein extraction that benefits high protein quantity and quality for studies of proteomic approaches.

In proteomic studies, the most critical step is the protein extraction and sample preparation, since outside their proper environment proteins may misfold, aggregate, and precipitate due to their instability when extracted from their *in vivo* context (Tan and Yiap 2009). Additionally, depending on the particular biochemical properties of each protein, the factors and conditions, which ensure protein stability upon extraction, can vary considerably (Andrés-Colás and Van Der Straeten 2017). During isolation and characterization of the proteins, proteases are released following cell or tissue lysis and degrade protein samples by endogenous proteolytic enzymes, which can reduce the quality for further analysis. In order to prevent degradation of the proteins, protease inhibitors, which are peptides or proteins proficient of impeding the catalytic activity of proteolytic enzymes, are recommended to be added for prevention of such unwanted biological phenomenon in protein chemistry and proteomics studies (Barbosa et al. 1992; Havanapan and Thongboonkerd 2009). Our results showed that the use of a protease inhibitor when extracting the proteins yielded two times more than without using it; confirming the great importance of this component when performing a proteomic approach.

The advantage of using phenol as an extracting agent resides in its capacity to disrupt membranes, leaving most of the water-soluble molecules in the aqueous phase, then proteins in the phenol phase can efficiently be purified and concentrated with the subsequent ammonium acetate/methanol precipitation; additionally, degradation of proteins is minimized. In the study performed by Contreras et al. (2008), five different extraction methods (urea extraction including ultracentrifugation and acetone precipitation; urea extraction, ultracentrifugation, and acetone precipitation; urea extraction, ultracentrifugation with TCA-acetone precipitation; phenol extraction; and phenol extraction with desalting steps) were tested using as model the brown seaweeds *S. gracilis* and *E. siliculosus*. The authors concluded that proteins from *S. gracilis* were better extracted using the phenol method, while for *E. siliculosus* all methods were adequate for the extraction. These results can be related with the nature of the biological material, as *E. siliculosus* is a delicate filamentous uniseriate alga with low amount of phenolic compounds (Zhang et al. 2007) and

polysaccharides. In contrast, *S. gracilis* is a cylindrical to flat and hollow alga with major cell biomass and consequently secondary metabolites as polyphenols (Lee et al. 2011) and polysaccharides than *Ectocarpus* species, in spite of both species are of the order Ectocarpales. However, when the authors tested protein quantity by a 2-DE gel, similar protein resolution level for both species was observed when using the phenol reagent. In the case of *S. gracilis*, the low yield efficiency of the other methods when compared *to E. siliculosus*, could be attributed to the presence of interfering charged polysaccharides and polyphenols, present in the protein extracts, probably because are much more abundant due the structure of the thallus, which presents a cortical layer and a relatively thick medulla whose cells have bulky cell walls rich in polysaccharides. Thus, we can expect that protein extracts from *S. filipendula* had this same characteristic due to its thallus complexity, making extraction difficult by TCA-acetone method. The same authors reported the phenol method allowed the extraction of both low and high molecular weight proteins, identifying proteins between 19 and 200 kDa. In our study, the same pattern was also observed, reporting proteins between 5 and 700 kDa, allowing a greater proteomic coverage including peptides of different molecular masses and a closer mid-scale proteomic approach. Similar results were observed by Nagai et al. (2008) when comparing various extraction protein methods, concluding that phenol extraction method produced high-quality protein extract from the laminar thallus of *E. kurome*, with the highest protein purity among the other methods examined.

In this regard, improvement of protein separation and identification techniques has led to the evolution of comparative proteomic as a powerful tool, being an important step for recognizing the mechanisms that participate in response to different abiotic stresses. In the present study, the proteomic profile of *S. filipendula* was evaluated after exposure to UV radiation treatments, where comparisons between the different radiations allowed identification of proteins that response to this factor under laboratorial conditions.

The identified proteins were searched against the database Sargassum_Uniprot, Fucales_Uniprot, and Ectocarpus_UniProt. However, the latter was the one that brought more useful information, allowing the recognition of hundreds of proteins presents in *S. filipendula*, together with a protein set that respond to the stimuli caused by UV radiation.

One of the reasons that could explain why this database gave us more informative results, is related to the fact that *E. siliculosus* genome has been sequenced and annotated (Cock et al. 2012), turn it into a model species for deeper explorations at molecular level. Additionally, the species presents particular characteristics as the small size of the thalli when mature, highly fertile, and rapidly progress through the life cycle, which are essential for the application of molecular approaches (Ritter et al. 2010).

The functional group with the largest number of protein altered by UV radiation was photosynthesis. Several reports have demonstrated that this stress may have alterations on photosynthesis rate and pigment concentration (Gómez and Figueroa 1998; Lopez et al. 1998; Figueroa and Vinegla 2001; Sampath-Wiley et al. 2008; Heo et al. 2009; Figueroa et al. 2014; Polo et al. 2014a). This fact could explain the lower abundance of proteins as photosystem II oxygen evolution complex, thylakoid lumen 15.0 kDa, and light harvesting complex in samples exposed UVB and cytochrome proteins for both types of UV radiation studied here. In the same way, key enzymes involved in energy metabolism as ATP synthase, which have a central role in oxidative phosphorylation and photosynthesis, presented a lower abundance after *S. filipendula* was exposed to PAR+UVB treatment. In this way, higher abundance of proteins involves in carbohydrate metabolism in UV radiation treatments, as phosporibulokinase (PRK), an enzyme unique to the reductive pentose phosphate pathway of $CO_2$ assimilation; and Ribulose bisphosphate carboxylase (RubisCo) large subunit, which catalyzes the first step in net photosynthetic $CO_2$ assimilation and photorespiratory carbon oxidation (Spreitzer and Salvucci 2002), may compensate the energy loss from photosynthesis through the catabolism of photoassimilates (Zhang et al. 2015).

UV radiation can also cause changes in nitrogen metabolism by decreasing nitrogen assimilation. It has been reported that glutamine synthetase, an enzyme that catalyzes the assimilation of ammonium to glutamine using glutamic acid as its substrate (Chen and Silflow 1996), can present a reduction under stress conditions. This behavior may be a protective mechanism because nitric oxide, an intermediate of nitrogen assimilation, is an active radical (Wang et al. 2004). Moreover, the reduction of enzymes involved in primary nitrogen indicates redirection of nitrogen resources into other pathways, such as those involved in repair or protection processes. However, glutamine synthase presented a higher

abundance for both PAR+UVA and PAR+UVB treatments; and in the case of proteins related to ROS scavenging and stress as superoxide dismutase (SOD), which constitute the first line of defense against oxidative damage caused (Alscher et al. 2002), did not presented differences in abundance for PAR and PAR+UVB treatments, suggesting that the antioxidant system is active at PAR control treatment and remains diligent under PAR+UVB condition.

As mentioned earlier, few proteomics studies have focused on cortical parenchymatous macroalgae and compared with other group of organisms (*e.g.* vascular plant) protein extraction has been extraordinary difficult, which results in a limited knowledge at biochemical and molecular levels. Additionally, all the performed proteomic works have used 2-DE gels, an approach that has some limits. The method could fail in its reproducibility, inability to detect low abundant and hydrophobic proteins, low sensitivity in identifying proteins with pH values too low (pH < 3) or too high (pH < 10) and molecular masses too small (Mr < 10 kD) or too large (Mr > 150 kD); moreover, proteins could be poorly separated do to streaking of the gels (Godovac-Zimmermann and Brown 2001). In this context, shotgun proteomics arrives as a powerful approach that allow identification and quantification of proteins presents in a mixture, that converted proteins to peptides by proteolytic digestion, and these peptides are used as surrogates for identification and quantitation of the proteins present in the original mixture (Liao et al. 2009). For the present research, the identification and quantification of a large number of proteins involved in several metabolic pathways in *S. filipendula*, demonstrated that this approach is reliable and feasible for the study of proteins that respond to abiotic stimuli as UV radiation. Moreover, mass spectrometry (MS)-based proteomic methods are a key technology for identification and quantification of complex protein mixtures with the potential to reveal unknown and novel changes in protein interactions and assemblies that regulate cellular and physiological processes.

Summarizing, the innovative proteomic approach with *S. filipendula* as biological model and the UV radiation effect constitutes a valuable international scientific contribution, as proclaims the successful benefit of large-scale high-quality protein extraction in a parenchymatous phenolic- and polysaccharide-rich macroalgae with a mid-scale proteomic profile approach on metabolic responses under UV radiation stress condition. Additionally, our research describes important difficulties related to the complexity of proteomic analyzes

in brown macroalgae, as well as opens major metabolic tools for understanding biological/physiological processes under stress abiotic conditions like UV radiation. In turn, this is the unique study, until the best of our knowledge of published literature, with a shotgun proteomic approach in macroalgae, in which the few available reports were performed with microalgae, making the contribution of this research even more valuable. Therefore, this investigation subscribes the scientific development by providing important insight for a better understanding of the biology of *S. filipendula*, as well as the responses to stress conditions and predicted global climate changes.

# Chapter IV

## Fatty acids and carotenoids

## Chapter IV

Impact of light quality on chemical composition of *Sargassum vulgare*: fatty acids and photosynthetic pigments profile


## ABSTRACT

Light is one of the major abiotic factors influencing diverse processes of seaweeds as growth and development, photosynthesis, acclimation, and regulation of several compounds as fatty acids and pigments. Seaweeds are a source of fatty acids with great interest as the long chain polyunsaturated fatty acids (LCPUFAs), especially those belonging to the omega-3 (ω-3) family due to the importance they represent for human metabolism, and are not produced by humans and animals. Additionally, pigments from these organisms represent a great commercial interest due to their biological properties. The present work was performed at the University of Málaga-Spain, in collaboration with Dr. Felix Lopez Figueroa, from the research group Photobiology and Biotechnology of Aquatic Organisms (FYBOA). The aimed this research was to evaluate the fatty acids and pigments profile of *Sargasum vulgare* after ten days of exposure to different light qualities: SOX (low pressure sodium lamps, used as control), SOX+Blue, SOX+Green, SOX+Red, and SOX+UV; regarding to possible application in the biotechnology area. Fatty acids were grouped in three main classes: saturated fatty acids (SFA, 41.18%), monounsaturated fatty acids (MUFAs, 11.76%); and polyunsaturated fatty acids (PUFAs, 47.1%). Light qualities increased the content of SFAs and MUFAs, while for PUFAs a decreased was observed in relation to the control. Pigment profile presented chlorophylls *a* and *b* (Chl *a* and Chl *c*), and carotenoids fucoxanthin, violaxanthin, neoxanthin, zeaxanthin and β-carotene. Green light was the only treatment that showed increased for these pigments in relation to the control. S. *vulgare*, presented a high percentage of PUFAs, with appropriate ratio ω6/ω3, indicating its potential as a valuable source of bioactive compounds. However, there is need to perform future researches that allow the establishment of light condition for the stimulation of these compounds from *S. vulgare*.

## INTRODUCTION

Seaweeds are key components within coastal ecosystem, being major biomass producers and fulfilling a multitude of functions as community ecosystem engineering. Additionally, these organisms are a rich source of nutrients (vitamins, pigments, minerals, proteins, fibers, and lipids), reason why are extensively explored; and researches related to their chemical composition, physiological, and biotechnological properties have become focus since there is a potential of seaweeds as the so-called functional or health-promoting foods (Sekmokienė et al. 2007).

As chemical composition is influenced by abiotic factors and consequently modify the quality of the biomass, a better understanding of the effective production of value compounds of interest is essential for diverse applications. Like any photosynthetic organism, light quantity and quality regard as one of the most important factors for macroalgal growth and development. As a result, biosynthesis or degradation of chemical cell constituents are sensitive to different characteristics of wavelength radiation. Studies with different light colors have been widely used for agricultural approaches (Aubé et al. 2013; Jou et al. 2015; Motogaito et al. 2017) and are less well-known in seaweeds.

In the marine environment, factors such as depth, high turbidity, and dissolved nutrients can affect the characteristics of light incidence on benthic communities (Monro and Poore 2005). Light, in its context of quantity, quality and duration has a significant influence on seaweed metabolism, affecting growth, reproduction (Henley and Ramus 1989), photosynthesizing performance and acclimation (Demmig et al. 1988; Aguilera et al. 1999; Dawes et al. 1999). Several studies have suggest that red, green, and blue lights have special influence on regulating algae growth and photosynthetic pigment synthesis. Dring (1986), reported that bright red and blue lights can increase the ratio of fucoxanthin to Chl *a* and Chl *c* in *Laminaria hyperborean* (Gunnerus) Foslie. Barufi et al. (2015) reported higher growth rates in *Gracilaria birdiae* E.M.Plastino & E.C.Oliveira exposed to white light and red light, and concluded that these spectral qualities could be utilized as a reproductive inductor to produce tetraspores. For *Halymenia floresia* (Clemente) C.Agardh, it has been reported that green light is suitable for the growth of the species (Godínez-Ortega et al. 2008).

Additionally, Kim et al. (2015) reported inferior growth rate for *G. tikvahiae* McLachlan under blue light in relation to red and green fluorescent lights.

Lipids and fatty acids, as constituents of commercial interest from marine sources, mainly by the polyunsaturated fatty acids (PUFAs) with healthy benefits, have risen up the effort for improving their production under controllable culture conditions. In algae, two classes of polar and nonpolar lipids can be found. Polar lipids, such as phospholipids, glycolipids, and sulfolipids, are mainly structural components as part of all cell membranes with crucial function for the living processes. Triacylglycerols, which are nonpolar lipids, have storage and energy reservoir functions, and compose most of the seaweed's lipids (Gerasimenko et al. 2010). Additionally, it can be found some unusual lipids in seaweeds that are characteristic of a particular genus or species (Kumari et al. 2013).

Lipids represent 1 to 5% of the dry weight of macroalgae and the composition of fatty acids is of great interest, mainly due to the composition of long chain polyunsaturated fatty acids (LCPUFAs), especially those belonging to the omega-3 (ω-3) family (Schmid et al. 2014). PUFAs are of great importance for human metabolism as they are the main component of the cell's phospholipid membranes and can be present in cellular storage compartments. In addition, they participate in the biosynthesis of eicosanoids, which are hormone-like signaling molecules that include thromboxanes, prostaglandins, and lucotrienes (Calder 2010), which participate in diverse physiological systems and pathological processes such as inflammation, allergy, fever, other immune responses, blood pressure control, among others. PUFAs have also biological activities already reported, such as antimicrobial (Guedes et al. 2011), heart disease preventer (Mozaffarian and Wu 2011), and inhibition of tumor progression (Field and Schley 2004).

The effect of PAR light on the composition of fatty acids in seaweeds has been examined only for a few species. For *Gracilaria* sp., the content of eicosapentaenoic acid, the main ω-3 PUFA for this species, increased with increasing photon flux density (Levy et al. 1992), whereas in *G. verrucosa* (Hudson) Papenfuss the proportion of arachidonic acid, the main ω-6 PUFA in the studied species, decreased under high light condition (Floreto and Teshima 1998). Despite these studies are focused on light intensity, the scientific background leads us to think about the role of the light quality as an effector of lipid composition. The effect of

UV radiation on total lipid content has only been studied in depth for microalgae species of interest for the production of transesterifiable lipids (Skerratt et al. 1998; Forján et al. 2011), and until our knowledge there is scarce scientific evidences on macroalgae.

Within brown seaweeds, *Sargassum* species, have been widely studies in relation to its fatty acid composition and researches are mainly focused on intraspecific variations and seasonal changes (Rajasulochana et al. 2010; Prabhakar et al. 2011; Van Ginneken et al. 2011; Silva et al. 2013; Chen et al. 2016; Bakar et al. 2017; Santos et al. 2019a). The study of Noaman et al. (2016) with *S. hornschuchii* C. Agardh reports significant increase on fatty acid content after three days of exposure to UVB radiation, with synthesis of two saturated fatty acids (capric acid (C10:0) and heneicosanoic acid (C21:0)) and depletion of one monounsaturated fatty acid (oleic acid (C18:1)). As UVB radiation impair physiological responses related to photostress, alterations in PUFAs as expected since some fatty acids are known to regulate physiological processes under stress.

Beside the composition of fatty acids from seaweed, carotenoid content has also been of great commercial interest, especially from brown algae. Carotenoids are recognized as important biomolecules for both their provitamin-A activity and their efficient antioxidative properties against oxidative damage (Riso et al. 2004; Hu et al. 2008). These compounds can act as quenchers of singlet molecular oxygen, convert hydroperoxides into more stable compounds, prevent formation of free radicals through the block of free radical oxidation, and convert iron and copper derivatives (metal prooxidants) into harmless molecules, acting as metal chelators, thus protecting the photosynthetic apparatus against oxidative stress (Stahl and Sies 2003).

Brown seaweeds, contains β-carotene, lutein, zeaxanthin, violaxanthin (Yoshii et al. 2005), and fucoxanthin as the main carotenoids (Lewey and Gorham 1984; Czeczuga and Taylor 1987). These pigments, have attracted considerable interest due to biological properties, such as antioxidant, anti-inflammatory, anticancer, anti-obese, antidiabetic, antiangiogenic, and antimalarial activities (D'Orazio et al. 2012), and help in cell communications and human health maintenance (Plaza et al. 2010). Therefore, they can be used as nutraceutical/cosmeceutical ingredients to prevent UV radiation-related damage and oxidative stress-related diseases (Nichols et al. 2011).

Currently, the commercialization of common carotenoids that is industrially produced by chemical synthesis increases production costs and waste material production with potential negative effects on the environment (Craft et al. 2012), bringing concern for human and environmental health. These issues have driven the growth of the market demand for natural carotenoids-based products; thus, the production of natural carotenoids from marine organisms such as seaweeds, has considerably increased, since they offer advantages in terms of costs, times and yields when compared to terrestrial plants or synthetic products (Galasso et al. 2017). Additionally, harvest of commercial algae can be considered beneficial for the environment, as they are carbon dioxide-absorbing organisms and thus their cultivation can limit greenhouse gas emissions (Christaki et al. 2013).

Inducing organisms through photoregulatory and nutritive strategies to control the synthesis of compounds of interest is a practice that is currently being applied and extended (Xue et al. 2005; Griffiths et al. 2016). In this regard, light sources for plant cultivation as light emitting diodes (LEDs) have recently attracted attention due to a number of advantages in that is possible to control the emission wavelength, the consumption power is smaller than that of other light sources, such as incandescent and fluorescent lamps, and they are capable of pulse irradiation, which is an advantage in plant photosynthesis (Motogaito et al. 2017). Additionally, UV radiation has been suggested as an inducing variable for the production of algal lipids in large-scale culture systems (Guihéneuf et al. 2010). Then this type of radiation under controlled conditions and doses would exert an inducer role for the biosynthesis of lipids at the cellular level (Sharma et al. 2012)

Light quality has a profound influence on seaweed, and among the different light spectra red and blue wavelengths have reported to play an important role in the photosynthesis and photomorphogenesis of these organisms, thus influencing their development and metabolism. However, the effects of light quality on seaweeds, aiming for a more effective production of compounds of interest has been little explored. Therefore, the present study aimed to characterize the profile of photosynthetic pigments (chlorophylls and carotenoids) and fatty acids in *S. vulgare* after the exposure to different light qualities and determine possible biotechnological applications.

## MATERIAL AND METHODS

**Collection site and algal material.** Specimens of *S. vulgare* were collected from the Málaga coast (Alboran Sea, south of the Iberian Peninsula) (Fig. 30), specifically in the upper infralittoral zone from rocky shore and pools, at Araña Beach (36°70'N; 4°33'W). This place is characterized by the preserved ecological status of the coastal waters of this area (Bermejo et al. 2013). The collected material was transported in an icebox to the laboratory, cleaned out from epibiota, and acclimated for one week under laboratory conditions in a ratio of 2-3 g of alga per 1 L of von Stosch culture medium, photosynthetically active radiation (PAR) 180 ± 5 μmol photons.$m^{-2}$.$s^{-1}$, 25 ± 1°C, 12h light:12h darkness regime, and continuous aeration.

**Experimental setup.** After acclimation, apical potions of 3 cm were exposed for one week to the following light treatments: Control, SOX lamp (low pressure sodium lamp), characterized by a yellow light (595 nm), at 250 μmol photons.$m^{-2}$.$s^{-1}$; SOX+Blue, SOX lamp supplemented by a blue light (400-450 nm) at 37.5 μmol photons.$m^{-2}$.$s^{-1}$; SOX+Green, SOX lamp supplemented by a green light (500-550 nm) at 37.5 μmol photons.$m^{-2}$.$s^{-1}$; SOX+Red, SOX lamp supplemented by a red light (600-650 nm) at 25 μmol photons.$m^{-2}$.$s^{-1}$; and SOX+UV lamp supplemented by UVA (315-400 nm) at 9.94 W.$m^{-2}$ and UVB (280-315 nm) at 0.43 W.$m^{-2}$. UV radiation was provided by using Q-Panel lamps radiation. Blue, green, and red lights were provided by blue, green, and red LEDs, respectively.

The light intensities where chosen based on initial photosynthetic measurements of saturation irradiance of the species, which was determined by a Junior PAM (Walz, Germany) and a rapid light curve. From the rapid light curve a light saturation point of 300 μmol photons.$m^{-2}$.$s^{-1}$ was obtained and this value was used as reference irradiance level, which was defined as 250 μmol photons.$m^{-2}$.$s^{-1}$ for SOX. This level of 250 μmol photons.$m^{-2}$.$s^{-1}$ corresponds to 15% of SOX lamp for blue and green LEDs, and 10% of SOX for red LED.

Each treatment was cultivated in three independent glass flask ($n$ = 3) (Fig. 31A-F) and the nutrient restitution (0.5 mM $KNO_3$) was provided weekly. At the end of the one week experimental period, samples were collected, freeze-dried, and stored at room temperature until the assessment of chlorophylls, carotenoids, and fatty acid profiles.

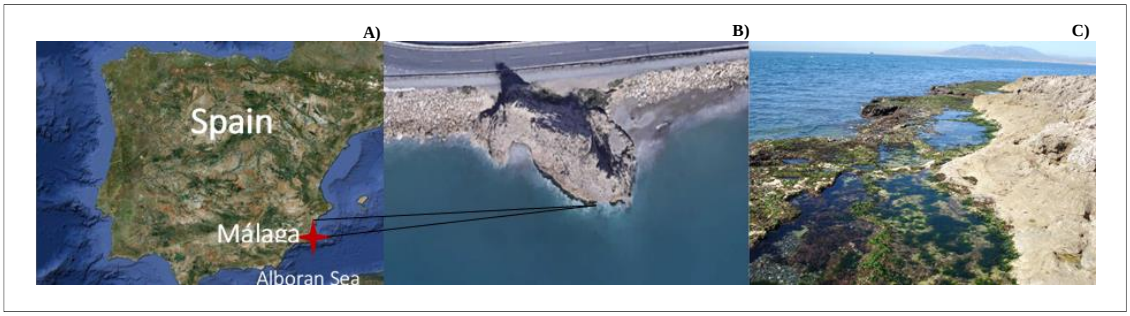


**Figure 30.** A) Spain map with the localization of Málaga coast, Spain; B) La Araña Beach (36°70´N; 4°33´W) and the localization of the rocky shore coast, which correspond to the collection site; C) Distribution of *Sargassum* bed along the lower intertidal and upper infralittoral zones of the littoral (photo: Felix L. Figueroa).

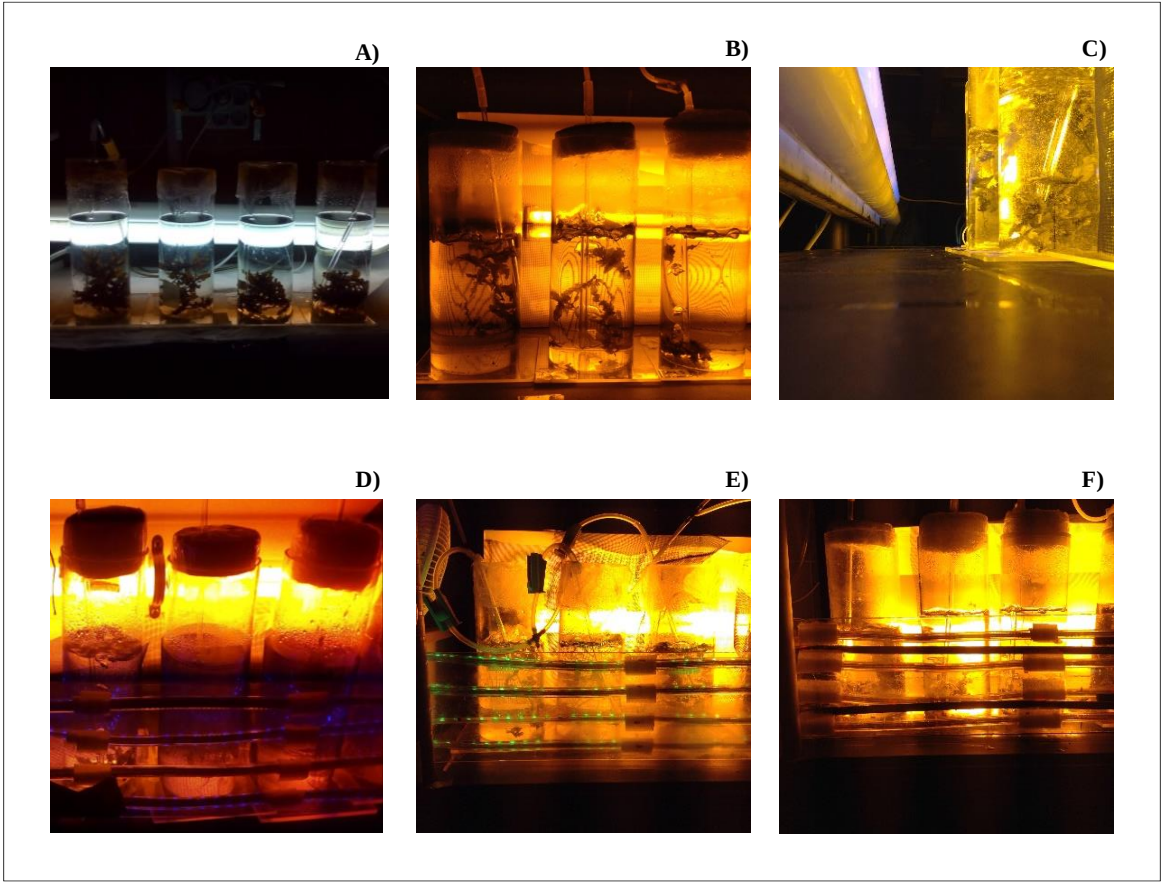


**Figure 31**. Exposure of *Sargassum vulgare* to different light quality treatments during one week (*n* = 3). A) algae under acclimation period under PAR light; B) SOX light (control); C) SOX+UV; D) SOX+Blue LEDs; E) SOX+Green LEDs; F) SOX+Red LEDs.

## Lipids and fatty acids

***Total lipids*.** Total lipids were analyzed by the gravimetric method following (Folch et al. 1957). Freeze-dried samples of approximately 200 mg DW were extracted in 20 mL of chloroform:methanol (2:1 v/v) with 0.01% BHT (butylated hydroxytoluene) as an antioxidant agent to avoid the oxidation of lipids during the whole process, by using an ultra-turrax disperser (T10, Ika Works Inc., USA), during 5 min in cold (Fig. 32A). Then, 2 mL of KCl 0.88% were added and centrifuged at 2000 rpm for 5 min to obtain the separation of phases (Fig. 32B). The upper phase, which contains salts and methanol was discarded by using a Pasteur pipette (Fig. 32C), and the bottom phase, which contains the lipids and the chloroform phase was filtered in a filter paper previous soaked with trichloromethane and sodium sulfate anhydrous to retain water (Fig. 32D). The samples were cooled to -20 °C for 20 min to remove the salt layer that forms, which was carefully removed by using a Pasteur pipette. The chloroform phase where the lipids are dissolved (Fig. 32E) was evaporated using rotaevaporator at room temperature. After the complete evaporation, samples were weighed.

The calculation of total lipid content was represented as yield of lipid percentage with respect to the initial freeze dry biomass:

**Lipids (%) = [Lipids (g) / Biomass (g DW)] x 100**

***Fatty acids.*** Samples for estimating fatty acid methyl esters (FAME) were prepared by acid-catalyzed transesterification of total lipids following the method of (Christie 1982). The samples containing total lipids were transmethylated overnight in 2 mL of sulfuric acid 1% in methanol (plus 1 mL of toluene to dissolve the neutral lipids) at 50 °C. Methyl esters were extracted twice in 5 mL of hexane-diethyl ether (1:1 v/v) after neutralization with 2 mL of $KHCO_3$ 2%, dried under gaseous nitrogen and redissolved in 1 mL of iso-hexane. FAME were characterized and quantified by gas-liquid chromatography in Servicios Centrales de Apoyo a la Investigación (SCAI), Unidad de Fotobiología at University of Málaga, Spain, using a gas chromatographer Focus GC (Thermo Scientifics, USA). For the separation method a forte column BPX70 (70% cyanopropyl polysilphenyleno-siloxane) (SGE Analytical Science, Australia; 60 m x 0.25 mm and 0.25 mm) was employed. Helium was used as the carrier gas at a pressure of 300 kPa. The initial temperature of the column was 140 °C for 10 min, then it was raised to 240 °C at a rate of 2.5 °C $min^{-1}$, and finally maintained

at 240 °C for 10 min. The detection of the FAMES was carried out through an FID detector and the peaks were identified by comparing their retention times with appropriate FAME standards (Supelco 37-Component FAME mix 47885-U, USA). The injection volume was 1 µL. Data for the individual fatty acids were expressed as percentage of total content. From the fatty acid composition were identified satured fatty acid (SFAs), monounsaturated fatty acid (MUFAs), and polyunsaturated fatty acid (PUFAs).

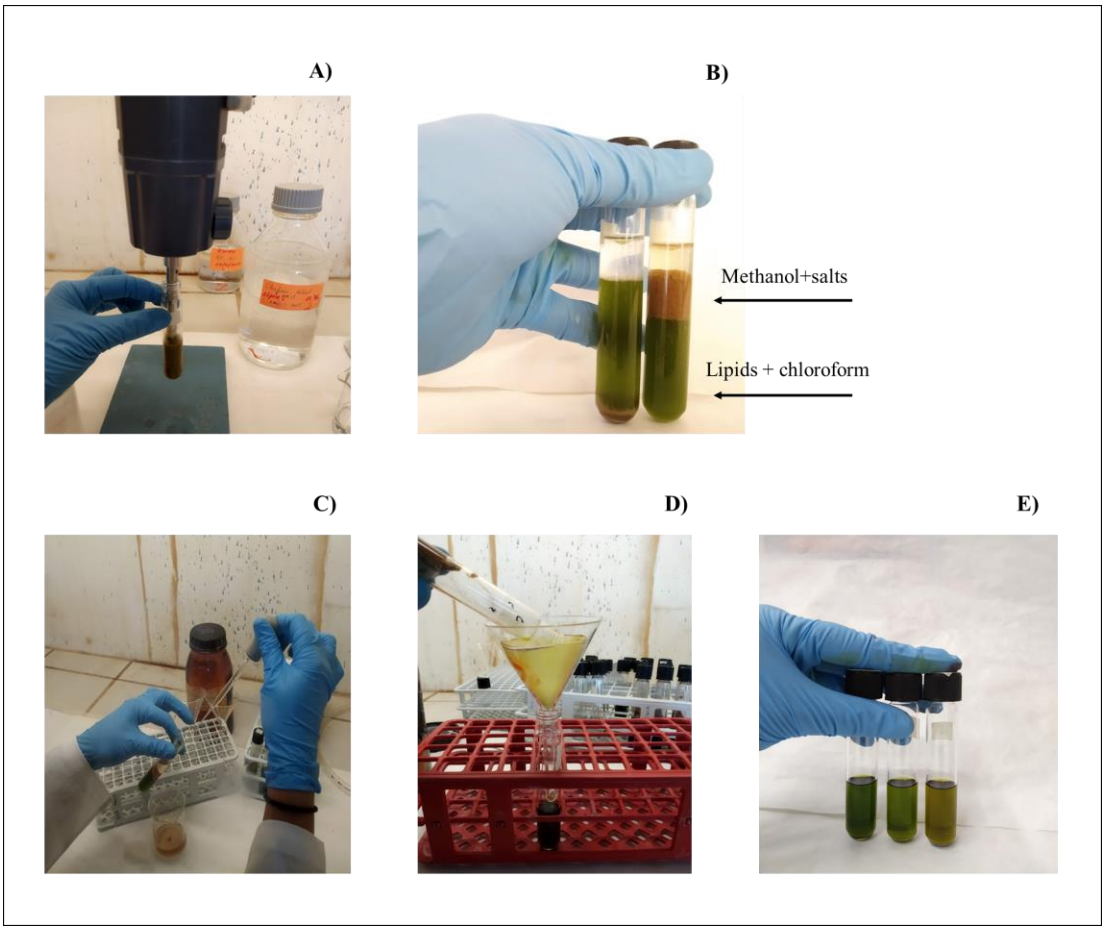


**Figure 32.** Lipid extraction procedure for *Sargassum vulgare* after one week of exposure to different light qualities. A) Sample homogenization by using an ultra-turrax disperser; B) Phase separation after the addition of 0.88% KCl with an upper phase containing salts and methanol, and a bottom phase with lipids and chloroform; C) Collection of upper phase with the help of Pasteur pipette for discard; D) Filtration of bottom phase by using a filter paper with sodium sulfate anhydrous; E) Final lipidic extract from samples after light treatments.

**Chlorophylls and carotenoids.** Pigment extraction was performed following Inskeep and Bloom (1985) from 20 mg freeze-dried samples (dry weight, DW) with 1 mL of DMF (dimethylformamide), and overnight at 4 °C. Sample extracts were filtered through 0.2 µm filters, and then analyzed by HPLC (Waters, USA; 996 photodiode array detector; 717 plus autosampler) as described in Lubián and Montero (1998) and García-Sánchez et al. (2012), using a column reverse phase column (Spheroclone, Phenomenex C18, Aschaffenburg, Germany; 15 cm x 4 mm) and 80 µL injection volume. Chlorophylls *a* and *c* and carotenoids were identified using commercial standards of chlorophyll *c*, antheraxanthin, β-carotene, fucoxanthin, lutein, neoxanthin, violaxanthin, and zeaxanthin (DHI LAB Products, Denmark). The pigment peaks were determined with a Waters Photodiode Array Detector at 350–800 nm, using the Empower 2 Chromatography Data Software. Data were expressed in $mg.g^{-1}$ DW.

**Data analysis.** All parameters were assessed in triplicate and the data were evaluated by analysis of variance (ANOVA) one-way, previous evaluation of normality (Kolmogorov-Smirnov's test) and homogeneity of variance (Bartlett's test) of the data set. When significant differences were evidenced, a *post-hoc* Student–Newman–Keuls (SNK) test was performed for a multiple comparison among the treatments set ($p < 0.05$). Analyses of data set were performed with the software STATISTICA (version 10.0).

## RESULTS

### Lipids and fatty acids

The percentage of total lipid content in *S. vulgare* after 10 days of exposure to different light qualities is represented in Figure 33A and the groups of total fatty acids summarizing all treatments is shown in Figure 33B. No variations in total lipid content were observed between the treatments, except for SOX+UV (Fig. 33A) with ~4% of total lipid. Total fatty acids from *S. vulgare* samples were classified in the three main classes as the sum and reported 41.18% for saturated fatty acids (SFAs), 11.76% for monounsaturated fatty acids (MUFAs), and 47.10% for polyunsaturated fatty acids (PUFAs) (Fig. 33B).

Fatty acid composition for *S. vulgare* within each treatment is presented in Table 8. Increase in the sum of SFAs content was observed for the diverse light qualities when comparing to the SOX control: SOX (17.42 ± 0.16%) > SOX+Green (23.20 ± 0.54%) >

SOX+UV (28.62 ± 0.85%) > SOX+Red (34.09 ± 1.53%) > SOX+Blue (45.34 ± 0.25%). Within this group palmitic acid (C16:0) presented the highest abundance (14.42 ± 0.78% to 37.77 ± 1.31%), followed by meristic acid (C14:0) (2.13 ± 0.07% to 4.68 ± 0.33%). For these both fatty acids, an increase was observed for almost all treatments when comparing to the control. Other SFAs as heptadecanoic acid (C17:0), stearic acid (C18:0), and behenic acid (C22:0) were identified in lower proportion. Additionally, arachidic acid (C20:0) was only detected in SOX+Blue treatment (0.33%) and lignoceric acid (C24:0) in SOX and SOX+Blue treatments.

Within MUFAs (Table 8), only two fatty acids were identified, palmitoleic acid (C16:1 7n) with increase for SOX+Red treatment (9.17 ± 0.82%), and oleic acid (C18:1 9n) with constant concentrations within the treatments. Between them, oleic acid was found in higher proportion.

In relation to PUFAs (Table 8), a general decrease in the sum of PUFAs was observed in relation to the control: SOX (62.49 ± 0.48%) > SOX+Green (53.15 ± 0.44%) > SOX+UV (49.42 ± 0.69%) > SOX+Red (40.61 ± 0.42) > SOX+Blue (31.64 ± 0.20). Within this group, arachidonic acid (ARA, C20:4 n6) was the main fatty acid among all PUFAs, with lower content for all light qualities in relation to the control (29.26 ± 1.55%); SOX > SOX+Green (25.02 ± 1.78%) > SOX+UV (20.31 ± 2.96%) > SOX+Red (16.92 ± 0.34%) > SOX+Blue (13.15 ± 0.51%). Linoleic acid (C18:2 n6) (from 7.87 ± 0.14% to 11.86 ± 0.15%) followed by α-linolenic acid (C18:3 n3) (from 4.97 ± 0.37% to 11.16 ± 0.47%) were the second most abundant PUFAs, with differences among the light treatments. Other fatty acids as eicosapentanoic acid (EPA, C20:5 n3), eicosatrienoic acid (C20:3 n6) and γ-linolenic acid (C18:3 n6) were present in lower proportion.

The sum of omega-3 (ω3; n3) and omega-6 (ω6; n6) fatty acids and the ratio between them are also presented in Table 8. The sum of ω3 ranged from 8.25 ± 0.24% to 17.61 ± 0.47%, while ω6 represented more than double that ω3 ranging between 22.97 ± 0.21% to 44.46 ± 0.67%. The ω3/ω6 ratio for *S. vulgare* presented differences between light treatments: SOX+Green (3.30) > SOX+UV (2.82) > SOX+Blue (2.78) > SOX+Red (2.69) > SOX (2.5) (Table 8).

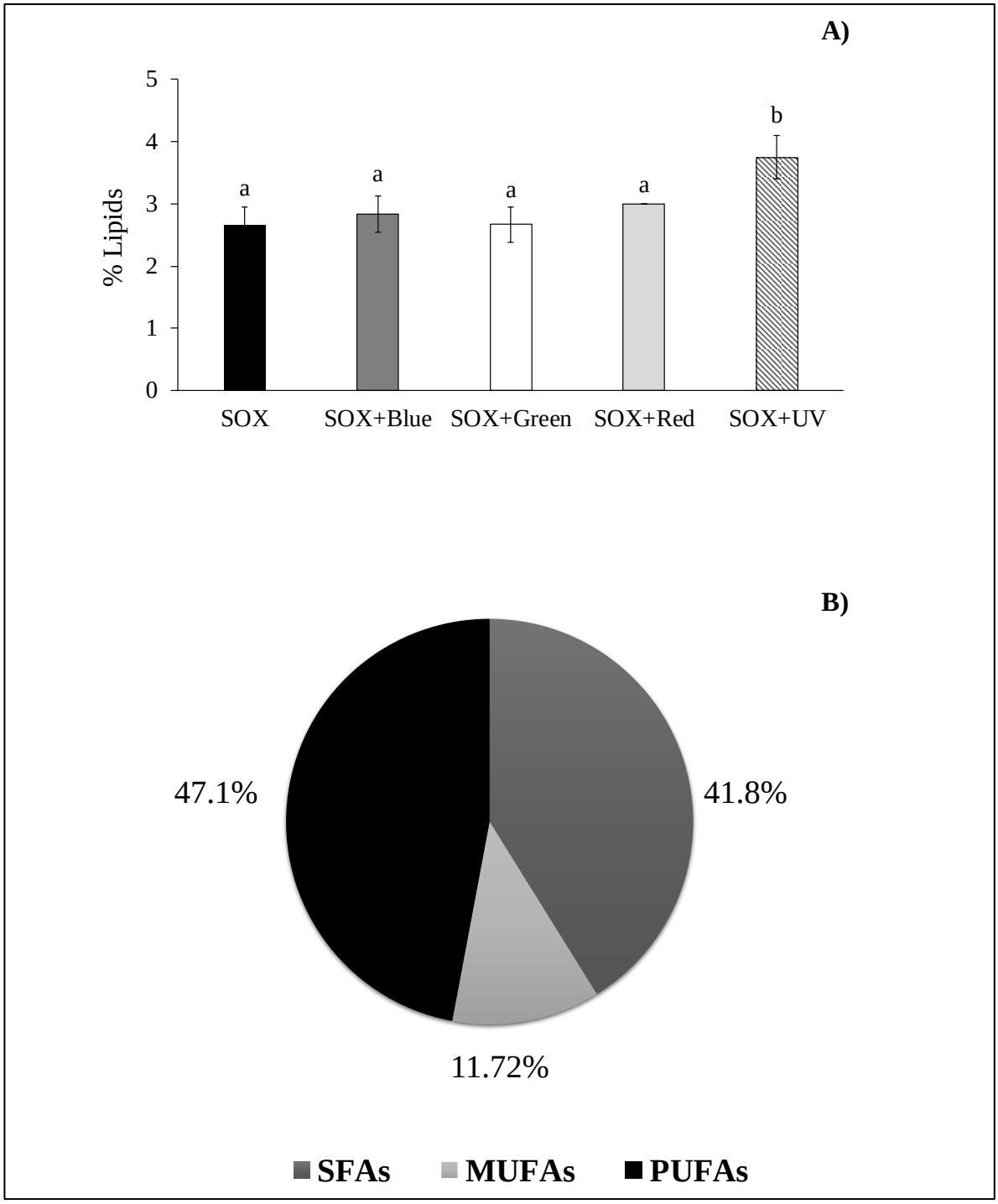


**Figure 33**.A) Percentage of total lipid content for *Sargassum vulgare* after 10 days of exposure to different light qualities ($n$ = 3; mean ± SD). Letters indicate differences according to one-way ANOVA and Newman-Keuls *post-hoc* test ($p < 0.05$). (B) Percentage of total amount of fatty acid classes as the sum of all treatments and grouped by SFAs (saturated fatty acids), MUFAs (monounsaturated fatty acids), and PUFAs (polyunsaturated fatty acids).

**Table 8.** Profile of total fatty acid composition (% TFA) in *Sargassum. vulgare* (n = 3; mean ± SD) after 10 days of exposure to different light qualities, classified in SFAs (saturated fatty acids), MUFAs (monounsaturated fatty acids), and PUFAs (polyunsaturated fatty acids) with the respective sum of them. ω3 = omega-3 (n3); ω6 = omega-6 (n6). Letters indicate differences according to one-way ANOVA and Newman-Keuls post-hoc test ($p < 0.05$). n.d = non-detected.

| TFA (%) | SOX | SOX + Blue | SOX + Green | SOX + Red | SOX + UV |
|---|---|---|---|---|---|
| **SFAs** | | | | | |
| C14:0 | 2.13 ± 0.07 $^{c}$ | 4.68 ± 0.33 $^{a}$ | 2.88 ± 0.37 $^{bc}$ | 3.88 ± 0.69 $^{ab}$ | 3.81 ± 0.55 $^{ab}$ |
| C16:0 | 14.52 ± 0.78 $^{d}$ | 37.77 ± 1.31 $^{a}$ | 19.37 ± 2.15 $^{cd}$ | 29.02 ± 6.64 $^{ab}$ | 23.71 ± 3.52 $^{bc}$ |
| C17:0 | 0.26 ± 0.00 $^{b}$ | 0.20 ± 0.02 $^{c}$ | 0.29 ± 0.03 $^{a}$ | 0.29 ± 0.03 $^{a}$ | 0.19 ± 0.01 $^{c}$ |
| C18: 0 | 0.3 ± 0.01 $^{c}$ | 0.87 ± 0.05 $^{a}$ | 0.37 ± 0.10 $^{c}$ | 0.61 ± 0.18 $^{b}$ | 0.58 ± 0.09 $^{b}$ |
| C20:0 | n.d | 0.33 ± 0.00 | n.d | n.d | n.d |
| C22:0 | 0.17 ± 0.09 $^{c}$ | 1.05 ± 0.07 $^{a}$ | 0.29 ± 0.05 $^{bc}$ | 0.42 ± 0.17 $^{b}$ | 0.34 ± 0.08 $^{bc}$ |
| C24:0 | 0.14 ± 0.00 $^{b}$ | 0.45 ± 0.02 $^{a}$ | n.d | n.d | n.d |
| **Sum SFAs** | 17.42 ± 0.16 $^{e}$ | 45.34 ± 0.25 $^{a}$ | 23.2 ± 0.54 $^{d}$ | 34.09 ± 1.53 $^{b}$ | 28.62 ± 0.85 $^{c}$ |
| **MUFAs** | | | | | |
| C16:1 7n | 7.29 ± 0.33 $^{b}$ | 7.53 ± 0.07 $^{b}$ | 7.81 ± 0.27 $^{b}$ | 9.17 ± 0.82 $^{a}$ | 7.80 ± 0.01 $^{b}$ |
| C18:1 9n | 12.16 ± 0.38 $^{b}$ | 14.68 ± 0.41 $^{ab}$ | 13.55 ± 1.22 $^{ab}$ | 14.91 ± 1.94 $^{ab}$ | 13.19 ± 1.15 $^{ab}$ |
| **Sum MUFAs** | 19.45 ± 0.71 $^{c}$ | 22.21 ± 0.48 $^{b}$ | 21.35 ± 1.50 $^{b}$ | 24.07 ± 2.76 $^{a}$ | 21.15 ± 1.6 $^{b}$ |
| **PUFAs** | | | | | |
| C18:2 n6c | 11.46 ± 0.49 $^{ab}$ | 7.87 ± 0.14 $^{c}$ | 11.86 ± 0.15 $^{ab}$ | 10.44 ± 1.19 $^{b}$ | 13.18 ± 0.75 $^{a}$ |
| C18:3 n3 | 11.16 ± 0.47 $^{a}$ | 4.97 ± 0.37 $^{d}$ | 7.03 ± 1.19 $^{bc}$ | 6.10 ± 0.58 $^{cd}$ | 8.18 ± 0.51 $^{b}$ |
| C18:3 n6 | 1.61 ± 0.08 $^{a}$ | 0.72 ± 0.09 $^{c}$ | 1.46 ± 0.20 $^{ab}$ | 0.84 ± 0.08 $^{c}$ | 1.17 ± 0.211 $^{b}$ |
| C20:2 | 0.43 ± 0.02 $^{b}$ | 0.42 ± 0.03 $^{b}$ | 0.41 ± 0.03 $^{b}$ | 0.49 ± 0.00 $^{a}$ | 0.51 ± 0.01 $^{a}$ |
| C20:3 n6 | 2.13 ± 0.30 $^{a}$ | 1.17 ± 0.09 $^{b}$ | 2.20 ± 0.07 $^{a}$ | 1.85 ± 0.29 $^{a}$ | 1.88 ± 0.04 $^{a}$ |
| C20:4 n6 | 29.26 ± 1.55 $^{a}$ | 13.15 ± 0.51 $^{d}$ | 25.02 ± 1.78 $^{b}$ | 16.92 ± 0.34 $^{d}$ | 20.31 ± 2.96 $^{c}$ |
| C20:5 n3 | 6.32 ± 0.91 $^{a}$ | 3.15 ± 0.32 $^{c}$ | 5.01 ± 0.22 $^{b}$ | 4.81 ± 0.47 $^{b}$ | 4.14 ± 0.8 $^{b}$ |
| C22:6 n3 | 0.10 ± 0.02 $^{a}$ | 0.13 ± 0.02 $^{a}$ | 0.14 ± 0.01 $^{a}$ | n.d | 0.49 ± 0.24 $^{a}$ |
| **Sum PUFAs** | 62.49 ± 0.48 $^{a}$ | 31.64 ± 0.20 $^{e}$ | 53.15 ± 0.44 $^{b}$ | 40.61 ± 0.42 $^{d}$ | 49.42 ± 0.69 $^{c}$ |
| **Sum ω3** | 17.61 ± 0.47 | 8.25 ± 0.24 | 12.19 ± 0.53 | 10.91 ± 0.53 | 12.821 ± 0.53 |
| **Sum ω6** | 44.46 ± 0.67 | 22.97 ± 0.21 | 40.54 ± 0.55 | 29.22 ± 0.48 | 36.69 ± 0.99 |
| **Ratio ω6/ω3** | 2.50 | 2.78 | 3.30 | 2.69 | 2.82 |

**Chlorophylls and carotenoids**

Identification and quantification of pigment content in *S. vulgare* were performed after ten days of exposure to different light qualities. From the samples, it was identified chlorophylls *a* and *c* (Chl *a* and Chl *c*, respectively), and the carotenoids fucoxanthin, violaxanthin, neoxanthin, zeaxanthin, and β-carotene.

Similar trend of Chl *a* and Chl *c* were observed for *S. vulgare* under the light quality treatments, which control treatment (SOX) showed 1.10 ± 0.02 $mg.g^{-1}$ DW Chl *a* (Fig. 34A) and 0.07 ± 0.00 $mg.g^{-1}$ DW Chl *b* (Fig. 33B). Lower values were registered at SOX+Blue and SOX+RED when compared to control, and the highest chlorophyll concentrations were at SOX+Green (Fig. 34A and 34B). The treatment SOX+UV displayed similar chlorophyll contents than SOX.

Within carotenoids, fucoxanthin was the most expressive carotenoid, from 0.19 ± 0.01 $mg.g^{-1}$ DW to 0.32 ± 0.00 $mg.g^{-1}$ DW (Fig. 34C), while the other carotenoids ranged between 0.001$mg.g^{-1}$ DW to 0.025 $mg.g^{-1}$ DW (Fig. 34D-G). In general, carotenoids presented differences in their abundance within the treatments, in which similar patterns than chlorophylls were observed for fucoxanthin (Fig. 34C) and violaxanthin (Fig. 34D) with decrease for SOX+Blue and SOX+Red and increase at SOX+Green treatment. Neoxanthin (Fig. 34E) showed equal amount within the treatments, except for SOX+Red with lower concentration than the other treatments. Additionally, neoxanthin was not identified for SOX+Green treatment (Fig. 34E). Zeaxanthin increased at SOX+Red treatment and reduced at SOX+UV (Fig. 34F) when compared to the control. For β-carotene, all treatments were lower than the SOX control (Fig. 34G), with the greatest reduction for SOX+UV, followed by SOX+Blue, and finally SOX+Green and SOX+Red.

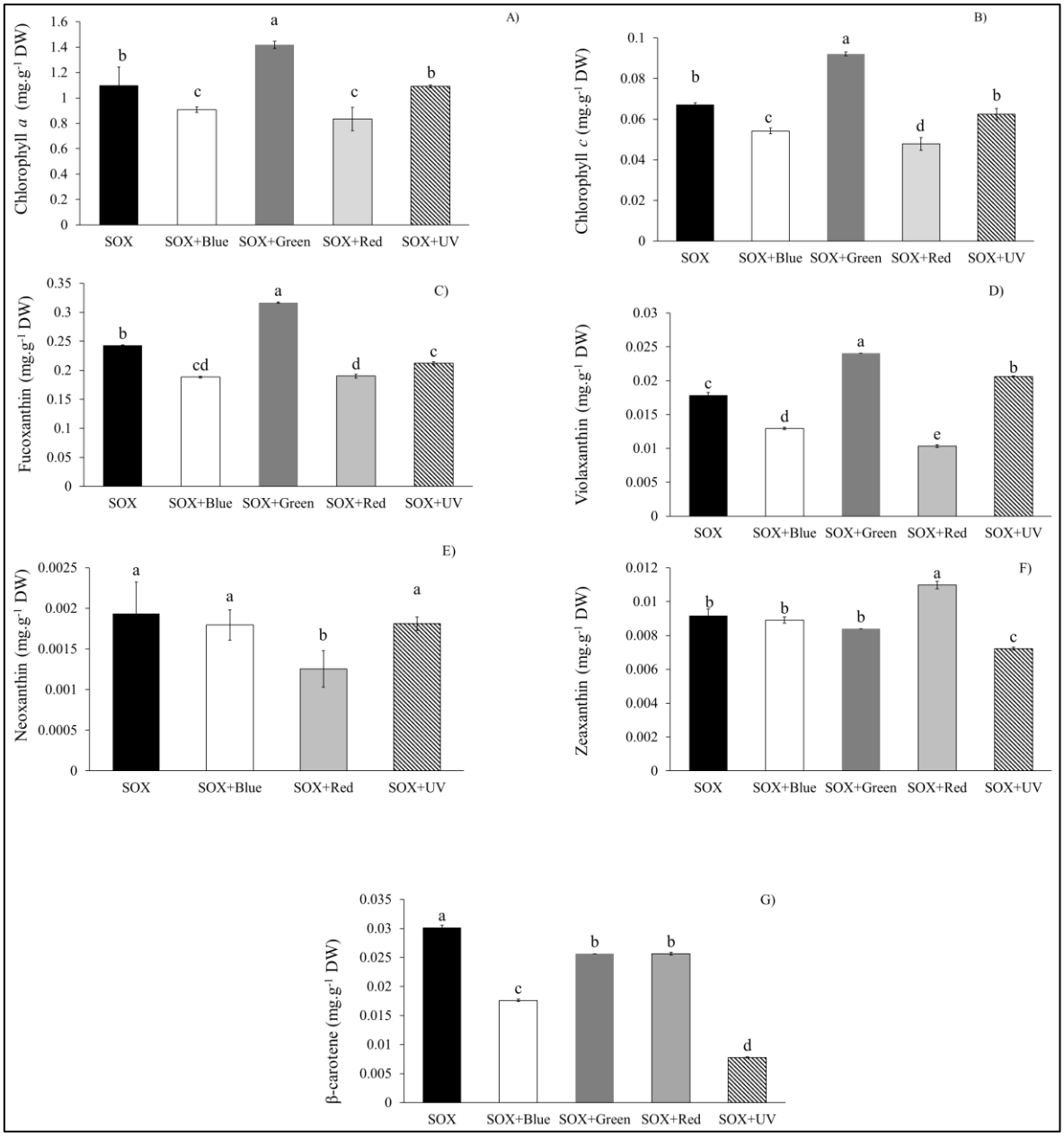


**Figure 34.** Pigment composition from *Sargassum vulgare* after exposure to different light qualities, assessed by HPLC ($n$ = 3; mean ± SD). A) Chlorophyll *a*; B) Chlorophyll *c*; C) Fucoxanthin; D) Violaxanthin; E) Neoxanthin; F) Zeaxanthin; G) β-carotene. Letters indicate differences according to one-way ANOVA and Newman-Keuls *post-hoc* test ($p < 0.05$).

## DISCUSSION

Marine environment is a unique rich source of biological and chemical diversity, presenting compounds of potential for pharmaceuticals, cosmetics, dietary supplements, and agrochemicals (Van Minh et al. 2005). Seaweeds are considered as a rich source of bioactive compounds as they are able to produce a great variety of metabolites characterized by a broad spectrum of biological activities (Rajasulochana et al. 2009). Brown seaweeds as *Sargassum* species are reported to produce metabolites with several therapeutic activities and due the many pharmacological properties they have been considered as a medicinal food of the twenty-first century (Kanimozhi and Joy Jeba Malar 2015).

Total lipid content in *S. vulgare* varied between ~2.7% and ~4.0% of DW, results that are in accordance with that commonly found for seaweeds (1-5% DW) (Banerjee et al. 2009). Within the SFAs, palmitic acid (C16:0) was the dominant for all treatments in *S. vulgare*, finding that is in agreement with other studies where reported that this fatty acid is the major for *Sargassum* species (Kumar et al. 2011; Noaman et al. 2016; Santos et al. 2019a). Two kind of MUFAs were detected for *S. vulgare*, palmitoleic (C16:1 n7) and oleic (C18:1 n9) acids, which also have been reported as the main for brown seaweeds (Schmid et al. 2014).

For PUFAs, arachidonic acid (ARA; C20:4 n3) was the major fatty acid within this group presenting percentages between 13.15% and 29.26%. Brown seaweeds have been reported to be a common source of this fatty acid (Schmid et al. 2014). Other PUFAs commonly found in this group of algae is eicosapentanoic acid (EPA; C20:5 n3). For the present work *S. vulgare* presented percentages within 3.15% and 6.32%, this values were higher when comparing to Santos et al. (2019) for the same species, whom reported range between 1.82% and 2.08%. However, our results showed lower content of EPA in relation to Pereira et al. (2012) that observed values of 8.60%, and have stated that levels of this fatty acid are often high in brown algae.

Light quality treatments used in this study modulated variations of fatty acid content after exposure, showing increase of SFAs and MUFAs and decrease of PUFAs in relation to the control. These results suggest that lipid composition of macroalgae can show changes during exposure to different light intensities and spectral availability, because there is a close

relationship between lipids and subcomplexes anchored to the photosystem within the membranes of the thylakoids (Thompson 1996; Klyachko-Gurvich et al. 1999).

SOX+Blue and SOX+Red presented the higher content of SFAs, increasing in 28% and 17% over the control, respectively. It has been demonstrated that LED light sources are a suitable choice for plant production and have the potential to produce major photosynthetically efficient light (Liu and Yang 2014). Additionally, there is a consensus that red and blue lights are essential wavelength that have higher relative quantum efficiency of photosynthesis, and can fulfill normal growth and development in land plants (Liu and Yang 2014). SFAs increase in 11% for UV radiation comparing to the control, fact that has also been observed for *S. hornschuchii* (Noaman et al. 2016). Increase in fatty acid concentrations under UV exposure, indicates an oxidative degradation of total lipids to form free fatty acids (Skerratt et al. 1998). Some studies have reported increase of unsaturated fatty acids after UV exposure for the cyanobacteria *Spirulina platensis* (Gomont) Geitler (Skerratt et al. 1998), the diatoms *Phaeodactylum tricornutum* Bohlin and *Chaetoceros mulleri* Lemmermann (Liang et al. 2006), and the brown seaweed *S. hornschuchii* (Noaman et al. 2016). However, for the present work, increase in unsaturated fatty acids from *S. vulgare* was only observed for palmitoleic acid (C16:1 7n) in SOX+Red and linoleic acid (C18:2 n6) in SOX+UV; however, this was slight.

In general, the different light treatments induced a reduction of PUFAs, suggesting lipid peroxidation or changes in lipid metabolism as has been reported by Hessen et al. (1997) for phytoplankton after exposure to UV radiation. Additionally, during fatty acid biosynthesis, the process of chain elongation and unsaturation requires a large amount of ATP compared to that required for the production of SFAs and MUFAs (Thompson 1996). Therefore, it seems likely that a limited supply of ATP may be the cause of the decrease in the concentrations of all long-chain unsaturated fatty acids, process that was more evident for SOX+Blue and SOX+Red. This fact explain why SFAs were higher for these light qualities.

The evaluation of the chemical composition of macroalgae is quite interesting, since these organisms may be an important nutritional source. Then the evaluation of chemical constituents is the first step towards the valorization of algal biomass as a food supplement (Balboa et al. 2016). Lipid content has been described to be very low in seaweeds; however

their PUFAs content can be as high as that of land plants (Darcy-Vrillon 1993), facts that were corroborated for the present work. We identified PUFAs, as linoleic acid (C18:2 n6), α-linolenic acid (C18: n3), ARA (C20:4), EPA (C20:5 n3), eicosatrienoic acid (C20:3 n6), and docosahexaenoic acid (DHA C22:6 n3) with similar values as reported for other *Sargussum* species as *S. fusiforme*, *S. pallidum*, *S. thunbergii*, and *S. hornii* (Li et al. 2002; Terasaki et al. 2009; Chen et al. 2016).

Thus, PUFAs are found in high proportions in some seaweed species and are important from a nutritional and medical point of view (Sánchez-Machado et al. 2004; Schmid et al. 2014). For example, the ω3 fatty acid docosahexaenoic acid (DHA) has the property of reducing blood pressure, and other ω3 acids, especially from marine sources, have been reported to reduce the plasma cholesterol and triacyleglycerol levels, thereby decreasing the chances of thrombosis and related cardiac complications. Likewise ARA which is a major constituent of cell membranes, plays an important role in the production of prostaglandins in the body (Prabhakar et al. 2011).

Moreover, ω6/ω3 ratio is fundamental for the correct performance of this group of fatty acid in human health (Simopoulos 2004). Although the different light qualities did not improve this ratio in *S. vulgare*, values varied between 2.5 to 3.3; which is still within the limit recommended by the World Health Organization (WHO), whose dietary intake ratio should be less than 10 (Matanjun et al. 2009).

Currently, the main source of PUFAs comes from fish oils, since only marine organisms have the ability to synthesize very long chain PUFA (VLCPUFA). However, the abusive exploitation of this matrix together with the increasing sea pollution, has led to the decline of this resource, leading to the search of alternative fonts of this resource (Pereira et al. 2012). In this regard, an intensive examination of the natural fatty acid composition of macroalgae have increase. For example, studies with macroalgae species showed that most of these species, although they have low levels of lipids and fatty acids with respect to microalgae, are rich in PUFAs and have a good ω6/ω3 ratio, a suitable amount for human consumption (approximately 1-2/1) (Simopoulos 2002; Stengel and Connan 2015). Therefore, these organisms can be an excellent source of fatty acids as some are essential in nutrition and are not present in terrestrial plants (Kumari et al. 2013). These properties can propose that the

fatty acids of macroalgae, which are still largely unexplored, may represent another interesting resource for nutraceutical and pharmaceutical applications as biofunctional ingredient.

Pigment composition in *S. vulgare* showed fucoxanthin, Chl *a*, and β-carotene as the main pigments, while other minor pigments such as, zeaxanthin, violaxanthin, neoxanthin, and Chl *c* were also observed. Our results are in accordance with other studies on pigment characterization from brown seaweeds (Terasaki et al. 2009, 2012; Sudhakar et al. 2013; Heriyanto et al. 2017). It is known that specific photosynthetic pigments and their concentrations in brown seaweeds could present fluctuations that depend on several environmental factors. For the present work, variations of the content of pigments from *S. vulgare* were observed in relation to light qualities. Light is important for the chlorophyll synthesis and algal pigment synthesis is regulated by various photoreceptors that absorb lighting for different wavelengths (Lopez-Figueroa et al. 1989; López-Figueroa and Niell 1990).

In general, light SOX+Blue and SOX+Red did not stimulate increase on pigment concentrations. In previous studies was reported that in favorable conditions of light quantity and quality the accumulation of photosynthetic pigments might be induced (Rüdiger and López-Figueroa 1992). Among various light spectra, red and blue wavelengths play an important role in the photosynthesis and photomorphogenesis, thus influencing plant development and metabolism (Manivannan et al. 2015). For *L. hyperborea* , a decrease in all pigments was observed after exposure to blue and red lights (Dring 1986). Similar findings are reported for the present work, where a significant reduction of almost all identified pigments was observed, which can be related to abatement of photosynthesis rate in *S. vulgare.* SOX+Green was the only light that induced increase in pigments from *S. vulgare*, except for β-carotene that was reduced under this light quality. For other species as the red seaweeds *Corallina elongata* Ellis, *Plocamium cartilagineum* (Linnaeus) P.S. Dixon (López-Figueroa and Niell 1990), and *Pyropia haitanensis* (T.J. Chang & B.F. Zheng) N. Kikuchi & M. Miyata (Wu 2016) increase in Chl *a* content by blue light was reported, suggesting that blue light have special influence on regulating algae growth and photosynthetic pigments synthesis (Wu 2016). It has been reported that this light could benefit algal growth and

pigments as Chl *a*, *α*-carotene, and lutein synthesis for the red macroalga *Halymenia floresia* (Clemente) C. Agardh that could be related to a higher efficiency of light absorption (Godínez-Ortega et al. 2008). It is known that UV radiation has negative consequences on photosynthetic pigments from seaweeds, either by degradation or by inhibition of enzymes involved in their biosynthetic pathway (Ranjbarfordoei et al. 2011). However, slightly variation on pigment content in *S. vulgare* was observed for SOX+UV, and as in green light only notorious decrease was observed for β-carotene. This finding could be related to the fact that seaweeds have developed efficient photoprotective mechanisms against excessive solar radiation (Gates 2014).

From a biotechnological point of view, seaweeds can potentially be induced to the synthesis and accumulation of compounds derived from secondary metabolism as pigments, and within this group, carotenoids, are widely used in the food and feed industries. Currently, there is a strong demand for natural pigments instead of those obtained by chemical synthesis, since it is suspected that compounds of synthetic origin could be promoters for carcinogenesis processes as well as produce liver and kidney toxicity (Abd et al. 2007). In this way, natural carotenoids began to be used in the food industry, replacing synthetic ones (Kelloff et al. 2018), being widely used in foods and beverages to improve the organoleptic properties and in nutraceutical products due to the antioxidant properties they present (Burton and Ingold 1984).

The potential uses of brown seaweeds has been recognized due to the presence of compounds with several beneficial effects on human health. In addition to sodium alginate, fucoxanthin, the major marine carotenoid, has demonstrated anti-inflammatory (Shiratori et al. 2005), anticancer (Kotake-Nara et al. 2001), and anti-obesity activities (Miyashita 2009). In the same way *β*-carotene, besides being one of the leading food colorant, has strong antioxidant capacity that could enhance immunity against various infectious diseases and acts as photoprotective agent (Boominathan and Mahesh 2015). Zeaxanthin, other carotenoid found in brown seaweeds, has been applied in pigmentation of animal tissues and foods; moreover, they are the primary pigments for the yellowing and the maintenance of normal visual function of the human eye macula and play a crucial role in prevention of stroke and lung cancer (Michaud et al. 2000)

Summarizing, light characteristics as spectral quality, quantity, and duration, have a profound influence on plant and seaweed metabolism and development. Characteristics that are of great relevance to determine a suitable photo environment for stable productive culture of brown seaweeds with the aim of improving induction of the synthesis and accumulation of compounds of biotechnological interest. For the present work, we describe fatty and pigment profiles for *S. vulgare* submitted to different light qualities, and results showed a variable response in regards to treatments. Green light was the one that stimulated an increase in most of the pigments; while blue, red, and green lights increased SFAs, MUFAs, and PUFAs contents, respectively. These interesting results indicate that future researches should be performed to stablish suitable light condition for the stimulation of both pigments and fatty acids from *S. vulgare* or another species of *Sargassum*. Additionally, the species presented a high percentage of PUFAs, with appropriate ratio of ω6/ω3, indicating its potential as a valuable source of bioactive compounds that can contribute to consumer's well-being, by being a part of new functional foods and pharmaceuticals.

# Final considerations

# FINAL CONSIDERATIONS

The present study showed that UV radiation under moderate doses is an abiotic factor that influences the physiology of *Sargassum filipendula* and potential threat of biological processes are counteracted by several adaptive strategies activating different protective and repair mechanisms.

Effects of UVA radiation are less severe than those from UVB for growth rate of *S. filipendula*, however photosynthetic pigments showed little variation in response to both kind of radiations.

*Sargassum filipendula* presented a high antioxidant activity for PAR samples that could be attributed to the presence of phenolic compounds as phlorotannins. However, under UV radiation treatments especially UVB, decrease of this activity was observed into the thallus, which can be related to the exudation of phenolic compounds as phlorotannins that act as a defense mechanism by the formation of a "UV-refuge". This behavior could be supported by the yellowish coloration of seawater, feature that has been observed in brown seaweeds.

High antiviral activity of *S. filipendula* against HIV-1 reverse transcriptase was observed for the aqueous extracts, which could be related to sulfated polysaccharides. These compounds have attracted the attention for play an important role against this bioactivity.

By the application of a proteomic approach, it was possible to identify proteins from *S. filipendula* involved in several metabolisms as energy, photosynthesis, and carbohydrate. Several target proteins respond distinctively after the exposure to UV radiation. However, the knowledge of the molecular mechanisms triggering acclimation strategies are scarce, then these kind of researches are essential for further elucidation of the ability of the species to adapt to this type of stress.

Fatty acid profile of *S. vulgare* showed that the species is a source of PUFAs, presenting high content of these fatty acids that are important from a nutritional and medical point of view. Additionally, fatty acid content varied in relation to the different light qualities, where SFAs and MUFAs increased, while PUFAs decreased in relation to the control.

Important pigments as chlorophylls *a* and *c*, fucoxanthin, and β-carotene, among others, were identified for *S. vulgare*. SOX+Green light was the only treatment that increased the pigments of the species.

In relation to light treatments, it is recommended further studies that allow our understanding how to optimize lighting systems for seaweeds cultivation for further developing of modern ecological agriculture.

# References

## REFERENCES


Abd H, El-baz F, Boroty G (2007) Production of carotenoids from marine microalgae and its evaluation as safe food colorant and lowering cholesterol agents. Am J Agric Environ Sci 2:792–800.

European Environment Agency (2018) Ozone-depleting substances. Aggregated data reported by companies on the import, export, production, destruction, feedstock and process agent use of ozone-depleting substances in the European Union, 2006-2017 pp 32.

Aguilera J, Karsten U, Lippert H, et al (1999) Effects of solar radiation on growth, photosynthesis and respiration of marine macroalgae from the Arctic. Mar Ecol Prog Ser 191:109–119.

Ahn M-J, Yoon K-D, Min S-Y, et al (2004) Inhibition of HIV-1 reverse transcriptase and protease by phlorotannins from the brown alga *Ecklonia cava*. Biol Pharm Bull 27:544–547.

Ahn MJ, Yoon KD, Kim CY, et al (2006) Inhibitory activity on HIV-1 reverse transcriptase and integrase of a carmalol derivative from a brown alga, *Ishige okamurae*. Phyther Res 20:711–713.

Aigner S, Remias D, Karsten U, Holzinger A (2013) Unusual phenolic compounds contribute to ecophysiological performance in the purple-colored green alga *Zygogonium ericetorum* (Zygnematophyceae, Streptophyta) from a high-alpine habitat. J Phycol 49:648–660.

Al-Azzawie HF, Alhamdani MSS (2006) Hypoglycemic and antioxidant effect of oleuropein in alloxan-diabetic rabbits. Life Sci 78:1371–1377.

Alscher R, Erturk N, Heath L (2002) Role of superoxide dismutases (SODs) in controlling oxidative stress in plants. J Exp Bot 53:1331–1341

Altamirano M, Flores-Moya A, Figueroa FL (2003) Effects of UV radiation and temperature on growth of germlings of three species of *Fucus* (Phaeophyceae). Aquat Bot 75:9–20.

Altschul SF, Gish W, Miller W, et al (1990) Basic local alignment search tool. J Mol Biol 215:403–410.

Álvarez-Gómez F, Bouzon ZL, Korbee N, et al (2017) Combined effects of UVR and nutrients on cell ultrastructure, photosynthesis and biochemistry in *Gracilariopsis longissima* (Gracilariales, Rhodophyta). Algal Res 26:190–202.

Amado Filho GM, Andrade LR, Karez CS, et al (1999) Brown algae species as biomonitors of Zn and Cd at Sepetiba Bay, Rio de Janeiro, Brazil. Mar Environ Res 48:213–224.

Anderson JG, Wilmouth DM, Smith JB, Sayres DS (2012) UV dosage levels in summer: increased risk of ozone loss from convectively injected water vapor. Science 337:835–839.

Andrés-Colás N, Van Der Straeten (2017) Optimization of non-denaturing protein extraction conditions for plant PPR proteins. PLoS One 12:1–15.

Ang Junior P. (1985) Phenology of *Sargassum siliquosum* J. Ag. and *S. paniculatum* J. Ag. (Sargassaceae, Phaeophyta) in the reef flat of Balibago (Calatagan, Philippines). In: V International Coral Reef Congress. pp 51–57.

Apak R, Özyürek M, Güçlü K, Çapanoğlu E (2016) Antioxidant activity/capacity measurement. 1. Classification, physicochemical principles, mechanisms, and electron transfer (ET)-based assays. J Agric Food Chem 64:997–1027.

Arasaki S, Arasaki T (1981) Vegetables from the sea, first edit. Japan Pubns.

Aro EM, Virgin I, Andersson B (1993) Photoinhibition of Photosystem II. Inactivation, protein damage and turnover. BBA - Bioenerg 1143:113–134.

Artan M, Li Y, Karadeniz F, et al (2008) Anti-HIV-1 activity of phloroglucinol derivative, 6,6′-bieckol, from *Ecklonia cava*. Bioorganic Med Chem 16:7921–7926.

Aubé M, Roby J, Kocifaj M (2013) Evaluating potential spectral impacts of various artificial lights on melatonin suppression, photosynthesis, and star visibility. PLoS One 8:1-15.

Ayres-Ostrock LM, Plastino EM (2014) Effects of short-term exposure to ultraviolet-B radiation on photosynthesis and pigment content of red (wild types), greenish-brown,

and green strains of *Gracilaria birdiae* (Gracilariales, Rhodophyta). J Appl Phycol 26:867–879.

Bais AF, McKenzie RL, Bernhard G, et al (2015) Ozone depletion and climate change: impacts on UV radiation. Photochem Photobiol Sci 14:1955.

Bakar K, Mohamad H, Latip J, et al (2017) Fatty acids compositions of *Sargassum granuliferum* and *Dictyota dichotoma* and their anti-fouling activities. J Sustain Sci Manag 12:8–16.

Balboa EM, Gallego-Fábrega C, Moure A, Domínguez H (2016) Study of the seasonal variation on proximate composition of oven-dried *Sargassum muticum* biomass collected in Vigo Ria, Spain. J Appl Phycol 28:1943–1953.

Bandy B, Davison A (1990) Mitochondrial mutations may increase oxidative stress: implications for carcinogenesis and aging? Free Radic Biol Med 8:523–539.

Banerjee K, Ghosh R, Homechaudhuri S, Mitra A (2009) Biochemical composition of marine macroalgae from Gangetic Delta at the apex of Bay of Bengal. African J Basic Appl Sci 1:96–104.

Barbosa EB, Vidotto A, Polachini GM, et al (1992) Proteomics: methodologies and applications to the study of human diseases. Rev Assoc Med Bras 58:366–375.

Barufi J, Figueroa F, Plastino EM (2015) Effects of light quality on reproduction, growth and pigment content of *Gracilaria birdiae* (Rhodophyta: Gracilariales). Sci Mar 79:14–24.

Barufi J, Korbee N, Oliveira M, López-Figueroa F (2011) Effects of N supply on the accumulation of photosynthetic pigments and photoprotectors in *Gracilaria tenuistipitata* (Rhodophyta) cultured under UV radiation. J Appl Phycol 23:457–466.

Behrenfeld MJ, Lean DRS, Lee H (1995) Ultraviolet-B radiation effects on inorganic nitrogen uptake by natural assemblages of oceanic plankton. J Phycol 31:25–36.

Berglin M, Delage L, Potin P, et al (2004) Enzymatic cross-linking of a phenolic polymer extracted from the marine alga *Fucus serratus.* Biomacromolecules 5:2376–2383.

Bermejo R, de la Fuente G, Vergara JJ, Hernández I (2013) Application of the CARLIT index

along a biogeographical gradient in the Alboran Sea (European Coast). Mar Pollut Bull 72:107–118.

Bischof K (2002) Effects of solar UV-B radiation on canopy structure of *Ulva* communities from southern Spain. J Exp Bot 53:2411–2421.

Bischof K, Gómez I, Molis M, et al (2007) Ultraviolet radiation shapes seaweed communities. Life Extrem Environ 2:187–212.

Bischof K, Hanelt D, Tüg H, et al (1998) Acclimation of brown algal photosynthesis to ultraviolet radiation in Arctic coastal waters (Spitsbergen, Norway). Polar Biol 20:388–395.

Bischof K, Hanelt D, Wiencke C (2000a) Effects of ultraviolet radiation on photosynthesis and related enzyme reactions of marine macroalgae. Planta 211:555–562.

Bischof K, Kräbs G, Hanelt D, Wiencke C (2000b) Photosynthetic characteristics and mycosporine-like amino acids under UV radiation: A competitive advantage of *Mastocarpus stellatus* over *Chondrus crispus* at the Helgoland shoreline? Helgol Mar Res 54:47–52.

Björn LO (2007) Stratospheric ozone, ultraviolet radiation, and cryptogams. Biol Conserv 135:326–333.

Blumthaler M, Webb AR (2003) UVR climatology. In: Helbling EW, Zagarese HE (eds) UV Effects in Aquatic Organisms and Ecosystems. Comprehensive Series in Photochemical and Photobiological Sciences. The Royal Society of Chemistry, UK, pp 21–58.

Boominathan M, Mahesh A (2015) Seaweed carotenoids for cancer therapeutics. In: Handbook of Anticancer Drugs from Marine Origin. pp 185–203.

Bornman JF, Teramura AH (1993) Effects of enhanced UV-B radiation on terrestrial plants. UV-B Radiat ozone depletion 125–153 verificar a referencia, qual o nome da revista e volume?

Bouzon ZL, Chow F, Zitta CS, et al (2012) Effects of natural radiation, photosynthetically active radiation and artificial ultraviolet radiation-b on the chloroplast organization and

metabolism of *Porphyra acanthophora* var. *brasiliensis* (Rhodophyta, Bangiales). Microsc Microanal 18:1467–1479.

Bradford MM (1976) A rapid and sensitive method for the quantitation of microgram quantities of protein utilizing the principle of protein-dye binding. Anal Biochem 72:248–254.

Brand-Williams W, Cuvelier ME, Berset C (1995) Use of a free radical method to evaluate antioxidant activity. LWT - Food Sci Technol 28:25–30.

Britt AB, May GD (2003) Re-engineering plant gene targeting. Trends Plant Sci 8:90–95.

Budhiyanti SA, Raharjo S, Marseno DW, Lelana IYB (2012) Antioxidant activity of brown algae *Sargassum* species extract from the coastline of java island. Am J Agric Biol Sci 7:337–346.

Buma AGJ, Oijen T Van, Poll W Van De, et al (2000) The sensitivity of *Emiliania huxley* (Primnesiophyceae) to ultraviolet-B radiation. J Phycol 36:296–303.

Buma AGJ, Walter Helbling E, Karin De Boer M, Villafañe VE (2001) Patterns of DNA damage and photoinhibition in temperate South-Atlantic picophytoplankton exposed to solar ultraviolet radiation. J Photochem Photobiol B Biol 62:9–18.

Burton GW, Ingold KU (1984) β-Carotene: An unusual type of lipid antioxidant. Science 224:569–573.

Calder PC (2010) Omega-3 fatty acids and inflammatory processes. Nutrients 2:355–374.

Carpentier SC, Witters E, Laukens K, et al (2005) Preparation of protein extracts from recalcitrant plant tissues: An evaluation of different methods for two-dimensional gel electrophoresis analysis. Proteomics 5:2497–2507.

Carter P (1971) Spectrophotometric determination of serum iron at the submicrogram level with a new reagent (ferrozine). Anal Biochem 40:450–458.

Castelo-Branco VN, Torres AG (2011) Capacidade antioxidante total de óleos vegetais comestíveis: Determinantes químicos e sua relação com a qualidade dos óleos. Rev Nutr 24:173–187.

Chakraborty K, Maneesh A, Makkar F (2017) Antioxidant activity of brown seaweeds. J Aquat Food Prod Technol 26:406–419.

Chandraraj S, Prakash B, Navanath K (2010) Immunomodulatory activities of ethyl acetate extracts of two marine sponges *Gelliodes fibrosa* and *Tedania anhelans* and brown algae *Sargassum ilicifolium* with reference to phagocytosis. Res J Pharm Biol Chem Sci 1:302–307.

Chen Q, Silflow CD (1996) Isolation and characterization of glutamine synthetase genes in *Chlamydomonas reinhardtii*. Plant Physiol 112:987–96.

Chen Q, Vazquez EJ, Moghaddas S, et al (2003) Production of reactive oxygen species by mitochondria: Central role of complex III. J Biol Chem 278:36027–36031.

Chen Z, Xu Y, Liu T, et al (2016) Comparative studies on the characteristic fatty acid profiles of four different Chinese medicinal *Sargassum* seaweeds by GC-MS and chemometrics. Mar Drugs 14:1–11.

Chitra R, Ali M S, Anuradha V, Shantha M (2018) Antioxidant activity of polysaccharide from *Sargassum* sp. IOSR J Pharm 8:24–31.

Chiu IM, Yaniv A, Dahlberg JE, Gazit A, Skuntz S, Tronick S, Aaronson A (1985) Nucleotide sequence evidence for relationship of AIDS retrovirus to lentiviruses. Nature 317:366–368.

Cho S, Kang S, Cho J, et al (2007) The antioxidant properties of brown seaweed (S*argassum siliquastrum*) extracts. J Med Food 10:479–485.

Chow F, Oliveira MC (2008) Rapid and slow modulation of nitrate reductase activity in the red macroalga *Gracilaria chilensis* (Gracilariales, Rhodophyta): Influence of different nitrogen sources. J Appl Phycol 20:775–782.

Christaki E, Bonos E, Giannenasa I, Florou-Paneria P (2013) Functional properties of carotenoids originating from algae. J Sci Food Agric 93:5–11.

Christie WW (1982) A simple procedure for rapid transmethylation of glycerolipids and cholesteryl esters. J Lipid Res 23:1072–1075.

Cock JM, Sterck L, Ahmed S, et al (2012) The *Ectocarpus* genome and brown algal genomics. The *Ectocarpus* Genome Consortium. Adv Bot Res 64:141-184.

Connan S, Delisle F, Deslandes E, Ar Gall E (2006) Intra-thallus phlorotannin content and antioxidant activity in Phaeophyceae of temperate waters. Bot Mar 49:39–46.

Contreras L, Ritter A, Dennett G, et al (2008) Two-dimensional gel electrophoresis analysis of brown algal protein extracts. J Phycol 44:1315–1321.

Cornish ML, Garbary DJ (2010) Antioxidants from macroalgae: potential applications in human health and nutrition. Algae 25:155–171.

Correa MP (2015) Solar ultraviolet radiation: properties, characteristics and amounts observed in Brazil and South America. An Bras Dermatol 90:297–313.

Cruces E, Huovinen P, Gómez I (2013) Interactive effects of UV radiation and enhanced temperature on photosynthesis, phlorotannin induction and antioxidant activities of two sub-Antarctic brown algae. Mar Biol 160:1–13.

Cullen J, Neale P (1994) Ultraviolet radiation, ozone depletation, and marine photosynthesis. Photosynth Res 39:303–320.

Czeczuga B, Taylor FJ (1987) Carotenoid content in some species of the brown and red algae from the coastal area of New Zealand. Biochem Syst Ecol 15:5–8.

D'Orazio N, Gemello E, Gammone MA, et al (2012) Fucoxantin: A treasure from the sea. Mar Drugs 10:604–616.

Dahms HU, Dobretsov S, Lee JS (2011) Effects of UV radiation on marine ectotherms in polar regions. Comp Biochem Physiol - C Toxicol Pharmacol 153:363–371.

Dalton TP, Shertzer HG, Puga A (1999) Regulation of gene expression by reactive oxygen. Annu Rev Pharmacol Toxicol 39:67–101.

Dang TT, Bowyer MC, Van Altena IA, Scarlett CJ (2018) Comparison of chemical profile and antioxidant properties of the brown algae. Int J Food Sci Technol 53:174–181.

Darcy-Vrillon B (1993) Nutritional aspects of the developing use of marine macroalgae for the human food industry. Int J Food Sci Nutr 44:23–25.

Davison IR, Jordan TL, Fegley JC, Grobe CW (2007) Response of *Laminaria saccharina* (Phaeophyta) growth and photosynthesis to simultaneous ultraviolet radiation and nitrogen limitation. J Phycol 43:636–646.

Dawes CJ, Orduña-Rojas J, Robledo D (1999) Response of the tropical red seaweed Gracilaria cornea to temperature, salinity and irradiance. J Appl Phycol 10:419–425.

De Clercq E (2000) Current lead natural products for the chemotherapy of human immunodeficiency virus (HIV) infection. Med Res Rev 20:323–349.

de Eston VR, Bussab WO (1990) An experimental analysis of ecological dominance in a rocky subtidal macroalgal community. J Exp Mar Bio Ecol 136:179–195.

de la Coba F, Aguilera J, Figueroa FL, et al (2008) Antioxidant activity of mycosporine-like amino acids isolated from three red macroalgae and one marine lichen. J Appl Phycol 21:161–169.

de Nadal E, Ammerer G, Posas F (2011) Controlling gene expression in response to stress. Nat Rev Genet 12:833–845.

Demirel Z, Yilmaz-Koz F, Karabay-Yavasoglu U, et al (2009) Antimicrobial and antioxidant activity of brown algae from the Aegean sea. J Serbian Chem Soc 74:619–628.

Demmig B, Winter K, Krüger A, Czygan F-C (1988) Zeaxanthin and the heat dissipation of excess light energy in Nerium oleander exposed to a combination of high light and water stress. Plant Physiol 87:17–24.

Dieter H, Wiencke C, Nultsch W (1997) Influence of UV radiation on the photosyntesis of Arctic macroalgae in the field. J Photochem Photobiol B Biol 38:40–47.

Diffey BL (1991) Solar ultraviolet radiation effects on biological systems. Phys Med Biol 36:299–328.

Diffey BL (2002) Sources and measurement of ultraviolet radiation. Methods 28:4–13.

Dohler G (1997) Impact of UV radiation of different wavebands on pigments and assimilation of 15N-ammonium and 15N-nitrate by natural phytoplankton and ice algae in Antarctica. J Plant Physiol 151:550–555.

Dring MJ (1986) Pigment composition and photosynthetic action spectra of sporophytes of *Laminaria* (Phaeophyta) grown in different light qualities and irradiances. Br Phycol J 21:199–207.

Edwards P (1970) Illustrated guide of seaweeds and sea grasses in vicinity of Porto Arkansas, Texas. Contrib Mar Sci 15:1–228.

Essen LO, Klar T (2006) Light-driven DNA repair by photolyases. Cell Mol Life Sci 63:1266–1277.

Environmental Protection Agency (2010). EPA Progress Report. https://www.epa.gov/sites/production/files/2013-12/documents/annual-report-2010.pdf. Accesed 19 November 2019.

Falkowski P, LaRoche J (1990) Acclimation to spectral irradiance in algae. J Phycol 27:8–14.

Field CJ, Schley PD (2004) Evidence for potential mechanisms for the effect of conjugated linoleic acid on tumor metabolism and immune function: lessons from n-3 fatty acids. Am J Clin Nutr 79:1190S–1198.

Figueroa FL, Viñegla B (2001) Effects of solar UV radiation on photosynthesis and enzyme activities (carbonic anhydrase and nitrate) in marine macroalgae from southern Spain. Rev Chil Hist Nat 74:237–249.

Figueroa FL, Domínguez-González B, Korbee N (2014) Vulnerability and acclimation to increased UVB radiation in three intertidal macroalgae of different morpho-functional groups. Mar Environ Res 97:30–38.

Floreto EAT, Teshima S (1998) The fatty acid composition of seaweeds exposed to different levels of light intensity and salinity. Bot Mar 41:467–481.

Folch J, Lees M, Sloane S (1957) A simple method for the isolation and purification of total lipids from animal tissues. J Biol Chem 226:497–509.

Folin O, Ciocalteu V (1927) Tyrosine and tryptophan determinations proteins. J Biol Chem 73:627–650.

Forján E, Garbayo I, Henriques M, et al (2011) UV-A mediated modulation of photosynthetic effficiency, xanthophyll cycle and fatty acid production of *Nannochloropsis*. Mar Biotechnol 13:366–375.

Freile-Pelegrin Y, Robledo, D. Bioactive Phenolic Compounds from Algae. In: Hernández-Ledesma B, Herrero M (ed). Bioactive Compounds from Marine Foods: Plant and Animal Sources, 1st edn. John Wiley & Sons. pp 113-219.

Fujimura T, Tsukahara K, Moriwaki S, et al (2000) Effects of natural products extracts on contraction and mechanical properties of fibroblast populated collagen gel. Biol Pharm Bull 23:291–297.

Gagné J, Mann K, Chapman R (1982) Seasonal patterns of growth and storage in *Laminaria longicruris* in relation to differing patterns of availability of nitrogen in the water. Mar Biol 69:91–101.

Galasso C, Corinaldesi C, Sansone C (2017) Carotenoids from marine organisms: biological functions and industrial applications. Antioxidants 6:96.

Ganapathi K, Subramanian V, Mathan S (2013) Bioactive potentials of brown seaweeds, *Sargassum myriocystum* J. Argadh, *S. plagiaphyllum* C. Agardh and *S. ilicifolium* (Turner) J. Argadh. Int Res J Pharm Appl Sci 3:105–111.

Gao K, Xu J (2008) Effects of solar UV radiation on diurnal photosynthetic performance and growth of *Gracilaria lemaneiformis* (Rhodophyta). Eur J Phycol 43:297–307.

Gerasimenko NI, Busarova NG, Logvinov SV (2010) Seasonal changes in the content of lipids and photosynthetic pigments in a brown alga *Saccharina cichorioides*. Russ J Plant Physiol 61:893–898.

Ghazalpou A, Bennett B, Petyuk V, et al (2011) Comparative analysis of proteome and transcriptome variation in mouse. PLoS Genet 7:1001393.

Ghilardi NP (2007) Settlements method for the characterization of hard bottom benthic communities in an infralittoral stretch in Palmas Bay, Anchieta Island, Ubatuba (SP). Thesis, University of São Paulo.

Godínez-Ortega JL, Snoeijs P, Robledo D, et al (2008) Growth and pigment composition in the red alga *Halymenia floresii* cultured under different light qualities. J Appl Phycol 20:253–260.

Godovac-Zimmermann J, Brown LR (2001) Perspectives for mass spectrometry and functional proteomics. Mass Spectrom Rev 20:1–57.

Goes JI, Handa N, Taguchi S, Hama T (1994) Effect of UV-B radiation on the fatty-acid composition of the marine-phytoplankton *Tetraselmis* sp. - relationship to cellular pigments. Mar Ecol Prog Ser 114:259–274.

Gómez I, Figueroa FL (1998) Effects of solar UV stress on chlorophyll fluorescence kinetics of intertidal macroalgae from southern Spain: a case study in *Gelidium* species. J Appl Phycol 10:285–297.

Gorostiaga JM, Díez I (1996) Changes in the sublittoral benthic marine macroalgae in the polluted area of Abra de Bilbao and proximal coast (Northern Spain). Mar Ecol Prog Ser 130:157–167.

Gouveia C (2012) Praias arenosas oceânicas do estado de São Paulo (Brasil): síntese dos conhecimentos sobre morfodinâmica, sedimentologia, transporte costeiro e erosão costeira. Rev do Dep Geogr - USP 30:307–371.

Griffiths M, Harrison T, Smit M, Maharajh D (2016) Major commercial products from micro- and macroalgae melinda. In: F. Bux and Y. Chisti (ed) Algae Biotechnology. Springer International Publishing Switzerland, pp 269–300.

Guedes AC, Amaro HM, Barbosa CR, et al (2011) Fatty acid composition of several wild microalgae and cyanobacteria, with a focus on eicosapentaenoic, docosahexaenoic and α-linolenic acids for eventual dietary uses. Food Res Int 44:2721–2729.

Guihéneuf F, Fouqueray M, Mimouni V, et al (2010) Effect of UV stress on the fatty acid and lipid class composition in two marine microalgae *Pavlova lutheri* (Pavlovophyceae) and *Odontella aurita* (Bacillariophyceae). J Appl Phycol 22:629–638.

Häder D-P, Helbling E, Williamson C, Worrest RC (2011) Effects of UV radiation on aquatic ecosystems and interactions with climate change. Photochem Photobiol Sci 10:242-260.

Häder D-P, Kumar HD, Smith RC, Worrest RC (2007) Effects of solar UV radiation on aquatic ecosystems and interactions with climate change. Photochem Photobiol Sci 6:267–285.

Harb TB, Torres PB, Pires JS, et al (2016) Ensaio em microplaca do potencial antioxidante através do sistema quelante de metais para extratos de algas. Instituto de Biociências. Universidade de São Paulo. ISBN 978-85-85658-63-2. 1-5.

Harnita ANI, Santosa IE, Martono S, et al (2013) Inhibition of lipid peroxidation induced by ultraviolet radiation by crude phlorotannis isolated from brown algae *Sargassum hystrix* v. *buxifolium* C. Agardh. Indones J Chem 13:14–20.

Hausladen A, Fridovich I (1996) Measuring nitric oxide and superoxide : constants for aconitase reactivity. Methods Enzymol 269:37–41.

Havanapan PO, Thongboonkerd V (2009) Are protease inhibitors required for gel-based proteomics of kidney and urine? J Proteome Res 8:3109–3117.

Hay ME, Fenical W (1988) Marine plant-herbivore interactions: the ecology of chemical defense. Annu Rev Ecol Syst 19:111–145.

Hayakawa K, Sugiyama Y (2008) Spatial and seasonal variations in attenuation of solar ultraviolet radiation in Lake Biwa, Japan. J Photochem Photobiol B Biol 90:121–133.

Henley WJ, Ramus J (1989) Time course of physiological response of *Ulva rotundata* to growth irradiance transition. Mar Ecol Prog Ser 54:171–177.

Heo SJ, Jeon YJ (2009) Protective effect of fucoxanthin isolated from *Sargassum siliquastrum* on UV-B induced cell damage. J Photochem Photobiol B Biol 95:101–107.

Heo SJ, Ko SC, Cha SH, et al (2009) Effect of phlorotannins isolated from *Ecklonia cava* on melanogenesis and their protective effect against photo-oxidative stress induced by UV-B radiation. Toxicol Vitr 23:1123–1130.

Heriyanto, Juliadiningtyas AD, Shioi Y, et al (2017) Analysis of pigment composition of brown seaweeds collected from Panjang Island, Central Java, Indonesia. Philipp J Sci 146:323–330.

Hermes-Lima M, Storey K (1998) Role of antioxidant defenses in the tolerance of severe dehydration by anurans. The case of the leopard frog *Rana pipiens*. Mol Cell Biochem 189:79–89.

Hessen DO, De Lange HJ, Van Donk E (1997) UV-induced changes in phytoplankton cells and its effects on grazers. Freshw Biol 38:513–524.

Hoepffner N (2008) Marine and coastal dimension of climate change in Europe. A report of the European Water Directors. European Communities. Institute for Environmental and Sustainability. Office for Official Publications of the European Communities, Luxembourg.

Holzinger A, di Piazza L, Lütz C, Roleda MY (2011) Sporogenic and vegetative tissues of *Saccharina latissima* (Laminariales, Phaeophyceae) exhibit distinctive sensitivity to experimentally enhanced ultraviolet radiation: photosynthetically active radiation ratio. Phycol Res 59:221–235.

Holzinger A, Lütz C (2006) Algae and UV irradiation: effects on ultrastructure and related metabolic functions. Micron 37:190–207.

Hu C, Lin J, Lu F, et al (2008) Determination of carotenoids in *Dunaliella salina* cultivated in Taiwan and antioxidant capacity of the algal carotenoid extract. Food Chem 109:439–446.

Huang D, Boxin OU, Prior RL (2005) The chemistry behind antioxidant capacity assays. J Agric Food Chem 53:1841–1856.

Hudson N, Baker A, Reynolds D (2007) Fluorescence analysis of dissolved organic matter in natural, waste and polluted waters: A review. River Res Appl 23:631–649.

Hwang PA, Wu CH, Gau SY, et al (2010) Antioxidant and immune-stimulating activities of hot-water extract from seaweed *Sargassum hemiphyllum*. J Mar Sci Technol 18:41–46.

Ikawa M, Schaper TD, Dollard CA, Sasner JJ (2003) Utilization of folin-ciocalteu phenol reagent for the detection of certain nitrogen compounds. J Agric Food Chem 51:1811–1815.

Ina A, Hayashi KI, Nozaki H, Kamei Y (2007) Pheophytin a, a low molecular weight compound found in the marine brown alga *Sargassum fulvellum*, promotes the differentiation of PC12 cells. Int J Dev Neurosci 25:63–68.

Ismail GA (2017) Biochemical composition of some Egyptian seaweeds with potent nutritive and antioxidant properties. Food Sci Technol 37:294–302.

Iwashima M, Mori J, Ting X, et al (2005) Antioxidant and antiviral activities of plastoquinones from the brown alga *Sargassum micracanthum*, and a new chromene derivative converted from the plastoquinones. Biol Pharm Bull 28:374–377.

Jeffrey SW (1963) Purification and properties of chlorophyll *c* from *Sargassum flavicans*. Biochem J 86:313–318.

Jiang Y, Ng TB, Wang CR, et al (2010) Inhibitors from natural products to HIV-1 reverse transcriptase, protease and integrase. Mini Rev Med Chem 10:1331–1344.

Joint United Nations Programme on HIV/AIDS (UNAIDS) (2018) Global AIDS Update.

Jormalainen V, Honkanen T (2008) Macroalgal chemical defenses and their roles in structuring temperate marine communities. Algal Chem Ecol 57–89. falta volume

Jou JH, Lin CC, Li TH, et al (2015) Plant growth absorption spectrum mimicking light sources. Materials (Basel) 8:5265–5275.

Jung HA, Oh SH, Choi JS (2010) Molecular docking studies of phlorotannins from *Eisenia bicyclis* with BACE1 inhibitory activity. Bioorganic Med Chem Lett 20:3211–3215.

Kanimozhi AS, Joy Jeba Malar RT (2015) Phytochemical composition of *Sargassum polycystum* C. Agardh and *Sargassum duplicatum* J. Agardh. Int J Pharm Pharm Sci 7:393–397.

Karadeniz F, Karagozlu MZ, Kim S (2015) Antiviral activities of marine algal extracts. In: Kim and Chojnacka (ed.) Marine Algae Extracts: Processes, Products, and Applications. Wiley-VCH Verlag GmbH & Co. KGaA, pp 371–379.

Karawita R, Siriwardhana N, Lee KW, et al (2005) Reactive oxygen species scavenging, metal chelation, reducing power and lipid peroxidation inhibition properties of different

solvent fractions from *Hizikia fusiformis*. Eur Food Res Technol 220:363–371.

Karentz D (1994) Ultraviolet tolerance mechanisms in Antarctic marine organisms. Antarct Res Ser 62:93–110.

Kelloff GJ, Crowell JA, Steele VE, et al (2018) Progress in cancer chemoprevention: development of diet-derived chemopreventive agents. J Nutr 130:467S–471S.

Khaled N, Hiba M, Asma C (2012) Antioxidant and antifungal activities of *Padina pavonica* and *Sargassum vulgare* from the Lebanese Mediterranean coast. Adv Environ Biol 6:42–48.

Khotimchenko S V, Yakovleva IM (2005) Lipid composition of the red alga *Tichocarpus crinitus* exposed to different levels of photon irradiance. Phytochemistry 66:73–79.

Kim EY, Kim DG, Kim YR, et al (2011) An improved method of protein isolation and proteome analysis with *Saccharina japonica* (Laminariales) incubated under different pH conditions. J Appl Phycol 23:123–130.

Kim JK, Mao Y, Kraemer G, Yarish C (2015) Growth and pigment content of *Gracilaria tikvahiae* McLachlan under fluorescent and LED lighting. Aquaculture 436:52–57.

Kim S-H, Choi D-S, Athukorala Y, et al (2007) Antioxidant activity of sulfated polysaccharides isolated from *Sargassum fulvellum*. J Food Sci Nutr 12:65–73.

Klyachko-Gurvich GL, Tsoglin LN, Doucha J, et al (1999) Desaturation of fatty acids as an adaptive response to shifts in light intensity. Physiol Plant 107:240–249.

Korbee N, Huovinen P, Figueroa FL, et al (2005) Availability of ammonium influences photosynthesis and the accumulation of mycosporine-like amino acids in two *Porphyra* species (Bangiales, Rhodophyta). Mar Biol 146:645–654.

Kosová K, Vítámvás P, Prášil IT, Renaut J (2011) Plant proteome changes under abiotic stress - Contribution of proteomics studies to understanding plant stress response. J Proteomics 74:1301–1322.

Kramer GD, Herndl GJ (2004) Photo- and bioreactivity of chromophoric dissolved organic matter produced by marine bacterioplankton. Aquat Microb Ecol 36:239–246.

Kremb S, Helfer M, Kraus B, et al (2014) Aqueous extracts of the marine brown alga *Lobophora variegata* inhibit HIV-1 infection at the level of virus entry into cells. PLoS One 9:1–12.

Kumar A, Tyagi MB, Jha PN (2004) Evidences showing ultraviolet-B radiation-induced damage of DNA in cyanobacteria and its detection by PCR assay. Biochem Biophys Res Commun 318:1025–1030.

Kumar M, Kumari P, Trivedi N, et al (2011) Minerals, PUFAs and antioxidant properties of some tropical seaweeds from Saurashtra coast of India. J Appl Phycol 23:797–810.

Kumari P, Reddy C, Kumar M, Jha B (2013) Algal lipids, fatty acids and sterols. In: Dominguez H (ed.) Functional ingredients from algae foods and nutraceuticals, 1rst edn. Woodhead Publishing Ltd, pp 87–134.

Lao K, Glazer AN (1996) Ultraviolet-B photodestruction of a light-harvesting complex. Proc Natl Acad Sci USA 93:5258–5263.

Lee JB, Takeshita A, Hayashi K, Hayashi T (2011) Structures and antiviral activities of polysaccharides from *Sargassum trichophyllum*. Carbohydr Polym 86:995–999.

Lee JH, Kim GH (2015) Evaluation of antioxidant activity of marine algae-extracts from Korea. J Aquat Food Prod Technol 24:227–240.

Lee KY, Mooney DJ (2012) Alginate: properties and biomedical applications. Prog Polym Sci 37:106–126.

Lee TM, Shiu CT (2009) Implications of mycosporine-like amino acid and antioxidant defenses in UV-B radiation tolerance for the algae species *Pterocladiella capillacea* and *Gelidium amansii*. Mar Environ Res 67:8–16.

Lerdau M, Coley PD (2002) Benefits of the carbon-nutrient balance hypothesis. Oikos 98:534–536.

Levy I, Maxim C, Friedlander M (1992) Fatty acid distribution among some red algal macrophytes. J Phycol 28:299–304.

Lewey SA, Gorham J (1984) Pigment composition and photosynthesis in *Sargassum*

*muticum*. Mar Biol 80:109–115.

Li X, Fan X, Han L, Lou Q (2002) Fatty acids of some algae from the Bohai Sea. Phytochemistry 59:157–161.

Li Y, Fu X, Duan D, et al (2017) Extraction and identification of phlorotannins from the brown alga *Sargassum fusiforme* (Harvey) Setchell. Mar Drugs 49:1-15.

Li YX, Wijesekara I, Li Y, Kim SK (2011) Phlorotannins as bioactive agents from brown algae. Process Biochem 46:2219–2224.

Liang Y, Beardall J, Heraud P (2006) Effects of nitrogen source and UV radiation on the growth, chlorophyll fluorescence and fatty acid composition of *Phaeodactylum tricornutum* and *Chaetoceros muelleri* (Bacillariophyceae). J Photochem Photobiol B Biol 82:161–172.

Liao L, McClatchy DB, Yates JR (2009) Shotgun proteomics in neuroscience. Neuron 63:12–26.

Lichtenthaler HK (1987) Chlorophylls and carotenoids: pigments of photosynthetic biomembranes. Methods Enzymol 148:350–382.

Lichtenthaler HK, Buschmann C (2001) Chlorophylls and carotenoids: measurement and characterization by UV-VIS spectroscopy. Curr Protoc Food Anal Chem 1–8. F4.3.1-F4.

Lim SN, Cheung PCK, Ooi VEC, Ang PO (2002) Evaluation of antioxidative activity of extracts from a brown seaweed, *Sargassum siliquastrum*. J Agric Food Chem 50:3862–3866.

Lippert H, Iken K, Rachor E, Wiencke C (2001) Macrofauna associated with macroalgae in the Kongsfjord (Spitsbergen). Polar Biol 24:512–522.

Liu W, Yang Q (2014) Development status of plant photobiology with LED monochromatic light and plant factory. Sci Technol Rev 32:25–28.

López-Figueroa F, Niell FX (1990) Effects of light quality on chlorophyll and biliprotein accumulation in seaweeds. Mar Biol 104:321–327.

Lopez-Figueroa F, Perez R, Niell FX (1989) Effects of red and far-red light pulses on the chlorophyll and biliprotein accumulation in the red alga *Corallina elongata*. J Photochem Photobiol B Biol 4:185–193.

Lopez F, Mercado J, Jiménez C, et al (1998) Relation between the bio-optical characteristics of phytoplankton and photoinhibition by solar radiation. Aquat Bot 59:237–251.

Madronich S, McKenzie RL, Björn LO, Caldwell MM (1998) Changes in biologically active ultraviolet radiation reaching the Earth's surface. J Photochem Photobiol B Biol 46:5–19.

Makarov M (1999) Influence of ultraviolet radiation on the growth of the dominant macroalgae of the Barents Sea. Chemosph - Glob Chang Sci 1:461–467.

Maneesh A, Chakraborty K, Makkar F (2017) Pharmacological activities of brown seaweed *Sargassum wightii* (Family Sargassaceae) using different in vitro models. Int J Food Prop 20:931–945.

Manivannan A, Soundararajan P, Halimah N, et al (2015) Blue LED light enhances growth, phytochemical contents, and antioxidant enzyme activities of *Rehmannia glutinosa* cultured in vitro. Hortic Environ Biotechnol 56:105–113.

Manojkumar K (2013) *In vitro* cancer chemopreventive properties of polysaccharide extracts from the brown alga *Sargassum wightii*. J Pharm Biol Sci 8:06-11.

Mao W, Li H, Li Y, et al (2009) Chemical characteristic and anticoagulant activity of the sulfated polysaccharide isolated from *Monostroma latissimum* (Chlorophyta). Int J Biol Macromol 44:70–74.

Marín A, Casas-Valdez M, Carrillo S, et al (2009) The marine algae *Sargassum* spp. (Sargassaceae) as feed for sheep in tropical and subtropical regions. Rev Biol Trop 57:1271–1281.

Matanjun P, Mohamed S, Mustapha NM, et al (2008) Antioxidant activities and phenolics content of eight species of seaweeds from north Borneo. J Appl Phycol 20:367–373.

Matanjun P, Mohamed S, Mustapha NM, Muhammad K (2009) Nutrient content of tropical

edible seaweeds, *Eucheuma cottonii*, *Caulerpa lentillifera* and *Sargassum polycystum.* J Appl Phycol 21:75–80.

McCree K (1981) Photosynthetically Active Radiation. In: Lange O, Nobel P, Osmond C, Zieglr H (eds) Physiological Plant Ecology I. Springer Berlin Heidelberg, pp 41–55.

Michaud D, Feskanich D, Rimm E, et al (2000) Intake of specific carotenoids and risk of lung cancer in 2 prospective US cohorts. Am J Clin Nutr 72:990–997.

Michler T, Aguilera J, Hanelt D, et al (2002) Long-term effects of ultraviolet radiation on growth and photosynthetic performance of polar and cold-temperate macroalgae. Mar Biol 140:1117–1127.

Min B, McClung AM, Chen M-H (2011) Phytochemicals and antioxidant capacities in rice brans of different color. J Food Sci 76:C117–C126.

Miyashita K (2009) The carotenoid fucoxanthin from brown seaweed affects obesity. Lipid Technol 21:186–190.

Monro K, Poore AGB (2005) Light quantity and quality induce shade-avoiding plasticity in a marine macroalga. J Evol Biol 18:426–435.

Monteoliva L, Albar JP (2004) Differential proteomics: an overview of gel and non-gel based approaches. Briefings Funct Genomics Proteomics 3:220–239.

Moreira DC, Oliveira MF, Liz-Guimarães L, et al (2017) Current trends and research challenges regarding “preparation for oxidative stress”. Front Physiol 8:1–8.

Motogaito A, Hashimoto N, Hiramatsu K, Murakami K (2017) Study of plant cultivation using a light-emitting diode illumination system to control the spectral irradiance distribution. Opt Photonics J 07:101–108.

Movahedinia A, Heydari M (2014) Antioxidant activity and total phenolic content in two alga species from the Persian Gulf in Bushehr Province, Iran. Int J Sci Res 3:954–958.

Mozaffarian D, Wu JHY (2011) Omega-3 fatty acids and cardiovascular disease: effects on risk factors, molecular pathways, and clinical events. J Am Coll Cardiol 58:2047–2067.

Munir N, Sharif N, Naz S, Farkhanda M (2013) Algae: a potent antioxidant source. Sky J

Microbiol Res 1:22–31.

Na YS, Kim WJ, Kim SM, et al (2010) Purification, characterization and immunostimulating activity of water-soluble polysaccharide isolated from *Capsosiphon fulvescens*. Int Immunopharmacol 10:364–370.

Nagai K, Yotsukura N, Ikegami H, et al (2008) Protein extraction for 2-DE from the lamina of *Ecklonia kurome* (laminariales): recalcitrant tissue containing high levels of viscous polysaccharides. Electrophoresis 29:672–681.

Navarro NP, Figueroa FL, Korbee N, et al (2016) Differential responses of tetrasporophytes and gametophytes of *Mazzaella laminarioides* (Gigartinales, Rhodophyta) under solar UV radiation. J Phycol 52:451–462.

Niki E, Noguchi N (2000) Evaluation of antioxidant capacity. What capacity is being measured by which method? IUBMB Life 50:323–329.

Noaman N, Akl F, Shakik M, et al (2016) Effect of ultraviolet-B irradiation on fatty acids, amino acids, protein contents, enzyme activities and ultrastructure of some algae. Adv Biol Earth Sci 1:126–152.

O'farrell PH (1975) High resolution two-dimensional electrophoresis of proteins. J Biol Chem 250:4007–4021.

Ohno M, Arai S, Watanabe M (1990) Seaweed succession on artificial reefs on different bottom substrata. J Appl Phycol 2:327–332.

Okamoto OK, Pinto E, Latorre LR, et al (2001) Antioxidant modulation in response to metal-induced oxidative stress in algal chloroplasts. Arch Environ Contam Toxicol 40:18–24.

Okuno E, Nakajima T, Yoshimura E, et al (1996) Radiação ultravioleta solar em S. Paulo, Chiba, Calafate e Ilha de Pascoa. RBE-Cuaderno Ingenheria Biomed 12:143'153.

Ossó A, Sola Y, Bech J, Lorente J (2011) Evidence for the influence of the North Atlantic Oscillation on the total ozone column at northern low latitudes and midlatitudes during winter and summer seasons. J Geophys Res Atmos 116:1-12.

Oueslati S, Ksouri R, Falleh H, et al (2012) Phenolic content, antioxidant, anti-inflammatory

and anticancer activities of the edible halophyte *Suaeda fruticosa* Forssk. Food Chem 132:943–947.

Ouriques LC, Pereira DT, Simioni C, et al (2017) Physiological, morphological and ultrastructural responses to exposure to ultraviolet radiation in the red alga *Aglaothamnion uruguayense* (W.R. Taylor). Rev Bras Bot 40:783–791.

Panche AN, Diwan AD, Chandra SR (2016) Flavonoids: an overview. J Nutr Sci 5:1-15.

Paula ÉJ De (1988) O gênero S*argassum* C. Ag. (Pharophyta - Fucales) no Litoral do Estado de São Paulo, Brasil. Bolm Botânica Univ São Paulo 10:65–118.

Paula EJ, Eston VR (1987) Are there other *Sargassum* species potentially as invasive as S. *muticum*? Bot Mar 30:405–410.

Penniman CA, Mathieson AC, Penniman CE (1986) Reproductive phenology and growth of *Gracilaria tikvahiae* McLachlan (Gigartinales, Rhodophyta) in the Great Bay Estuary, New Hampshire. Bot Mar 29:147–154.

Pereira DT, Simioni C, Ouriques LC, et al (2017) Comparative study of the effects of salinity and UV radiation on metabolism and morphology of the red macroalga *Acanthophora spicifera* ( Rhodophyta , Ceramiales ). Photosynthetica 55:1–12.

Pereira H, Barreira L, Figueiredo F, et al (2012) Polyunsaturated fatty acids of marine macroalgae: Potential for nutritional and pharmaceutical applications. Mar Drugs 10:1920–1935.

Pereira R (2002) Ecologia química marinha. In: Ribeiro Henriques R (ed) Biologia Marinha. Rio de Janeiro, pp 282–310.

Pessoa MF (2012) Harmful effects of UV radiation in algae and aquatic macrophytes - A review. Emirates J Food Agric 24:510–526.

Piazena H, Perez-Rodrigues E, Häder DP, Lopez-Figueroa F (2002) Penetration of solar radiation into the water column of the central subtropical Atlantic Ocean - Optical properties and possible biological consequences. Deep Res Part II Top Stud Oceanogr 49:3513–3528.

Pires J, Torres PB, Dos Santos D, Chow F (2017a) Ensaio em microplaca do potencial antioxidante através do método de sequestro do radical livre DPPH para extratos de algas. Instituto de Biociências, Universidade de São Paulo. ISBN 978-85-85658-71-7. 1-6.

Pires JS, Torres PB, Dos Santos D, Chow F (2017b) Ensaio em microplaca de substâncias redutoras pelo método do Folin-Ciocalteu para extratos de algas. Instituto de Biociências, Universidade de São Paulo. ISBN 978-85-85658-70-0. 1-5.

Plaza M, Santoyo S, Jaime L, et al (2010) Screening for bioactive compounds from algae. J Pharm Biomed Anal 51:450–455.

Polo LK, de L Felix MR, Kreusch M, et al (2014a) Photoacclimation responses of the brown macroalga sargassum cymosum to the combined influence of UV radiation and salinity: cytochemical and ultrastructural organization and photosynthetic performance. Photochem Photobiol 90:560–573.

Polo LK, Felix MRL, Kreusch M, et al (2014b) Metabolic profile of the brown macroalga Sargassum cymosum (Phaeophyceae, Fucales) under laboratory UV radiation and salinity conditions. J Appl Phycol 27:887–899.

Poppe F, Schmidt R, Hanelt D, Wiencke C (2003) Effects of UV radiation on the ultrastructure of several red algae. Phycological 51: 11–19.

Portmann RW, Daniel JS, Ravishankara AR (2012) Stratospheric ozone depletion due to nitrous oxide: influences of other gases. Philos Trans R Soc B Biol Sci 367:1256–1264.

Prabhakar V, Anandan R, Aneesh T, et al (2011) Fatty acid composition of *Sargassum wightii* and *Amphiroa anceps* collected from the Mandapam coast Tamil Nadu, India. J Chem Pharm Res Prep 3:210–216.

Quaite FE, Takayanagi S, Ruffini J, et al (1994) DNA damage levels determine cyclobutyl pyrimidine dimer repair mechanisms in alfalfa seedlings. Plant Cell 6:1635–1641.

Queiroz KCS, Medeiros VP, Queiroz LS, et al (2008) Inhibition of reverse transcriptase activity of HIV by polysaccharides of brown algae. Biomed Pharmacother 62:303–307.

Rabilloud T, Lelong C (2011) Two-dimensional gel electrophoresis in proteomics: A tutorial. J Proteomics 74:1829–1841.

Raimbault P, Kawamura K, Miller WL, et al (2007) High penetration of ultraviolet radiation in the south east Pacific waters. Geophys Res Lett 34:1–5.

Rajasulochana P, Dhamotharan R, Krishnamoorthy P, Murugesan S (2009) Antibacterial activity of the extracts of marine red and brown algae. Marsl Press J Am Sci 5:20–25.

Rajasulochana P, Krishnamoorthy P, Dhamotharan R (2010) Amino acids, fatty acids and minerals in *Kappaphycus* sps. J Agric Biol Sci 5:1–12.

Ranjbarfordoei A, Samson R, Van Damme P (2011) Photosynthesis performance in sweet almond [*Prunus dulcis* (Mill) D. Webb] exposed to supplemental UV-B radiation. Photosynthetica 49:107–111.

Rastian Z, Mehranian M, Vahabzadeh F, Sartavi K (2016) Antioxidant activity of extract from a brown alga, *Sargassum boveanum*. African J Biotechnol 6:2740–2745.

Riso P, Visioli F, Erba D, et al (2004) Lycopene and vitamin C concentrations increase in plasma and lymphocytes after tomato intake. Effects on cellular antioxidant protection. Eur J Clin Nutr 58:1350–1358.

Ritchie RJ (2008) Universal chlorophyll equations for estimating chlorophylls a, b, c, and d and total chlorophylls in natural assemblages of photosynthetic organisms using acetone, methanol, or ethanol solvents. Photosynthetica 46:115–126.

Ritter A, Ubertini M, Romac S, et al (2010) Copper stress proteomics highlights local adaptation of two strains of the model brown alga *Ectocarpus siliculosus*. Proteomics 10:2074–2088.

Roleda MY, Hanelt D, Kräbs G, Wiencke C (2004a) Morphology, growth, photosynthesis and pigments in *Laminaria ochroleuca* (Laminariales, Phaeophyta) under ultraviolet radiation. Phycologia 43:603–613.

Roleda MY, Hanelt D, Wiencke C (2006a) Growth and DNA damage in young *Laminaria* sporophytes exposed to ultraviolet radiation: implication for depth zonation of kelps on

Helgoland (North Sea). Mar Biol 148:1201–1211.

Roleda MY, Lüder UH, Wiencke C (2010a) UV-susceptibility of zoospores of the brown macroalga *Laminaria digitata* from Spitsbergen. Polar Biol 33:577–588.

Roleda MY, Van De Poll WH, Hanelt D, Wiencke C (2004b) PAR and UVBR effects on photosynthesis, viability, growth and DNA in different life stages of two coexisting Gigartinales: Implications for recruitment and zonation pattern. Mar Ecol Prog Ser 281:37–50.

Roleda MY, Wiencke C, Hanelt D, et al (2005) Sensitivity of Laminariales zoospores from Helgoland (North Sea) to ultraviolet and photosynthetically active radiation: Implications for depth distribution and seasonal reproduction. Plant, Cell Environ 28:466–479.

Roleda MY, Wiencke C, Hanelt D, Bischof K (2007a) Sensitivity of the early life stages of macroalgae from the Northern Hemisphere to Ultraviolet Radiation. Photochem Photobiol 83:851–862.

Roleda MY, Wiencke C, Lüder UH (2006b) Impact of ultraviolet radiation on cell structure, UV-absorbing compounds, photosynthesis, DNA damage, and germination in zoospores of Arctic *Saccorhiza dermatodea*. J Exp Bot 57:3847–3856.

Roleda MY, Zacher K, Wulff A, et al (2007b) Photosynthetic performance, DNA damage and repair in gametes of the endemic Antarctic brown alga *Ascoseira mirabilis* exposed to ultraviolet radiation. Austral Ecol 32:917–926.

Rosenberg G, Ramus J (1982) Ecological growth strategies in the seaweeds G*racilaria foliifera* (Rhodophyceae) and *Ulva* sp. (Chlorophyceae): photosynthesis and antenna composition. Mar Ecol Prog Ser 8:233–241.

Rothäusler E, Gómez I, Karsten U, et al (2011) Physiological acclimation of floating *Macrocystis pyrifera* to temperature and irradiance ensures long-term persistence at the sea surface at mid-latitudes. J Exp Mar Bio Ecol 405:33–41.

Rüdiger W, López-Figueroa F (1992) Photoreceptors in algae. Photochem Photobiol 55:949–954.

Rufino M do S, Alves RE, Bito ES De, et al (2007a) Metodologia científica: determinação da atividade antioxidante total em frutas pela captura do radical Livre DPPH. Embrapa. - Comun. Técnico 3-6.

Rufino M do S, Alves Ri, Brito E, Morais S (2006) Metodologia científica: determinação da atividade antioxidante total em frutas pelo métodos de redução do ferro (FRAP). I Embrapa - Comun. Técnico 1–4

Rufino M do SM, Alves RE, Brito ES de, et al (2007b) Metodologia científica: determinação da atividade antioxidante total em frutas pela captura do radical livre ABTS. Embrapa - Comun. Técnico 127:1–3

Ruhland CT, Fogal MJ, Buyarski CR, Krna MA (2007) Solar ultraviolet-B radiation increases phenolic content and ferric reducing antioxidant power in *Avena sativa*. Molecules 12:1220–1232.

Salgado LT, Andrade LR, Amado GM (2005) Localization of specific monosaccharides in cells of the brown alga *Padina gymnospora* and the relation to heavy-metal accumulation. Protoplasma 225:123–128.

Salgado LT, Tomazetto R, Cinelli LP, et al (2007) The influence of brown algae alginates on phenolic compounds capability of ultraviolet radiation absorption in vitro. Brazilian J Oceanogr 55:145–154.

Sampath-Wiley P, Neefus CD, Jahnke LS (2008) Seasonal effects of sun exposure and emersion on intertidal seaweed physiology: fluctuations in antioxidant contents, photosynthetic pigments and photosynthetic efficiency in the red alga *Porphyra umbilicalis*. J Exp Mar Bio Ecol 361:83-91.

Sánchez-Machado DI, López-Cervantes J, López-Hernández J, Paseiro-Losada P (2004) Fatty acids, total lipid, protein and ash contents of processed edible seaweeds. Food Chem 85:439–444.

Sánchez-Moreno C (2002) Methods used to evaluate the free radical scavenging activity in foods and biological systems. Food Sci Technol Int 8:121–137.

Santos JP, Guihéneuf F, Fleming G, et al (2019a) Temporal stability in lipid classes and fatty

acid profiles of three seaweed species from the north-eastern coast of Brazil. Algal Res 41:1-12.

Santos JP, Torres PB, dos Santos DYAC, et al (2019b) Seasonal effects on antioxidant and anti-HIV activities of Brazilian seaweeds. J Appl Phycol 31:1333–1341.

Schaeffer DJ, Krylov VS (2000) Anti-HIV activity of extracts and compounds from algae and cyanobacteria. Ecotoxicol Environ Saf 45:208–227.

Schmid M, Guihéneuf F, Stengel DB (2014) Fatty acid contents and profiles of 16 macroalgae collected from the Irish Coast at two seasons. J Appl Phycol 26:451–463.

Schmidt ÉC, dos Santos R, Horta PA, et al (2010a) Effects of UVB radiation on the agarophyte *Gracilaria domingensis* (Rhodophyta, Gracilariales): Changes in cell organization, growth and photosynthetic performance. Micron 41:919–930.

Schmidt ÉC, dos Santos RW, de Faveri C, et al (2012a) Response of the agarophyte *Gelidium floridanum* after *in vitro* exposure to ultraviolet radiation B: Changes in ultrastructure, pigments, and antioxidant systems. J Appl Phycol 24:1341–1352.

Schmidt ÉC, Kreusch M, Marthiellen MR, et al (2015) Effects of ultraviolet radiation (UVA+UVB) and copper on the morphology, ultrastructural organization and physiological responses of the red alga *Pterocladiella capillacea*. Photochem Photobiol 91:359-370.

Schmidt ÉC, Maraschin M, Bouzon ZL (2010b) Effects of UVB radiation on the carragenophyte *Kappaphycus alvarezii* (Rhodophyta, Gigartinales): Changes in ultrastructure, growth, and photosynthetic pigments. Hydrobiologia 649:171–182.

Schmidt ÉC, Nunes BG, Maraschin M, Bouzon ZL (2010c) Effect of ultraviolet-B radiation on growth, photosynthetic pigments, and cell biology of *Kappaphycus alvarezii* (Rhodophyta, Gigartinales) macroalgae brown strain. Photosynthetica 48:161–172.

Schmidt ÉC, Pereira B, Pontes CLM, et al (2012b) Alterations in architecture and metabolism induced by ultraviolet radiation-B in the carragenophyte *Chondracanthus teedei* (Rhodophyta, Gigartinales). Protoplasma 249:353–367.

Schmidt ÉC, Scariot LA, Rover T, Bouzon ZL (2009) Changes in ultrastructure and histochemistry of two red macroalgae strains of *Kappaphycus alvarezii* (Rhodophyta, Gigartinales), as a consequence of ultraviolet B radiation exposure. Micron 40:860–869.

Schoenwaelder ME (2002) The occurrence and cellular significance of physodes in brown algae. Phycologia 41:125–139.

Sekmokienė D, Liutkevičius A, Malakauskas M (2007) Functional food and it's ingredients. Vet Zootech 37:72–78.

Senger H, Bauer B (1987) The influence of light quality on adaptation and function of the photosynthetic apparatus. Photochem Photobiol 45:939–946.

Sharma KK, Schuhmann H, Schenk PM (2012) High lipid induction in microalgae for biodiesel production. Energies 5:1532–1553.

Shibata T, Ishimaru K, Kawaguchi S, et al (2008) Antioxidant activities of phlorotannins isolated from Japanese Laminariaceae. J Appl Phycol 20:705–711.

Shiratori K, Ohgami K, Ilieva I, et al (2005) Effects of fucoxanthin on lipopolysaccharide-induced inflammation *in vitro* and *in vivo*. Exp Eye Res 81:422–428.

Silva G, Pereira RB, Valentão P, et al (2013) Distinct fatty acid profile of ten brown macroalgae. Brazilian J Pharmacogn 23:608–613.

Simioni C, Schmidt ÉC, Felix MRDL, et al (2014) Effects of ultraviolet radiation (UVA+UVB) on young gametophytes of *Gelidium floridanum*: Growth rate, photosynthetic pigments, carotenoids, photosynthetic performance, and ultrastructure. Photochem Photobiol 90:1050-1060.

Simopoulos AP (2004) Importance of the ratio of omega-6/omega-3 essential fatty acids: evolutionary aspects. World Rev Nutr Diet. 92:1–22.

Simopoulos AP (2002) Omega-3 fatty acids in inflammation and autoimmune diseases. J Am Coll Nutr 21:495–505.

Singleton VL, Rossi JA (1965) Colorimetry of total phenolics with phosphomolybdic-phosphotungstic acid reagents. Am J Enol Vitic 16:144–158.

Sinha S, Astani A, Ghosh T, et al (2010) Polysaccharides from *Sargassum tenerrimum*: Structural features, chemical modification and anti-viral activity. Phytochemistry 71:235–242.

Sinjal CA, Rompas RM, Sumilat DA, Suryanto E (2018) Antioxidant and photoprotective activity of brown seaweed from North Sulawesi Coast. Int J ChemTech Res 11:121–133.

Skerratt JH, Davidson AD, Nichols PD, Mcmeekin TA (1998) Effect of UV-B on lipid content of three antarctic marine phytoplankton. Phytochemistry 49:999–1007.

Smith JA, Daniel R (2006) Following the path of the virus: the exploitation of host DNA repair mechanisms by retroviruses. ACS Chem Biol 1:217–226.

Spreitzer RJ, Salvucci ME (2002) RUBISCO: Structure, regulatory interactions, and possibilities for a better enzyme. Annu Rev Plant Biol 53:449–475.

Stahl W, Sies H (2003) Antioxidant activity of carotenoids. Mol Aspects Med 24:345–351.

Stengel DB, Connan S (2015) Natural products from marine algae: Methods and protocols. Springer Science+Business Media New York.

Strid Å, Chow WS, Anderson JM (1994) UV-B damage and protection at the molecular level in plants. Photosynth Res 39:475–489.

Sudhakar MP, Ananthalakshmi JS, Nair BB (2013) Extraction, purification and study on antioxidant properties of fucoxanthin from brown seaweeds. J Chem Pharm Res 5:169–175.

Svensson CJ, Pavia H, Toth GB (2007) Do plant density, nutrient availability, and herbivore grazing interact to affect phlorotannin plasticity in the brown seaweed *Ascophyllum nodosum*? Mar Biol 151:2177–2181.

Synytsya A, Kim WJ, Kim SM, et al (2010) Structure and antitumour activity of fucoidan isolated from sporophyll of Korean brown seaweed *Undaria pinnatifida*. Carbohydr Polym 81:41–48.

Széchy MTM, Paula ÉJ De (2000) Padrões estruturais quantitativos de bancos de *Sargassum*

(Phaeophyta, Fucales) do litoral dos estados do Rio de Janeiro e São Paulo, Brasil. Rev Bras Botânica 23:121–132.

Széchy MTM, Veloso VG, De Paula ÉJ (2001) *Brachyura* (Decapoda, Crustacea) of phytobenthic communities of the sublittoral region of rocky shores of Rio de Janeiro and São Paulo, Brazil. Trop Ecol 42:231–242.

Széchy MTM, Galliez M, Marconi MI (2006) Quantitative variables applied to phenological studies of *Sargassum vulgare* C. Agardh (Phaeophyceae - Fucales) from Ilha Grande Bay, State of Rio de Janeiro. Rev Bras Bot 29:27–37.

Tamura K, Peterson D, Peterson N, et al (2011) MEGA5: Molecular evolutionary genetics analysis using maximum likelihood, evolutionary distance, and maximum parsimony methods. Mol Biol Evol 28:2731–2739.

Tan SC, Yiap BC (2009) DNA, RNA, and protein extraction: the past and the present. J Biomed Biotechnol 2009:1–10.

Tandon S, Arora A, Singh S, et al (2012) Antioxidant profiling of *Triticum aestivum* (wheatgrass) and its antiproliferative activity in MCF-7 breast cancer cell line. J Pharm Res 4:8–12.

Taskin E, Caki Z, Ozturk M (2010) Assessment of *in vitro* antitumoral and antimicrobial activities of marine algae harvested from the eastern Mediterranean sea. African J Biotechnol 9:4272–4277.

Teramura AH (1983) Effects of ultraviolet B radiation on the growth and yield of crop plants. Physiol Plant 58:415–427.

Terasaki M, Hirose A, Narayan B, et al (2009) Evaluation of recoverable functional lipid components of several brown seaweeds (Phaeophyta) from Japan with special reference to fucoxanthin and fucosterol contents1. J Phycol 45:974–980.

Terasaki M, Narayan B, Kamogawa H, et al (2012) Carotenoid profile of edible japanese seaweeds: An improved hplc method for separation of major carotenoids. J Aquat Food Prod Technol 21:468–479.

Thambiraj J, Lingakumar K, Paulsamy S (2012) Effect of seaweed liquid fertilizer (SLF) prepared from *Sargassum wightii* and *Hypnea musciformis* on the growth and biochemical constituents of the pulse, *Cyamopsis tetragonoloba* (L.) J Res Agric 1:65–70.

Thomas DN, Norman L, Zhang C, et al (2009) Exudation and decomposition of chromophoric dissolved organic matter (CDOM) from some temperate macroalgae. Estuar Coast Shelf Sci 84:147–153.

Thomas NV, Kim SK (2011) Potential pharmacological applications of polyphenolic derivatives from marine brown algae. Environ Toxicol Pharmacol 32:325–335.

Thomas P., Subbaramaiah K (1991) Seasonal variations in growth, reproduction, alginic acid, mannitol, iodine and ash contents of brown alga Sargassum wightii. Indian J Mar Sci 10:169–175.

Thompson GA (1996) Lipids and membrane function in green algae. Biochim Biophys Acta - Lipids Lipid Metab 1302:17–45.

Thuy TTT, Ly BM, Van TTT, et al (2015) Anti-HIV activity of fucoidans from three brown seaweed species. Carbohydr Polym 115:122–128.

Torres PB, Pires JS, Dos Santos D, Chow F (2017) Ensaio do potencial antioxidante de extratos de algas através do sequestro do ABTS•+ em microplaca. Instituto de Biociências, Universidade de São Paulo. ISBN 978-85-85658-69-4. 1-4.

Trevisan M, Browne R, Ram M, et al (2001) Correlates of markers of oxidative status in the general population. Am J Epidemiol 154:348–356.

Trono GC, Lluisma AO (1990) Seasonality of standing crop of a *Sargassum* (Fucales, Phaeophyta) bed in Bolinao, Pangasinan, Philippines. Hydrobiologia 204/205:331–338.

Tsang CK, Kamei Y (2004) Sargaquinoic acid supports the survival of neuronal PC12D cells in a nerve growth factor-independent manner. Eur J Pharmacol 488:11–18.

Turrens JF (1997) Superoxide production by the mitochondrial respiratory chain. Biosci Rep 17:3–8.

Turrens JF, Boveris A (1980) Generation of superoxide anion by the NADH dehydrogenase of bovine heart mitochondria. Biochem J 191:421–427.

U.S. EPA. 2010 U.S. Environmental Protection Agency (EPA) Decontamination Research and Development Conference (2010) Environmental Protection Agency (EPA).

Urquiaga I, Leighton F (2003) Plant polyphenol antioxidants and oxidative stress. Biol Res 33:55–64.

Urrea-victoria V, Pires J, Torres PB, Santos DYAC (2016) Ensaio antioxidante em microplaca do poder de redução do ferro (FRAP) para extratos de algas. Instituto de Biociências, Universidade de São Paulo. ISBN 978-85-85658-62-5. 1-6.

Ursi S, Plastino EM (2001) Crescimento *in vitro* de linhagens de coloração vermelha e verde clara de *Gracilaria birdiae* (Gracilariales, Rhodophyta) em dois meios de cultura: análise de diferentes estádios reprodutivos. Rev Bras Botânica 24:587–594.

Van de Poll WH, Eggert A, Buma AGJ, Breeman AM (2001) Effects of UV-B-induced DNA damage and photoinhibition on growth of temperate marine red macrophytes: Habitat-related differences in UV-B tolerance. J Phycol 37:30–37.

Van de Poll WH, Hanelt D, Hoyer K, et al (2002) Ultraviolet-B-induced cyclobutane-pyrimidine dimer formation and repair in Arctic marine macrophytes. Photochem Photobiol 76:493–500.

Van Ginneken VJT, Helsper JPFG, De Visser W, et al (2011) Polyunsaturated fatty acids in various macroalgal species from north Atlantic and tropical seas. Lipids Health Dis 10:104.

Van Minh C, Van Kiem P, Hai Dang N (2005) Marine natural products and their potential application in the future. ASEAN J Sci Technol Dev 22:297–311.

Vasconcelos JB, de Vasconcelos ERTPP, Urrea-Victoria V, et al (2018) Antioxidant activity of three seaweeds from tropical reefs of Brazil: potential sources for bioprospecting. J Appl Phycol 31:835–846.

Vass I, Szilard A, Sicora C (2005) Adverse Effects of UV-B light on the structure and

function of the photosynthetic apparatus. In: Handbook of photosynthesis pp 931–949.

Viennois E, Chen F, Laroui H, et al (2013) Dextran sodium sulfate inhibits the activities of both polymerase and reverse transcriptase: Lithium chloride purification, a rapid and efficient technique to purify RNA. BMC Res Notes 6:1-8.

Villafañe VE, Sundback K, Figueroa FL, Helbing W (2003) Environment, photosynthesis in the aquatic UVR, as affected by UVR. In: Helbling E, Zagarese H (eds) UV Effects in Aquatic Organisms and Ecosystems. Comprehensive Series in Photochemical and Photobiological Sciences. pp 359–383.

Vinayak RC, Sabu AS, Chatterji A (2011) Bio-prospecting of a few brown seaweeds for their cytotoxic and antioxidant activities. Evidence-based Complement Altern Med 2011:1-9.

Vinegla B, Figueroa F (2009) Effect of solar and artificial UV radiation on photosynthetic performance and carbonic anhydrase activity in intertidal macroalgae from southern Spain. Ciencias Mar 35:59–74.

Wang SB, Chen F, Sommerfeld M, Hu Q (2004) Proteomic analysis of molecular response to oxidative stress by the green alga *Haematococcus pluvialis* (Chlorophyceae). Planta 220:17–29.

Wang T, Jónsdóttir R, Ólafsdóttir G (2009) Total phenolic compounds, radical scavenging and metal chelation of extracts from Icelandic seaweeds. Food Chem 116:240–248.

Wang W, Wang SX, Guan HS (2012) The antiviral activities and mechanisms of marine polysaccharides: An overview. Mar Drugs 10:2795–2816.

Waterman PG, Mole S (1994) Analysis of phenolic plant metabolites. Blackwell Scientific.

Wiencke C, Gómez I, Pakker H, et al (2000) Impact of UV-radiation on viability, photosynthetic characteristics and DNA of brown algal zoospores: Implications for depth zonation. Mar Ecol Prog Ser 197:217–229.

Williams A, Feagin R (2010) *Sargassum* as a natural solution to enhance dune plant growth. Environ Manage 46:738–747.

Williamson CE, Zepp RG, Lucas RM, et al (2014) Solar ultraviolet radiation in a changing climate. Nat Clim Chang 4:434–441.

Wondrak GT, Jacobson MK, Jacobson EL (2006) Endogenous UVA-photosensitizers: Mediators of skin photodamage and novel targets for skin photoprotection. Photochem Photobiol Sci 5:215–237.

Wong CK, Ooi VEC, Ang PO (2000) Protective effects of seaweeds against liver injury caused by carbon tetrachloride in rats. Chemosphere 41:173–176.

Woradulayapinij W, Soonthornchareonnon N, Wiwat C (2005) *In vitro* HIV type 1 reverse transcriptase inhibitory activities of Thai medicinal plants and *Canna indica* L. rhizomes. J Ethnopharmacol 101:84–89.

Worm SW, Sabin C, Weber R, et al (2010) Risk of myocardial infarction in patients with hiv infection exposed to specific individual antiretroviral drugs from the 3 major drug classes: The data collection on adverse events of Anti-HIV drugs (D:A:D) astudy. J Infect Dis 201:318–330.

Wu H (2016) Effect of different light qualities on growth, pigment content, chlorophyll fluorescence, and antioxidant enzyme activity in the red alga *Pyropia haitanensis* (Bangiales, Rhodophyta). Biomed Res Int 2016:1-8.

Xu J, Gao K (2010) UV-A enhanced growth and UV-B induced positive effects in the recovery of photochemical yield in *Gracilaria lemaneiformis* (Rhodophyta). J Photochem Photobiol B Biol 100:117–122.

Xu J, Li Y, Sun J, et al (2013) Comparative physiological and proteomic response to abrupt low temperature stress between two winter wheat cultivars differing in low temperature tolerance. Plant Biol (Stuttg) 15:292–303.

Xue L, Zhang Y, Zhang T, et al (2005) Effects of enhanced ultraviolet-B radiation on algae and cyanobacteria. Crit Rev Microbiol 31:79–89.

Yang H, Dong Y, Du H, et al (2011) Antioxidant compounds from propolis collected in Anhui, China. Molecules 16:3444–3455.

Yende SR, Harle UN, Chaugule BB (2014) Therapeutic potential and health benefits of *Sargassum* species. Pharmacogn Rev 8:1–7.

Yoshida T, Stiger V, Horiguchi T (2000) *Sargassum boreale* sp. nov. (Fucales, Phaeophyceae) from Hokkaido, Japan. Phycol Res 48:125–131.

Yotsukura N, Nagai K, Kimura H, Morimoto K (2010) Seasonal changes in proteomic profiles of Japanese kelp: *Saccharina japonica* (Laminariales, Phaeophyceae). J Appl Phycol 22:443–451.

Yotsukura N, Nagai K, Tanaka T, et al (2012) Temperature stress-induced changes in the proteomic profiles of *Ecklonia cava* (Laminariales, Phaeophyceae). J Appl Phycol 24:163–171.

Zaid SAA-L, Abdel-Wahab KSE-D, Abed NN (2017) Screening for antiviral activities of aqueous extracts of some egyptian seaweeds. Egypt J Hosp Med 64:430–435.

Zandi K, Ahmadzadeh S, Tajbakhsh S, et al (2010) Anticancer activity of *Sargassum oligocystum* water extract against human cancer cell lines. Eur Rev Med Pharmacol Sci 14:669–673.

Zepp RG, Erickson DJ, Paul ND, Sulzberger B (2011) Effects of solar UV radiation and climate change on biogeochemical cycling: Interactions and feedbacks. Photochem Photobiol Sci 10:261-279.

Zhang A, Xu T, Zou H, Pang Q (2015) Comparative proteomic analysis provides insight into cadmium stress responses in brown algae *Sargassum fusiforme*. Aquat Toxicol 163:1–15.

Zhang Y, Fonslow B, Shan B, et al (2013) Protein analysis by shotgun/bottom-up proteomics. Chem Rev 113:2343–2394.

Zhang Y, Liu M, Qin B, Feng S (2009) Photochemical degradation of chromophoric-dissolved organic matter exposed to simulated UV-B and natural solar radiation. Hydrobiologia 627:159–168.

Zhang Y, Marcillat O, Giulivi C, et al (1990) The oxidative inactivation of mitochondrial

electron transport chain components and ATPase. J Biol Chem 265:16330–16336.

Zhu W, Chiu LCM, Ooi VEC, et al (2004) Antiviral property and mode of action of a sulphated polysaccharide from *Sargassum patens* against herpes simplex virus type 2. Int J Antimicrob Agents 24:81–85.

Zhu W, Chiu LCM, Ooi VEC, et al (2006) Antiviral property and mechanisms of a sulphated polysaccharide from the brown alga *Sargassum patens* against *Herpes simplex* virus type 1. Phytomedicine 13:695–701.

Zhu W, Smith JW, Huang CM (2010) Mass spectrometry-based label-free quantitative proteomics. J Biomed Biotechnol 2010:1-6.

Zou H-X, Pang Q-Y, Zhang A-Q, et al (2015) Excess copper induced proteomic changes in the marine brown algae *Sargassum fusiforme*. Ecotoxicol Environ Saf 111:271–280.

Zubia M, Fabre MS, Kerjean V, et al (2009) Antioxidant and antitumoural activities of some Phaeophyta from Brittany coasts. Food Chem 116:693–701.

Zubia M, Robledo D, Freile-Pelegrin Y (2007) Antioxidant activities in tropical marine macroalgae from the Yucatan Peninsula, Mexico. J Appl Phycol 19:449–458.

# Supplements

## SUPPLEMENTS

### Supplement 1. Taxonomic and molecular identification of *Sargassum*

Analysis from the taxonomic identification allowed to identify the species as *Sargassum filipendula* C. Agardh. Figure S1.1-A shows the general habit of a representative individual of the species for this study, which presents a main axis from whose apex arise numerous, primary laterals branches with lateral laminar ramifications that resemble the leaves of the angiosperms, called phylloids. Figure S1.1-B highlights the holdfast, which is disciform and constituted by filaments that are compactly superimposed and interlaced. Figure S1.1-C shows in detail the phylloids that could be simple or occasionally forked, wavy or with small teeth and with few cryptostomata arranged in a row on each side of the midrib. Figure S1.1-D highlights the receptacles in dichotomic-branched group, which arise from the axil of the phylloids.

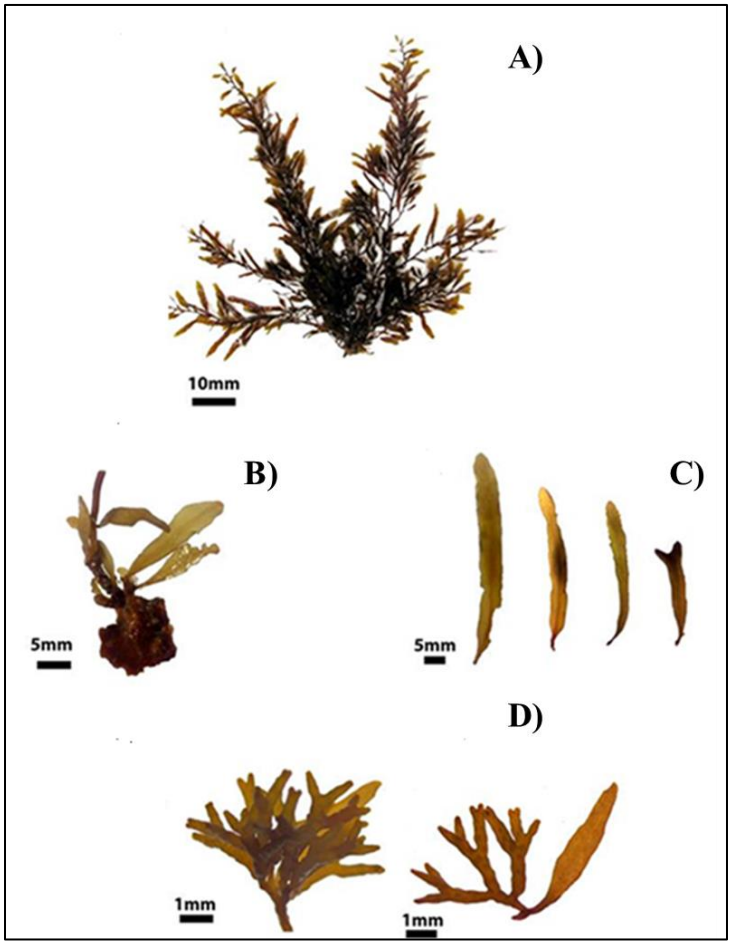


**Figure 1-S1.**. General habit and detailed morphological characters used for the taxonomic identification of *Sargassum filipendula*. A) General appearance of an representative individual; B) Details of the holdfast; C) General aspect of simple, flat, and linear-lanceolate phylloids; D) Detail of tuberculated receptacles.

## Detailed description and morphological traits for identification of *Sargassum filipendula* C. Agardh.

**Type specimen.** Agardh Herbarium no. 3253 (LD). Lectotype, designated from the syntype collection by Hanisak & Kilar (1990).

**Type locality.** West Indies 'India Occidentalis, Aspegren' [as 'In sinu mexicano?' in C. Agardh 1824.

Thallus light brown when alive, yellowish brown or greenish when dry; when fertile up to 30- (40-50) -60 cm length. Holdfast up to 1.5 cm of diameter with few main branches up

to 3 cm length. Main lateral branches cylindrical, smooth and long, with long first-order phylloids and branches in loose spiral. Phylloids simple, flat and linear-lanceolate, and the lowers being able to branched once; with tapered base resembling a “petiole”. 3-(4-5) -8 cm length and 3-(4-5) -6 mm wide; sawed margin and evident midrib. Vesicles numerous, distributed throughout the specimen when present; elliptic, about 3 mm diameter, apiculated or ended by phylloid expansion. Pedicle about 3-4 mm length. Cryptostomata numerous, irregularly distributed on the surface of the phylloids. Dioecious organism. Receptacles arranged in clusters, with the last ramifications being dichotomous, produced especially in the ramifications of the primary sides. Female receptacle tuberculated up to 1.3 cm and male finer and more branched up to of 2.5 cm.

The measurements of the morphological characteristics observed from the collected specimens that corroborate the identification as *S. filipendula* are listed Table S1.1

**Table 1-S1.** Summary of the morphological characteristics of *Sargassum filipendula* collected at Cigarras Beach, used for identification.

| ***Morphological characteristics*** | ***Sargassum filipendula*** |
|---|---|
| Habitat | Lower intertidal region |
| Color | Yellowish brown |
| Height (cm) | 19.73 ± 1.94 |
| Leaves long (cm) | 2.45 ± 0.16 |
| Leaves width (cm) | 0.27 ± 0.01 |
| Cryptostomata | Irregularly distributed on the surface of the phylloids |

Results from the molecular analysis gave a different identity for the study species, which was identify as *Sargassum vulgare* C. Agardh by using ITS molecular marker. Table S2 shows the sequences present in GenBank database for ITS-2 marker used in the NJ cluster analysis (Fig. S2). The tree shows the clustering of *Sargassum* species by Neighbor-Joining (NJ) based on the alignment of the internal transcribed spacer 2 (ITS-2) and 2000 replicates bootstrap, which presents 71 species of the genus, including 55 species of the Brazilian flora and sequences obtained from GenBank corresponding to different works. Tree topology shows two major groups: 1) where all the Brazilian sequences (dash-dot rectangle; sequences gently provided by Professor Mariana Cabral de Oliveira and the student Vitoria Miranda)

are grouped with the sequences of the specimens collected for the present work (dashed rectangle), with 42 bootstrap; and 2) sequences from the GenBank (dotted rectangle).

**Table 2-S1.**Specifications of *Sargassum* sequences present in GenBank database for ITS-2 marker used in the NJ cluster analysis of Figure S1.2.

| ***Species*** | ***Accession-GenBank*** | ***Local*** | ***References*** |
|---|---|---|---|
| *S. aquifolium* | FJ170435 | New Caledonia | Mattio and Payri (2008) |
| *S. echinocarpum* | EU100795 | French Polynesia | Mattio et al. (2008) |
| *S. fallax* | JN243808 | Australia | Dixon et al. (2012) |
| *S. herporhizum* | JX560130 | Mexico | Andrade-Sorcia et al. (2012) |
| *S. horneri* | AY149999 | South Korea | Oak et al. (2002) |
| *S. johnstonii* | JX560129 | Mexico | Andrade-Sorcia et al. (2012) |
| *S. lapazeanum* | JX560125 | Mexico | Andrade-Sorcia et al. (2012) |
| *S. muticum* | AB043503 | Pacific Basin | Stiger et al. (2000) |
| *S. obtusifolium* | EU100787 | French Polynesia | Mattio et al. (2008) |
| *S. polyphyllum* | EU833424 | Western and Central Pacific | Mattio et al. (2009) |
| *S. scabridum* | FJ170451 | New Caledonia | Mattio and Payri (2009) |
| *S. sinclairii* | FJ170459 | New Caledonia | Mattio and Payri (2008) |
| *S. sinicola* | JX560124 | Mexico | Andrade-Sorcia et al. (2012) |
| *S. spinuligerum* | FJ170462 | New Caledonia | Mattio and Payri (2009) |
| *S. swartzii* | EU882254 | New Caledonia | Mattio et al. (2010) |
| ***S. thunbergii*** | KF281927 | Australia | Dixon et al. (2014) |

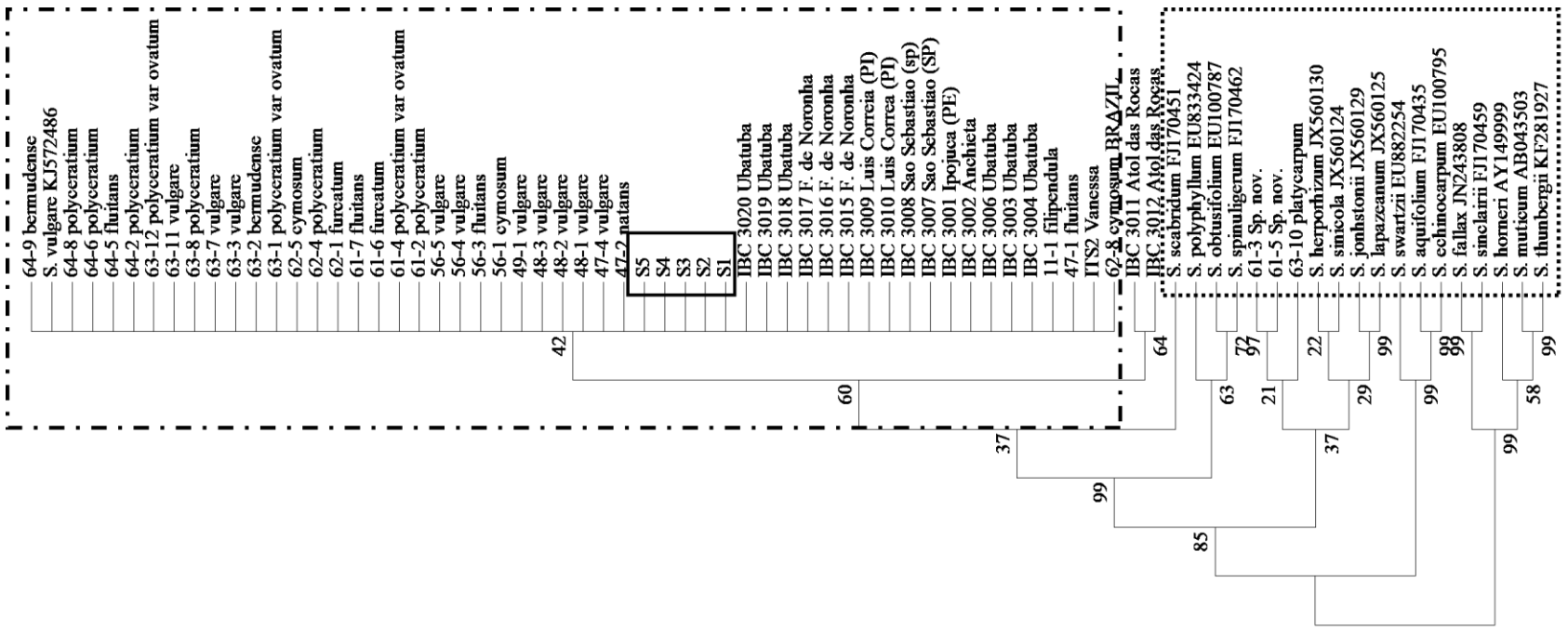


**Figure 2-S1.** Neighbor-joining (NJ) tree based on the alignment of the ITS-2 marker. Bootstrap for 2000 replicates. Dot-dashed rectangle indicates the species from Brazilian flora gently provided by Professor Mariana Cabral de Oliveira and the student Vitoria Miranda. Continuous rectangle indicates the specimens for the present work. Dotted rectangle indicates sequences obtained from GenBank database.

**General considerations about the identification of the species**

*Sargassum* C. Agardh, Agardh is one of the most diverse and widely distributed genera of the Phaeophyceae (Guiry and Guiry 2014). Species are distributed worldwide and the genus is especially well represented in tropical and inter-tropical regions where it forms dense submarine forests (Thibaut et al. 2005).

Nomenclatural ambiguities have been documented since the establishment of *Sargassum* (Silva et al. 1996) and the origin of the taxonomic confusions is probably linked to its high polymorphism and consequently, identifying species often remains uncertain. Due to the intra-specific morphological plasticity, either between populations, within populations or even within individuals, which depends on the seasons, habitat features, and water motion, *Sargassum* has been recognized as a complex genus with critical need of taxonomic reassessment (Mattio et al. 2010). Nowadays, is well recognized that the use of molecular markers to assess species delimitation in *Sargassum* is of great importance, considering the large variability of morphological traits among and within taxa (Mattio and Payri 2011), which have led to significant new insights on the genus' phylogeny and allowed reconsidering the taxonomic placement of several entities.

For the present work, both morphological and molecular approaches were used to identify the species; nevertheless, the results were not concordant between them, giving two different identities for the species: *Sargassum filipendula* C. Agardh for the identification by morphological characters and *Sargassum vulgare* C. Agardh by molecular markers. Thus, with the obtained results we can concluded that the use of one molecular marker, ITS-2 for this case, was not conclusive for the identification and we determined the name of species based on the morphological characters following Paula (1988), Camacho et al. (2015), AlgaeBase and with wide discussion with expert taxonomists. Therefore, the species was defined as *Sargassum filipendula.* Thus, we suggest that further analyses need to be done considering at least three biological markers, nuclear ITS-2, partial sequence of the chloroplastidial gene RubisCO (ribulose-1,5-bisphosphate carboxylase/oxygenase) and the mitochondrial gene *cox*3 (cytochrome *c* oxidase subunit III), for a more accurate results, as it has been proposed by several authors (Phillips and Frederico 2000; Mattio et al. 2008; Cho et al. 2012; Camacho et al. 2015).

## Supplement 2.

**Table 1-S2.** Main effects and interactions related to growth rate of repeated measures of ANOVA of *S. filipendula* cultivated under different radiation treatments over time. SS – square sum, d.f. – degree of freedom, MS – medium square, *F* – statistic index, *p* – probability ($p < 0.05$).

| | SS | d.f. | MS | *F* | *p* |
|---|---|---|---|---|---|
| | | | **Growth rate** | | |
| **Intercept** | 33.92 | 1 | 33.92 | 4.02 | 0.07 |
| **Radiation** | 15.27 | 2 | 7.64 | 0.90 | 0.43 |
| **Error** | 101.25 | 12 | 8.44 | | |
| **Time** | 17.26 | 3 | 5.75 | 4.39 | 0.01 |
| **Time*Radiation** | 7.04 | 6 | 1.17 | 0.90 | 0.51 |
| **Error** | 47.19 | 36 | 1.31 | | |

**Table 2-S2.** Main effects and interactions related to contents of soluble proteins, chlorophylls *a* and *c*, and carotenoids of bifactorial ANOVA of *S. filipendula* cultivated under different radiation treatments over time. SS – square sum, d.f. – degree of freedom, MS – medium square, *F* – statistic index, *p* – probability ($p < 0.05$).

| | SS | d.f. | MS | *F* | *p* |
|---|---|---|---|---|---|
| | | | **Soluble proteins** | | |
| **Intercept** | 20181680 | 1 | 20181680 | 560.3709 | < 0.001 |
| **Radiation** | 338506 | 2 | 169253 | 4.6995 | 0.023 |
| **Time** | 3672367 | 2 | 1836184 | 50.9841 | < 0.001 |
| **Time*Radiation** | 7661408 | 4 | 1915352 | 53.1823 | < 0.001 |
| **Error** | 648267 | 18 | 36015 | | |
| | | | **Chlorophyll *a*** | | |
| **Intercept** | 19493570 | 1 | 19493570 | 9294.069 | < 0.001 |
| **Radiation** | 97712 | 2 | 48856 | 23.293 | < 0.001 |
| **Time** | 18083 | 2 | 9041 | 4.311 | 0.024 |
| **Time*Radiation** | 132036 | 4 | 33009 | 15.738 | < 0.001 |
| **Error** | 52436 | 25 | 2097 | | |
| | | | **Chlorophyll *c*** | | |
| **Intercept** | 6729174 | 1 | 6729174 | 1835.130 | < 0.001 |
| **Radiation** | 251325 | 2 | 125662 | 34.270 | < 0.001 |
| **Time** | 55001 | 2 | 27500 | 7.500 | 0.003 |
| **Time*Radiation** | 218473 | 4 | 54618 | 14.895 | < 0.001 |
| **Error** | 80671 | 22 | 3667 | | |
| | | | **Carotenoids** | | |
| **Intercept** | 19143.83 | 1 | 19143.83 | 81.09105 | < 0.001 |
| **Radiation** | 5353.13 | 2 | 2676.56 | 11.33762 | < 0.001 |
| **Time** | 12616.12 | 2 | 6308.06 | 26.72022 | < 0.001 |
| **Time*Radiation** | 10620.88 | 4 | 2655.22 | 11.24721 | < 0.001 |
| **Error** | 5665.88 | 24 | 236.08 | | |

## Supplement 3.

**Table 1-S3.** Main effects related to the formation of CPDs of unifactorial ANOVA of *S. filipendula* cultivated under different radiation. SS – square sum, d.f. – degree of freedom, MS – medium square, *F* – statistic index, *p* – probability ($p < 0.05$).

| | SS | d.f | MS | *F* | *p* |
|---|---|---|---|---|---|
| | | | **CPDs formation** | | |
| **Intercept** | 3.34401 | 1 | 3.34401 | 14.84694 | 0.030874 |
| **Radiation** | 5.63743 | 2 | 2.81871 | 12.51469 | 0.035016 |
| **Error** | 0.67570 | 3 | 0.22523 | | |

**Table 2-S3.** Main effects and interactions related to the percentage of antioxidant activity of bifactorial ANOVA of *S. filipendula* cultivated under different radiation treatments at different concentration of crude extract [CE]. SS – square sum, d.f. – degree of freedom, MS – medium square, *F* – statistic index, *p* – probability ($p < 0.05$).

| | SS | d.f | MS | *F* | *p* |
|---|---|---|---|---|---|
| | | | **ABTS** | | |
| **Intercept** | 34.33687 | 1 | 34.33687 | 48103.09 | < 0.001 |
| **Radiation** | 0.02411 | 2 | 0.01206 | 16.89 | < 0.001 |
| **[CE]** | 0.55673 | 5 | 0.11135 | 155.99 | < 0.001 |
| **[CE] *Radiation** | 0.03712 | 10 | 0.00371 | 5.20 | < 0.001 |
| **Error** | 0.03640 | 51 | 0.00071 | | |
| | | | **DPPH** | | |
| **Intercept** | 32.02063 | 1 | 32.02063 | 55115.51 | < 0.001 |
| **Radiation** | 0.15165 | 2 | 0.07582 | 130.51 | < 0.001 |
| **[CE]** | 0.84049 | 5 | 0.16810 | 289.34 | < 0.001 |
| **[CE] *Radiation** | 0.03362 | 10 | 0.00336 | 5.79 | < 0.001 |
| **Error** | 0.02963 | 51 | 0.00058 | | |
| | | | **Folin-Ciocalteu (phenolic compounds)** | | |
| **Intercept** | 28.34552 | 1 | 28.34552 | 44690.89 | < 0.001 |
| **Radiation** | 0.12870 | 2 | 0.06435 | 101.46 | < 0.001 |
| **[CE]** | 1.19205 | 5 | 0.23841 | 375.89 | < 0.001 |
| **[CE] *Radiation** | 0.01491 | 10 | 0.00149 | 2.35 | 0.021 |
| **Error** | 0.03615 | 57 | 0.00063 | | |
| | | | **FRAP** | | |
| **Intercept** | 36.48947 | 1 | 36.48947 | 30139.22 | < 0.001 |
| **Radiation** | 0.12741 | 2 | 0.06370 | 52.62 | < 0.001 |
| **[CE]** | 0.92650 | 5 | 0.18530 | 153.05 | < 0.001 |
| **[CE] *Radiation** | 0.01051 | 10 | 0.00105 | 0.87 | 0.568 |
| **Error** | 0.06296 | 52 | 0.00121 | | |
| | | | **Quelant** | | |
| **Intercept** | 13.31193 | 1 | 13.31193 | 3418.80 | < 0.001 |
| **Radiation** | 0.05390 | 2 | 0.02695 | 6.92 | < 0.001 |
| **[CE]** | 0.23095 | 5 | 0.04619 | 11.86 | < 0.001 |
| **[CE] *Radiation** | 0.07985 | 10 | 0.00798 | 2.05 | 0.04 |
| **Error** | 0.21416 | 55 | 0.00389 | | |

**Table 3-S3.** Main effects and interactions related to the antioxidant activity expressed as µg GAE.g$^{-1}$ of algae of bifactorial ANOVA of *S. filipendula* cultivated under different radiation treatments at different concentration of crude extract [CE]. SS – square sum, d.f. – degree of freedom, MS – medium square, *F* – statistic index, *p* – probability ($p < 0.05$).

| | SS | d.f. | MS | *F* | *p* |
|---|---|---|---|---|---|
| | | | **ABTS** | | |
| **Intercept** | 3.93590 | 1 | 3.93590 | 6972.23 | < 0.001 |
| **Radiation** | 0.01542 | 2 | 0.00771 | 13.66 | < 0.001 |
| **[CE]** | 0.68032 | 5 | 0.13606 | 241.03 | < 0.001 |
| **[CE] *Radiation** | 0.02293 | 10 | 0.00229 | 4.06 | < 0.001 |
| **Error** | 0.02879 | 51 | 0.00057 | | |
| | | | **DPPH** | | |
| **Intercept** | 7.80611 | 1 | 7.80611 | 4560.04 | < 0.001 |
| **Radiation** | 0.31124 | 2 | 0.15562 | 90.91 | < 0.001 |
| **[CE]** | 0.14165 | 5 | 0.02833 | 16.55 | < 0.001 |
| **[CE] *Radiation** | 0.13689 | 10 | 0.01369 | 8.00 | < 0.001 |
| **Error** | 0.08730 | 51 | 0.00171 | | |
| | | | **Folin-Ciocalteu (phenolic compounds)** | | |
| **Intercept** | 75.76493 | 1 | 75.76493 | 6109.42 | < 0.001 |
| **Radiation** | 1.70043 | 2 | 0.85022 | 68.56 | < 0.001 |
| **[CE]** | 1.98474 | 5 | 0.39695 | 32.01 | < 0.001 |
| **[CE] *Radiation** | 0.16683 | 10 | 0.01668 | 1.35 | < 0.001 |
| **Error** | 0.70688 | 57 | 0.01240 | | |
| | | | **FRAP** | | |
| **Intercept** | 6.08781 | 1 | 6.08781 | 6115.26 | < 0.001 |
| **Radiation** | 0.08676 | 2 | 0.04338 | 43.57 | < 0.001 |
| **[CE]** | 0.67560 | 5 | 0.13512 | 135.73 | < 0.001 |
| **[CE] *Radiation** | 0.01557 | 10 | 0.00156 | 1.56 | 0.143894 |
| **Error** | 0.05177 | 52 | 0.00100 | | |
| | | | **Quelant** | | |
| **Intercept** | 145.04420 | 1 | 145.04420 | 2362.21 | < 0.001 |
| **Radiation** | 0.60020 | 2 | 0.30010 | 4.89 | 0.011125 |
| **[CE]** | 50.46490 | 5 | 10.09300 | 164.38 | < 0.001 |
| **[CE] *Radiation** | 0.79180 | 10 | 0.07920 | 1.29 | 0.259245 |
| **Error** | 3.37710 | 55 | 0.06140 | | |

**Table 4-S3.** Main effects related to the EC50 of unifactorial ANOVA of *S. filipendula* cultivated under different radiation treatments at different concentration of crude extract [CE]. SS – square sum, d.f. – degree of freedom, MS – medium square, *F* – statistic index, *p* – probability ($p < 0.05$).

| | SS | d.f. | MS | *F* | *p* |
|---|---|---|---|---|---|
| | | | **ABTS** | | |
| **Intercept** | 101.2272 | 1 | 101.2272 | 4630.7350 | < 0.001 |
| **Radiation** | 1.7365 | 2 | 0.8683 | 39.7190 | < 0.001 |
| **Error** | 0.1093 | 5 | 0.0219 | | |
| | | | **DPPH** | | |
| **Intercept** | 191.1073 | 1 | 191.1073 | 3989.4500 | < 0.001 |
| **Radiation** | 13.1125 | 2 | 6.5563 | 136.8650 | < 0.001 |
| **Error** | 0.2395 | 5 | 0.0479 | | |
| | | | **Folin-Ciocalteu (phenolic compounds)** | | |
| **Intercept** | 471.5424 | 1 | 471.5424 | 15293.8400 | < 0.001 |
| **Radiation** | 20.9100 | 2 | 10.4550 | 339.0900 | < 0.001 |
| **Error** | 0.1850 | 6 | 0.0308 | | |
| | | | **FRAP** | | |
| **Intercept** | 107.4522 | 1 | 107.4522 | 2733.3570 | < 0.001 |
| **Radiation** | 9.3973 | 2 | 4.6986 | 119.5230 | < 0.001 |
| **Error** | 0.1572 | 4 | 0.0393 | | |

**Table 5-S3.** Main effects and interactions related to the antiviral activity expressed as percentage of inhibition of bifactorial ANOVA of *S. filipendula* cultivated under different radiation treatments at different concentration of methanolic and aqueous extracts [CE]. SS – square sum, d.f. – degree of freedom, MS – medium square, *F* – statistic index, *p* – probability ($p < 0.05$).

| | **SS** | **d.f.** | **MS** | ***F*** | ***p*** |
|---|---|---|---|---|---|
| | | | **% inhibition** | | |
| **Methanolic extract** | | | | | |
| **Intercept** | 0.206931 | 1 | 0.206931 | 11598.32 | < 0.001 |
| **Radiation** | 0.003452 | 3 | 0.001151 | 64.50 | < 0.001 |
| **[CE]** | 0.009879 | 3 | 0.003293 | 184.57 | < 0.001 |
| **[CE] *Radiation** | 0.002859 | 9 | 0.000318 | 17.81 | < 0.001 |
| **Error** | 0.000535 | 30 | 0.000018 | | |
| | | | | | |
| **Aqueous Extract** | | | | | |
| **Intercept** | 42.40265 | 1 | 42.40265 | 12847853 | < 0.001 |
| **Radiation** | 0.00037 | 3 | 0.00012 | 37 | < 0.001 |
| **[CE]** | 0.00009 | 4 | 0.00002 | 7 | < 0.001 |
| **[CE] *Radiation** | 0.00011 | 12 | 0.00001 | 3 | < 0.001 |
| **Error** | 0.00013 | 38 | 0.00000 | | |

## Supplement 4.

**Table 1-S4.** Main effects related to the fatty acids of unifactorial ANOVA of *S. vulgare* cultivated under different light qualities treatments. SS – square sum, d.f. – degree of freedom, MS – medium square, *F* – statistic index, *p* – probability ($p < 0.05$).

| | SS | d.f. | MS | *F* | *p* |
|---|---|---|---|---|---|
| | | **C14:0** | | | |
| **Intercept** | 218.0332 | 1 | 218.0332 | 1160.3870 | < 0.001 |
| **Light** | 16.0565 | 5 | 3.2113 | 17.0910 | < 0.001 |
| **Error** | 1.8790 | 10 | 0.1879 | | |
| | | **C16:0** | | | |
| **Intercept** | 10423.3300 | 1 | 10423.3300 | 837.6093 | < 0.001 |
| **Light** | 1080.8400 | 5 | 216.1700 | 17.3711 | < 0.001 |
| **Error** | 112.0000 | 9 | 12.4400 | | |
| | | **C17:0** | | | |
| **Intercept** | 0.7602 | 1 | 0.7602 | 782.0053 | < 0.001 |
| **Light** | 0.0269 | 5 | 0.0054 | 5.5299 | < 0.001 |
| **Error** | 0.0078 | 8 | 0.0010 | | |
| | | **C18:0** | | | |
| **Intercept** | 4.7548 | 1 | 4.7548 | 683.5729 | < 0.001 |
| **Light** | 0.6538 | 5 | 0.1308 | 18.7995 | 0.154914 |
| **Error** | 0.0556 | 8 | 0.0070 | | |
| | | **C20:0** | | | |
| **Intercept** | 0.5671 | 1 | 0.5671 | 2249.3470 | < 0.001 |
| **Light** | 0.0018 | 1 | 0.0018 | 7.3340 | 0.053645 |
| **Error** | 0.0010 | 4 | 0.0003 | | |
| | | **C22:0** | | | |
| **Intercept** | 3.7940 | 1 | 3.7940 | 865.2846 | < 0.001 |
| **Light** | 1.6541 | 5 | 0.3308 | 75.4511 | < 0.001 |
| **Error** | 0.0351 | 8 | 0.0044 | | |
| | | **C24:0** | | | |
| **Intercept** | 0.835555 | 1 | 0.835555 | 923.0709 | < 0.001 |
| **Light** | 0.123531 | 2 | 0.061765 | 68.2347 | < 0.001 |
| **Error** | 0.004526 | 5 | 0.000905 | | |
| | | **C16:1 7n** | | | |
| **Intercept** | 881.9538 | 1 | 881.9538 | 4641.2590 | < 0.001 |
| **Light** | 7.4282 | 5 | 1.4856 | 7.8180 | 0.004281 |
| **Error** | 1.7102 | 9 | 0.1900 | | |

**Continuation Table 1-S4.**

| | SS | d.f. | MS | *F* | *p* |
|---|---|---|---|---|---|
| | | **C18:1 9nc** | | | |
| **Intercept** | 3314.8470 | 1 | 3314.8470 | 2595.5510 | < 0.001 |
| **Light** | 27.5880 | 5 | 5.5180 | 4.3200 | 0.020233 |
| **Error** | 14.0480 | 11 | 1.2770 | | |
| | | **C18:2 n6c** | | | |
| **Intercept** | 1595.9360 | 1 | 1595.9360 | 2683.5560 | < 0.001 |
| **Light** | 99.1180 | 5 | 19.8240 | 33.3330 | < 0.001 |
| **Error** | 5.9470 | 10 | 0.5950 | | |
| | | **C18:3 n3** | | | |
| **Intercept** | 662.4877 | 1 | 662.4877 | 1986.7430 | < 0.001 |
| **Light** | 67.8450 | 5 | 13.5690 | 40.6920 | < 0.001 |
| **Error** | | | | | |
| | | **C18:3 n6** | | | |
| **Intercept** | 13.8709 | 1 | 13.8709 | 805.6963 | < 0.001 |
| **Light** | 1.6118 | 5 | 0.3224 | 18.7245 | < 0.001 |
| **Error** | 0.1033 | 6 | 0.0172 | | |
| | | **C20:2** | | | |
| **Intercept** | 2.5055 | 1 | 2.5055 | 3990.4610 | < 0.001 |
| **Light** | 0.0524 | 5 | 0.0105 | 16.6950 | < 0.001 |
| **Error** | 0.0050 | 8 | 0.0006 | | |
| | | **C20:3 n6** | | | |
| **Intercept** | 37.4026 | 1 | 37.4026 | 1378.4430 | < 0.001 |
| **Light** | 4.2031 | 5 | 0.8406 | 30.9800 | < 0.001 |
| **Error** | 0.2171 | 8 | 0.0271 | | |
| | | **C20:4 n6** | | | |
| **Intercept** | 5212.9240 | 1 | 5212.9240 | 2499.3480 | < 0.001 |
| **Light** | 478.3560 | 5 | 95.6710 | 45.8700 | < 0.001 |
| **Error** | 16.6860 | 8 | 2.0860 | | |
| | | **C20:5 n3** | | | |
| **Intercept** | 298.9681 | 1 | 298.9681 | 893.0605 | < 0.001 |
| **Light** | 14.4162 | 5 | 2.8832 | 8.6126 | 0.003057 |
| **Error** | 3.0129 | 9 | 0.3348 | | |
| | | **C22:6 n3** | | | |
| **Intercept** | 0.218654 | 1 | 0.218654 | 364.2239 | < 0.001 |
| **Light** | 0.001585 | 4 | 0.000396 | 0.6602 | 0.641786 |
| **Error** | 0.003602 | 6 | 0.000600 | | |

**Table 2-S4.** Main effects related to the pigments of unifactorial ANOVA of *S. vulgare* cultivated under different light qualities treatments. SS – square sum, d.f. – degree of freedom, MS – medium square, *F* – statistic index, *p* – probability ($p < 0.05$).

| | SS | d.f. | MS | *F* | *p* |
|---|---|---|---|---|---|
| | | | **Chlorophyll *a*** | | |
| **Intercept** | 11.444170 | 1 | 11.444170 | 10985.9300 | < 0.001 |
| **Light** | 0.409610 | 4 | 0.102400 | 98.3000 | < 0.001 |
| **Error** | 0.005210 | 5 | 0.001040 | | |
| | | | **Chlorophyll *c*** | | |
| **Intercept** | 0.045000 | 1 | 0.045000 | 8606.0840 | < 0.001 |
| **Light** | 0.002579 | 4 | 0.000645 | 123.3230 | < 0.001 |
| **Error** | 0.000031 | 6 | 0.000005 | | |
| | | | **Fucoxanthin** | | |
| **Intercept** | 0.520291 | 1 | 0.520291 | 5857.5770 | < 0.001 |
| **Light** | 0.024370 | 4 | 0.006093 | 68.5920 | < 0.001 |
| **Error** | 0.000444 | 5 | 0.000089 | | |
| | | | **Neoxanthin** | | |
| **Intercept** | 0.000023 | 1 | 0.000023 | 381.2592 | < 0.001 |
| **Light** | 0.000001 | 3 | 0.000000 | 3.0475 | 0.154914 |
| **Error** | 0.000000 | 4 | 0.000000 | | |
| | | | **Violaxanthin** | | |
| **Intercept** | 0.002946 | 1 | 0.002946 | 8802.4870 | < 0.001 |
| **Light** | 0.000248 | 4 | 0.000062 | 185.4310 | < 0.001 |
| **Error** | 0.000002 | 5 | 0.000000 | | |
| | | | **Zeaxanthin** | | |
| **Intercept** | 0.000847 | 1 | 0.000847 | 1534.499 | < 0.001 |
| **Light** | 0.000009 | 4 | 0.000002 | 4.271 | 0.071559 |
| **Error** | 0.000003 | 5 | 0.000001 | | |
| | | | **β-carotene** | | |
| **Intercept** | 0.004569 | 1 | 0.004569 | 5748.2980 | < 0.001 |
| **Light** | 0.000625 | 4 | 0.000156 | 196.5340 | < 0.001 |
| **Error** | 0.000004 | 5 | 0.000001 | | |

**Supplement 5.** Identified protein from *S. vulgare* after ten days exposure to radiation treatments.

**Table 1-S5.** Identified protein from *Sargassum vulgare* after ten days exposure to radiation treatments matched with Ectocarpus_Uniprot database. Proteins were searched and classified by their metabolism or function using the information content on the UniProt database (http://www.ebi.uniprot.org).

| Metabolism/ Function | Accession | Protein name |
|---|---|---|
| Photosynthesis | D7FJ97 | Thylakoid lumenal protein |
| | D8LD75 | Thylakoid lumen 15.0 kDa protein |
| | D8LBZ8 | Protochlorophyllide reductase, putative chloroplast |
| | D7FML1 | PS II stability/assembly factor HCF136 |
| | D1GJN7 | PS II reaction center Psb28 protein |
| | D1J6Z2 | PS II protein D1 |
| | D8LJF7 | PS II oxygen evolution complex protein PsbP |
| | D1GJP1 | PS II D2 protein |
| | D1GJP8 | PS II CP47 reaction center protein |
| | D1J718 | PS II CP47 reaction center protein |
| | D1GJP0 | PS II CP43 reaction center protein |
| | D7G9E0 | PS II 12 kDa extrinsic protein |
| | D8LJ72 | PS II 11 kDa protein |
| | D1J7A8 | PS I subunit III |
| | D1GJL5 | PS I reaction center subunit XI |
| | D1J785 | PS I reaction center subunit II |
| | D1GJK8 | PS I protein F |
| | D1GJJ2 | Photosystem I P700 chlorophyll a apoprotein A2 |
| | D1GJJ1 | Photosystem I P700 chlorophyll a apoprotein A1 |
| | D1J7C7 | Photosystem I iron-sulfur center |
| | D1GJH0 | Photosystem I ferredoxin-binding protein |
| | D7FNE6 | NADH-cytochrome b5 reductase |
| | D1GJE7 | Mg-protoporphyrin IX chelatase |
| | D8LG03 | Manganese stabilising protein |
| | D7FQ20 | Magnesium-protoporphyrin IX methyltransferase, putative chloroplast |
| | D8LJH9 | Light harvesting complex protein |
| | D7FNP8 | Light harvesting complex protein |
| | D8LDI3 | Light harvesting complex protein |
| | D7G1R8 | Light harvesting complex protein |
| | D7FKU2 | Light harvesting complex protein |
| | D7FRX5 | Geranylgeranyl reductase geranylgeranyl diphosphate reductase geranylgeranyl hydrogenase |
| | D8LBE1 | FtsH protease OS=Ectocarpus siliculosus |

| | | |
|---|---|---|
| | D1GJK5 | Cytochrome f |
| | D1GJF8 | Cytochrome c6 |
| | D1GJF7 | Cytochrome c-550 |
| | D1J771 | Cytochrome c-550 |
| | D7FT78 | Cytochrome c |
| | D7FL45 | Cytochrome b6-f complex iron-sulfur subunit |
| | D1GJL9 | Cytochrome b559 subunit beta |
| | D1GJL8 | Cytochrome b559 subunit alpha |
| Carbohydrate | D7FQF5 | Transketolase |
| | D7FVZ8 | Transaldolase |
| | D8LMM8 | Transaldolase B |
| | D8LGS4 | Trans-2-enoyl-CoA reductase, mitochondrial |
| | D7FM01 | Sedoheptulose-bisphosphatase |
| | D7FKR0 | Sedoheptulose-bisphosphatase |
| | D8LBH8 | Ribulose-phosphate 3-epimerase |
| | D1GJJ0 | Ribulose-1,5-bisphosphate carboxylase/oxygenase small subunit |
| | D1J7D7 | Ribulose bisphosphate carboxylase small subunit |
| | Q32217 | Ribulose bis-phosphate carboxylase small subunit |
| | Q37063 | Ribulose bis-phosphate carboxylase small subunit |
| | Q2PQH5 | Ribulose bisphosphate carboxylase large chain |
| | P24313 | Ribulose bisphosphate carboxylase large chain |
| | Q8HW46 | Ribulose bisphosphate carboxylase large chain (Fragment) O |
| | D8LDV8 | Ribose-5-phosphate isomerase |
| | D8LBI0 | Phosphoribulokinase |
| | D7FWW3 | Phosphomannomutase |
| | D8LJG3 | Phosphoglycerate mutase |
| | D8LQF3 | Phosphoglycerate mutase |
| | D8LEV5 | Phosphoglycerate kinase |
| | D8LFP9 | Phosphoglycerate kinase |
| | D8LS77 | Phosphoglycerate kinase |
| | D8LRT8 | Phosphoglycerate kinase |
| | D8LTN1 | Phosphoenolpyruvate carboxylase |
| | D7FYY3 | Phosphoenolpyruvate carboxykinase (ATP) |
| | D8LQM3 | Malate dehydrogenase |
| | D7G2Q2 | Isocitrate dehydrogenase [NADP] |
| | D7FSU9 | Glyceraldehyde-3-phosphate dehydrogenase |
| | D7FZL5 | Glyceraldehyde-3-phosphate dehydrogenase |
| | D8LTZ6 | Glyceraldehyde-3-phosphate dehydrogenase |
| | D7FMT2 | Glyceraldehyde 3-phosphate dehydrogenase alternative name: imm downregulated 12 |
| | D8LTN7 | Gdp-d-mannose 4,6-dehydratase |
| | D7FW27 | GDP-4-keto-6-deoxy-D-mannose epimerase-reductase |

| | | |
|---|---|---|
| | D7FNZ9 | Fructose-bisphosphate aldolase |
| | D7FPZ7 | Fructose-1,6-bisphosphate aldolase |
| | D7FTT4 | Aldo/keto reductase |
| | D8LGX8 | Aldo/keto reductase family protein |
| | D7G0R3 | Aldehyde Dehydrogenase |
| | D7FMJ8 | Mannitol 1-phosphate dehydrogenase |
| | D7FU48 | Putative lactoylglutathione lyase, putative glyoxalase I, putative |
| | D7FLC9 | 6-phosphogluconate dehydrogenase, decarboxylating |
| Energy | D8LCT6 | Vacuolar ATP synthase subunit B |
| | D8LRC1 | UMP-CMP kinase |
| | D8LSQ1 | UDP-sulfoquinovose synthase, plastid OS=Ectocarpus siliculosus |
| | D7FGR7 | UDP-glucose 6-dehydrogenase |
| | D7G3K4 | UDP-glucose 6-dehydrogenase |
| | D8LNT5 | Tryptophan--tRNA ligase |
| | D8LLB1 | Tryptophan synthase (Alpha / beta chains) |
| | D7FP79 | Triosephosphate isomerase/glyceraldehyde-3-phosphate dehydrogenase |
| | D7G091 | Triosephosphate isomerase |
| | D7G0B9 | Succinate--CoA ligase [ADP-forming] subunit beta, mitochondrial |
| | D7FJ40 | Succinate--CoA ligase [ADP-forming] subunit alpha, mitochondrial |
| | D7FWF5 | Succinate dehydrogenase [ubiquinone] iron-sulfur subunit, mitochondrial |
| | D8LTH1 | Shikimate Kinase |
| | D8LSF2 | SDH1, succinate dehydrogenase subunit 1 |
| | D7FN56 | S-adenosylmethionine synthase |
| | D7FUQ8 | RME1L3, RME1-like GTPase/ATPase without a C-terminal EH domain |
| | D8LI11 | Pyruvate, phosphate dikinase |
| | D8LP24 | Pyruvate kinase |
| | D7FPK7 | Pyruvate kinase |
| | D7FYR2 | Pyruvate kinase |
| | D8LEK3 | Pyruvate dehydrogenase |
| | D8LIJ4 | Pyruvate dehydrogenase E1 component subunit beta |
| | D7FIP4 | Pyruvate dehydrogenase E1 component alpha subunit, mitochondrial (PDHE1-A) |
| | D8LCR8 | Pyruvate carboxylase |
| | D7FRM0 | Pyrophosphate-dependent phosphofructose kinase |
| | D7FWB4 | Putative ATP-dependent proteinase, possible LON protease |
| | D7G0Y3 | Prohibitin complex subunit 2 |
| | D7FVV6 | Prohibitin complex subunit 1 |
| | D7FKZ0 | Oxoglutarate dehydrogenase, N-terminal part |
| | D8LSE9 | Obg-like ATPase 1 |
| | D8LDR9 | NUOI homolog, NADH dehydrogenase (Ubiquinone) subunit OS=Ectocarpus siliculosus |

| | | |
|---|---|---|
| | D8LSE6 | NUOE homolog, NADH dehydrogenase (Ubiquinone) subunit |
| | D8LIF1 | NUO10 homolog, NADH dehydrogenase (Ubiquinone) subunit 10 |
| | D7FSV9 | NADH-dependent fumarate reductase |
| | D8LEE1 | NADH:ubiquinone oxidoreductase complex I |
| | D7FZX3 | NADH dehydrogenase [ubiquinone] flavoprotein 1, mitochondrial |
| | D7FKA9 | Mitochondrial carrier family |
| | D8LKN5 | Mitochondrial ADP/ATP translocator |
| | D7FTF5 | NADH dehydrogenase (Ubiquinone) |
| | D8LNJ3 | NADH dehydrogenase (Ubiquinone) (Partial) (Fragment) |
| | D7FZC8 | N/a |
| | D8LE50 | N/a |
| | D7G305 | N/a |
| | D8LQV8 | Glucose-6-phosphate isomerase |
| | D7FTB9 | Glucose-6-phosphate 1-epimerase |
| | D7FQL5 | Glucose-6-phosphate 1-epimerase |
| | D7FLD0 | Glucose-6-phosphate 1-dehydrogenase |
| | D7FN31 | Fumarate hydratase |
| | D8LDX4 | Fumarate hydratase (Fumarase) |
| | D8LRL3 | ATP-sulfurylase |
| | D1GJQ2 | ATP-dependent zinc metalloprotease FtsH |
| | D8LNX4 | ATP-dependent protease peptidase subunit |
| | D7FZH9 | ATP-dependent DNA helicase |
| | D8LGQ4 | ATP-dependent Clp protease proteolytic subunit |
| | D7G416 | ATP-dependent Clp protease proteolytic subunit |
| | D1GJJ8 | ATP-dependent clp protease ATP-binding subunit |
| | D1J7B8 | ATP-dependent Clp protease ATP-binding subunit clpA homolog |
| | D7FN48 | ATP-citrate synthase |
| | D7FMK6 | ATPase |
| | D1GJK2 | ATP synthase subunit beta, chloroplastic |
| | D1J7B4 | ATP synthase subunit beta, chloroplastic |
| | D7FXG1 | ATP synthase subunit beta |
| | D1GJI2 | ATP synthase subunit alpha, chloroplastic |
| | D1J797 | ATP synthase subunit alpha, chloroplastic |
| | D7FJT6 | ATP synthase O subunit, mitochondrial |
| | D8LBF0 | ATP synthase gamma chain |
| | D1GJK3 | ATP synthase epsilon chain, chloroplastic |
| | D7FQE8 | Adenylate kinase |
| | D7FV44 | Adenylate kinase |
| | D7FQN5 | Aconitate hydratase |
| | D7FXW6 | ABC transporter ATP-binding protein |
| Amino acid | D8LDZ7 | Serine/threonine-protein phosphatase |

| | | |
|---|---|---|
| | D7FZ88 | Serine/threonine kinase, putative |
| | D7FQZ4 | Ketol-acid reductoisomerase |
| | D8LKW5 | Chorismate Synthase |
| | D7FQ51 | Aspartate-semialdehyde dehydrogenase |
| | D7FVQ6 | Alanine transaminase |
| Amonia assimilation | D7G5Q0 | Glutamate-1-semialdehyde 2,1-aminomutase, putative chloroplast |
| | D8LCE0 | Glutamate synthase (NADH/NADPH-dependent), C-terminal part |
| | D7FVE7 | Glutamate synthase (NADH/NADPH-dependent) |
| | D8LK56 | Glutamate dehydrogenase |
| | D7G3Q6 | Glutamate dehydrogenase 2 (NADP-dependent) |
| Arginine biosynthetic process | D8LSF8 | N-acetyl-gamma-glutamyl-phosphate reductase, C-terminal part |
| | D8LD12 | Argininosuccinate synthetase |
| | D7G2H9 | Arginine biosynthesis bifunctional protein ArgJ, mitochondrial |
| ATP-binding | D7FI32 | T-complex protein, epsilon subunit |
| | D8LU47 | T-complex protein 1 subunit gamma |
| | D7FKP3 | Similar to doublecortin and CaM kinase-like 3 |
| | D8LIL8 | Nucleoside diphosphate kinase |
| | D8LI58 | Molecular chaperones HSP70/HSC70, HSP70 superfamily |
| | D7FZN2 | Molecular chaperones HSP70/HSC70, HSP70 superfamily |
| | D7FNT3 | Molecular chaperones HSP70/HSC70, HSP70 superfamily |
| | D7FQC8 | Molecular chaperones GRP78/BiP/KAR2, HSP70 superfamily |
| | D7FKD7 | Molecular chaperone, putative |
| | D7FZ99 | Kinase, CAMK CAMKL |
| | D1GJM5 | CfxQ protein homolog |
| | D8LPQ0 | CbbX protein |
| | D7FMN1 | Casein kinase (Serine/threonine/tyrosine protein kinase) |
| | D8LHK4 | Arsenical pump-driving ATPase (Partial) (Fragment) |
| | D8LHZ3 | Actin-related protein 2/3 complex subunit 3 |
| | D7FQK6 | Actin |
| Catalytic activity | D7FY07 | Pyridoxal-dependent decarboxylase, C-terminal sheet domain protein |
| | D8LRS9 | mRNA binding protein |
| | D7FZ95 | Branched chain alpha-keto acid dehydrogenase E1 beta subunit |
| | D8LDN8 | Amino acid adenylation domain protein OS=Ectocarpus siliculosus |
| | D8LDG3 | 38 kDa ribosome-associated protein |
| Cell redox homeostasis | D8LQL6 | Mercuric reductase |
| | D8LB56 | Glyoxalase domain containing protein |
| | D7G3G5 | Electron donor (NADH / NADPH)-dependent reductase |
| | D8LBF4 | Dihydrolipoyl dehydrogenase |
| | D7FM36 | Dihydrolipoamide S-acetyltransferase |
| | D8LL48 | Dihydrolipoamide dehydrogenase |
| | D8LL62 | Dihydrolipoamide acetyltransferase |

| | | |
|---|---|---|
| | D7G687 | Dihydrolipoamide acetyltransferase component of pyruvate dehydrogenase complex |
| | D8LS09 | AhpC/TSA family protein |
| | D7G6K3 | 2-cys peroxiredoxin |
| Subcellular modification process | D8LKK7 | Ubiquitin like protein 5 |
| | D7FVD5 | Small ubiquitin-like modifier |
| | D7FWC9 | Similar to ubiquitin |
| Fatty acid | D7FPP1 | Trifunctional enzyme subunit alpha |
| | D8LN46 | Malonyl-CoA:ACP transacylase |
| | D7FJ06 | Epimerase/dehydrogenase |
| | D8LLF7 | Enoyl-(Acyl carrier protein) reductase |
| | D8LRQ2 | Beta-ketoacyl synthase |
| | D7FWP0 | Beta-hydroxyacyl-ACP dehydratase |
| | D8LGX1 | Acyl-CoA dehydrogenase |
| | D8LLC3 | 3-oxoacyl-[acyl-carrier-protein] synthase |
| | D7FX87 | 3-ketoacyl-CoA thiolase |
| | D7FQ82 | 3-ketoacyl-(Acyl-carrier-protein) reductase, 3-oxoacyl-[acyl-carrier-protein] reductase |
| GTP binding | D8LJ21 | Filamentous temperature sensitive Z |
| | D1GJQ5 | Elongation factor Tu, chloroplastic |
| | D1J725 | Elongation factor Tu, chloroplastic |
| | D8LFY4 | Elongation factor G, mitochondrial |
| | D7FZS6 | Elongation factor 1-alpha |
| | D7FZQ6 | EF2, translation elongation factor 2 |
| | D7FGX4 | Arf1, ARF family GTPase |
| GTPase activity | D8LS40 | Rab50, RAB family GTPase |
| | D7FNV2 | Rab1B, RAB family GTPase |
| | D8LQC1 | Rab11A, RAB family GTPase |
| | D8LRP8 | Rab GDP dissociation inhibitor |
| Hydrolase activity | D7FJR9 | Similar to N(4)-(Beta-N-acetylglucosaminyl)-L-asparaginase (Glycosylasparaginase) (Aspartylglucosaminidase) (N4-(N-acetyl-beta-glucosaminyl)-L-asparagine amidase) (AGA) isoform 1 |
| | D7G484 | Lysophospholipase l2 pldb, hydrolase of alpha/beta superfamily |
| | D8LC90 | Haloacid dehalogenase-like hydrolase |
| | D7G792 | Haloacid dehalogenase-like hydrolase |
| | D7FWN8 | Haloacid dehalogenase-like hydrolase family protein |
| | D8LCA9 | Abhydrolase domain containing 14B |
| Lipid | D8LGE2 | Lipase |
| | D8LDK4 | Lipase |
| | D7FKG7 | Inorganic pyrophosphatase |
| | D7FZ60 | BiP |
| Metal ion binding | D7FRP4 | Similar to Iron-containing Alcohol Dehydrogenase |
| | D8LJJ8 | Protein phosphatase, putative |

| | | |
|---|---|---|
| | D7FHL9 | Mitochondrial protein import TIM8.13 complex subunit, Tim13 homolog |
| | D1GJM3 | Ferredoxin-thioredoxin reductase, catalytic chain |
| | D8LCX8 | Ferredoxin-NADP oxidoreductase |
| | D1GJP7 | Ferredoxin |
| | D7G5N8 | Ferredoxin |
| | D7FVZ4 | Ferredoxin nitrite reductase |
| | D8LQ48 | Ferredoxin component |
| Microtubule related | D8LIS3 | Tubulin beta chain |
| | D8LPR8 | Tubulin alpha chain |
| | D7FHD5 | Putative microtubule-associated protein EB1 |
| | D7FP80 | Flagellar associated protein |
| | D8LG52 | Flagellar associated protein |
| | D8LDT0 | Flagellar associated protein |
| | D7FLQ8 | Dynein heavy chain |
| | D8LF24 | Dynein heavy chain |
| NADP binding | D7FNG3 | Flavin-binding monooxygenase-like subfamily |
| | D7FJJ0 | D-3-phosphoglycerate dehydrogenase |
| | D7FLK7 | D-3-phosphoglycerate dehydrogenase |
| Nitrogen | D8LQI2 | NAD(P)H-Nitrate reductase |
| | D8LL91 | NAD(P)H-hydrate epimerase |
| | D7FPA7 | Glutamine synthetase |
| One carbon | D8LUA3 | Serine hydroxymethyltransferase |
| | D8LFD6 | Serine hydroxymethyltransferase |
| | D7G8Q4 | Adenosylhomocysteinase |
| nucleic acid binding | D7FRA4 | Plastid ribosomal protein S1 |
| | D7G9I0 | C2H2 zinc finger, ankyrin repeat protein |
| | D1J736 | 30S ribosomal protein S5, chloroplastic |
| | D1GJM7 | 30S ribosomal protein S16 |
| | D1GJQ4 | 30S ribosomal protein S10 |
| | D8LLY2 | 30S ribosomal protein S1 |
| oxidoreductase activity | D7FHR9 | Oxidoreductase, NAD-binding, myo-inositol 2-dehydrogenase |
| | D7FTB5 | Inositol 2-dehydrogenase |
| | D8LIK6 | Inositol 2-dehydrogenase |
| | D7G2B6 | Histidinol dehydrogenase |
| | D7FL60 | Coproporphyrinogen oxidase (Aerobic), putative chloroplast |
| Protein-protein interactions | D7FWZ8 | TPR repeat-containing protein |
| | D7G753 | Tetratricopeptide domain-containing protein |
| | D7FMW2 | Ankyrin repeat protein |
| | D8LMV4 | Ankyrin repeat protein |
| | D7G4T9 | Ankyrin domain protein |
| Protein folding | D7FR20 | Peptidylprolyl isomerase |

| | | |
|---|---|---|
| | D8LKW9 | Peptidylprolyl isomerase |
| | D7FP62 | Peptidylprolyl isomerase |
| | D7FP17 | Peptidylprolyl isomerase |
| | D8LGT5 | Peptidylprolyl isomerase |
| | D7FHE4 | Peptidyl-prolyl cis-trans isomerase |
| | D7G6P5 | Peptidyl-prolyl cis-trans isomerase |
| | D7G0Y5 | Peptidyl-prolyl cis-trans isomerase |
| | D8LET8 | Peptidyl-prolyl cis-trans isomerase |
| | D8LET7 | Peptidyl-prolyl cis-trans isomerase |
| | D8LI28 | Peptidyl-prolyl cis-trans isomerase (Rotamase)-cyclophilin family |
| | D7FZ58 | Immunophilin |
| | D8LHP1 | Cyclophilin |
| | D7FM88 | Chaperonin cpn60 |
| | D1GJG0 | Chaperone protein DnaK |
| | D1J774 | Chaperone protein DnaK |
| | D1GJF9 | 60 kDa chaperonin, chloroplastic |
| | D1J773 | 60 kDa chaperonin, chloroplastic |
| RNA metabolism | D7G3Y6 | Sm-like protein LSm6 |
| | D8LTD5 | Polyadenylate-binding protein |
| | D8LML1 | Heterogeneous nuclear ribonucleoprotein, putative |
| | D8LH21 | DEAD box helicase |
| | D7FNE7 | DEAD box helicase |
| | D8LK23 | DEAD box helicase |
| | D7FR54 | DEAD box helicase |
| ROS scavering, defense, stress related | D7FQ23 | Superoxide dismutase |
| | D7FPZ8 | Putative Glutathione S-transferase |
| | D7FUM6 | Phosphoadenylyl-sulfate reductase (Thioredoxin) |
| | D7G8P0 | Manganese superoxide dismutase |
| | D7G168 | L-ascorbate peroxidase |
| | D7FJU9 | Heat shock protein 90 |
| | D7G843 | Heat shock protein 90 |
| | D7FNB5 | Heat shock protein 70 |
| | D8LBY7 | Heat shock protein 70 |
| | D7G5X8 | Heat shock protein 70 |
| | D8LRH4 | Glutathione synthetase |
| | D8LHC1 | Glutathione reductase |
| | D8LHH9 | Glutathione peroxidase |
| | D8LC00 | Glutaredoxin |
| | D8LTP5 | Vanadium-dependent bromoperoxidase |
| | D7FM93 | Copper/zinc superoxide dismutase |
| | D7G1K9 | Catalase |

| | | |
|---|---|---|
| | D7G7J0 | Catalase |
| | D7FTZ8 | Catalase |
| | D7G613 | PUB domain, zinc finger protein Thioredoxin |
| | D8LK67 | Peroxiredoxin or Alkyl hydroperoxide reductase/ Thiol specific antioxidant |
| | D8LFG4 | Peroxiredoxin family protein |
| | D7G7J1 | Peroxidase |
| | D8LTK5 | Peroxidase |
| Spliceosome formation | D7FT20 | Small nuclear ribonucleoprotein-associated protein D3 |
| | D7FWG1 | Small nuclear ribonucleoprotein SmF |
| | D8LRR0 | Small nuclear ribonucleoprotein polypeptide G |
| | D7FW42 | Small nuclear ribonucleoprotein D2-like protein |
| Transcription | D8LJM6 | RuvB-like helicase |
| | D8LCR9 | NF-X1 finger and helicase domain protein, putative |
| | D7G5C4 | Nascent polypeptide-associated complex subunit beta |
| | D8LI33 | Histone-like transcription factor |
| | D7FWI5 | Histone H4 |
| | D7G4I4 | Histone H3 |
| | D7FWI8 | Histone H2B |
| | D7FWI9 | Histone H2A |
| Translation | D7G2D8 | Ribosome recycling factor |
| | D8LI35 | Ribosome biogenesis protein WDR12 homolog |
| | D8LN84 | Ribosomal protein rpl30 |
| | D7G033 | Ribosomal protein L35 |
| | D8LL36 | Ribosomal protein L18 |
| | D8LTT6 | Putative initiation factor eIF3 g subunit |
| | Q2PQH2 | Multifunctional fusion protein |
| | D8LER7 | Eukaryotic translation initiation factor 6 |
| | D7FNG1 | Eukaryotic translation initiation factor 3 subunit H |
| | D8LDJ7 | Eukaryotic translation initiation factor 3 subunit F |
| | D7G2M4 | Eukaryotic translation initiation factor 1-SUI1 |
| | D7FIB3 | Eukaryotic peptide chain release factor 1 |
| | D7FQL1 | Eukaryotic initiation factor 4A |
| | D8LC24 | Eukaryotic initiation factor 2A |
| | D7G233 | Eukaryotic initiation factor 2 beta subunit |
| | D7G6W9 | 60S ribosomal protein L13a |
| | D8LNU8 | 60S ribosomal protein L10A |
| | D1GJS2 | 50S ribosomal protein L14, chloroplastic |
| | D1GJP6 | 50S ribosomal protein L12, chloroplastic |
| | D1GJP4 | 50S ribosomal protein L11, chloroplastic |
| | D7FHP2 | 40S ribosomal protein AS |
| | D7FRM9 | 40S ribosomal protein S28 |

| | | |
|---|---|---|
| | D7FUE0 | 40S ribosomal protein S27 |
| | D7FYT5 | 40S ribosomal protein S17 |
| | D7FYS4 | 40S ribosomal protein S14 |
| | D7FHF7 | 40S ribosomal protein S12 |
| Vesicle related | D7G927 | Soluble NSF Attachment Protein (SNAP) Receptor (SNARE) |
| | D7FNJ2 | Clathrin light chain |
| | D7G9H3 | Clathrin light chain |
| | D7FWD1 | Clathrin heavy chain |
| Transport | D7FVE6 | Voltage Gated Calcium/Sodium Channel subunit alpha |
| | D7FZW9 | Vacuolar protein sorting-associated protein 29 |
| | D7FQ25 | Similar to ankyrin 2,3/unc44 |
| | D7FNZ6 | U3 snoRNP-associated protein Utp7 |
| | D7FWM8 | Vacuolar protein sorting-associated protein 28 homolog |
| | D8LDU1 | Carnitine/acylcarnitine carrier protein |
| | D7FKE2 | V-type proton ATPase subunit F |
| | D7FPY6 | V-type proton ATPase subunit a |
| | D7G8S5 | V-type proton ATPase proteolipid subunit |
| | D8LH70 | tRNA (guanine(26)-N(2))-dimethyltransferase |
| | D8LH70 | tRNA (guanine(26)-N(2))-dimethyltransferase |
| Zinc ion binding | D8LLJ1 | Carbonic anhydrase |
| | D7FJ29 | Carbonic anhydrase |
| | D7FMY1 | Aminotransferase |
| | D7FQZ3 | Aminopeptidase |
| Other functions | D8LT76 | Profilin |
| | D7G8H9 | VCBS protein |
| | D8LRH6 | Ornithine cyclodeaminase |
| | D7G2U5 | Autophagy-related protein |
| | D7FNY6 | SH2 domain containing protein |
| | D7G282 | 3-isopropylmalate dehydrogenase |
| | D8LRK8 | 3-isopropylmalate dehydratase |
| | D8LP22 | CDGSH iron sulfur domain-containing protein |
| | D8LK78 | Ubiquinol cytochrome c reductase subunit QCR7 |
| | D7FVX8 | Ubiquinol cytochrome c reductase cytochrome c1 prec (ISS) |
| | D8LH46 | Calmodulin OS=Ectocarpus siliculosus |
| | D8LGM4 | Putative carbonic anhydrase |
| | D8LCQ8 | Gamma carbonic anhydrase |
| | D8LTS6 | GatB/YqeY |
| | D8LPN3 | Amine oxidase |
| | D7FTN9 | 26S proteasome regulatory subunit |
| | D7FSE0 | 26S proteasome beta type 7 subunit |
| | D7G7T5 | Cyclin-dependent kinases regulatory subunit |

| | | |
|---|---|---|
| | D7FIY2 | Adenylyl cyclase-associated protein |
| | D7FV40 | Valine--tRNA ligase |
| | D7G804 | Squalene Monooxygenase (N-terminal region) |
| | D8LTQ9 | Basal body protein |
| | D7FSI9 | Villin villin |
| | D7G4M2 | Smc-like protein |
| | D7FUA1 | Putative Leucine Rich Repeat Protein |
| | D7FM46 | Putative Leucine Rich Repeat Protein Kinase |
| | D7G5A2 | Probable chromatin remodelling complex ATPase chain |
| | D8LFA5 | Phospho-2-dehydro-3-deoxyheptonate aldolase |
| | D8LBK0 | Bromodomain-containing protein |
| | D8LR14 | Flagellar associated protein, transcriptional coactivator-like protein |
| | D7G2X9 | eIF-2alpha kinase GCN2 similar to Eukaryotic translation initiation factor 2-alpha kinase 4 (GCN2-li) |
| | D8LM38 | Excision repair helicase ercc-6-related |
| | D7FPB6 | Ubiquitin-conjugating enzyme 1 |
| | D8LJN5 | Ubiquitin conjugating enzyme |
| | D8LRR5 | Similar to suppressor of ypt1 |
| | D8LKV0 | High mobility group protein |
| | D8LK79 | Uncharacterized protein (Fragment) |
| | D8LQX5 | Uncharacterized protein (Fragment) |
| | D7G5E4 | Similar to arginine/serine-rich splicing factor 7 |
| | D7FQT7 | RNA-binding protein, putative |
| | D7FKD2 | Coiled-coil domain 6-like protein |
| | D7FHS2 | Similar to PDGF associated protein |
| | D8LHP4 | Monogalactosyldiacylglycerol synthase, family GT28 |
| | D7FRW0 | Glycine cleavage system P protein |
| | D7FYQ9 | Enolase OS=Ectocarpus siliculosus |
| | D8LPQ9 | Dihydroxyacetone/glycerone kinase |
| | D7G5X0 | Putative homoaconitate hydratase, N-terminal part |
| | D7G5W8 | Putative homoaconitate hydratase, c-terminal part |
| | D7FUT9 | Myo-inositol-1-phosphate synthase |
| | D7FVN4 | Myo-inositol dehydrogenase myo-inositol dehydrogenase |
| | D8LHI5 | Protein disulfide isomerase |
| | D8LI73 | Prolyl 4-hydroxylase alpha-1 subunit-like protein |
| | D7FMW8 | Inositol triphosphate receptor (IP3R)/ Ryanodine receptor like protein |
| | D8LQ54 | Similar to leucine rich repeat containing 44 |
| | D8LCF6 | Mx2, Mx-like dynamin-related GTPase |
| | D8LHU2 | 2-Isopropylmalate synthase |
| | D7FLF2 | 1-deoxy-D-xylulose 5-phosphate reductoisomerase, chloroplast |
| | D7FLF2 | 1-deoxy-D-xylulose 5-phosphate reductoisomerase, chloroplast |

| | | |
|---|---|---|
| | D7FMJ8 | Mannitol 1-phosphate dehydrogenase |
| | D7FJC6 | LL-diaminopimelate aminotransferase diaminopimelate aminotransferase |
| | D7G034 | Diaminopimelate epimerase |
| | D8LGH6 | Cytosolic 5\'-nucleotidase III-like protein A (CN-III-like protein A) |
| | D7FLF2 | 1-deoxy-D-xylulose 5-phosphate reductoisomerase, chloroplast |
| | D7FJC6 | LL-diaminopimelate aminotransferase diaminopimelate aminotransferase |
| | D7G034 | Diaminopimelate epimerase |
| | D8LGH6 | Cytosolic 5\'-nucleotidase III-like protein A (CN-III-like protein A) |
| | D7FLF2 | 1-deoxy-D-xylulose 5-phosphate reductoisomerase, chloroplast |
| | D7FYV0 | Lactoylglutathione lyase, putative |
| | D7G588 | Histidyl-tRNA Synthetase Similar to Histidine Ammonia-Lyase |
| | D8LM83 | Sorting nexin 1 |
| | D8LHP7 | Mitogen-activated protein kinase |
| | D8LJF5 | Importin subunit alpha |
| | D8LK94 | Methionyl-tRNA synthetase |
| | D7FPC5 | Copper chaperone |
| | D7FVV9 | B1142C05.17 |
| | D7G747 | Similar to MGC83835 protein |
| | D8LQS5 | Short-chain dehydrogenase/reductase SDR |
| | D8LSP6 | Rad23b protein |
| | D8LDI6 | Glycolate Oxidase |
| | D7FT45 | Spermidine/spermine synthase |
| | D7FKW3 | Spermidine/spermine synthase |
| | D7G6X5 | Separin |
| | D8LBQ0 | Peroxisomal enoyl-coenzyme A hydratase |
| | D8LU94 | Coronin |
| | D7FJB9 | Catalytic/ hydrolase/ phosphoglycolate phosphatase/ phosphoric monoester hydrolase |
| | D7FLX5 | Aspartyl protease |
| | D7G5M6 | Delta-1-pyrroline-5-carboxylate synthase |
| | D8LDT2 | Tuf1, mitochondrial translation elongation factor EF-Tu |
| | D7FYP6 | Transcriptional activator |
| | D7FVL0 | Putative transmembrane protein |
| | D7G6H6 | Methionine-R-sulfoxide reductase |
| | D7FMY2 | Hydroxymethylbilane synthase, putative chloroplast |
| | D7G7A6 | GTP-binding nuclear protein |
| | D7FN58 | 14-3-3-like protein |
| | D8LNZ4 | Pyridoxal phosphate homeostasis protein |
| | D7FU83 | Protoporphyrinogen oxidase |
| | D8LKS8 | Probable bifunctional purine synthesis protein |
| | D8LJS6 | Cystathionine gamma-lyase |

| | | |
|---|---|---|
| | D7FXH2 | Inosine-5'-monophosphate dehydrogenase |
| | D7FYW5 | Flavine reductase |
| | D8LLC7 | 6,7-dimethyl-8-ribityllumazine synthase |
| | D7FZC9 | Regulator of ribonuclease activity A, RraA |
| | D8LP25 | 60S acidic ribosomal protein P0 |
| | D7G5F6 | Cysteine synthase |
| | D7FXN1 | Copine |
| | D8LP23 | Thiamine monophosphate synthase |
| | D8LSH6 | Cysteine desulfurase |
| | D8LF05 | Gamma-glutamyl transpeptidase |
| | D7FZ31 | Viral A-type inclusion protein |
| | D7G287 | Putative serine esterase |
| | D7G7C7 | Putative Ntdin |
| | D8LHI8 | Protein binding protein, putative |
| | D7FZR3 | Pentapeptide repeat |
| | D7FIV4 | NHL repeat-containing protein |
| | D7FVX5 | LRR-GTPase of the ROCO family |
| | D7FZ52 | Leucyl aminopeptidase |
| | D8LJM5 | Kinesin family member 3A |
| | D7G7Q2 | Imm downregulated 23 |
| | D8LNZ9 | Guanine nucleotide binding protein beta polypeptide 2-like 1 (Partial) (Fragment) |
| | D8LP49 | EsV-1-210/211 paralog |
| | D8LPL9 | EsV-1-210 |
| | D8LPL3 | EsV-1-192 |
| | Q8QKW6 | EsV-1-14 |
| | D8LB31 | Chromosome 22 open reading frame 13, isoform CRA_c |
| | D7FTS3 | CAB/ELIP/HLIP superfamily of protein |
| | D7FQ70 | Bcs1 aaa-type ATPase, putative |
| | D7FVR8 | Aspartate aminotransferase |
| | D8LF03 | Acetyl-coenzyme A synthetase |
| | D7G8S8 | Acetyl-CoA acetyltransferase |